AD-A114 117 FEDERAL AVIATION ADMINISTRATION TECHNICAL CENTER ATL--ETC F/G 1/3
A COMPENDIUM OF LIGHTNING EFFECTS ON FUTURE AIRCRAFT ELECTRONIC--ETC(U)
FEB 82 N O RASCH
UNCLASSIFIED DOT/FAA/CT-82/30 NL

1 OF 3

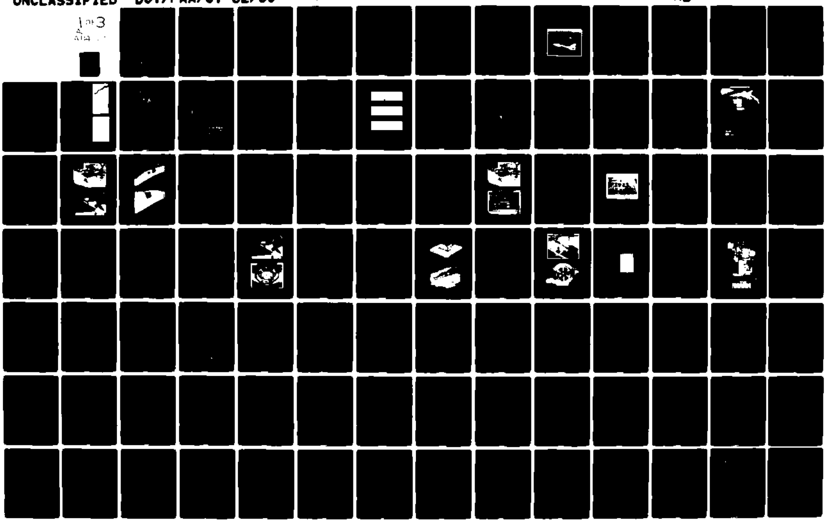

(14)

DOT/FAA/CT-82/30

A Compendium of Lightning Effects on Future Aircraft Electronic Systems

Nickolus O. Rasch

February 1982

Compendium

This document is available to the U.S. public through the National Technical Information Service, Springfield, Virginia 22161.

US Department of Transportation
Federal Aviation Administration
Technical Center
Atlantic City Airport, N.J. 08405

NOTICE

Technical Report Documentation Page

1. Report No. DOT/FAA/CT-82/30	2. Government Accession No. AD-A114 117	3. Recipient's Catalog No.
4. Title and Subtitle A COMPENDIUM OF LIGHTNING EFFECTS ON FUTURE AIRCRAFT SYSTEMS		5. Report Date February 1982
		6. Performing Organization Code
7. Author(s) Nickolus O. Rasch		8. Performing Organization Report No. ACT-340
9. Performing Organization Name and Address Federal Aviation Administration Technical Center Atlantic City Airport, New Jersey 08405		10. Work Unit No. (TRAIS)
		11. Contract or Grant No. 182-340-100
12. Sponsoring Agency Name and Address U.S. Department of Transportation Federal Aviation Administration Technical Center Atlantic City Airport, New Jersey 08405		13. Type of Report and Period Covered Final November 4-8, 1981
		14. Sponsoring Agency Code

15. Supplementary Notes

16. Abstract

This publication is a composite of presentations given at the NASA-Langley Research Center/FAA Technical Center "Lightning Effects on Future Aircraft Systems Workshop" held on November 4-6, 1981, at the NASA-Langley Research Center Facility.

The presentations encompassed the full spectrum of lightning research from lighting phenomonology, lightning modeling, electromagnetic issues associated with composite materials, to the lightning/aircraft electromagnetic interaction analysis. Also included are a total of five presentations assessing the Digital System upset phenomen.

17. Key Words	18. Distribution Statement
Triboelectrification Corona Stepped Leader Tortuous Channel	Document is available to the U.S. public through the National Technical Information Service, Springfield, Virginia 22161

19. Security Classif. (of this report)	20. Security Classif. (of this page)	21. No. of Pages	22. Price
Unclassified	Unclassified	251	

Form DOT F 1700.7 (8-72) Reproduction of completed page authorized

METRIC CONVERSION FACTORS

Approximate Conversions to Metric Measures

Symbol	When You Know	Multiply by	To Find	Symbol
	LENGTH			
in	inches	*2.5	centimeters	cm
ft	feet	30	centimeters	cm
yd	yards	0.9	meters	m
mi	miles	1.6	kilometers	km
	AREA			
in^2	square inches	6.5	square centimeters	cm^2
ft^2	square feet	0.09	square meters	m^2
yd^2	square yards	0.8	square meters	m^2
mi^2	square miles	2.6	square kilometers	km^2
	acres	0.4	hectares	ha
	MASS (weight)			
oz	ounces	28	grams	g
lb	pounds	0.45	kilograms	kg
	short tons (2000 lb)	0.9	tonnes	t
	VOLUME			
tsp	teaspoons	5	milliliters	ml
Tbsp	tablespoons	15	milliliters	ml
fl oz	fluid ounces	30	milliliters	ml
c	cups	0.24	liters	l
pt	pints	0.47	liters	l
qt	quarts	0.95	liters	l
gal	gallons	3.8	liters	l
ft^3	cubic feet	0.03	cubic meters	m^3
yd^3	cubic yards	0.76	cubic meters	m^3
	TEMPERATURE (exact)			
°F	Fahrenheit temperature	5/9 (after subtracting 32)	Celsius temperature	°C

*1 in = 2.54 (exactly). For other exact conversions and more detailed tables, see NBS Misc. Publ. 286, Units of Weights and Measures, Price $2.25, SD Catalog No. C13.10:286.

Approximate Conversions from Metric Measures

Symbol	When You Know	Multiply by	To Find	Symbol
	LENGTH			
mm	millimeters	0.04	inches	in
cm	centimeters	0.4	inches	in
m	meters	3.3	feet	ft
m	meters	1.1	yards	yd
km	kilometers	0.6	miles	mi
	AREA			
cm^2	square centimeters	0.16	square inches	in^2
m^2	square meters	1.2	square yards	yd^2
km^2	square kilometers	0.4	square miles	mi^2
ha	hectares (10,000 m^2)	2.5	acres	
	MASS (weight)			
g	grams	0.035	ounces	oz
kg	kilograms	2.2	pounds	lb
t	tonnes (1000 kg)	1.1	short tons	
	VOLUME			
ml	milliliters	0.03	fluid ounces	fl oz
l	liters	2.1	pints	pt
l	liters	1.06	quarts	qt
l	liters	0.26	gallons	gal
m^3	cubic meters	35	cubic feet	ft^3
m^3	cubic meters	1.3	cubic yards	yd^3
	TEMPERATURE (exact)			
°C	Celsius temperature	9/5 (then add 32)	Fahrenheit temperature	°F

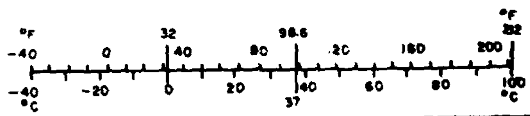

PREFACE

The "Lightning Effects on Future Aircraft Electronic Systems" workshop, November 4-6, 1981, sponsored by the NASA-Langley Research Center in conjunction with the Federal Aviation Administration (FAA) Technical Center, provided an ideal vehicle for information exchange. This workshop provided regional and headquarters personnel with an insight into the magnitude of the problem, and the progress being accomplished through existing and future FAA programs.

Protection of electrical and electronic subsystems and equipments against the atmospheric electricity hazards constituted by lightning and static electricity must be taken into special account in the design of advanced technology aircraft. Two primary factors have contributed to an increased potential hazard to new generation aircraft: (1) The increasingly widespread use of digital microelectronic subsystems and/or avionic equipment which are inherently susceptible to upset and damage caused by electrical transients to implement flight and mission critical functions; and (2) the reduced electromagnetic shielding provided by many advanced structural materials. Present military and civil design guides and standards are being reviewed to assure adequate protection for new generation aircraft.

The NASA-Langley Research Center Electronic System Branch of the Flight Electronic Division was the host for this workshop; which is a major element in the FAA Technical Center's Advanced Integrated Flight Systems (AIFS) program. The AIFS program objectives are to acquire and disseminate data, enhance communications, and provide Aviation Standards, lead and/or certify regions airworthiness/certification personnel with a vehicle for information transfer in this highly technological area of lightning research as related to aircraft flight safety.

The personnel from the NASA-Langley Research Center Aircraft Electronic System Branch and their associates exhibited professionalism in the planning, assembling the technical experts and material, and conducting this workshop. It is with a deep and sincere sense of gratitude that we of the FAA would like to extend our appreciation to those persons for a job well done.

TABLE OF CONTENTS

LIGHTNING EFFECTS RESEARCH PROGRAM

by

Mr. Felix Pitts

Langley Research Center
National Aeronautics and Space Administration

The current research program being pursued at the Langley Research Center on lightning and its effects on digital electronic systems will be presented.

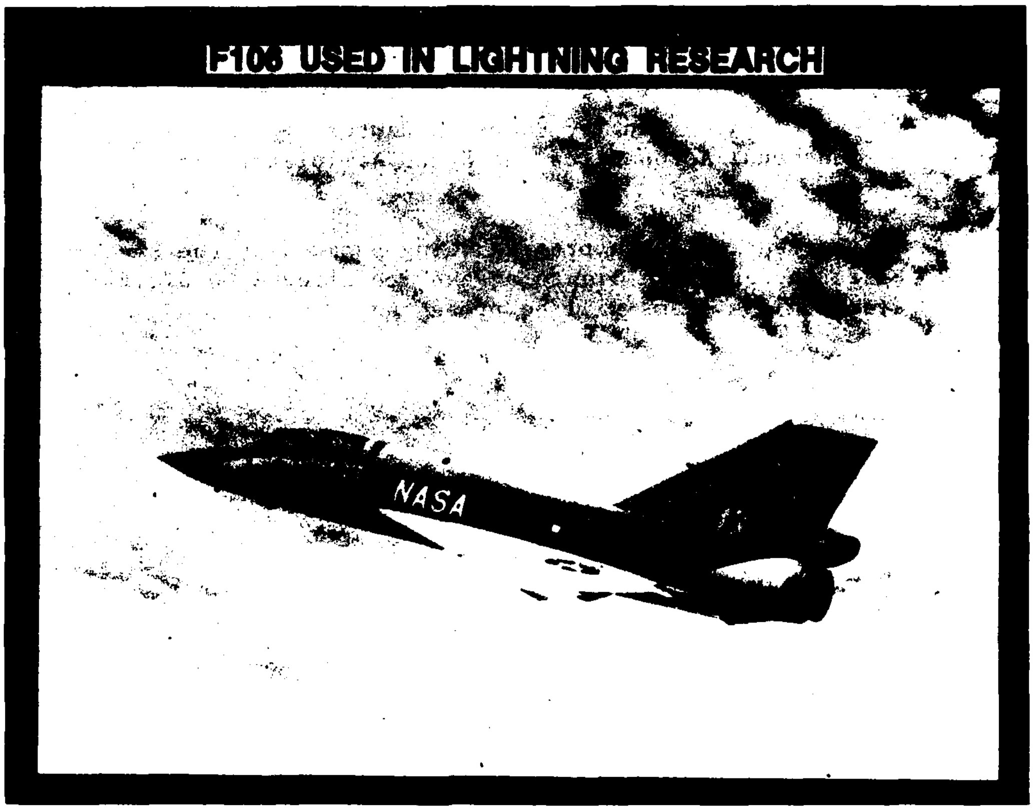
F106 USED IN LIGHTNING RESEARCH
NASA

LIGHTNING EFFECTS

- CURRENT TRANSPORT AIRCRAFT STRUCK ABOUT ONCE PER YEAR
  - ALUMINUM SKIN
  - HYDRAULIC/MECHANICAL PRIMARY CONTROLS
  - MOSTLY NUISANCE PROBLEMS CAUSED BY LIGHTNING
- FUTURE AIRCRAFT WILL EMPLOY
  - COMPOSITE STRUCTURE
  - DIGITAL AVIONICS/ELECTRONIC CONTROLS
    - SUSCEPTIBLE TO DISTURBANCE
    - POTENTIAL FOR UPSET
- NEED FOR FUTURE AIRCRAFT DESIGNS
  - BETTER UNDERSTANDING OF IN-FLIGHT LIGHTNING ENVIRONMENT
  - TECHNIQUES FOR ASSESSING DIGITAL SYSTEM PERFORMANCE IN LIGHTNING ENVIRONMENT

LIGHTNING EFFECTS RESEARCH PROGRAM

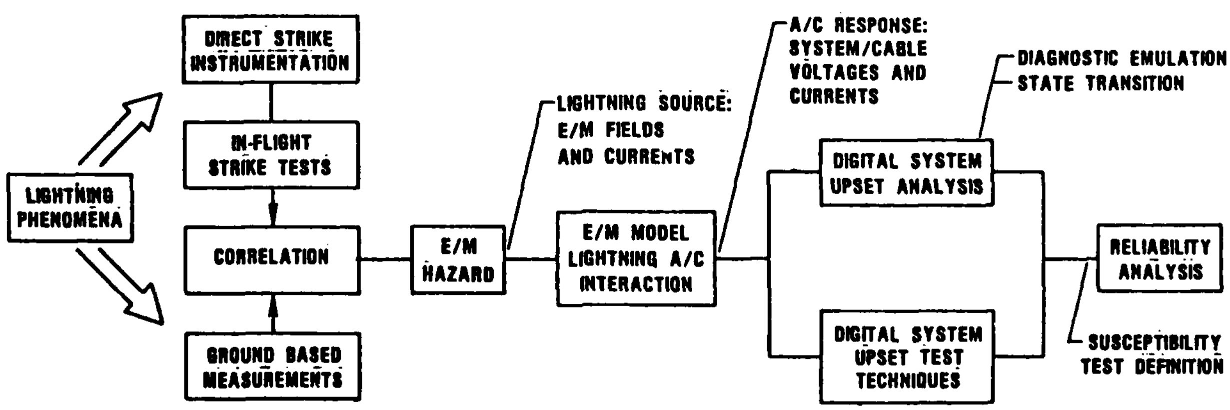

LIGHTNING PHENOMENOLOGY

by

Dr. M. LeVine

Goddard Space Flight Center
National Aeronautics and Space Administration

State-of-the-art of lightning knowledge: Theories of charge generation, the lightning discharge, stepped leaders, return strokes, fundamental electromagnetics of lightning, statistical distribution of lightning characteristics.

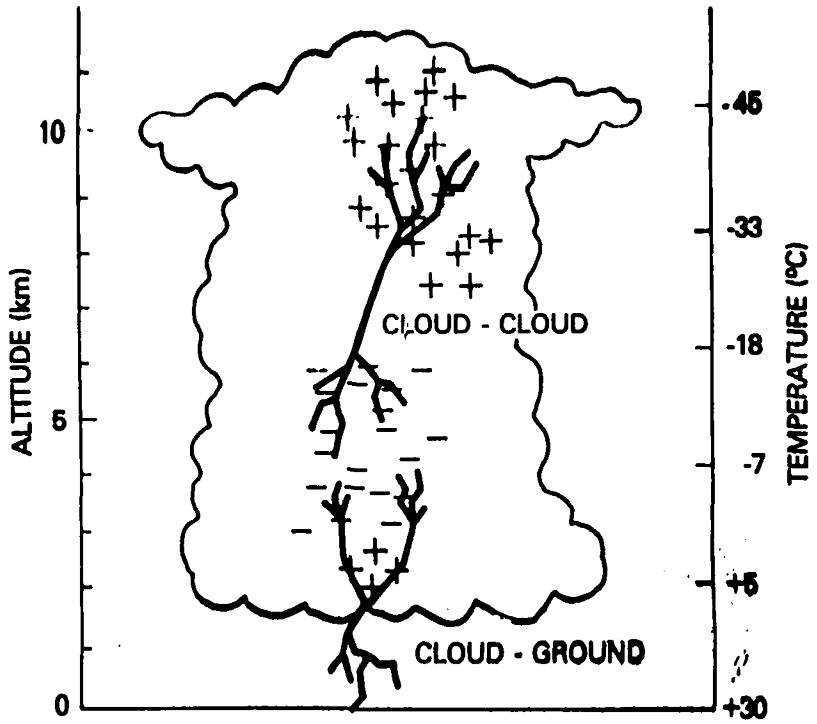

ALTITUDE (km)
TEMPERATURE (ºC)
10
5
0
-45
-33
-18
-7
+5
+30
CLOUD - CLOUD
CLOUD - GROUND

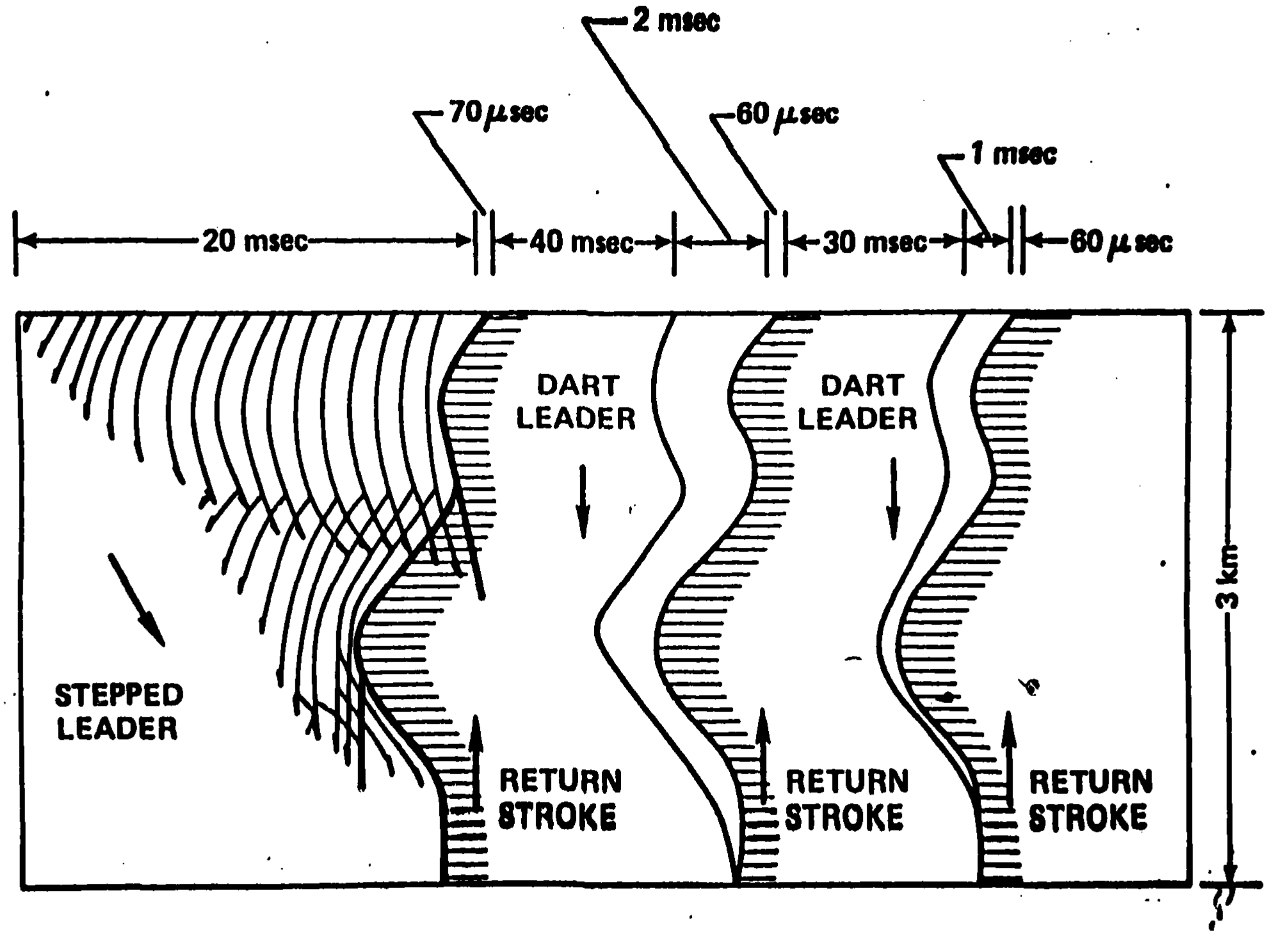

2 msec
70 μsec
60 μsec
1 msec
20 msec
40 msec
30 msec
60 μsec
DART LEADER
DART LEADER
STEPPED LEADER
RETURN STROKE
RETURN STROKE
RETURN STROKE
3 km

CLOUD-TO-GROUND LIGHTNING PARAMETERS

	MINIMUM*	REPRESENTATIVE	MAXIMUM*
STEPPED LEADER			
LENGTH OF STEP (m)	3	50	200
TIME INTERVAL BETWEEN STEPS (μsec)	30	50	125
AVERAGE VELOCITY OF PROPAGATION OF STEPPED LEADER (m/sec)	1.0×10^5	1.5×10^5	2.6×10^6
DART LEADER			
VELOCITY OF PROPAGATION (m/sec)	1.0×10^6	2.0×10^6	2.1×10^7
RETURN STROKE**			
PEAK CURRENT (ka)		10-20	110
TIME TO HALF OF PEAK CURRENT (μsec)	10	40	250
CHANNEL LENGTH (km)	2	5	14
VELOCITY OF PROPAGATION (m/sec)	2.0×10^7	5.0×10^7	1.4×10^8
LIGHTNING FLASH			
NUMBER OF STROKES PER FLASH	1	3-4	26
TIME INTERVAL BETWEEN STROKES (msec)	3	40	100
TIME DURATION OF FLASH (sec)	10^{-2}	0.2	2
CHARGE TRANSFERRED (coul)	3	25	90

*THE WORDS MAXIMUM AND MINIMUM ARE USED IN THE SENSE THAT MOST MEASURED VALUES FALL BETWEEN THESE LIMITS.

**FIRST RETURN STROKES HAVE SLOWER AVERAGE VELOCITIES OF PROPAGATION, SLOWER CURRENT RATES OF INCREASE, LONGER TIMES TO CURRENT PEAK, AND GENERALLY LARGER CHARGE TRANSFER THAN SUBSEQUENT RETURN STROKES IN A FLASH.

HISTORICAL PERSPECTIVE

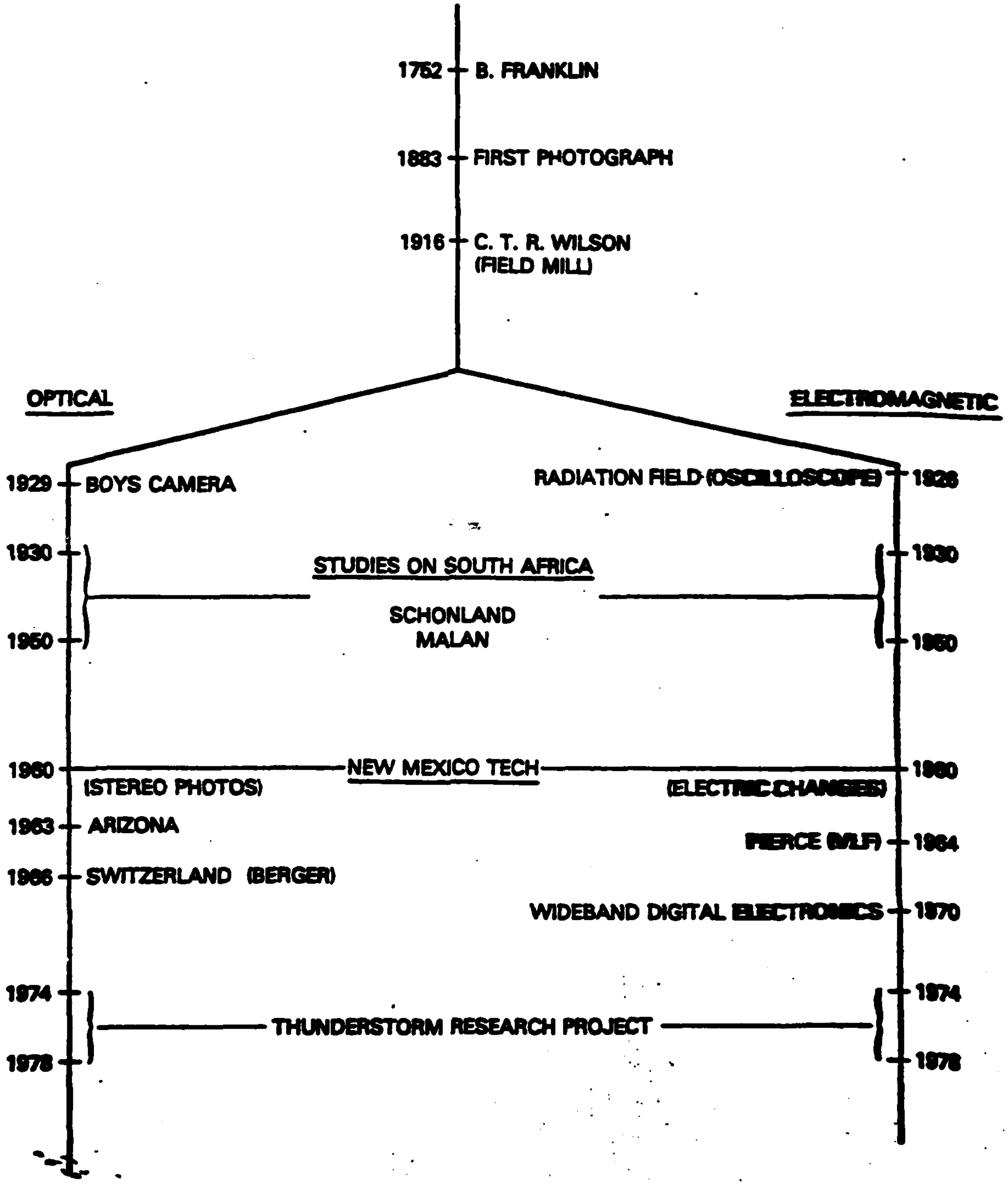

THE STREAK CAMERA

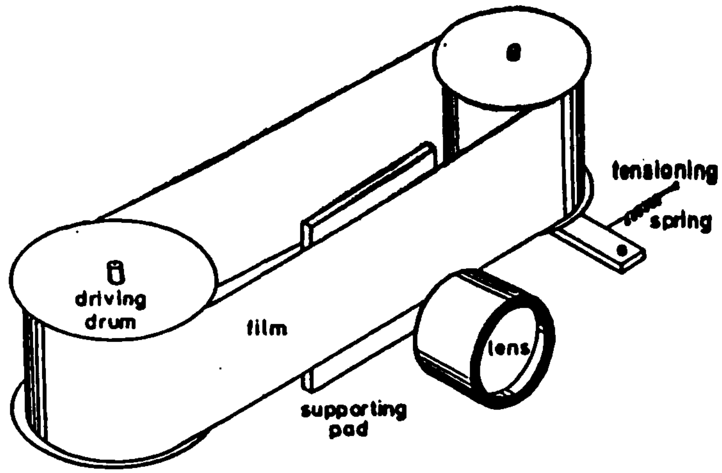

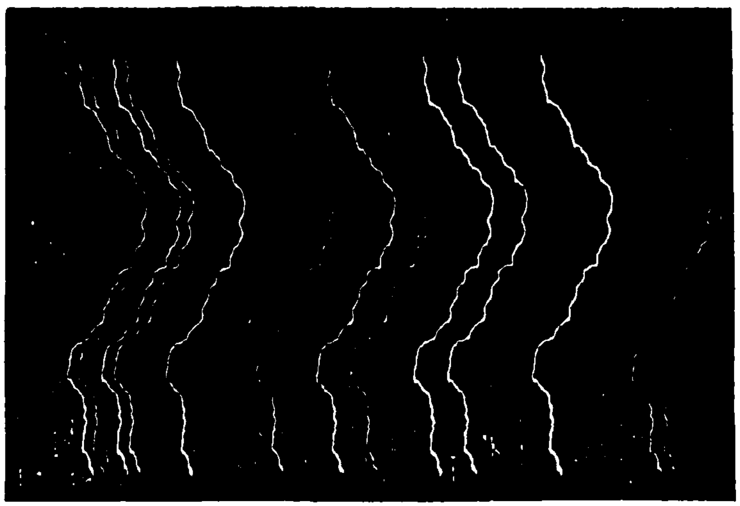

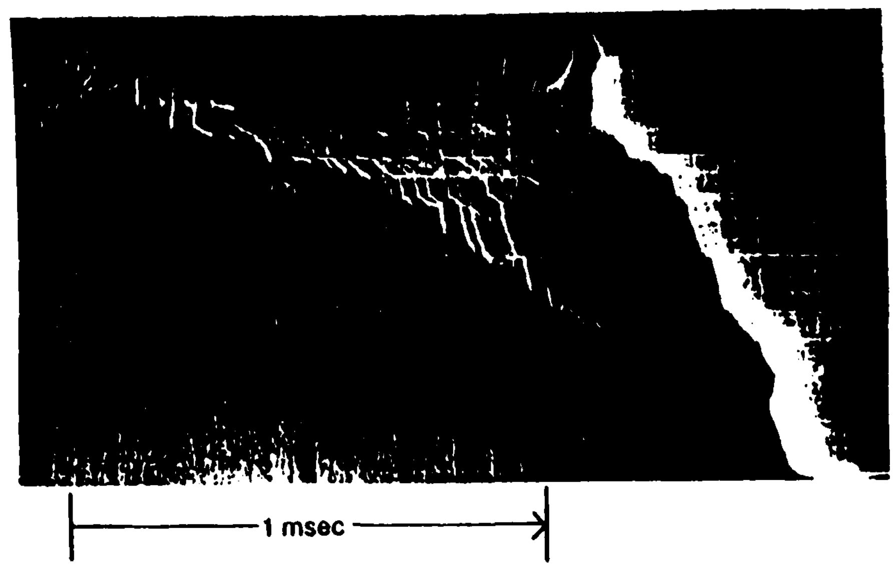

THE BOYS' CAMERA

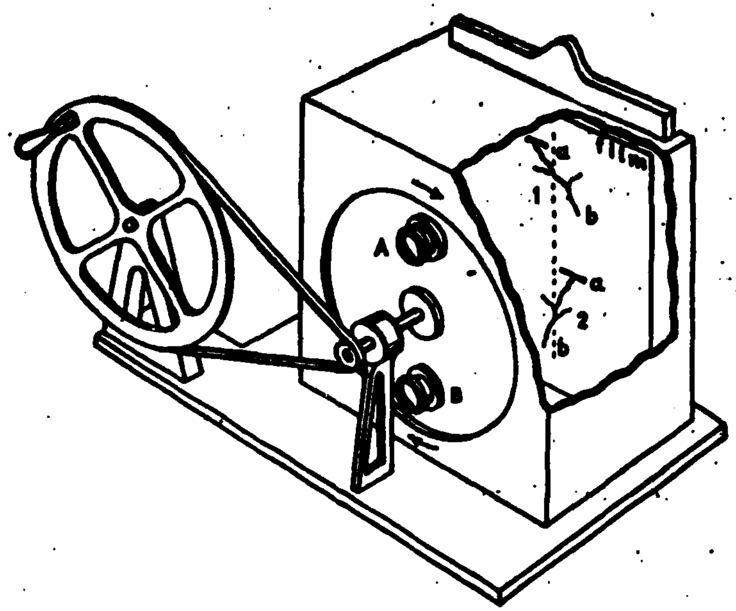

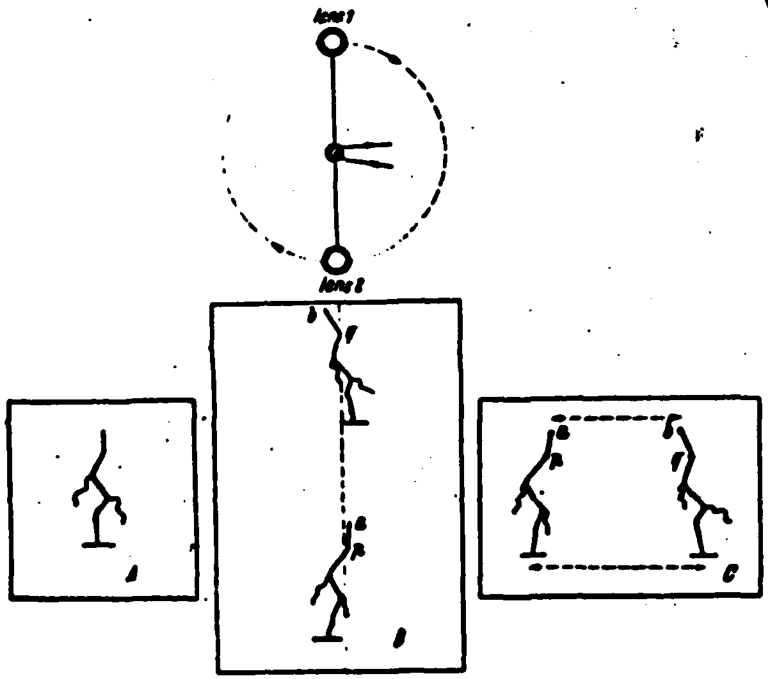

FIELD MILL

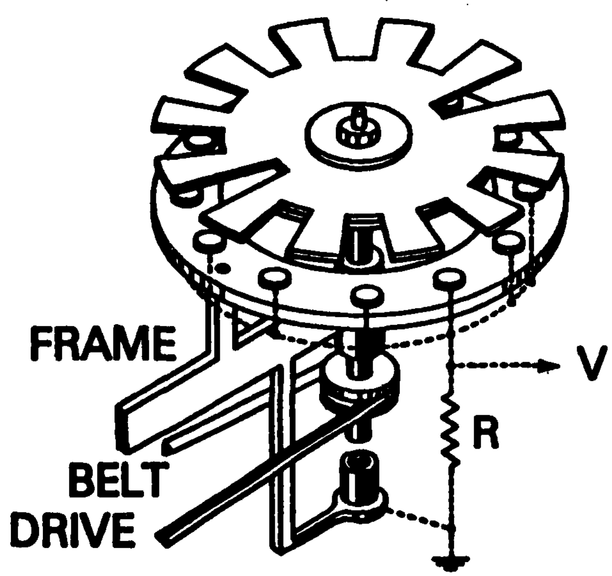

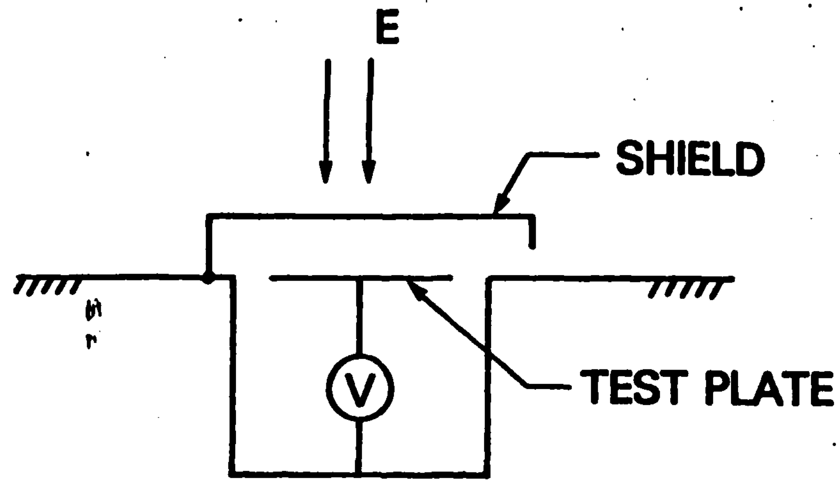

$$E_n = \frac{CV}{E_o A}$$

DISTRIBUTION OF CHARGE IN A THUNDERCLOUD

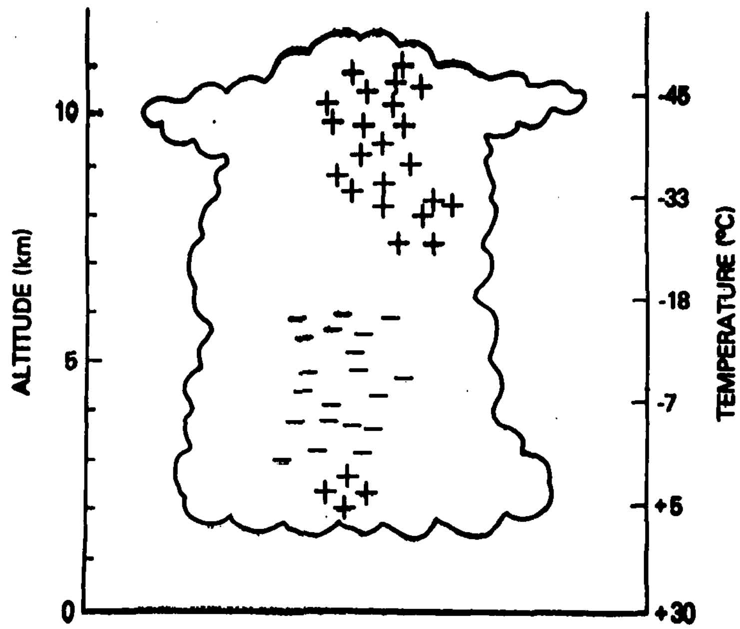

FIELD CHANGE SYSTEM

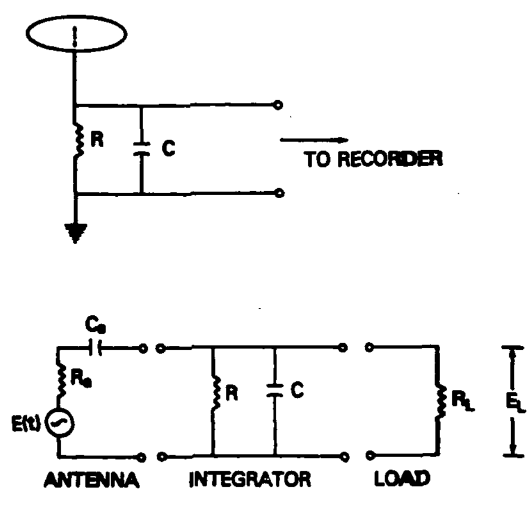

$$E_L = \begin{cases} \dfrac{C_a}{C_a + C} E & \text{INTEGRATOR} \\ R_L C_a \dfrac{dE}{dt} & \text{NO INTEGRATOR} \end{cases}$$

SLOW ELECTRIC FIELD CHANGES

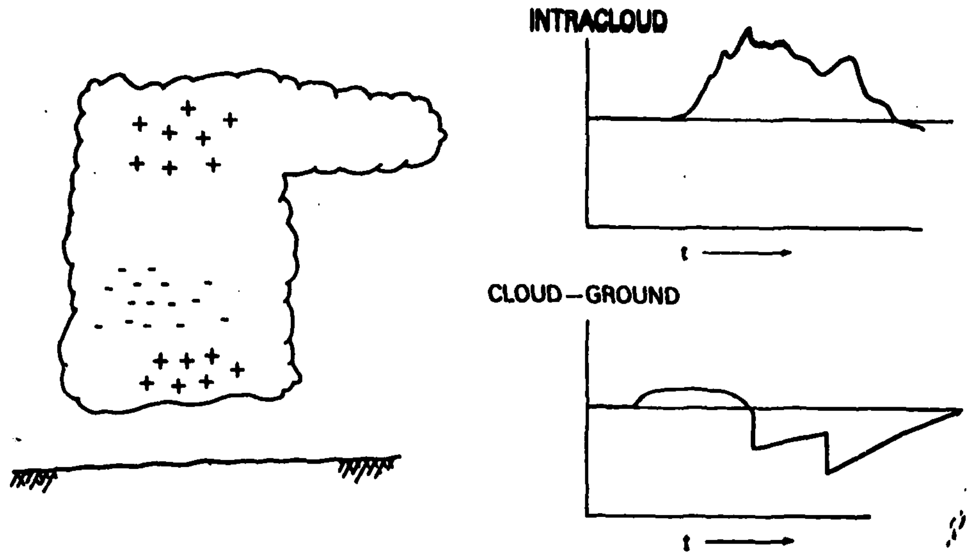

FAST ELECTRIC FIELD CHANGES

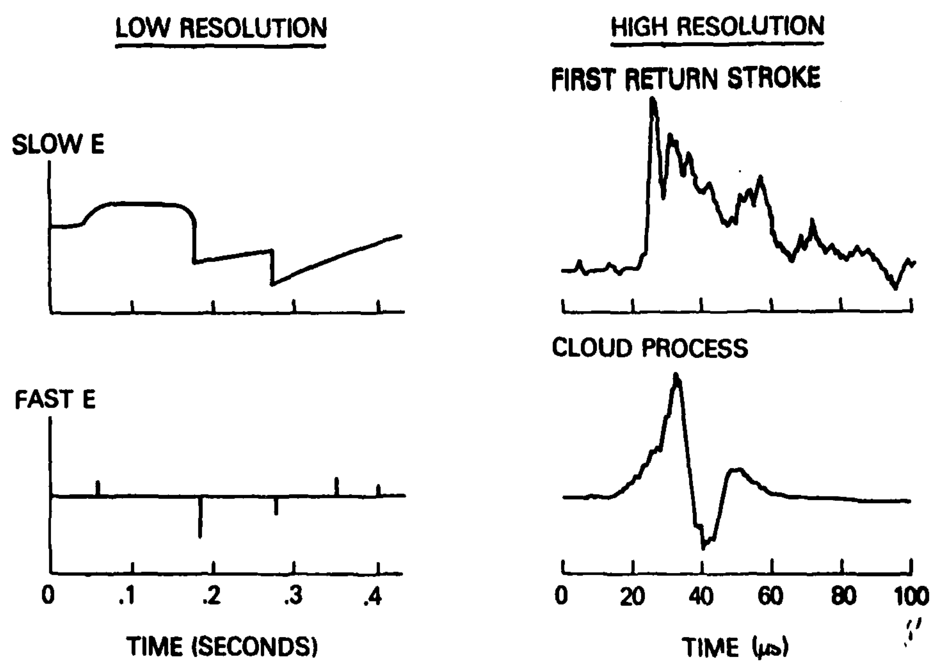

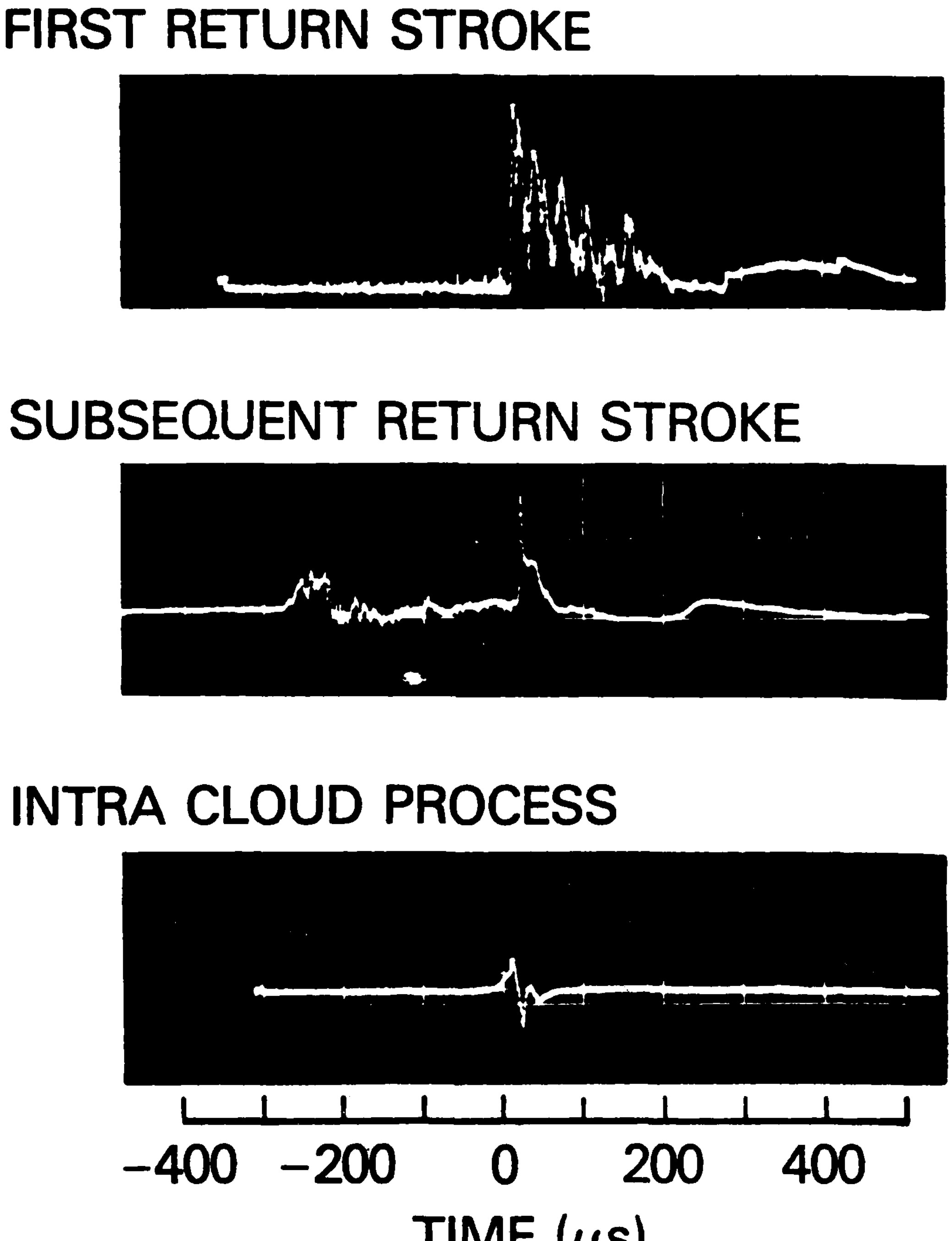
FIRST RETURN STROKE
SUBSEQUENT RETURN STROKE
INTRA CLOUD PROCESS
−400 −200 0 200 400
TIME (μs)

RADIO RECEIVER

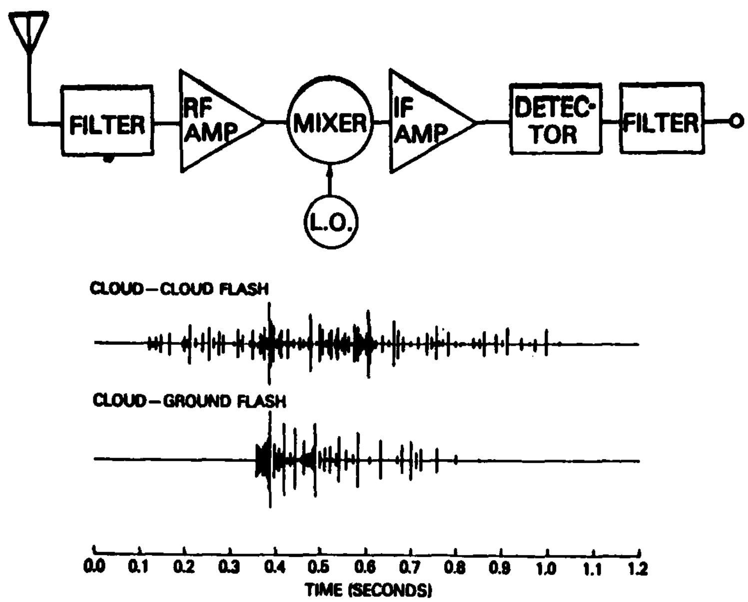

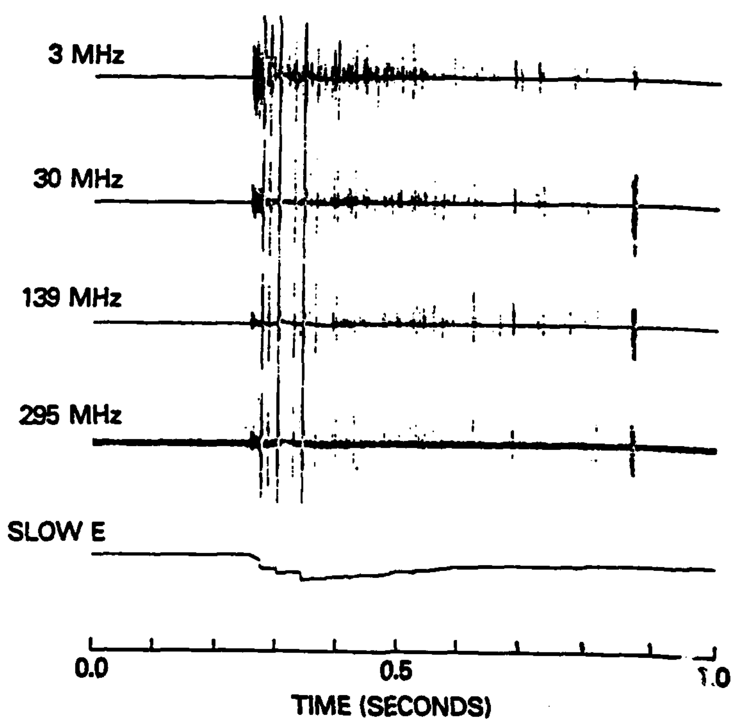

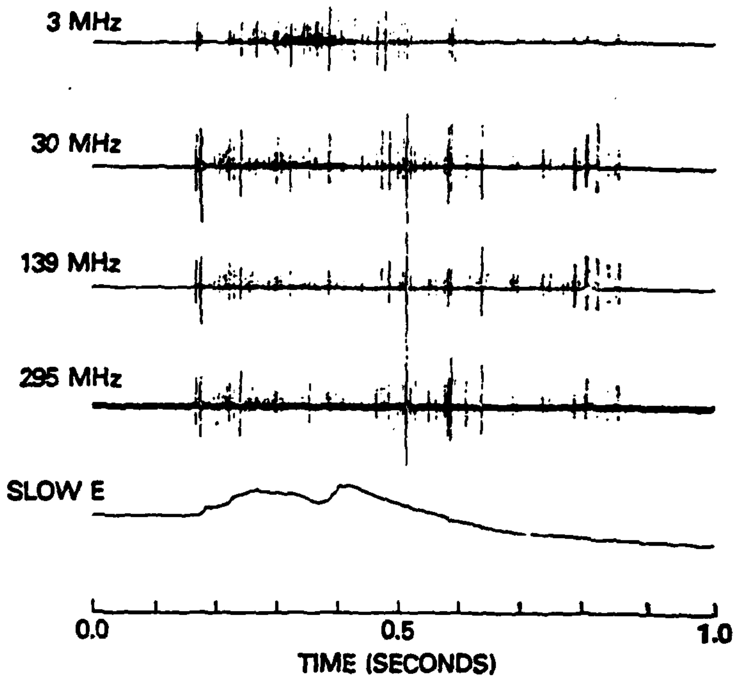
3 MHz
30 MHz
139 MHz
295 MHz
SLOW E
0.0
0.5
1.0
TIME (SECONDS)

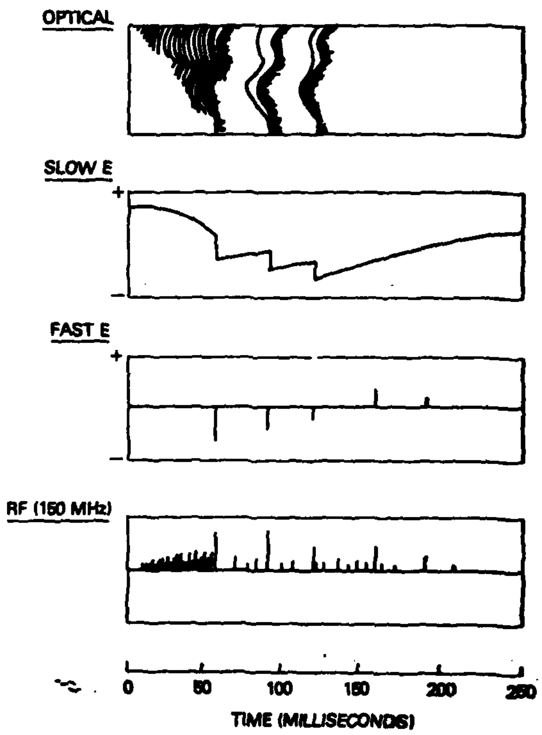
OPTICAL
SLOW E
FAST E
RF (150 MHz)
0
50
100
150
200
250
TIME (MILLISECONDS)

MAPPING USING RF RADIATION

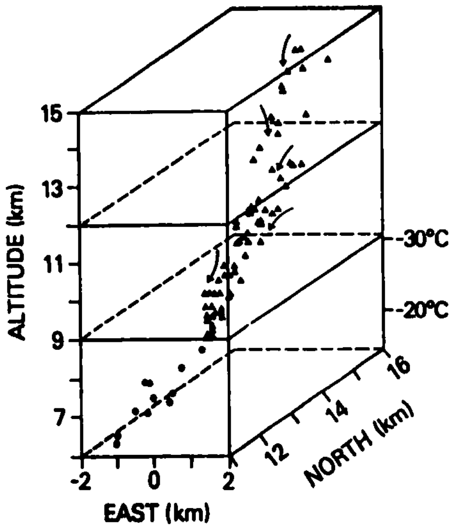

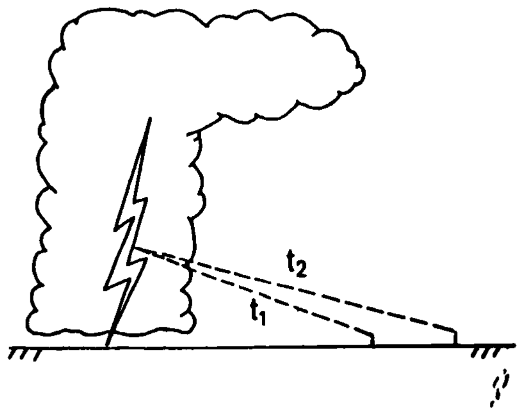

CURRENT WAVEFORMS

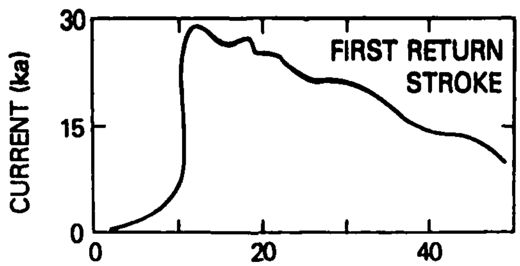

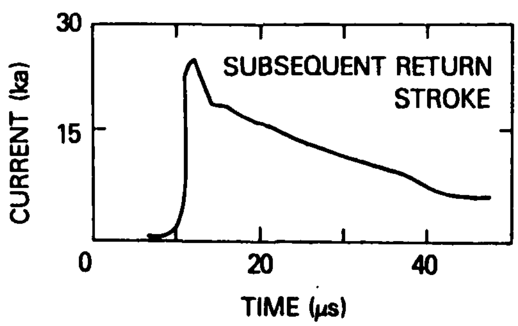

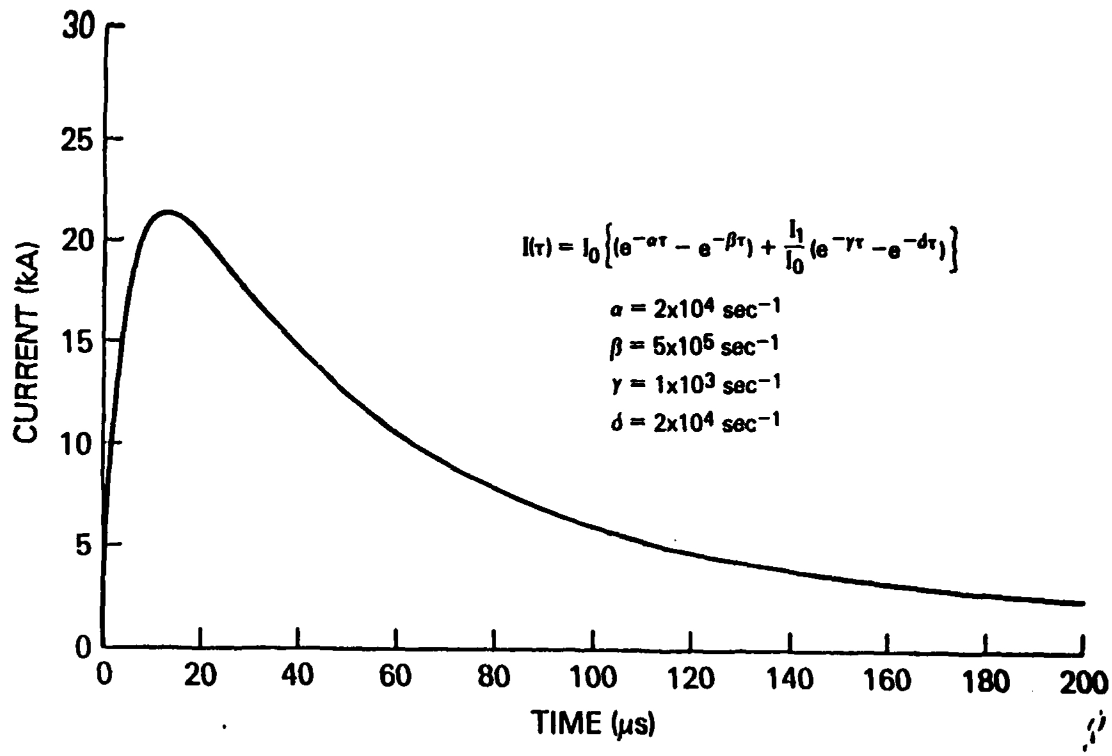

30
25
20
15
10
5
0
CURRENT (kA)
0
20
40
60
80
100
120
140
160
180
200
TIME (μs)
$I(\tau) = I_0 \left\{ (e^{-\alpha\tau} - e^{-\beta\tau}) + \frac{I_1}{I_0} (e^{-\gamma\tau} - e^{-\delta\tau}) \right\}$
$\alpha = 2x10^4$ sec^{-1}
$\beta = 5x10^5$ sec^{-1}
$\gamma = 1x10^3$ sec^{-1}
$\delta = 2x10^4$ sec^{-1}

FLIGHT EXPERIMENT DEFINITION AND SUMMARY

by

Mr. Felix Pitts

Langley Research Center
National Aeronautics and Space Administration

Description of NASA F-106B in-flight direct strike measurement program. Electromagnetic measurements, instrumentation concept, and results summary.

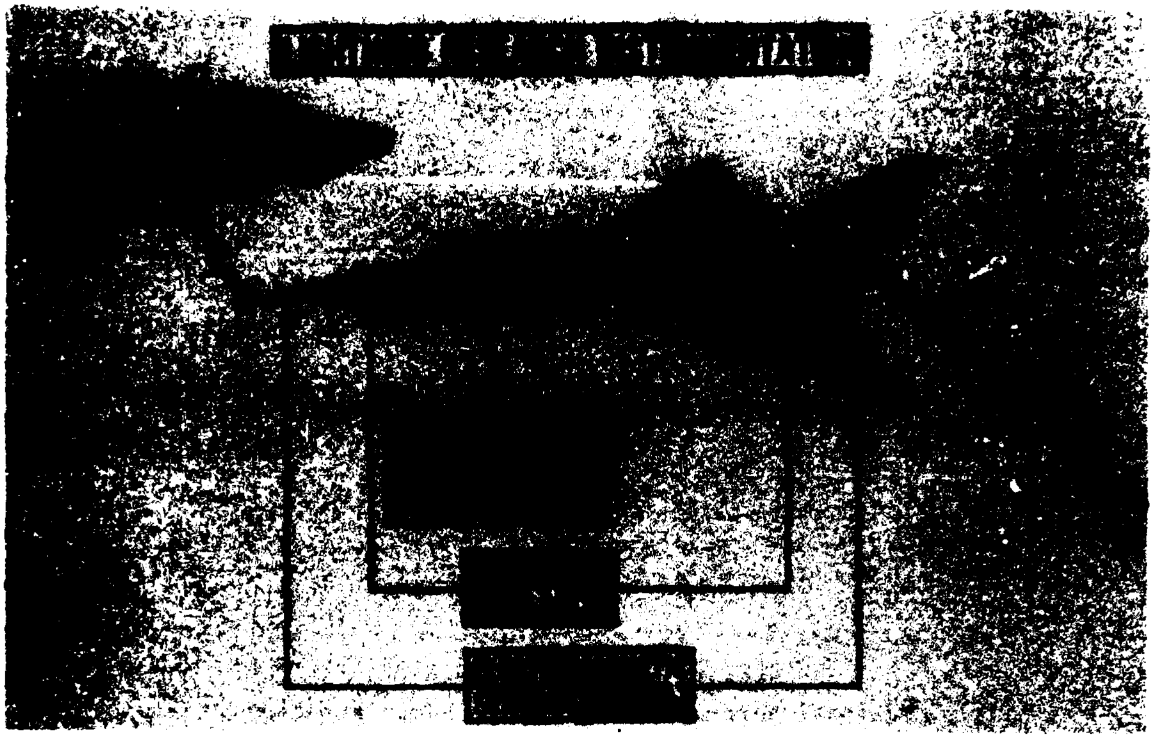

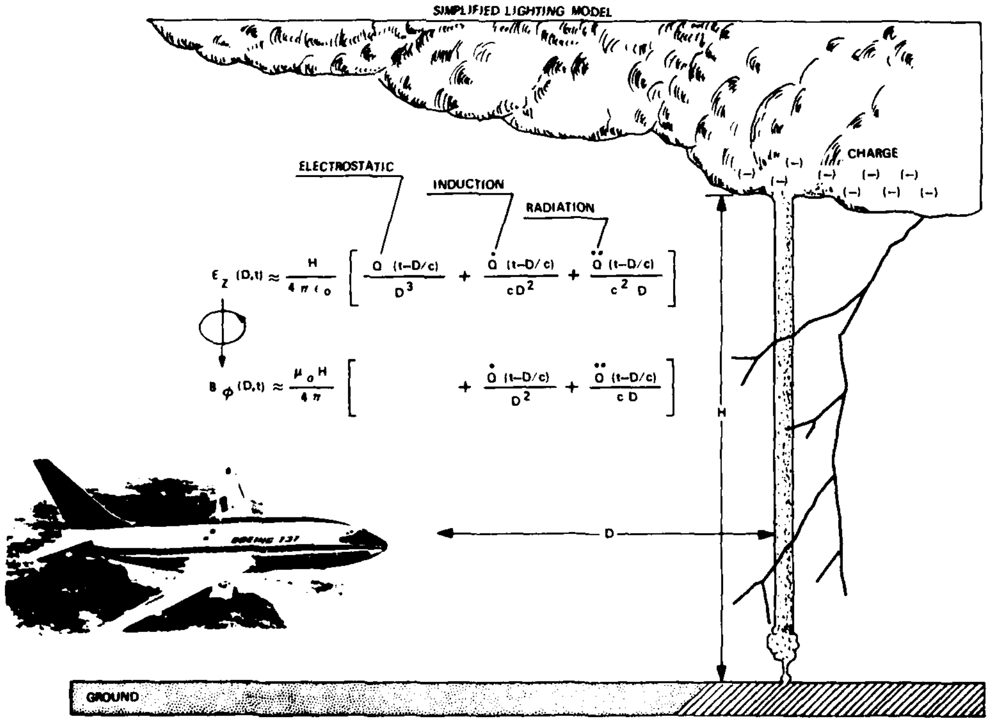

SIMPLIFIED LIGHTING MODEL
ELECTROSTATIC
INDUCTION
RADIATION
CHARGE
$E_z(D,t) \approx \frac{H}{4\pi\epsilon_o}\left[\frac{Q(t-D/c)}{D^3} + \frac{\dot{Q}(t-D/c)}{cD^2} + \frac{\ddot{Q}(t-D/c)}{c^2 D}\right]$
$B_\phi(D,t) \approx \frac{\mu_o H}{4\pi}\left[+ \frac{\dot{Q}(t-D/c)}{D^2} + \frac{\ddot{Q}(t-D/c)}{cD}\right]$
H
D
GROUND

MEASUREMENTS SUMMARY

MEASUREMENT	SYMBOL	AMPLITUDE RANGE	SENSOR TYPE
RATE OF CHANGE OF ELECTRIC FLUX DENSITY	$\dot{D}$	50 A/M^2	FLUSH PLATE DIPOLE
RATE OF CHANGE OF MAGNETIC FLUX DENSITY	$\dot{B}$	2×10^4 TESLA/SEC	MULTIGAP LOOP
RATE OF CHANGE OF CURRENT	$\dot{I}$	10^{11} A/SEC	INDUCTIVE CURRENT PROBE

MEASUREMENTS SUMMARY

MEASUREMENT	SYMBOL	DIMENSION	SENSOR TYPE
• RATE OF CHANGE OF ELECTRIC FLUX DENSITY	$\dot{D}$	A/M^2	FLUSH PLATE DIPOLE
• RATE OF CHANGE OF MAGNETIC FLUX DENSITY	$\dot{B}$	TESLA/SEC	MULTIGAP LOOP
• RATE OF CHANGE OF CURRENT	$\dot{I}$	A/SEC	INDUCTIVE CURRENT-PROBE
• ELECTRIC FIELD	E	V/M	FIELD MILL
• CURRENT	I	A	CURRENT TRANSFORMER

MEASUREMENT LOCATIONS - 1980

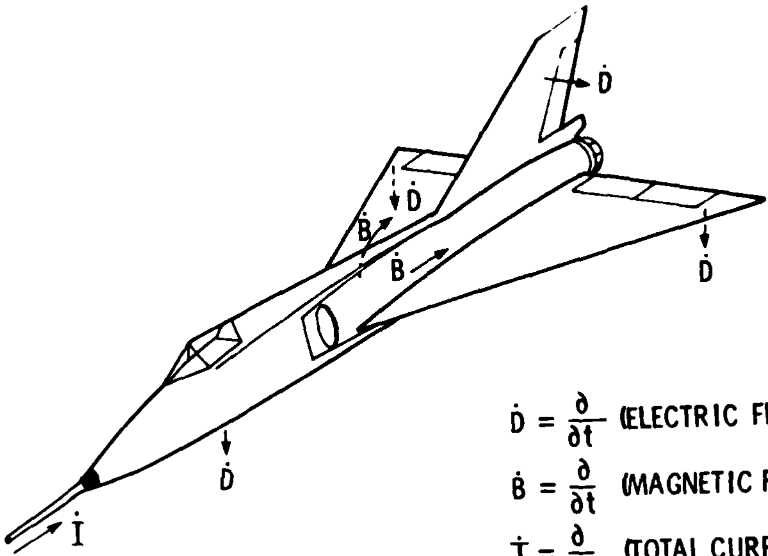

$\dot{D} = \frac{\partial}{\partial t}$ (ELECTRIC FLUX DENSITY)

$\dot{B} = \frac{\partial}{\partial t}$ (MAGNETIC FLUX DENSITY)

$\dot{I} = \frac{\partial}{\partial t}$ (TOTAL CURRENT)

1980 LIGHTNING OCCURRENCES

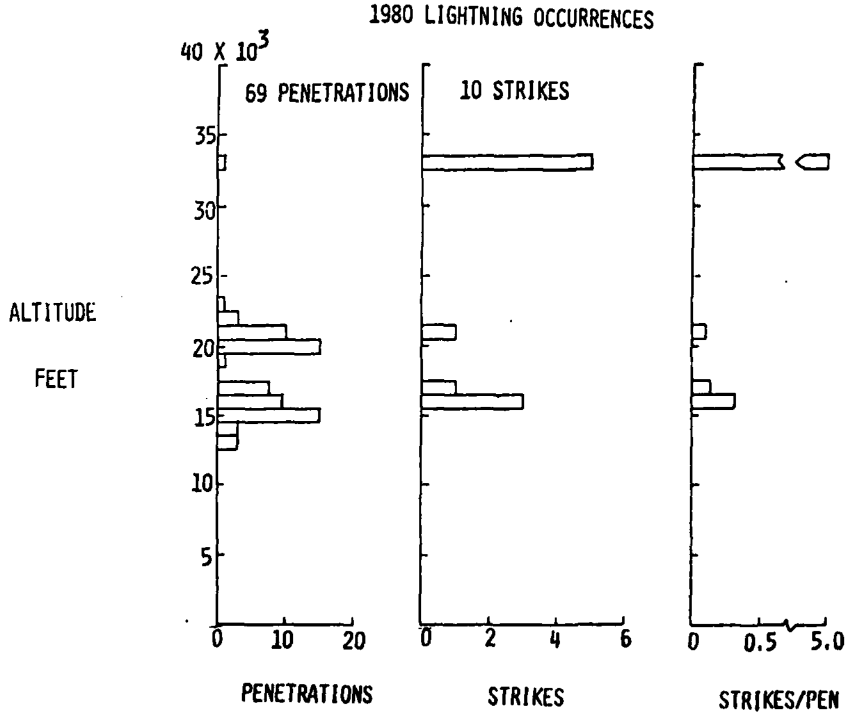

INSTRUMENTATION SYSTEM

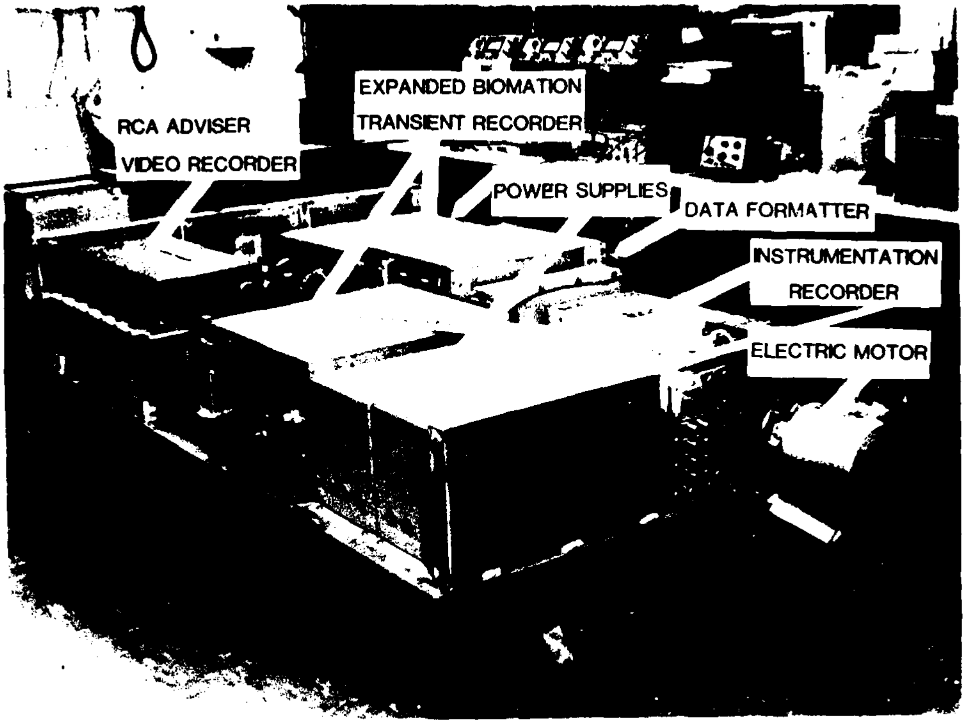

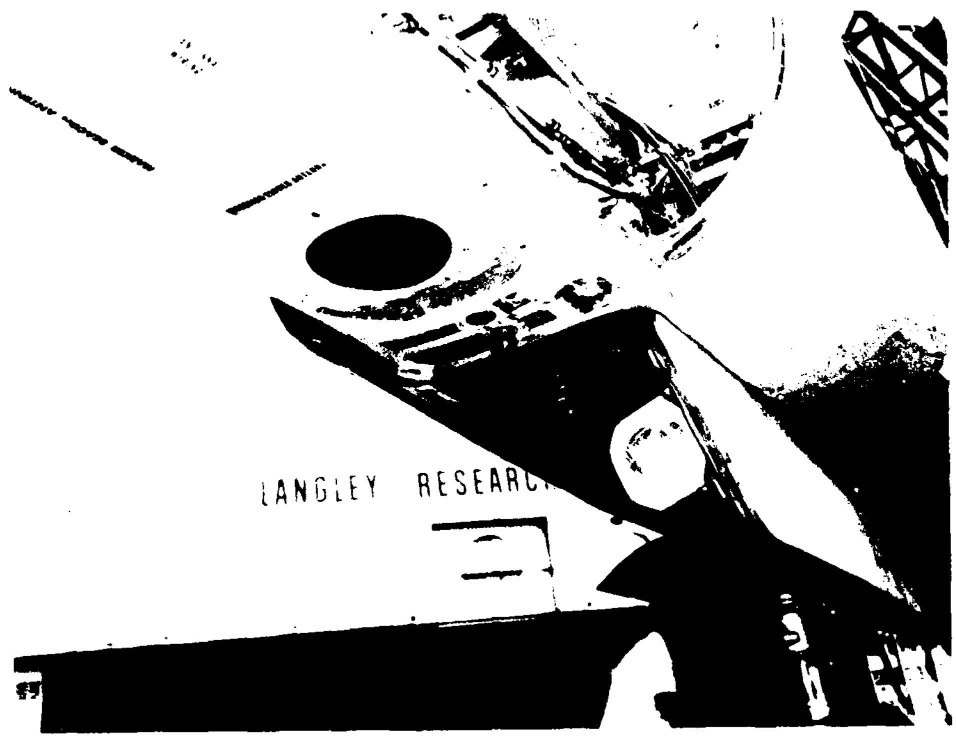

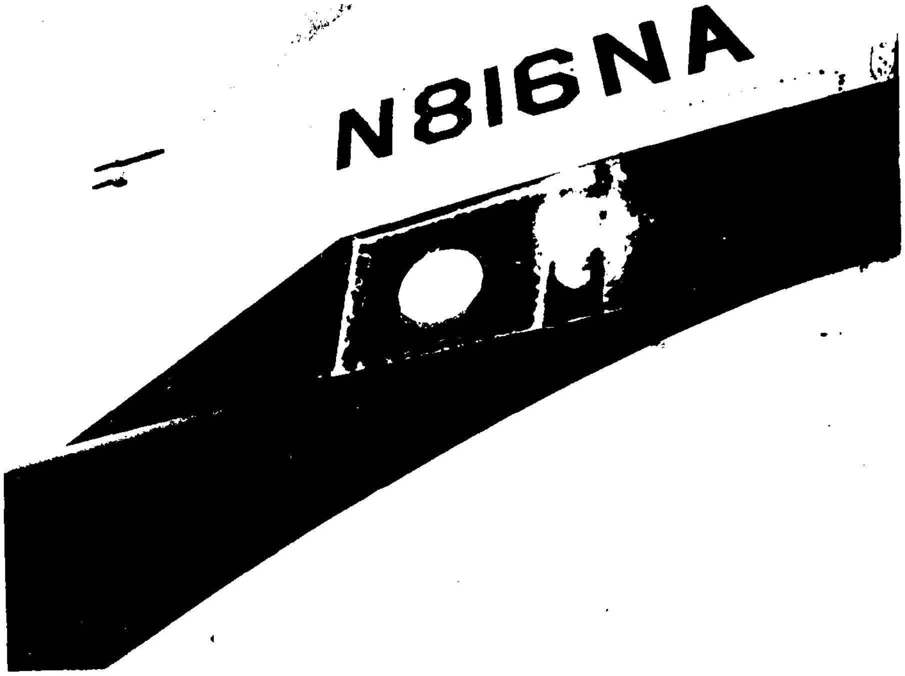
N816NA

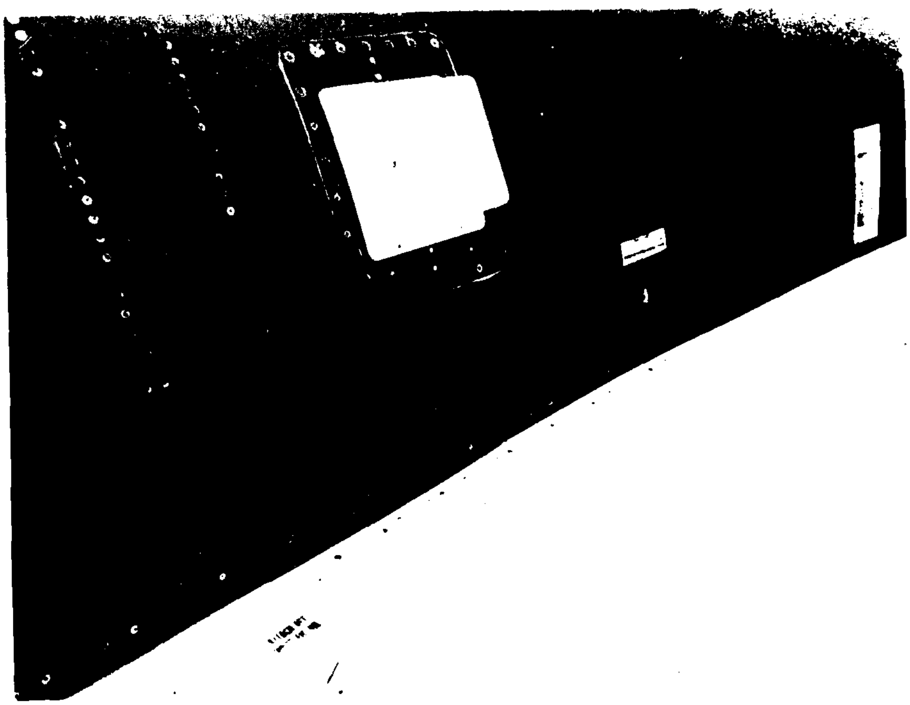

TYPICAL DIRECT STRIKE LIGHTNING RESULTS

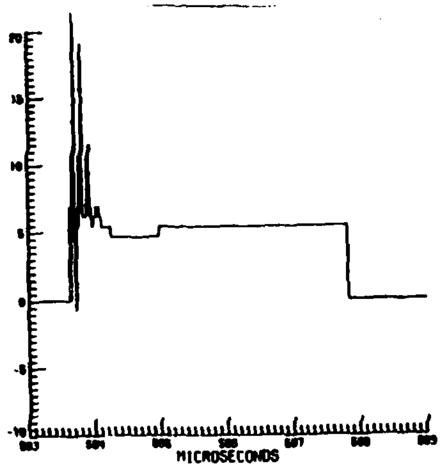

Fig. 10 D-dot sensor (flight #80-018).

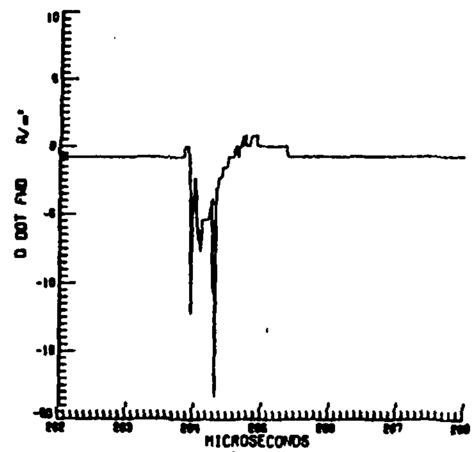

Fig. 11 D-dot sensor (flight #80-036).

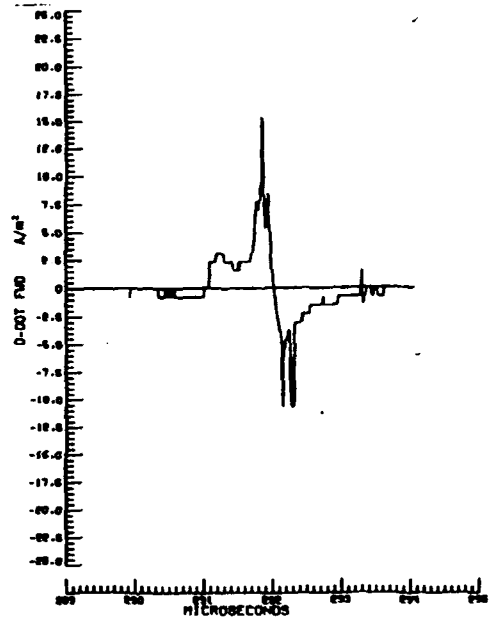

Fig. 12 D-dot sensor (flight #80-038).

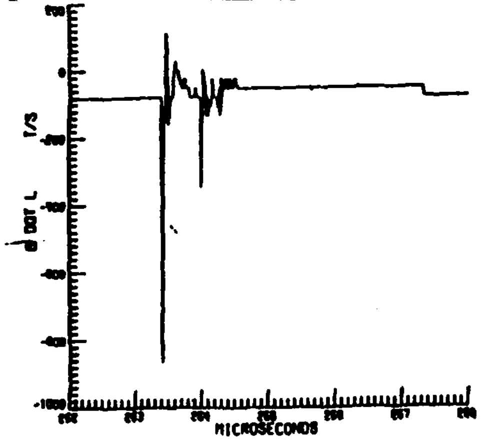

Fig. 13 B-dot sensor (flight #80-036).

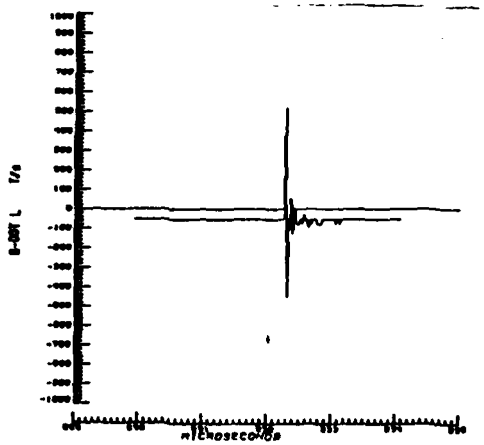

Fig. 14 B-dot sensor (flight #80-038).


Fig. 15 I-dot sensor (flight #80-038).

86%

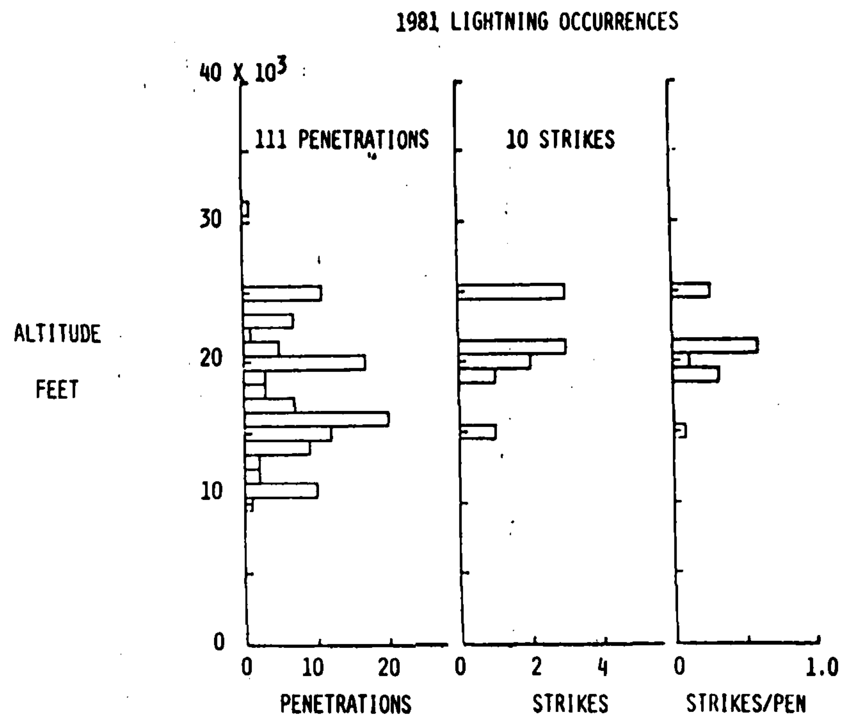

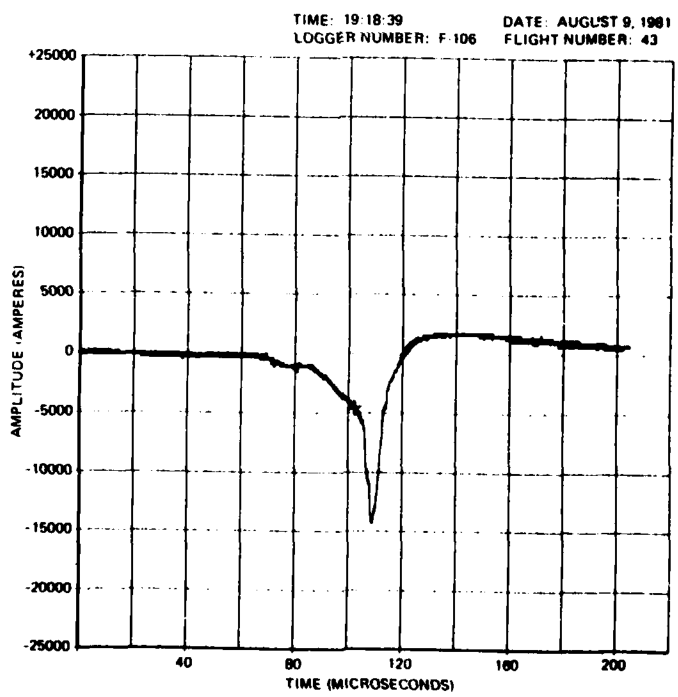

X - INDICATES TRIGGER POINT

DATA SUMMARY

- o 1980
  - 19 FLIGHTS 69 STORM PENETRATIONS
  - 10 STRIKES 17 TRANSIENTS: (7 $\dot{D}$, 5 $\dot{B}$, 5 I)
  - RESULTS REPORTED:
    NASA TM 81946 "1980 DIRECT STRIKE LIGHTNING DATA"
    AIAA 81-0083 "E/M MEASUREMENT OF DIRECT LIGHTNING STRIKES TO A/C"
- o 1981
  - 24 FLIGHTS 111 STORM PENETRATIONS
  - 10 STRIKES 27 TRANSIENTS
    1 BOOM CURRENT (BOEING)
    16 $\dot{B}$, 10 $\dot{D}$ (DISTANT)
- o MAXIMUM MEASURED VALUES

$\dot{D}$ 30.5 A/M² ⟶ 340 KV/0.1 μs
$\dot{B}$ 1160 T/s ⟶ 2 KA/0.1 μs
I 15 KA

OTHER F-106 LIGHTNING EXPERIMENTS

- ATMOSPHERIC CHEMISTRY EXPERIMENTS - LaRC
  1980 - SHOWED N_2O ENHANCEMENT NEAR LIGHTNING
  1981 - SHOWED CO ENHANCEMENT NEAR LIGHTNING
- X-RAY EXPERIMENT - U. WASHINGTON
  1980 - SHOWED INCREASED COUNT NEAR LIGHTNING
  1981 - BEING EVALUATED
- OPTICAL SIGNATURE EXPERIMENT - NSSL
  - PROTOTYPE FOR ORBITAL LIGHTNING MAPPER
  - RESULTS BEING ANALYZED AT NSSL
- STORM SCOPE
  - TURBULENCE/LIGHTNING DO NOT ALWAYS CORRELATE
  - LIGHTNING LOCATIONS DISPLAYED TEND TO BE FURTHER FROM AIRCRAFT POSITION THAN RADAR CONTOURS (BUT AT SAME BEARING)
- BOEING DATA LOGGER
  - FIRST BOOM CURRENT RECORDED AUGUST 1981

DATA SYSTEM DESCRIPTION

by

Mr. Mitchel E. Thomas

Langley Research Center
National Aeronautics and Space Administration

The research data-gathering system on the F-106B aircraft developed for in-flight measurement of direct and nearby lightning strike characteristics is described. Details of the design and performance are presented for system components including the digital transient recorders, wideband analog recorder, fiber optic control and diagnostic links, power system isolation, and system shielding.

LIGHTNING INSTRUMENTATION SYSTEM

- WIDE BANDWIDTH FOR SUBMICROSECOND SIGNAL RESOLUTION
  - 10 NS SAMPLE INTERVAL
- CONTINUOUS RECORDS FOR DEFINITION OF FULL LIGHTNING SCENARIO
  - 15 MHz ANALOG BANDWIDTH
- PROTECT AGAINST SPURIOUS RESPONSES (EMI)
  - SHIELDED ENCLOSURE
  - MOTOR-GENERATOR POWER ISOLATION
  - FIBER OPTIC CONTROL
- AUTOMATIC OPERATION

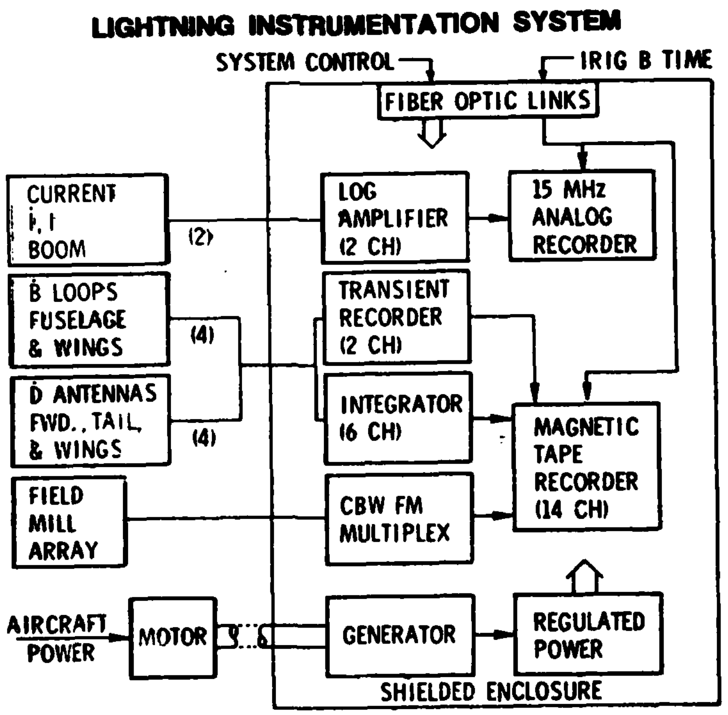

INSTRUMENTATION SYSTEM

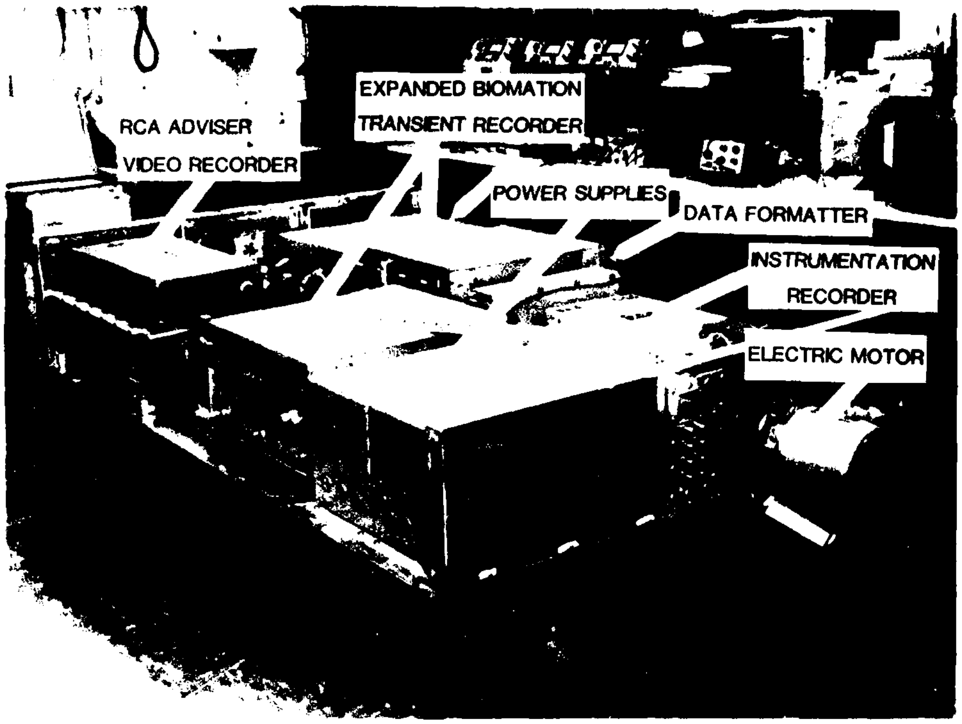

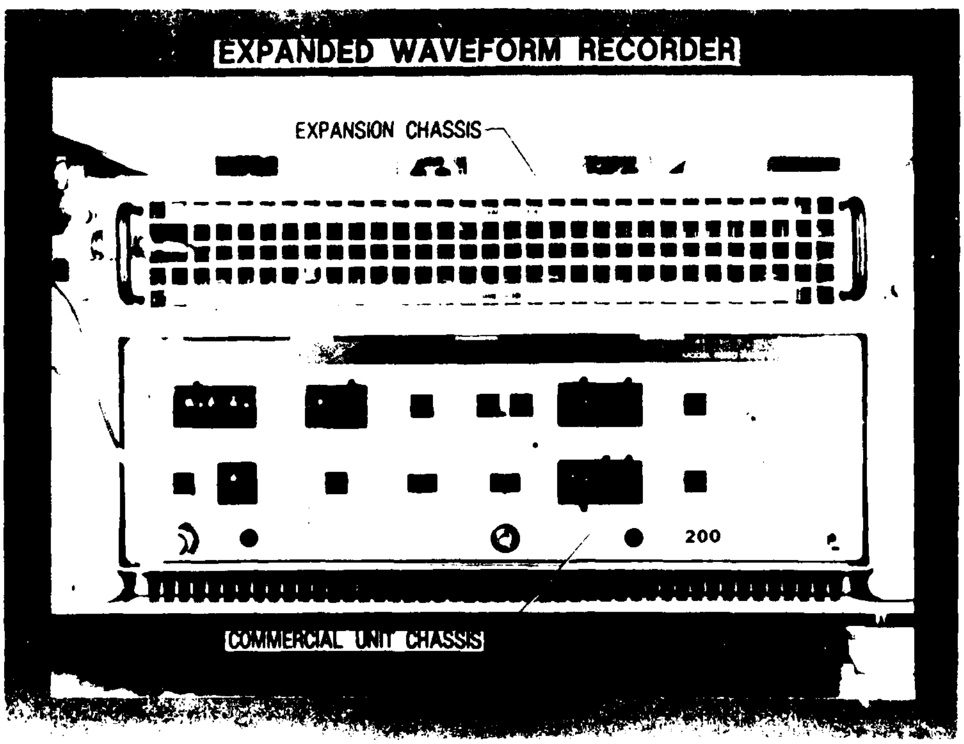

TRANSIENT RECORDER

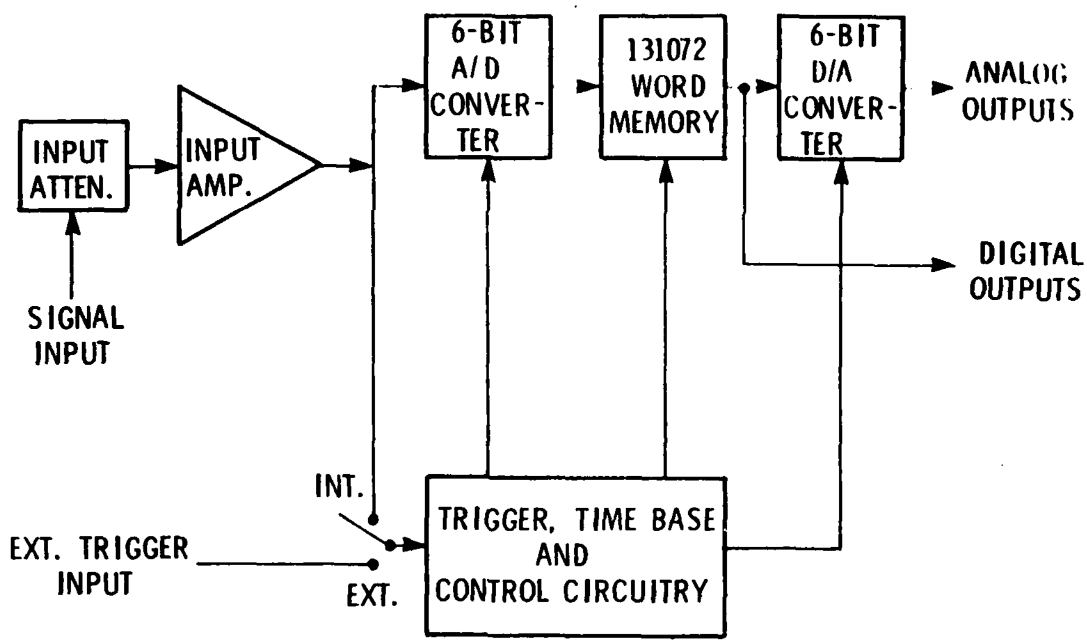

EXPANDED TRANSIENT WAVEFORM RECORDER FEATURES

- 6-BIT AMPLITUDE RESOLUTION (1.56%)
- FREQUENCY RESPONSE - DC TO 50 MHz
- 131072 (2^{17}) DATA WORD CAPACITY
- SAMPLE RATES UP TO 100 MHz
- DATA WINDOW LENGTH OF 1310 MICROSECONDS AT 100 MHz
- INTERNAL OR EXTERNAL TRIGGERING
- DATA WINDOW SELECTION WHICH IS BEFORE, DURING, OR AFTER TRIGGER EVENT

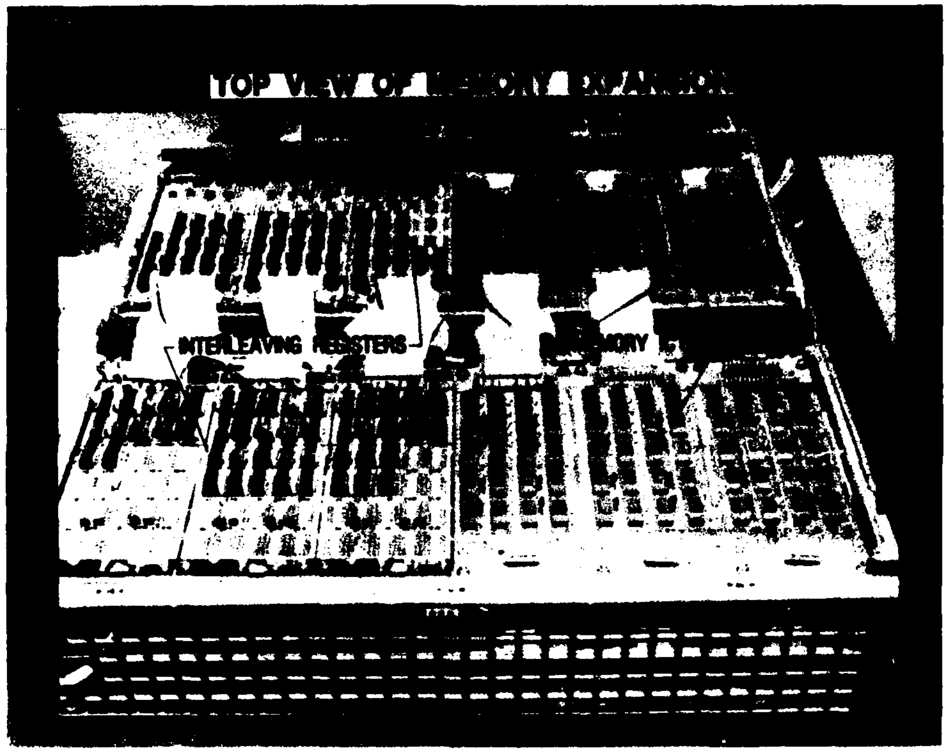
TOP
INTERLEAVING REGISTERS

- VIDEO RECORD TECHNIQUES
- FREQUENCY MODULATED CARRIER
- 10 Hz TO 15 MHz BANDWIDTH
- 12 MINUTES RECORD TIME
- 2 CHANNELS & 2 AUXILIARY

LOGARITHMIC AMPLIFIER

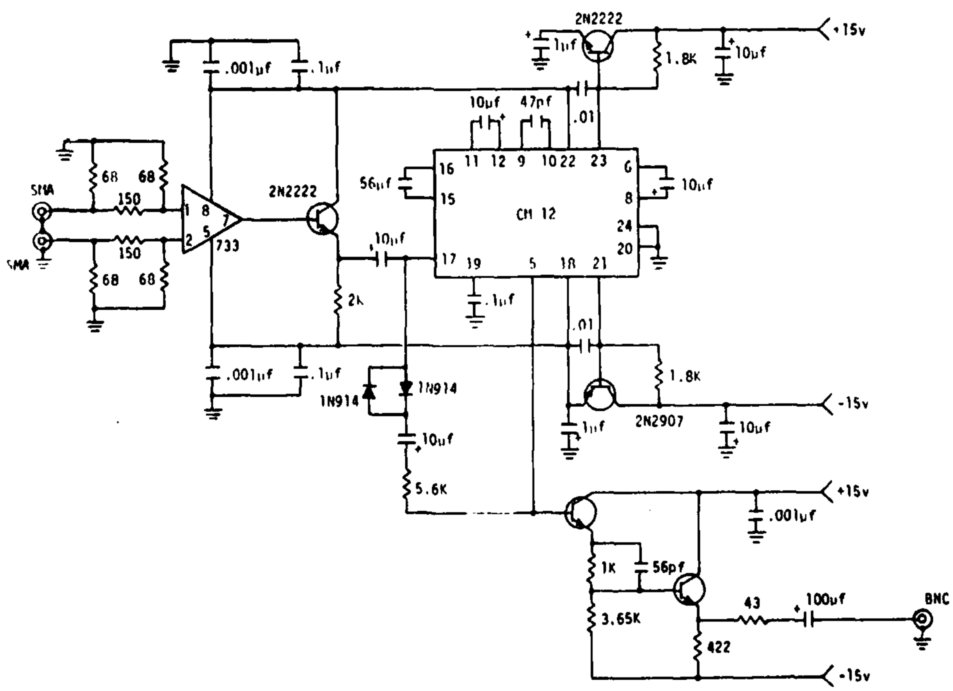

COMPRESSION AMPLIFIER

- 15 MHz BANDWIDTH
- DIFFERENTIAL INPUT, 50 OHM IMPEDANCE
- $E_0 = 1 + .3 \log E_{IN}$
- 60 dB DYNAMIC RANGE

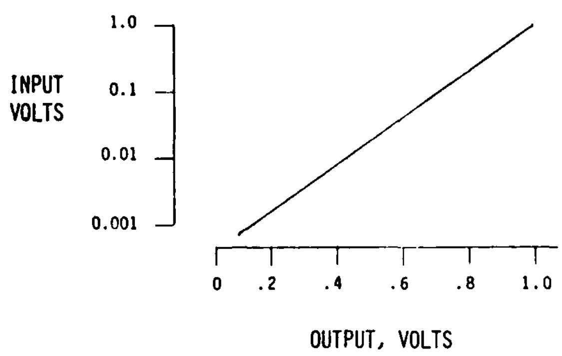

SIMPLIFIED SHIELDING TOPOLOGY

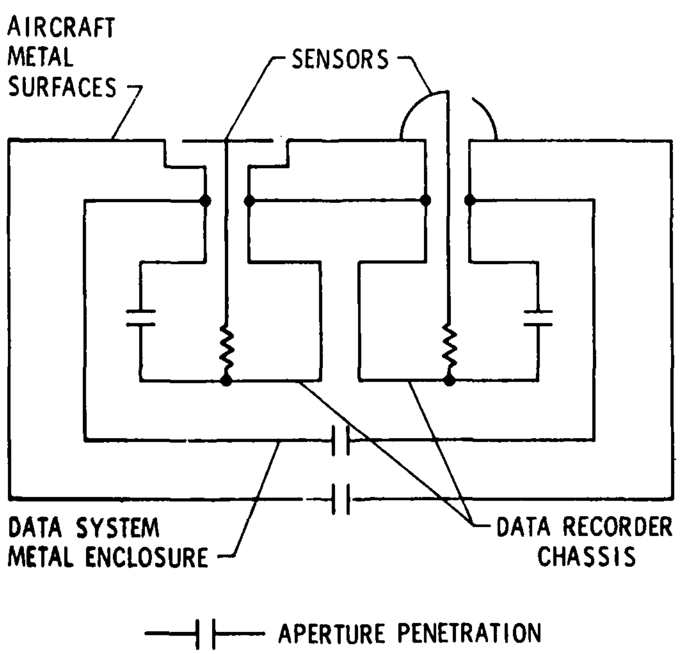

LIGHTNING INSTRUMENTATION CONTROL

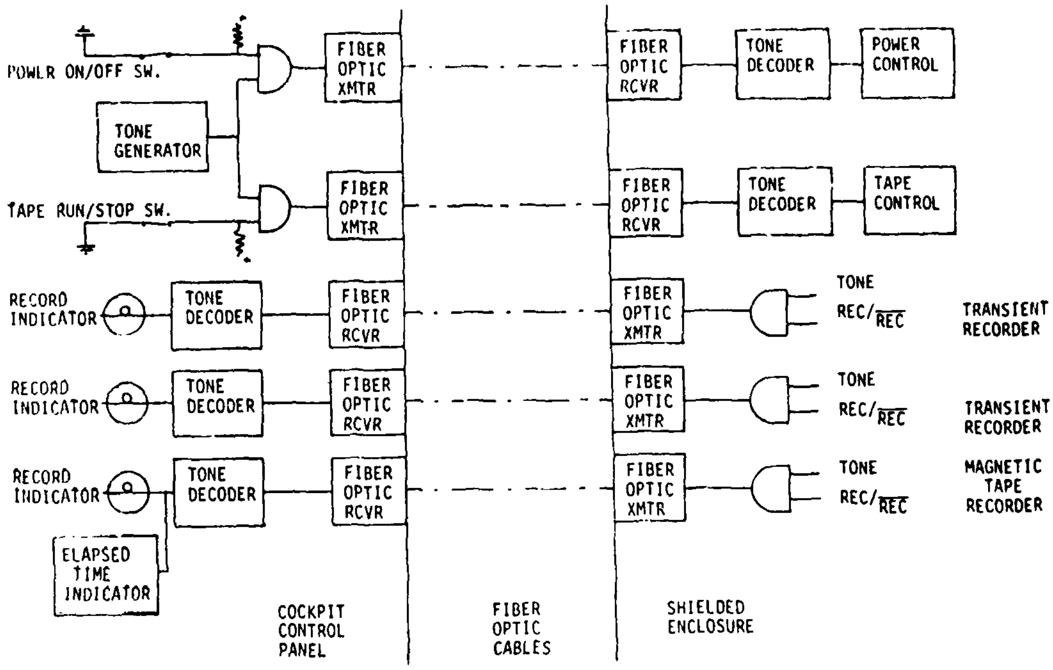

I-DOT SENSOR RESPONSE

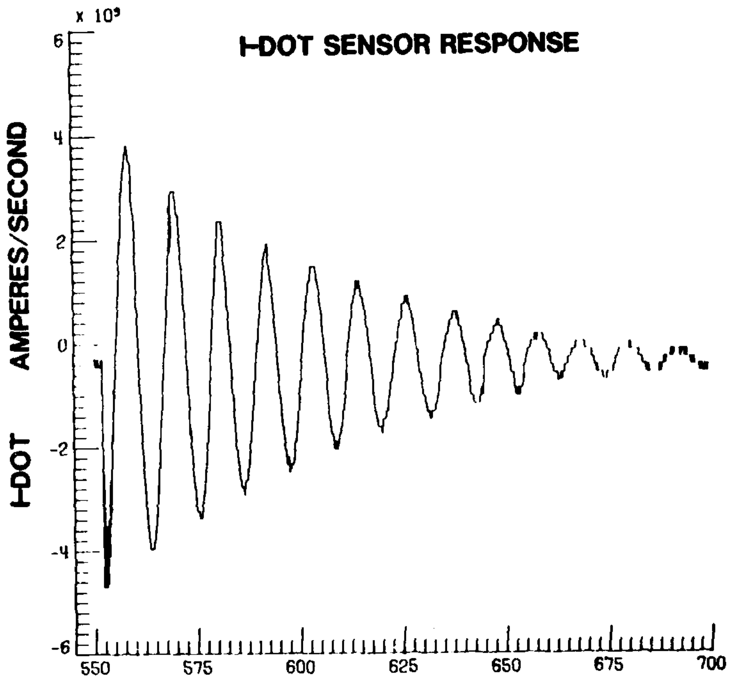

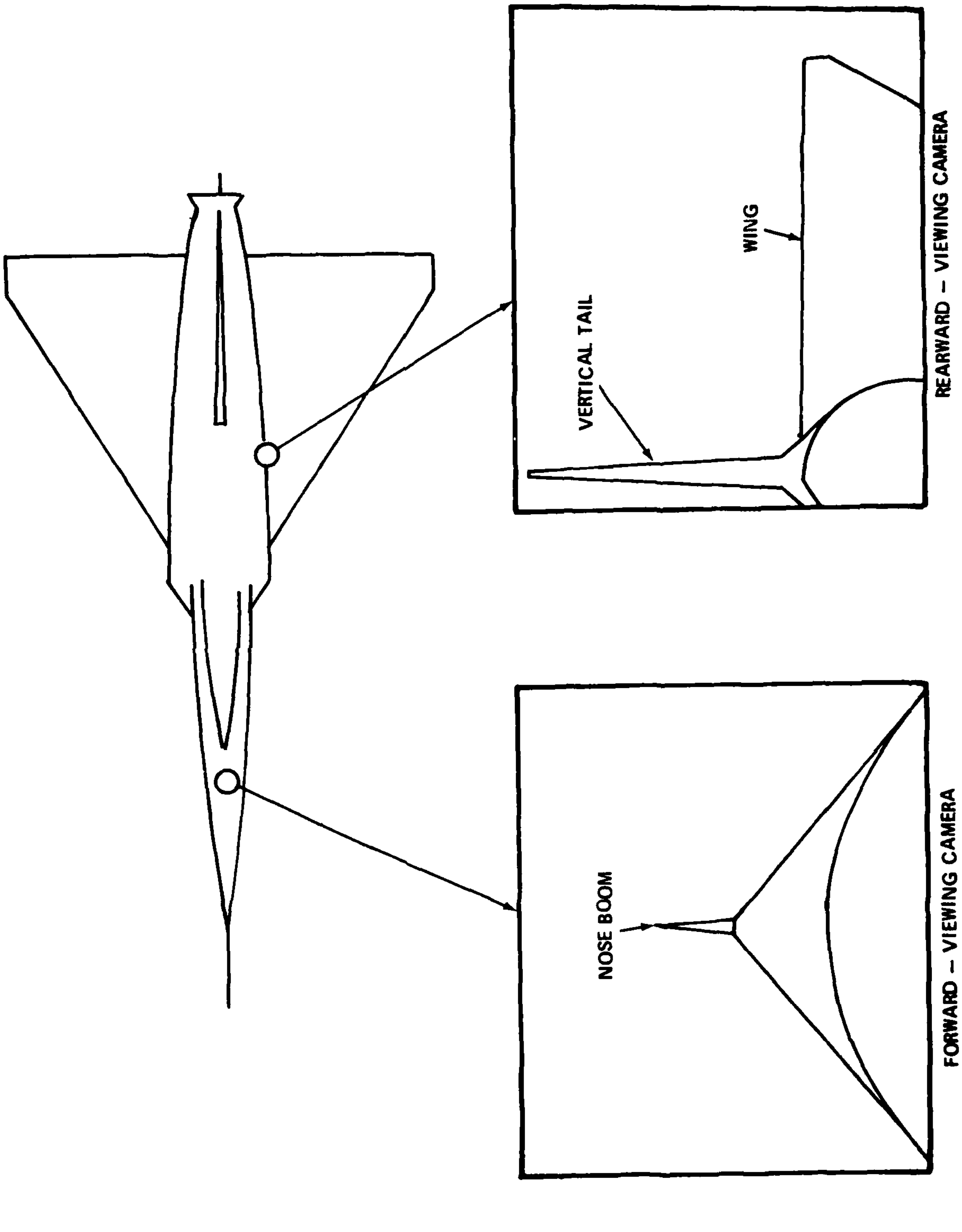
VERTICAL TAIL
WING
REARWARD – VIEWING CAMERA
NOSE BOOM
FORWARD – VIEWING CAMERA

ELECTROMAGNETIC SENSORS FOR AIRCRAFT LIGHTNING RESEARCH

by

Mr. Klaus P. Zaepfel

Langley Research Center
National Aeronautics and Space Administration

Electromagnetic sensors designed for measuring EM fields and currents during lightning strikes to the F-106B research aircraft are described. Sensor theoretical basis, performance, and parallel-plate transmission line used to check and calibrate these sensors are described.

MEASUREMENT REQUIREMENTS

MEASUREMENT	FIELD CHANGE	SENSOR OUTPUT
J_T	$50A/m^2$ ($\Delta E \approx 6 \times 10^5 \frac{V}{m}$ per $0.1\mu s$)	> 100V
$\dot{B}$	2×10^4 Tesla/s	> 100V
$\dot{I}$	10kA per $0.1\mu s$	> 100V

SENSOR CHARACTERISTICS

- DESIGN PRINCIPLES DEVELOPED BY AIR FORCE WEAPONS LAB FOR NEMP
- WIDE BANDWIDTH: $\geq$80 MHz ($t_R \leq 4.4$ ns)
- SIMPLE GEOMETRY: CALIBRATION BY RULER
- APPROXIMATELY 100 V OUTPUT FOR FULL-SCALE DIRECT STRIKE

DEFINITIONS: ELECTRIC FIELDS

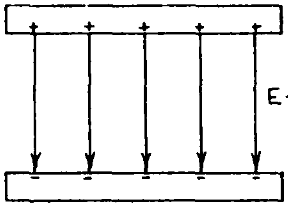

E-FIELD, V/m
(Electric Field Intensity)

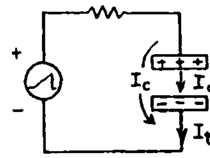

No Corona, $I_t = \dot{D}\cdot\text{Area}$

In Corona, $I_t = (J_c + \dot{D})\text{Area} = J_t\text{Area}$

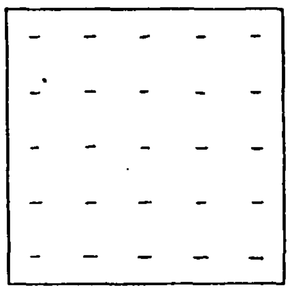

D, C/m^2
(Electric Flux Density)

ρ_s, C/m^2
(Surface Charge Density)

For flat plate, $D = \rho_s$

$D = \epsilon E$ where ϵ is permittivity of dielectric

SENSOR FUNDAMENTALS

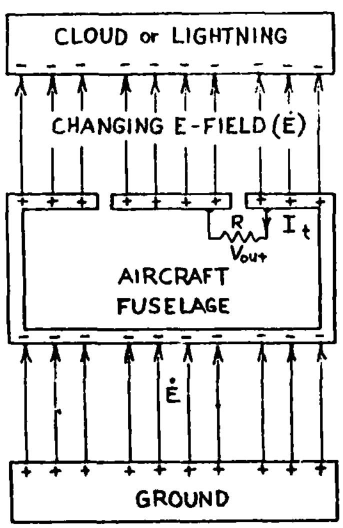

NO CORONA	CORONA
$\dot{D} = \epsilon\dot{E}$	
$I_t = I_d = \dot{D}\cdot\text{AREA}$	$I_t = (J_c + \dot{D})\,\text{AREA}$

$V_{OUT} = R\,I_t$

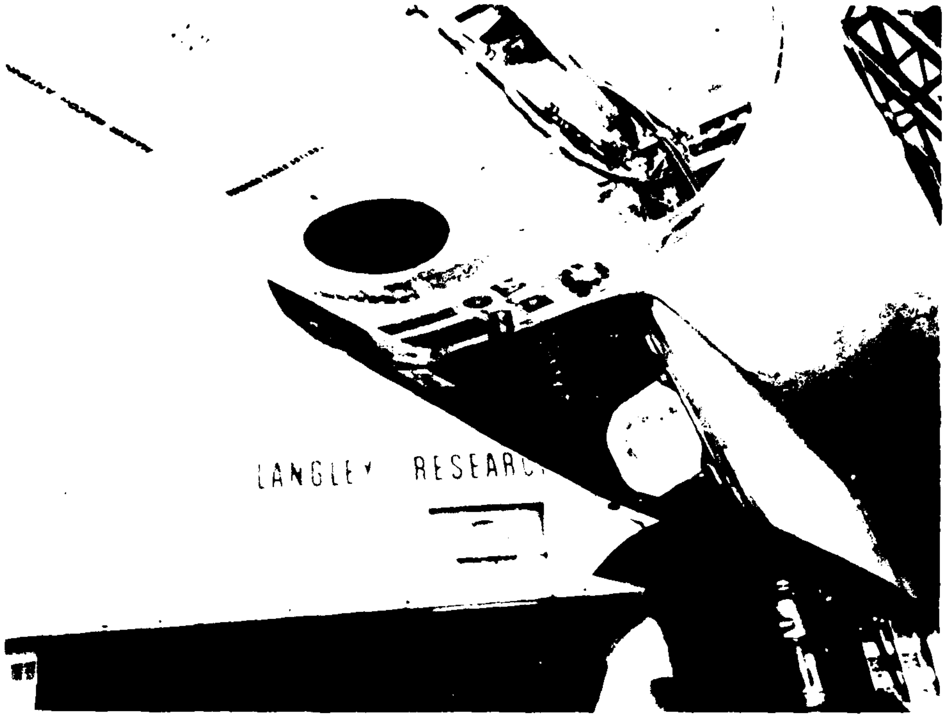
LANGLEY RESEARC

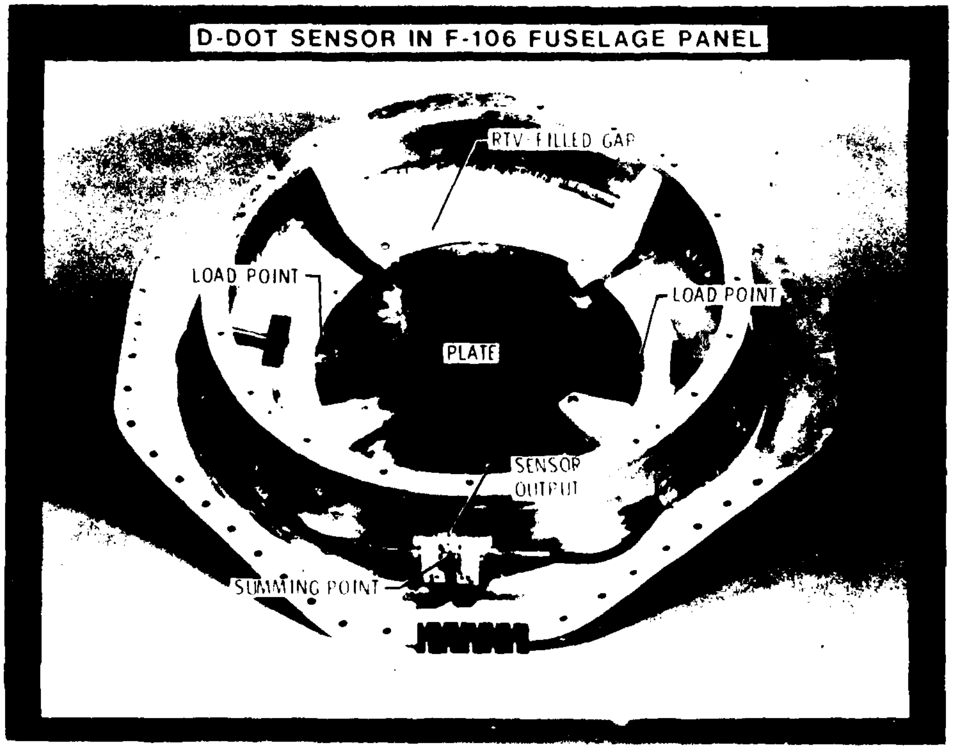
D-DOT SENSOR IN F-106 FUSELAGE PANEL
RTV-FILLED GAP
LOAD POINT
LOAD POINT
PLATE
SENSOR
OUTPUT
SUMMING POINT

J_T SENSOR

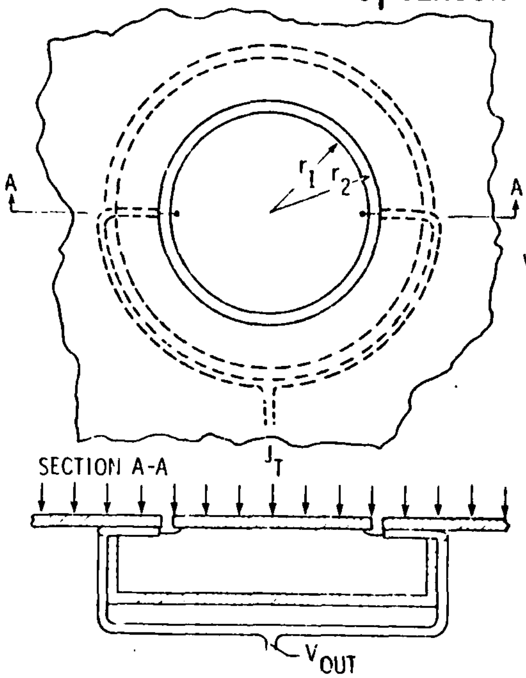

$t_r = 2.2\ RC,\ R = 50\Omega$

$t_{rt} = t_r$ + PROPAGATION TIME

$$V_{out} = A_J J_T R$$

$$= A_J(\dot{D} + J)R$$

$$A_J = \pi r^2,\ r^2 = r_1 r_2$$

DEFINITION: MAGNETIC FIELDS

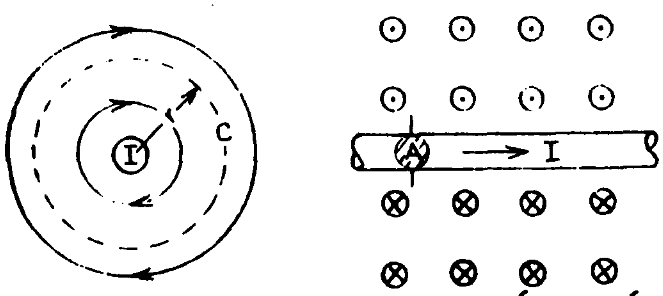

MAXWELL-AMPERE LAW: $\oint_C H \cdot dl = \int_A J \cdot dA$ $\qquad H = \frac{B}{\mu}$

$$\frac{B}{\mu} 2\pi r = I$$

$$B = \frac{\mu}{2\pi r} I$$

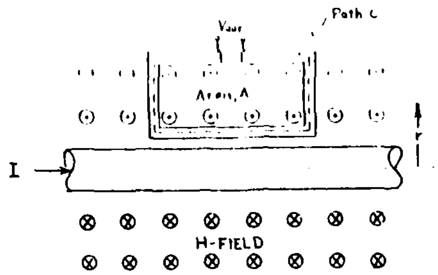

$$B = \frac{\mu}{2\pi r} I$$

MAXWELL-FARADAY LAW: $\oint_c E \cdot dl = -\int_A \frac{dB}{dt} \cdot dA$

$V_{OUT} = -\int_A \frac{dB}{dt} \cdot dA$ B-DOT Sensor

$= -\int_A \left(\frac{\mu}{2\pi r} \cdot \frac{dI}{dt}\right) dA$

$= -\frac{dI}{dt} \int_A \frac{\mu}{2\pi r} dA$

$V_{OUT} = -M\dot{I}$, $M = \frac{\mu}{2\pi} \int_A \frac{1}{r} dA$ I-DOT Sensor

B-DOT SENSOR

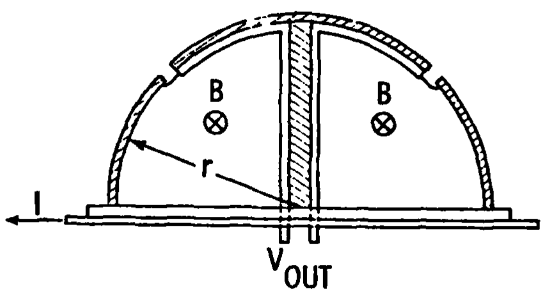

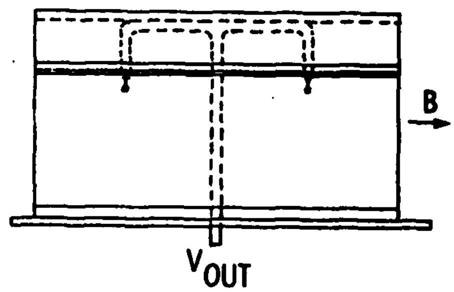

$t_r = 2.2 \frac{L}{R}$, $R = 100\Omega$

$V_{out} = A_B \dot{B}$

$A_B \approx \frac{1}{2} \pi r^2$

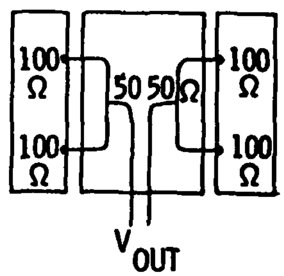

B DOT SENSOR ON F 106 FUSELAGE PANEL

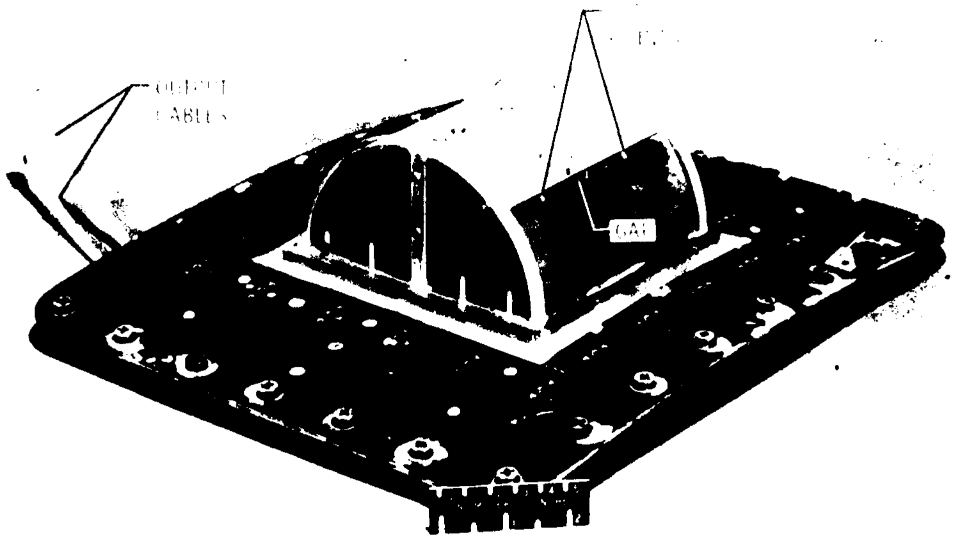

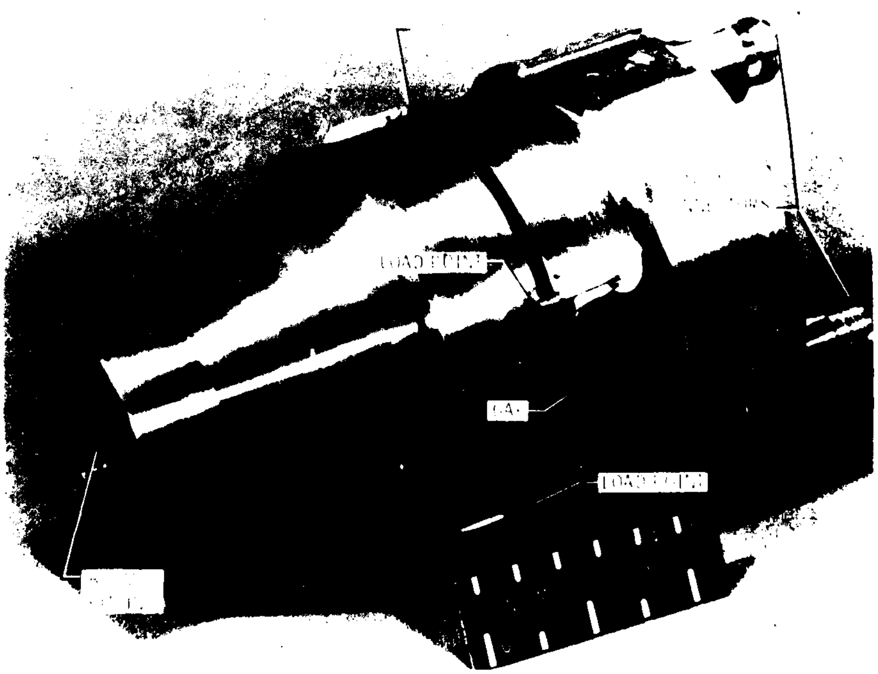

I-DOT SENSOR

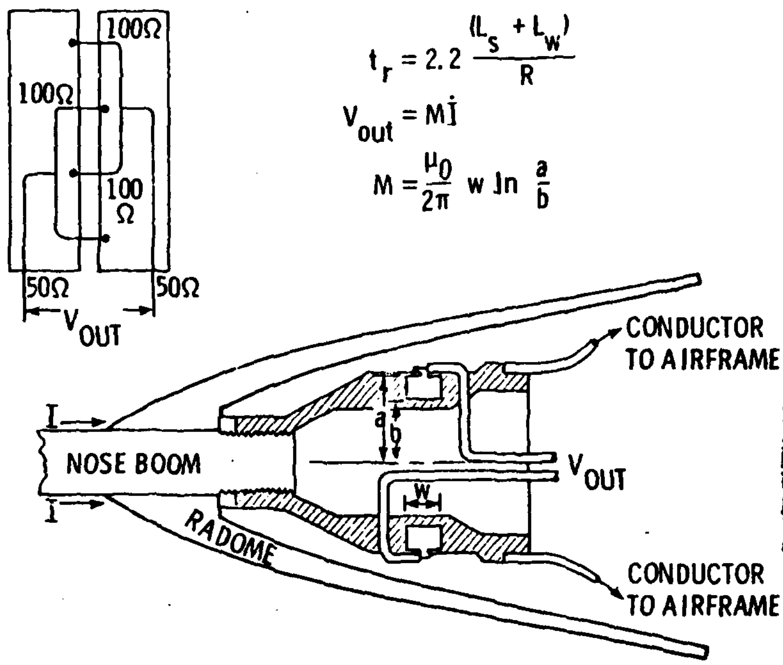

FLAT-PLATE TRANSMISSION LINE CALIBRATOR

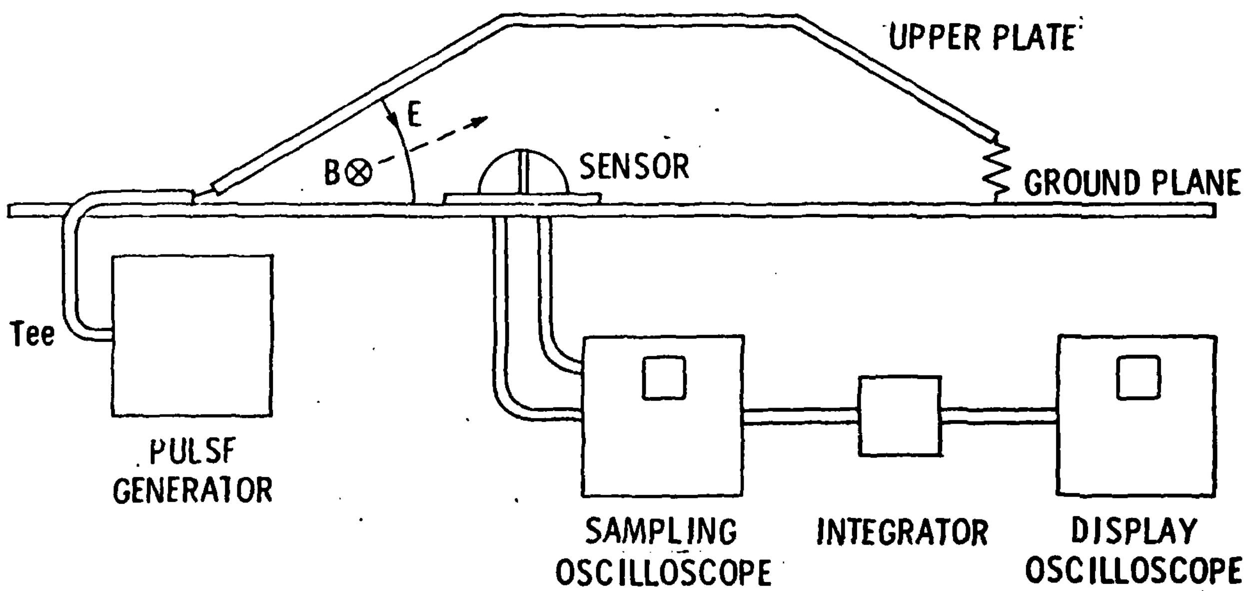

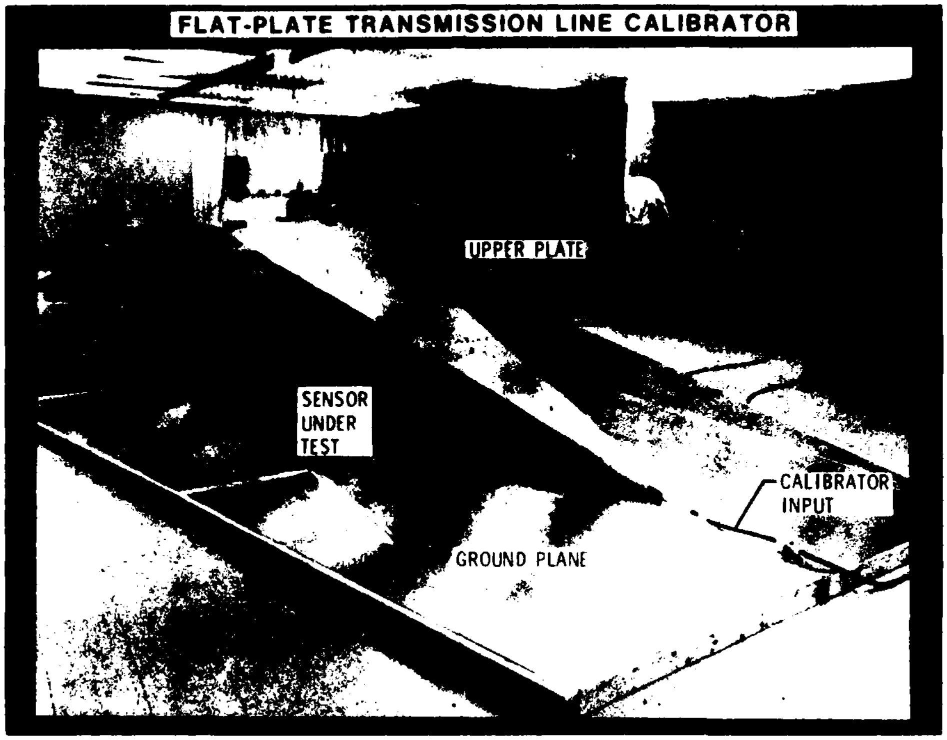
FLAT-PLATE TRANSMISSION LINE CALIBRATOR
UPPER PLATE
SENSOR
UNDER
TEST
CALIBRATOR
INPUT
GROUND PLANE

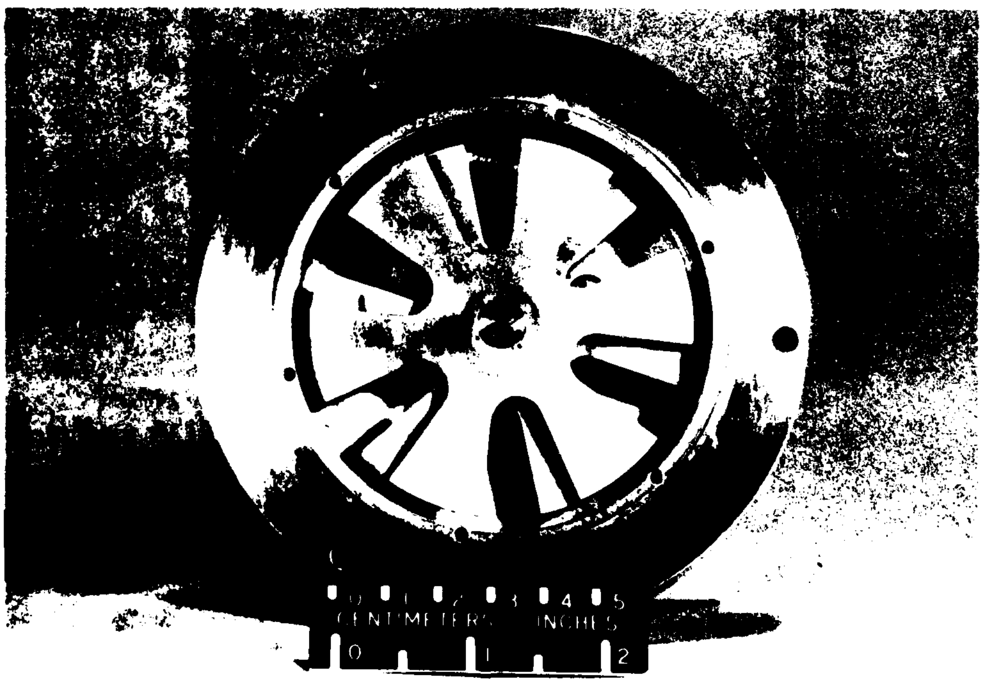
CENTIMETERS
INCHES

B-DOT SENSOR DIFFERENTIAL AND INTEGRATED OUTPUTS

a: 200m V/div.

b: 1.4×10^{-10} V - s/div.

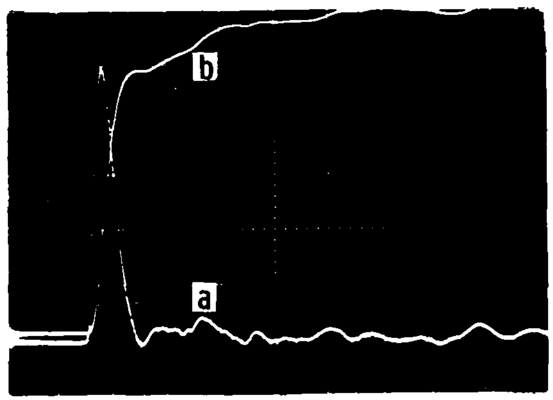

2ns/div.

STEP RESPONSE

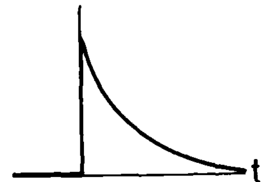

$$v(t) = \frac{RA_B B_0}{L} e^{\frac{-Rt}{L}} u(t)$$

INTEGRATED STEP RESPONSE

$$\int_{-\infty}^{t} v(t')dt'$$

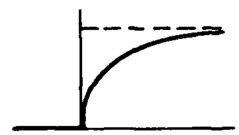

SUMMARY OF SENSOR PARAMETERS

SENSOR	LOCATION	DESIGN	SENSITIVITY	RISETIME (10%-90%)
J_T	FUSELAGE/TAIL	CIRCULAR	$4.1\times10^{-2}m^2$	2.4 ns
J_T	WINGS	RECTANGULAR	$2.7\times10^{-2}m^2$	3.0 ns
B-DOT	FUSELAGE	2 GAPS, 4 LOAD POINTS	$5.7\times10^{-3}m^2$	.85 ns
B-DOT	WINGS	1 GAP, 1 LOAD POINT	$5.5\times10^{-3}m^2$	2.0 ns
I-DOT	RADOME	1 GAP, 4 LOAD POINTS	$2.1\times10^{-9}H$	0.8 ns

FIELD MILLS

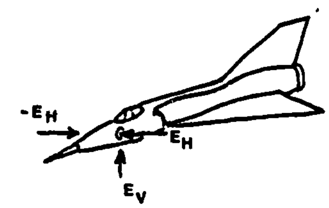

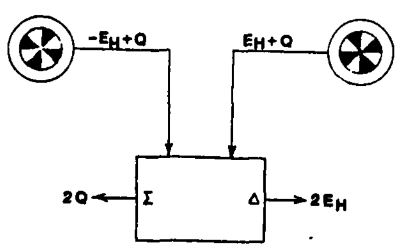

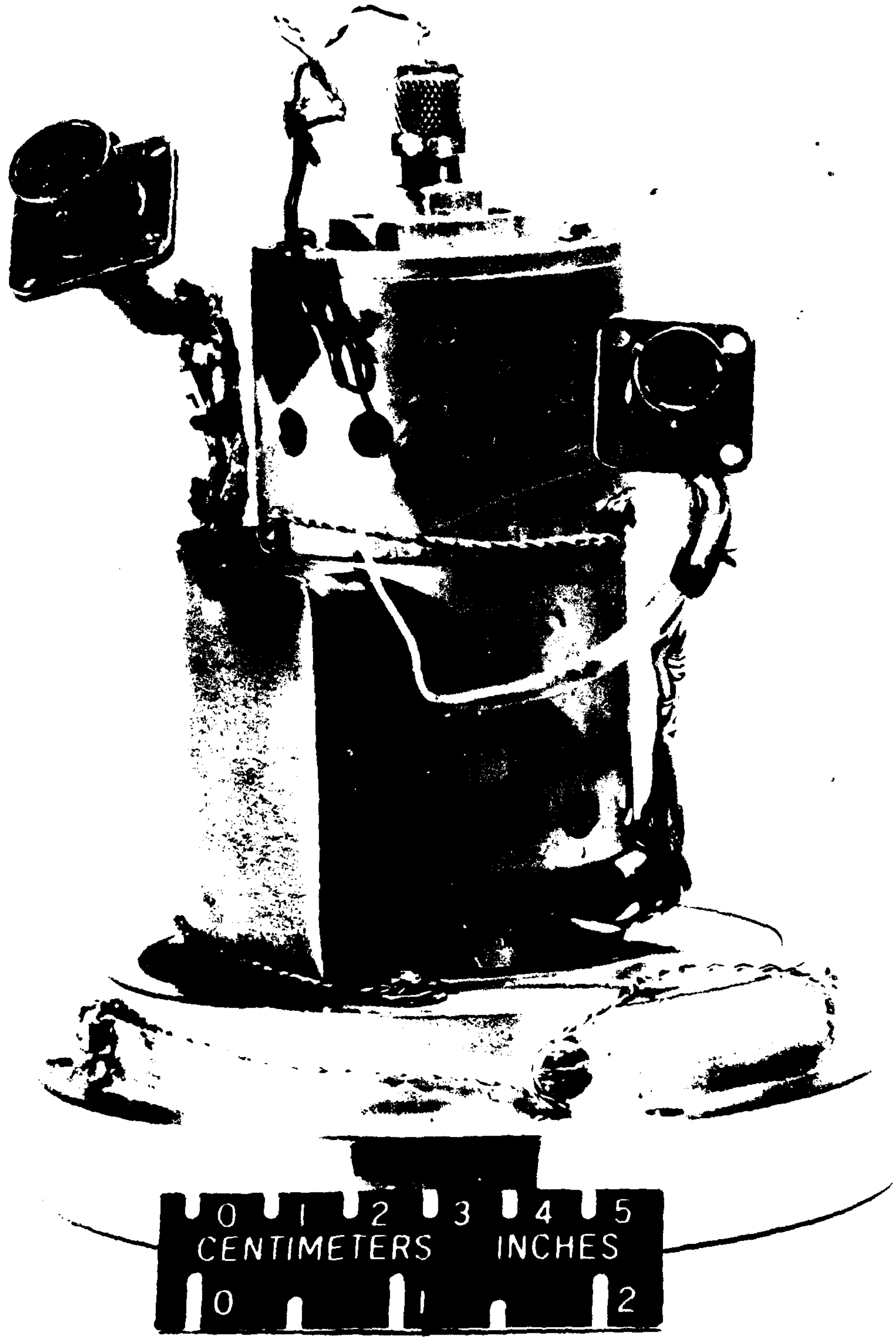
0 1 2 3 4 5
CENTIMETERS INCHES
0 1 2

LIGHTNING MODELING

by

Dr. M. LeVine

Goddard Space Flight Center
National Aeronautics and Space Administration

The ground-based lightning measurements made at Wallops Flight Center concurrently with the in-flight direct strike measurements are described. Lightning mathematical model development to arrive at credible lightning models for use in induced effects electromagnetic coupling studies is discussed.

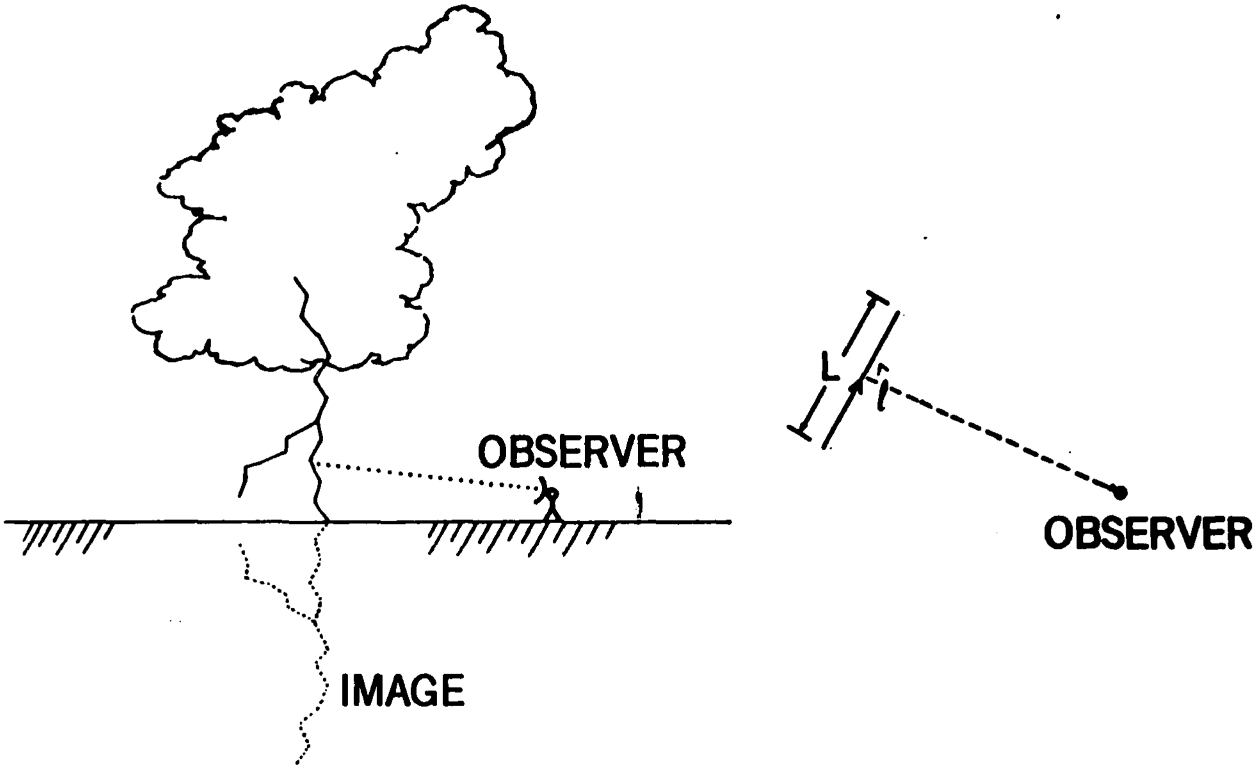

CHANNEL GEOMETRY

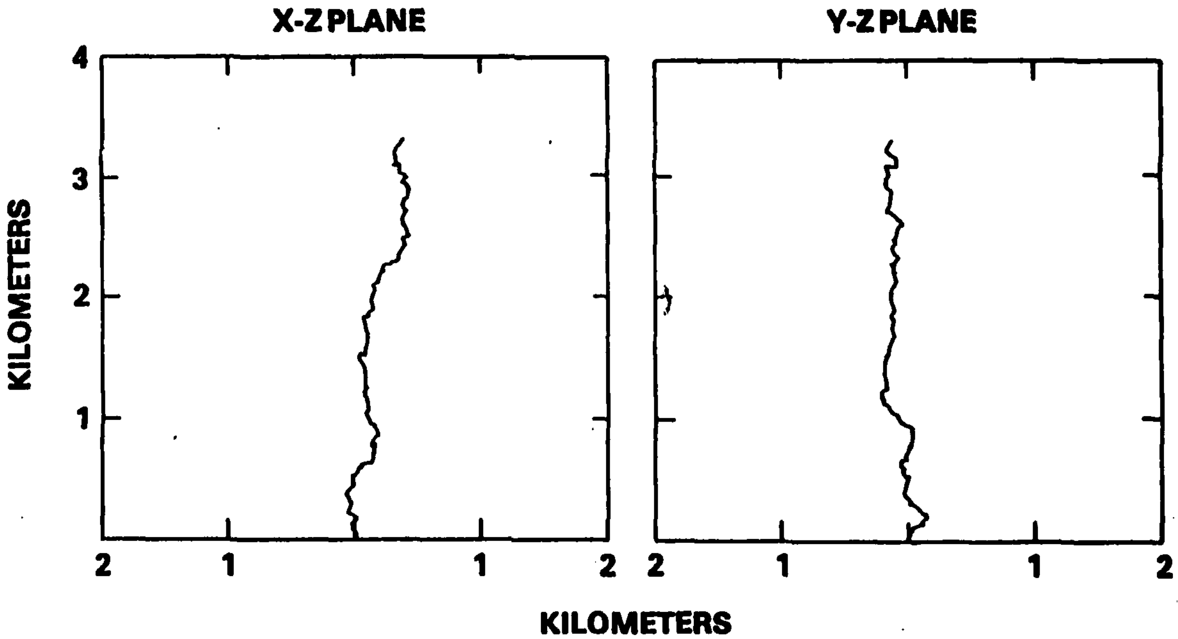

CHANNEL GEOMETRY

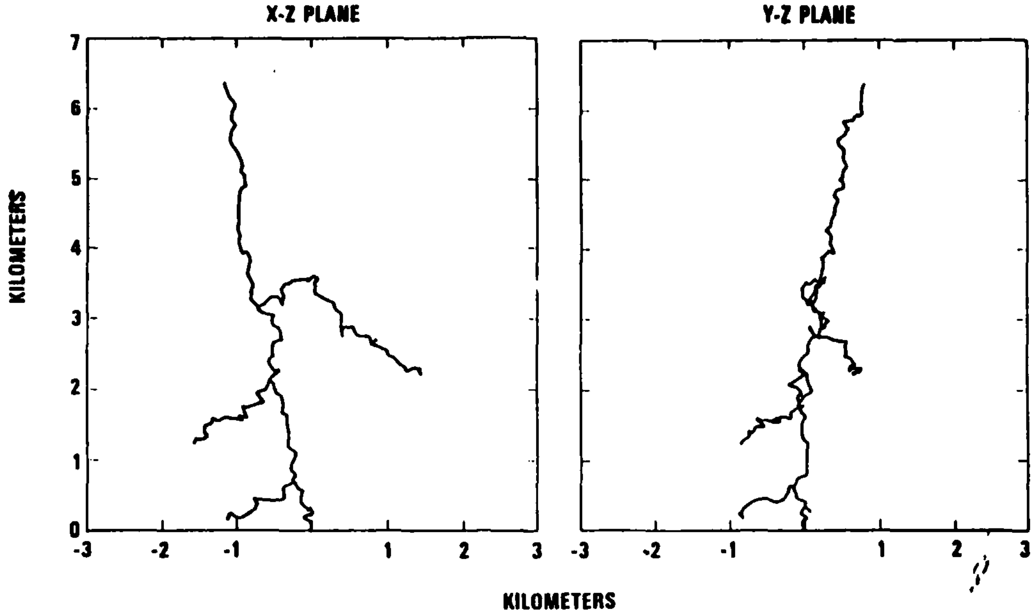

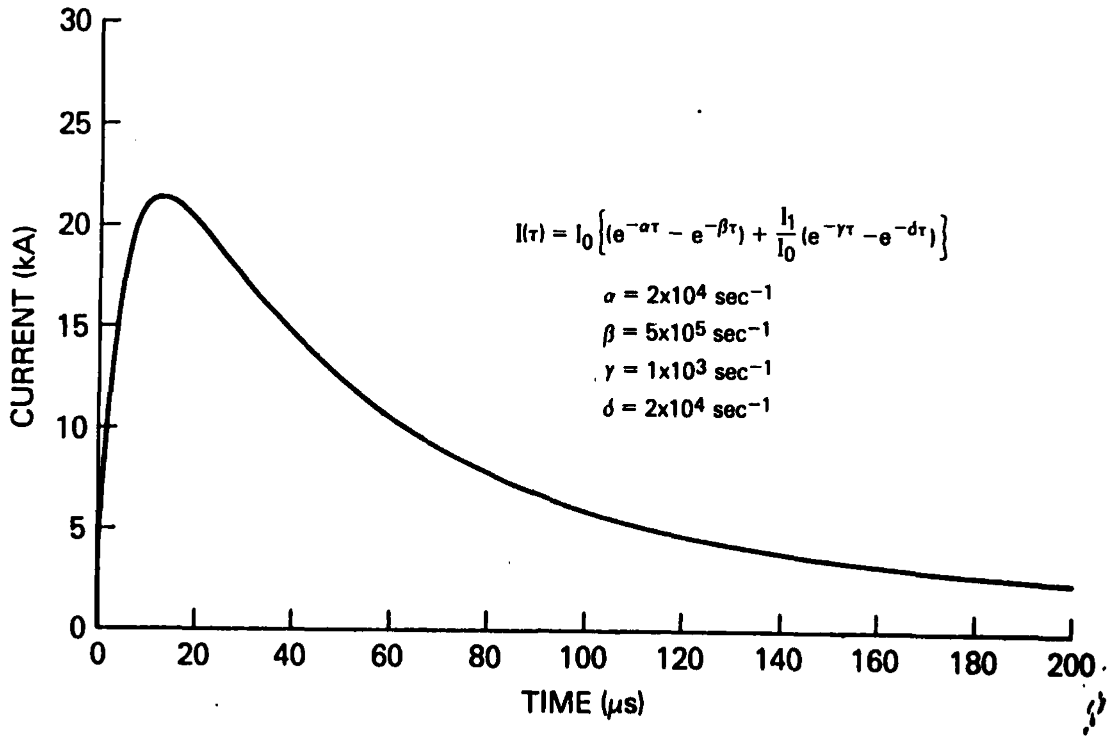

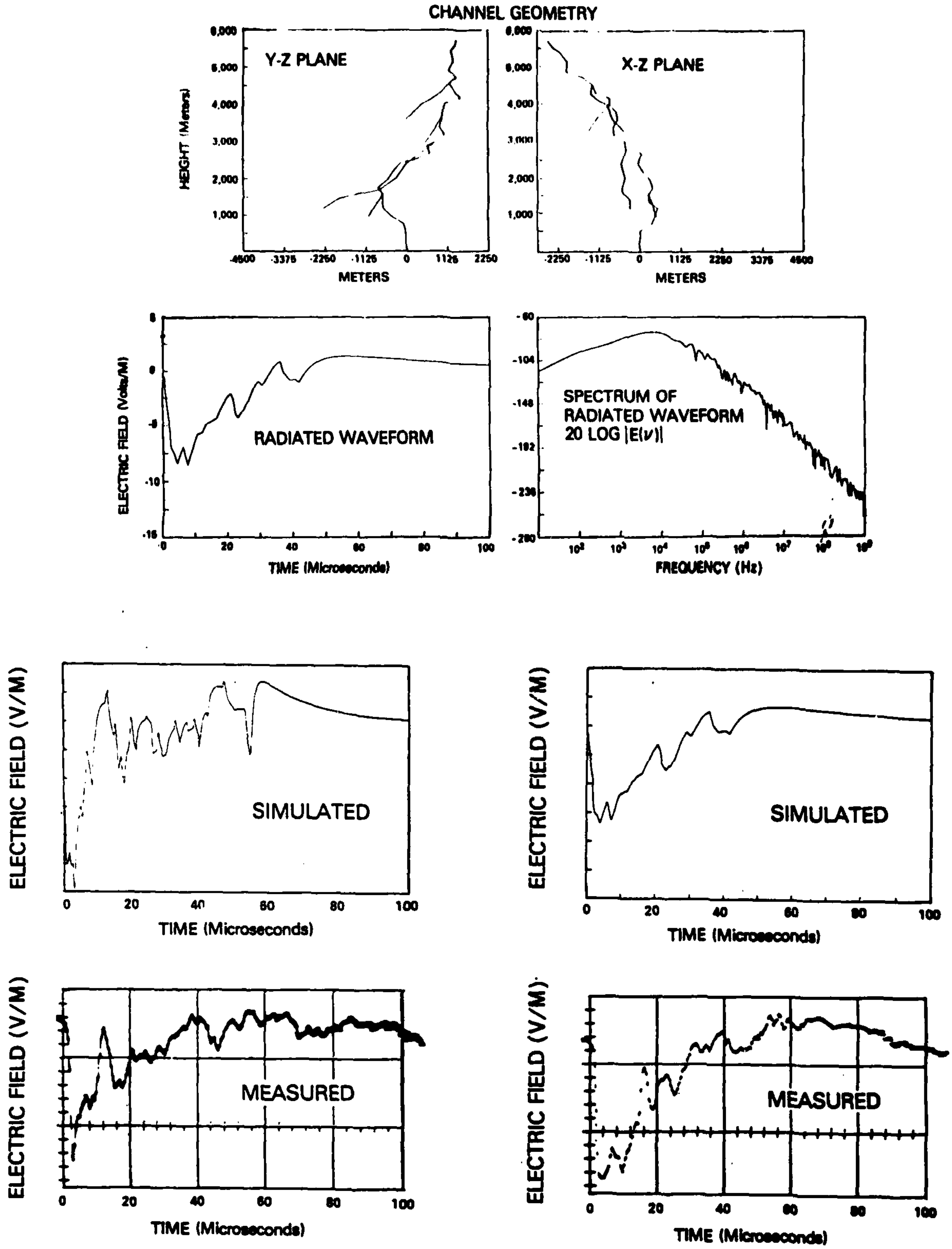
CHANNEL GEOMETRY
Y-Z PLANE
X-Z PLANE
HEIGHT (Meters)
METERS
METERS
RADIATED WAVEFORM
ELECTRIC FIELD (Volts/M)
TIME (Microseconds)
SPECTRUM OF
RADIATED WAVEFORM
20 LOG |E(ν)|
FREQUENCY (Hz)
SIMULATED
SIMULATED
MEASURED
MEASURED
ELECTRIC FIELD (V/M)
TIME (Microseconds)

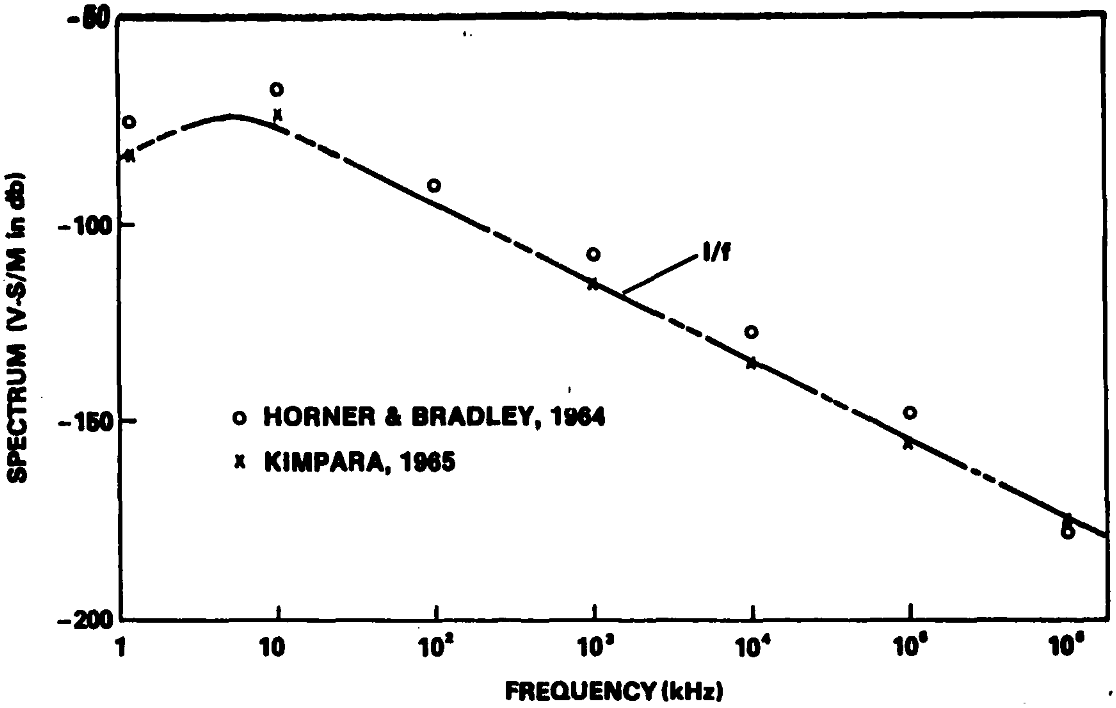
-50
-100
-150
-200
SPECTRUM (V-S/M in db)
1/f
o HORNER & BRADLEY, 1964
x KIMPARA, 1965
1
10
10^2
10^3
10^4
10^5
10^6
FREQUENCY (kHz)

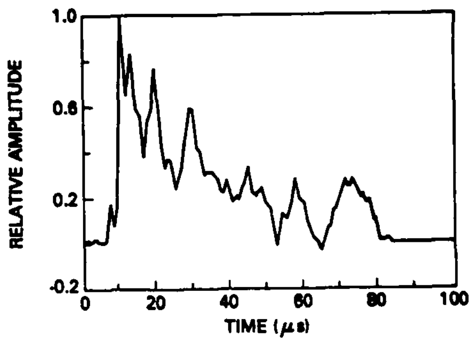
1.0
0.6
0.2
-0.2
RELATIVE AMPLITUDE
0
20
40
60
80
100
TIME (μs)

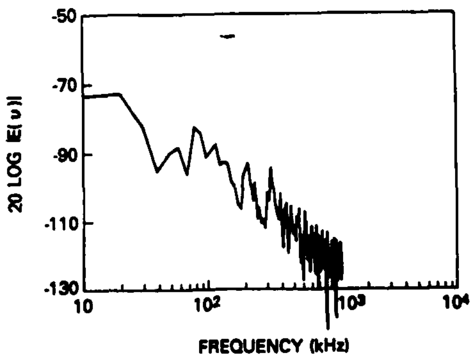
-50
-70
-90
-110
-130
20 LOG |E(ν)|
10
10^2
10^3
10^4
FREQUENCY (kHz)

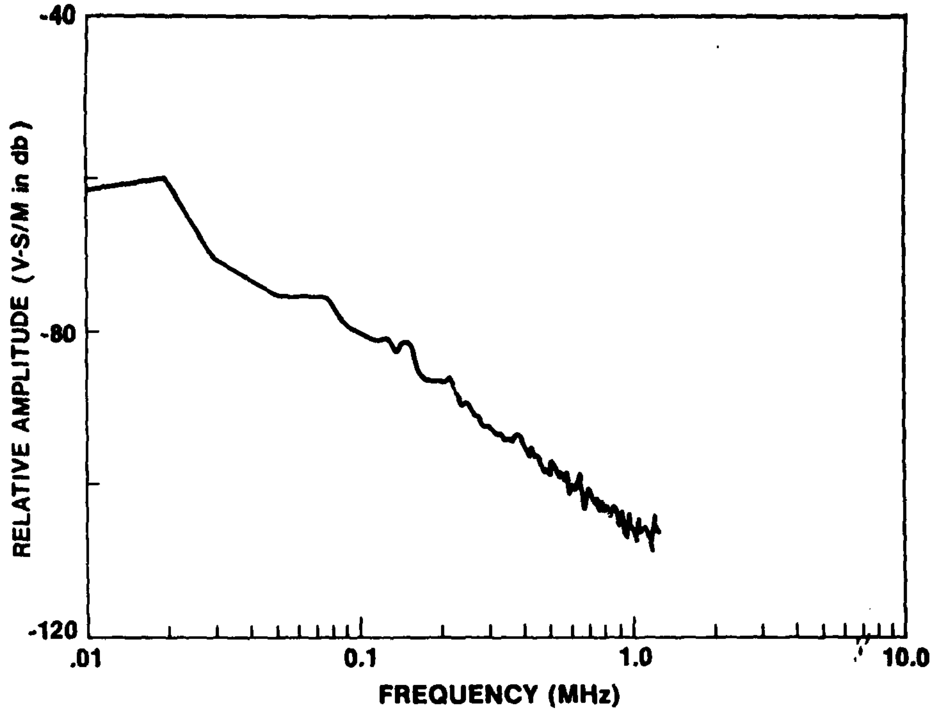
-40
-80
-120
RELATIVE AMPLITUDE (V-S/M in db)
.01
0.1
1.0
10.0
FREQUENCY (MHz)

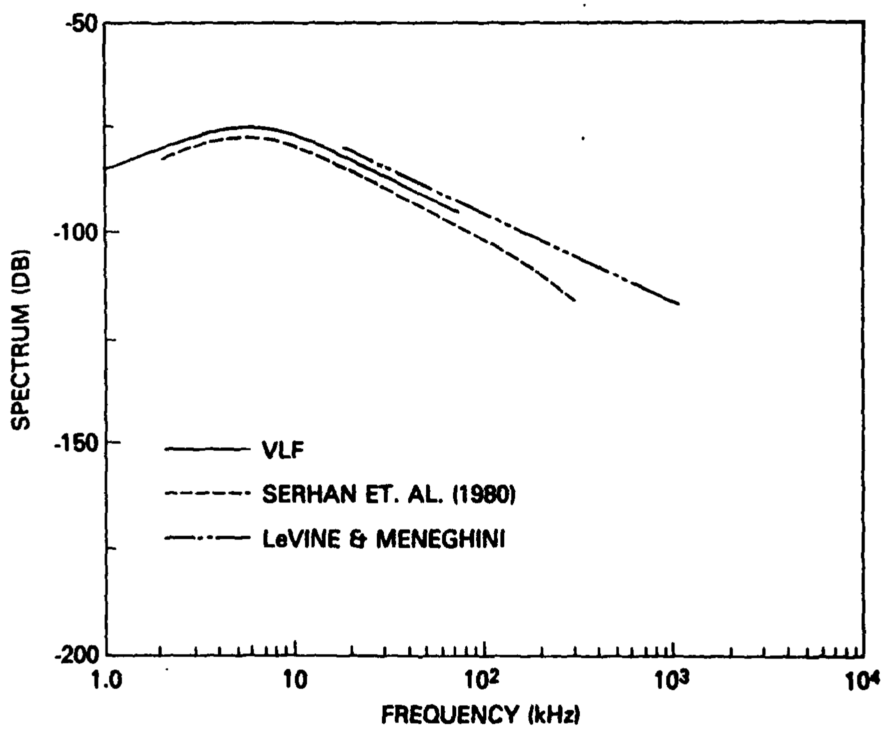
-50
-100
-150
-200
SPECTRUM (DB)
VLF
SERHAN ET. AL. (1980)
LeVINE & MENEGHINI
1.0
10
10^2
10^3
10^4
FREQUENCY (kHz)

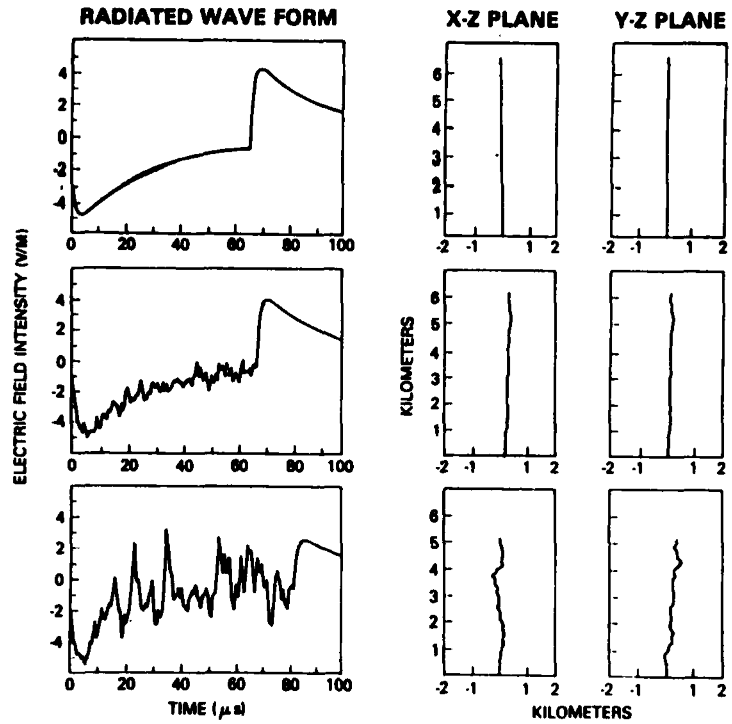
RADIATED WAVE FORM
X-Z PLANE
Y-Z PLANE
ELECTRIC FIELD INTENSITY (V/M)
TIME (μs)
KILOMETERS
KILOMETERS

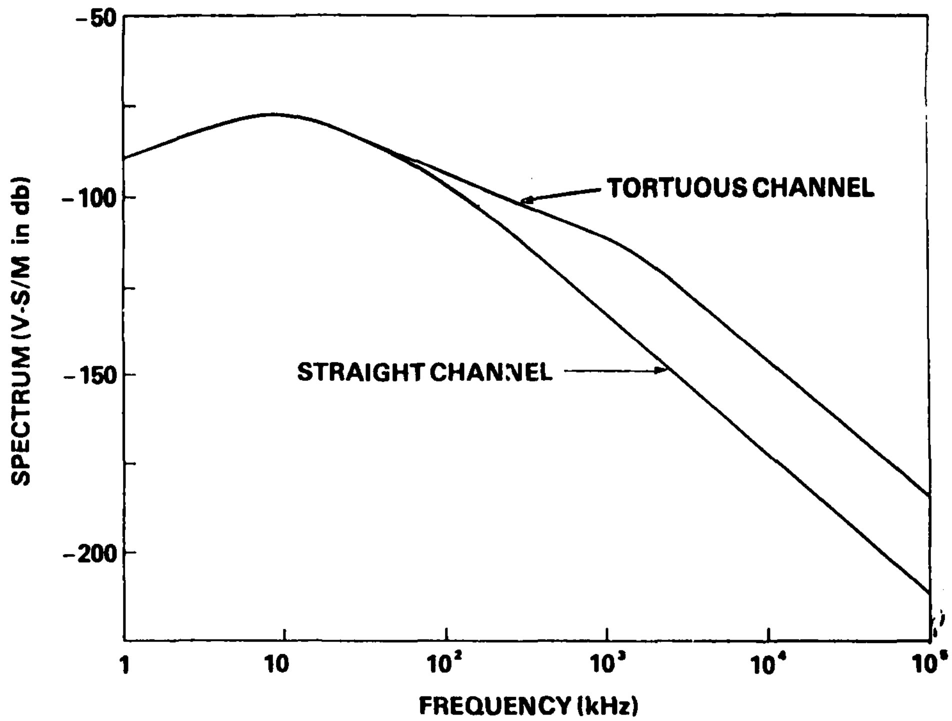
TORTUOUS CHANNEL
STRAIGHT CHANNEL
SPECTRUM (V-S/M in db)
FREQUENCY (kHz)

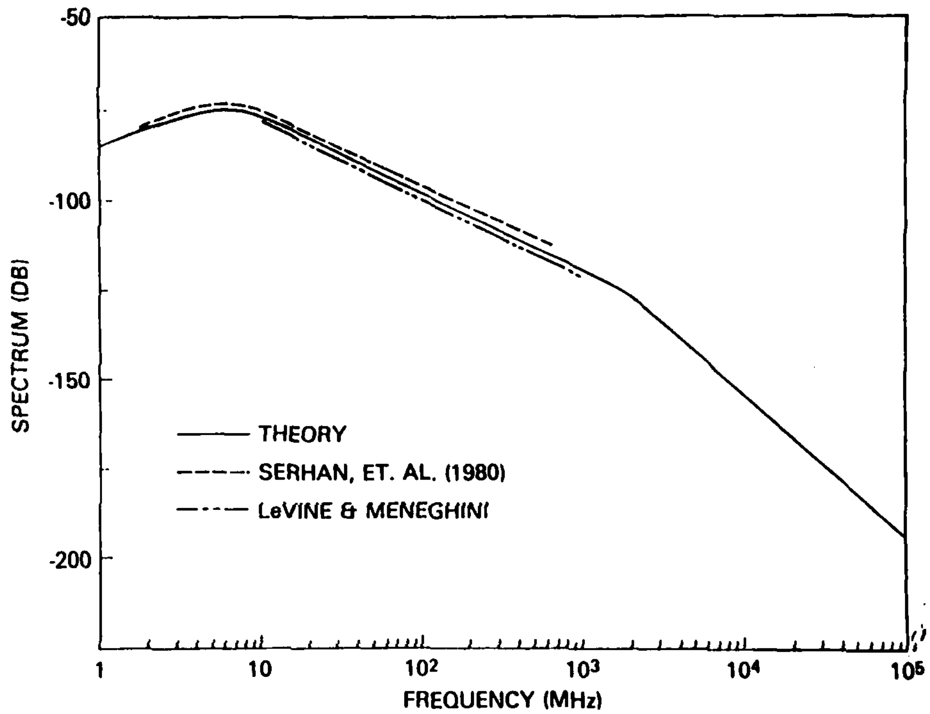
-50
-100
-150
-200
SPECTRUM (DB)
THEORY
SERHAN, ET. AL. (1980)
LeVINE & MENEGHINI
1
10
10^2
10^3
10^4
10^5
FREQUENCY (MHz)

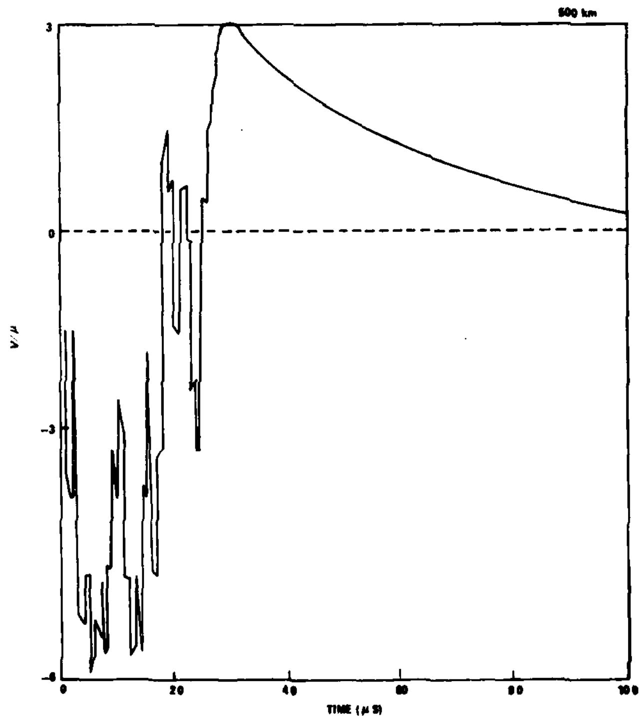
3
0
-3
20
40
100
TIME (μS)

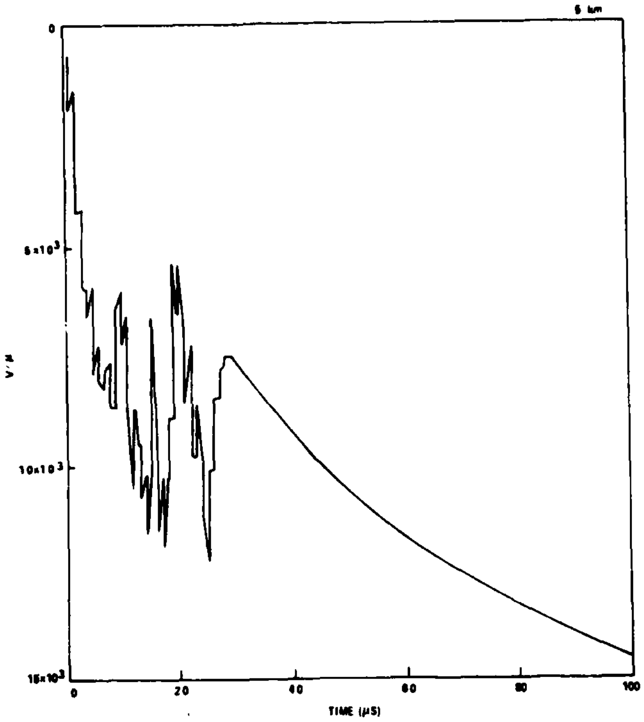
5 km
0
5x10³
10x10³
15x10³
V/M
0
20
40
60
80
100
TIME (μS)

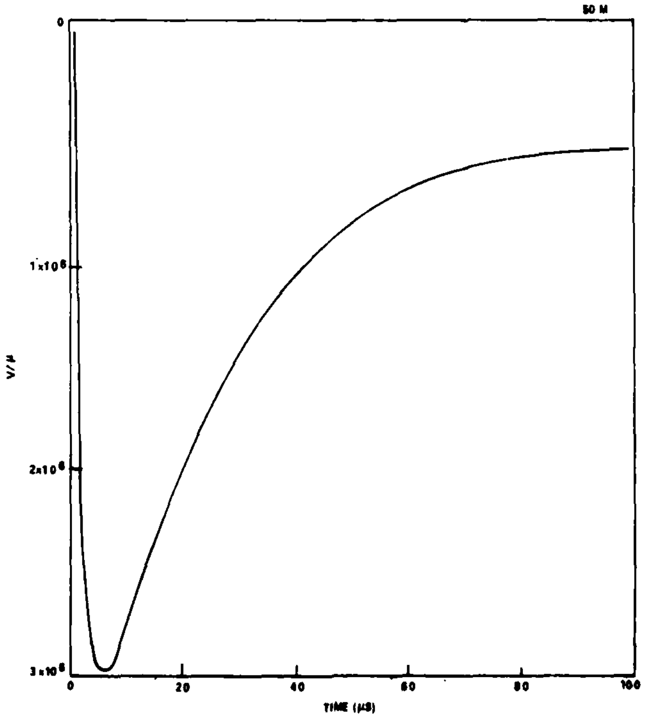
50 M
0
1x10⁶
2x10⁶
3x10⁶
V/M
0
20
40
60
80
100
TIME (μS)

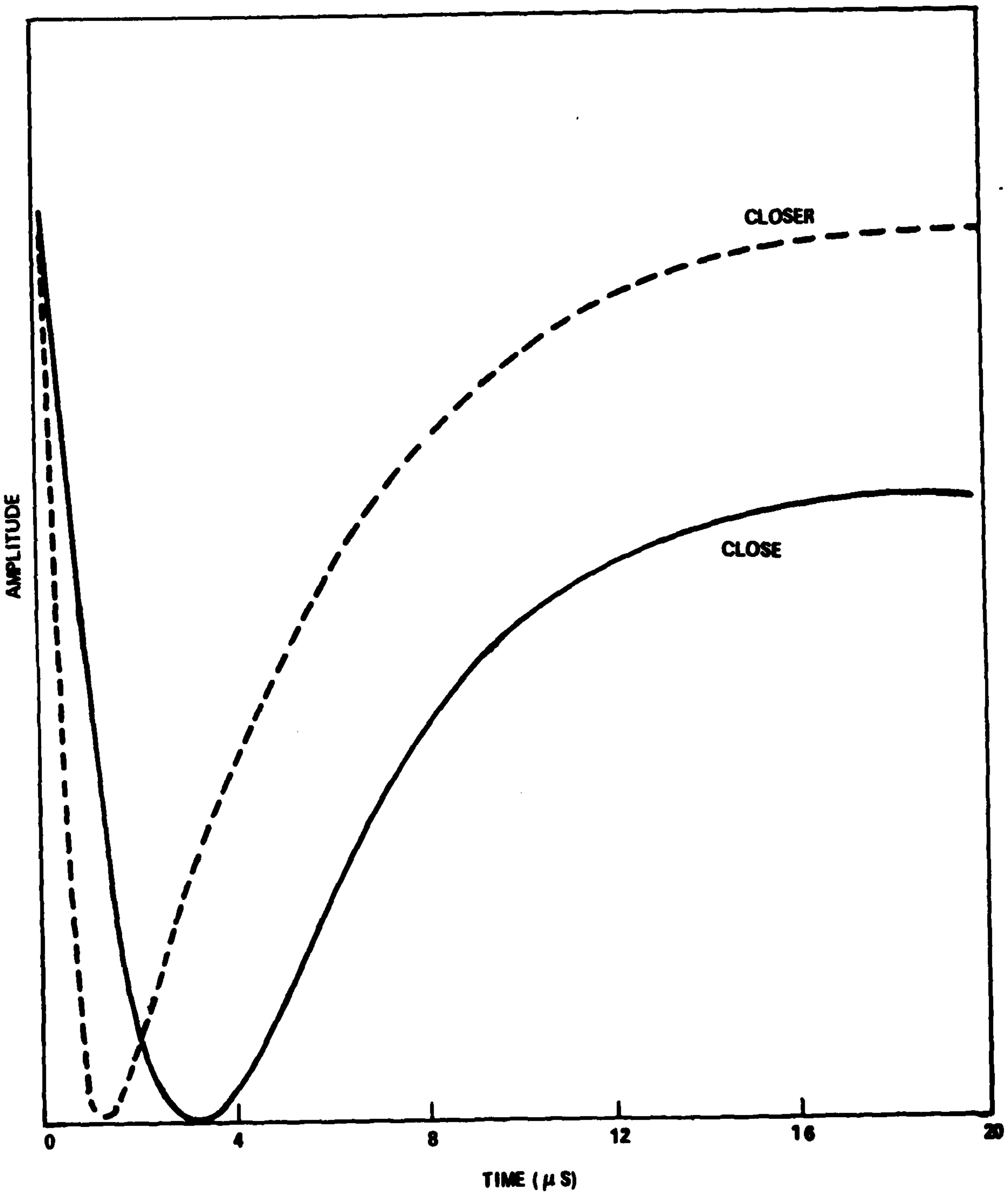

CLOSER
CLOSE
AMPLITUDE
0
4
8
12
16
20
TIME (μ S)

INTERPRETATION OF IN-FLIGHT TEST DATA APPROACH, PROBLEMS, AND OUTLOOK

by

Dr. R. A. Perala

Electromagnetic Applications, Incorporated

Discussion of the direct strike data interpretation problem and issues to be resolved. Review of lightning/aircraft interaction process and aircraft electrical resonance considerations. Approach for generalization of F-106 data to other aircraft classes.

OUTLINE

- THE LIGHTNING/AIRCRAFT INTERACTION PROCESS
- THE NEED FOR IN-FLIGHT TEST DATA
- EXTENSION OF DATA TO OTHER AIRCRAFT
- LIGHTNING MODELING
- AIRCRAFT MODELING
- EXAMPLES

STEPPED LEADER APPROACHING AIRCRAFT

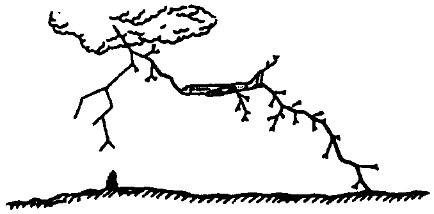

RETURN STROKE THROUGH THE AIRCRAFT

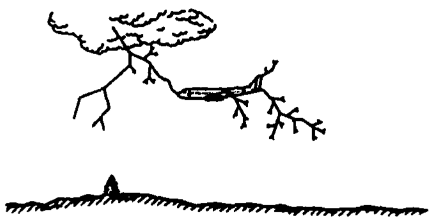

STEPPED LEADER ATTACHMENT AND CONTINUED PROPAGATION FROM AN AIRCRAFT

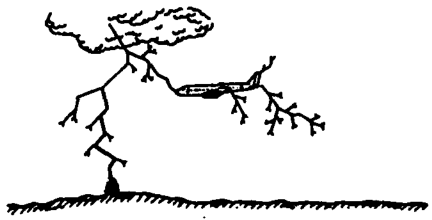

NO RETURN STROKE THROUGH THE AIRCRAFT

LIGHTNING/AIRCRAFT INTERACTION DESCRIPTION

- AIRCRAFT IN LARGE STATIC ELECTRIC FIELD, 10-100 kV/M TYPICAL
- AIRCRAFT PROBABLY ALREADY CHARGED BY TRIBOELECTRIFICATION
- APPROACHING STEPPED LEADER GIVES LARGE E, $\partial E/\partial t$
- WHEN E LARGE ENOUGH, AIRCRAFT STREAMERS
- STREAMER ATTACHES TO APPROACHING LEADER
- CHARGE FROM LEADER DEPOSITED ON AIRCRAFT AND ELEVATES ITS POTENTIAL
- WHEN ITS POTENTIAL IS HIGH ENOUGH, LEADER CONTINUES FROM AIRCRAFT TO DESTINATION
- STEPPED LEADER CURRENT FLOWS THROUGH AIRCRAFT UNTIL RETURN STROKE
- RETURN STROKE CURRENT LOWERS AIRCRAFT POTENTIAL
- AIRCRAFT IN CORONA DURING MUCH OF THIS TIME

APPROACHING LEADER E FIELDS

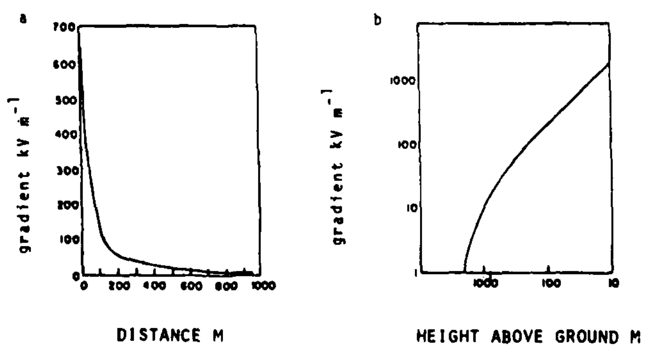

ELECTRIC GRADIENT BELOW LEADER CHANNEL: (a) AS FUNCTION OF HORIZONTAL DISTANCE AND (b) AS FUNCTION OF HEIGHT OF LEADER TIP ABOVE GROUND

ASSUME $\frac{\partial E}{\partial t} = \frac{\partial E}{\partial h}\frac{\partial h}{\partial t}$ and $\frac{\partial h}{\partial t} = 1.5 \times 10^5$ m/sec

WE GET $\frac{\partial E}{\partial t} = 1.2 \times 10^7$ at 1000 m

$= 1.5 \times 10^{10}$ at 10-20 m

AIRCRAFT STREAMERING

- CURRENTS PROBABLY LESS THAN 100A, BASED ON GROUND STREAMER DATA
- WAVESHAPES: 10 μsec RISETIMES
- NEGATIVE CHARGE ENTERING AIRCRAFT AT STREAMER POINT
- STREAMERING CAN OCCUR FROM CRITICAL POINTS
- STREAMERING INFLUENCED BY STATIC FIELD
- ELECTRIC FIELD ON AIRCRAFT REVERSES AT ATTACHMENT

STEPPED LEADER CURRENT FLOW THROUGH AIRCRAFT

- AIRCRAFT NEEDS TO ACCUMULATE ≥100 μC OF CHARGE FOR STEPPED LEADER TO CONTINUE ON FROM AIRCRAFT
- IF LEADER CURRENT IS 1000A RISING IN 100 ns, CHARGING TIME IS ABOUT 150 ns
- DURING THIS TIME AIRCRAFT NORMAL ELECTRIC FIELDS APPROACH 3 MV/m
- THIS GIVES $\partial E/\partial t \approx 2 \times 10^{13}$ V/m/sec
- LEADER CURRENT CONTINUES THROUGH AIRCRAFT AND ELECTRIC FIELD STAYS CONSTANT AND CURRENT ASSUMES THE SLOWLY INCREASING ARC CURRENT UPON WHICH IS SUPERIMPOSED LEADER PULSE CURRENTS
- AIRCRAFT IS IN CORONA DURING THIS PHASE

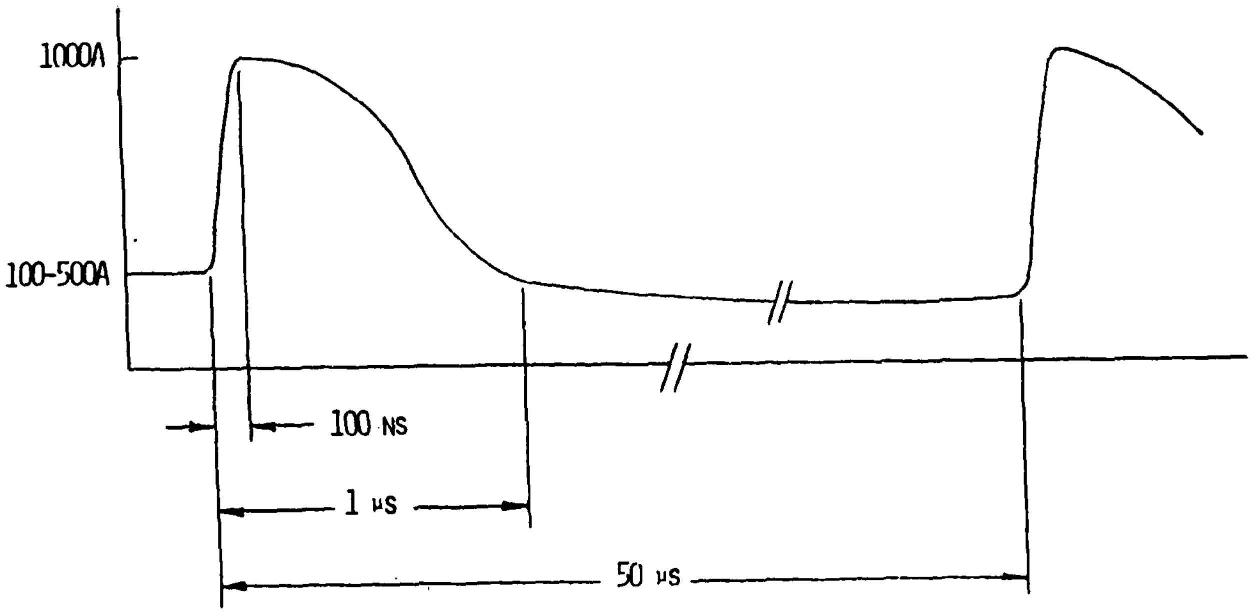

STEPPED LEADER CURRENTS

J- AND K- CHANGES

J-CHANGES: SLOW, 100A CURRENTS

K-CHANGES: SEVERAL THOUSAND AMPS
POSSIBLY 50 NS RISE TIMES

ISSUES OF INTEREST AND THE NEED FOR IN-FLIGHT TEST DATA

- ATTACHMENT PROCESS
  - WHAT ARE E AND $\frac{\partial E}{\partial t}$?
  - HOW IMPORTANT ARE NONLINEAR (CORONA, STREAMERS) EFFECTS?
  - WHAT IS THE EQUIVALENT CIRCUIT OF THE LEADER (CHANNEL IMPEDANCE, NORTON CURRENT SOURCE)
- RETURN STROKE
  - WHAT ARE E AND $\frac{\partial E}{\partial t}$?
  - WHAT ARE H AND $\frac{\partial H}{\partial t}$?
  - HOW IMPORTANT ARE NONLINEAR EFFECTS?
  - WHAT IS THE RETURN STROKE EQUIVALENT CIRCUIT?
- NEARBY LIGHTNING: HOW IMPORTANT IS IT?
- HOW APPLICABLE ARE STATE OF THE ART LIGHTNING MODELS AT AIRCRAFT ALTITUDES?
  - MODELS SO FAR ARE BASED ON TERRESTRIAL OBSERVATIONS
  - MODELS HAVE NOT BEEN TESTED AT AIRCRAFT ALTITUDES
- OBTAIN DATA ON INTRACLOUD LIGHTNING
- HOW DOES THE AIRCRAFT INTERACT WITH LIGHTNING? IS THE LIGHTNING ENVIRONMENT ITSELF MODEIFIED BY THE PRESENCE OF AN AIRCRAFT? IS IT DIFFERENT FOR DIFFERENT AIRCRAFT.

THE OBJECTIVE OF DATA INTERPRETATION

- **WHAT ARE THE LIGHTNINGS THAT CAUSE THE F106B RESPONSES? (AN INVERSE PROBLEM)**
- **WHAT WOULD BE THE RESPONSE OF A DIFFERENT AIRCRAFT?**
- **CAN A METHODOLOGY BE DEVELOPED FOR EXTENDING IN-FLIGHT DATA FROM ANY AIRCRAFT TO ANY OTHER AIRCRAFT?**

APPROACH

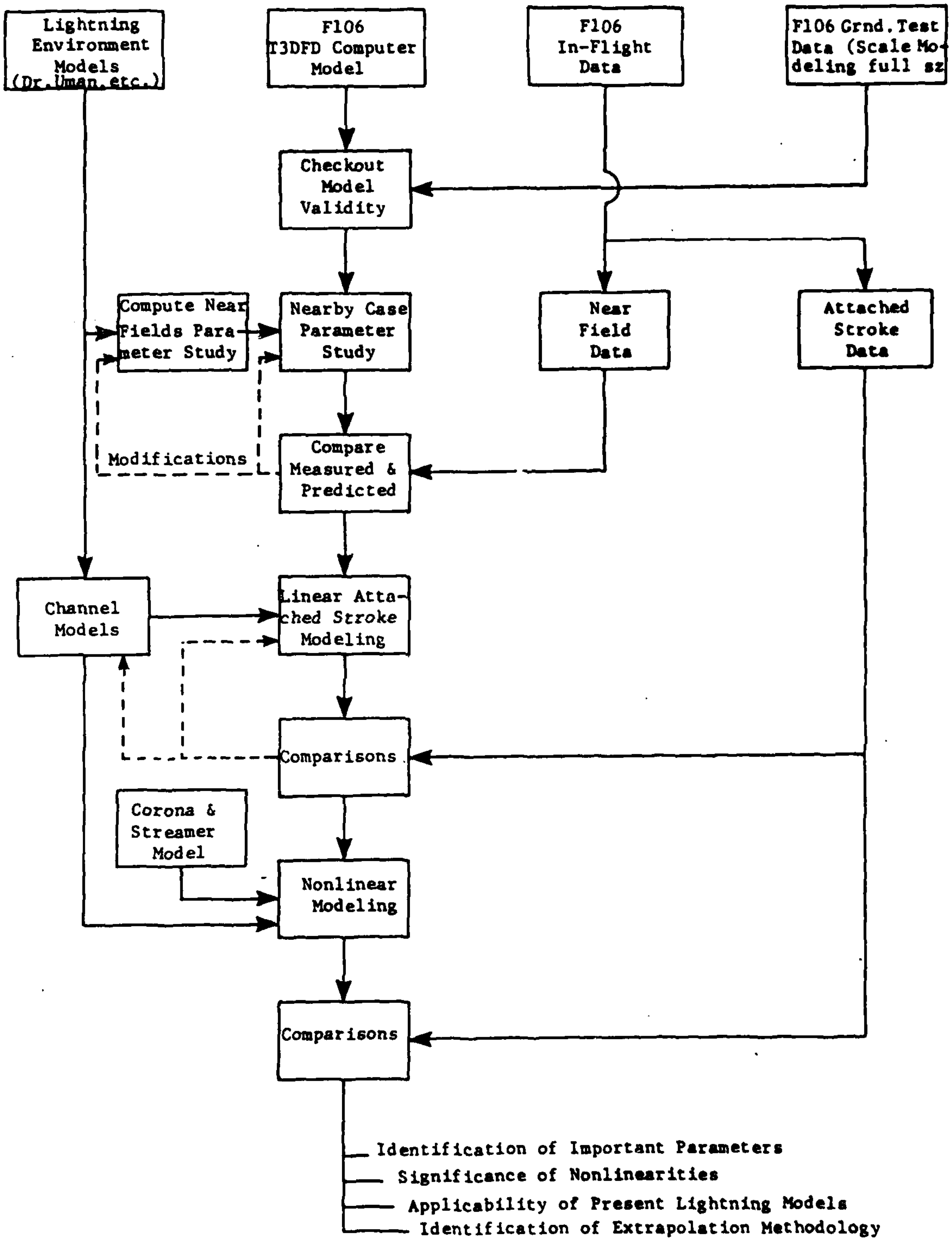

Lightning Environment Models (Dr. Uman, etc.)
F106 T3DFD Computer Model
F106 In-Flight Data
F106 Grnd. Test Data (Scale Modeling full sz
Checkout Model Validity
Compute Near Fields Parameter Study
Nearby Case Parameter Study
Near Field Data
Attached Stroke Data
Modifications
Compare Measured & Predicted
Channel Models
Linear Attached Stroke Modeling
Comparisons
Corona & Streamer Model
Nonlinear Modeling
Comparisons
Identification of Important Parameters
Significance of Nonlinearities
Applicability of Present Lightning Models
Identification of Extrapolation Methodology

IMPORTANCE OF NEAR MISS DATA

- INTERACTION CALCULATIONS CAN BE DONE LINEARLY, WITHOUT COMPLICATIONS INTRODUCED BY NONLINEARITIES

- DATA CAN BE USED TO INFER NEARBY LIGHTNING ELECTROMAGNETIC WAVEFORMS AT AIRCRAFT ALTITUDES TO CORRELATE WITH PREDICTIONS

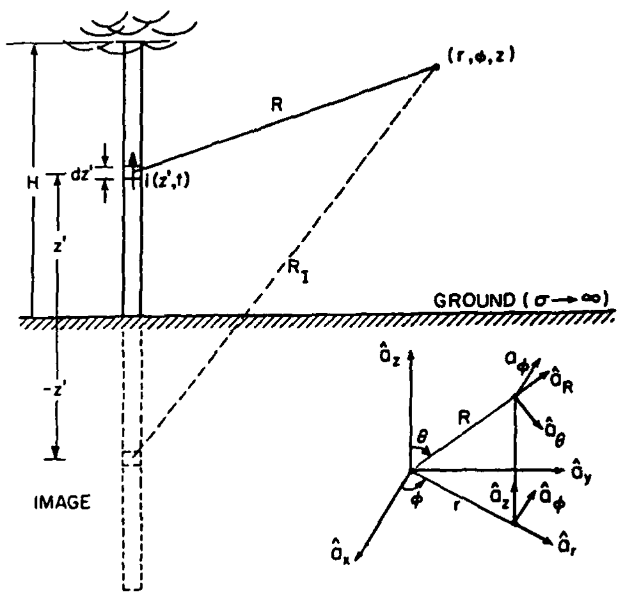

A DRAWING DEFINING ALL GEOMETRICAL PARAMETERS NEEDED IN THE CALCULATION OF ELECTRIC AND MAGNETIC FIELDS. (FROM UMAN)

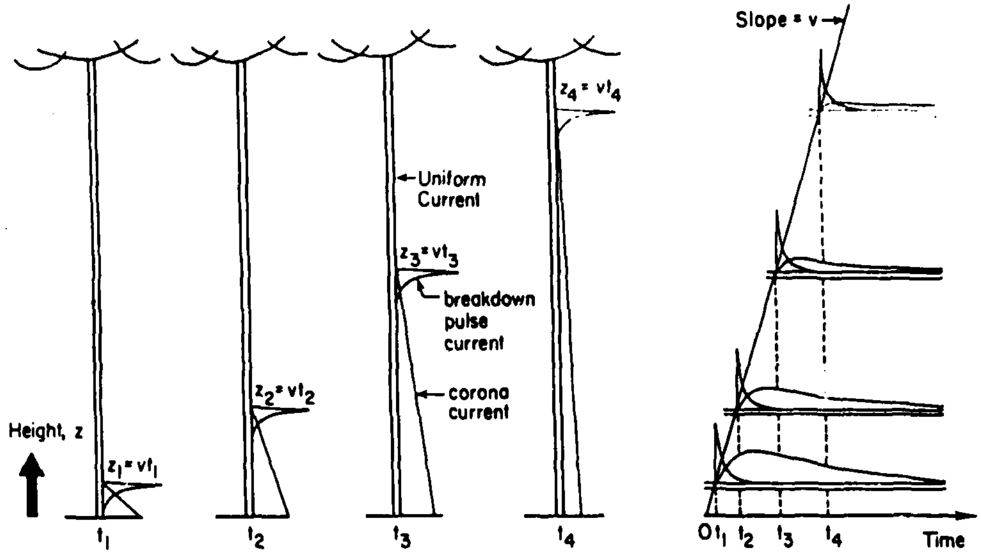

CURRENT DISTRIBUTION FOR THE MODEL OF LIN ET AL. (1980) IN WHICH THE BREAKDOWN PULSE CURRENT IS CONSTANT WITH HEIGHT. THE CONSTANT VELOCITY OF THE BREAKDOWN PULSE CURRENT IS v. CURRENT PROFILES ARE SHOWN AT FOUR DIFFERENT TIMES t_1 THROUGH t_4, WHEN THE RETURN STROKE WAVEFRONT AND THE BREAKDOWN PULSE CURRENT ARE AT FOUR DIFFERENT HEIGHTS z_1 THROUGH z_4, RESPECTIVELY. (FROM UMAN)

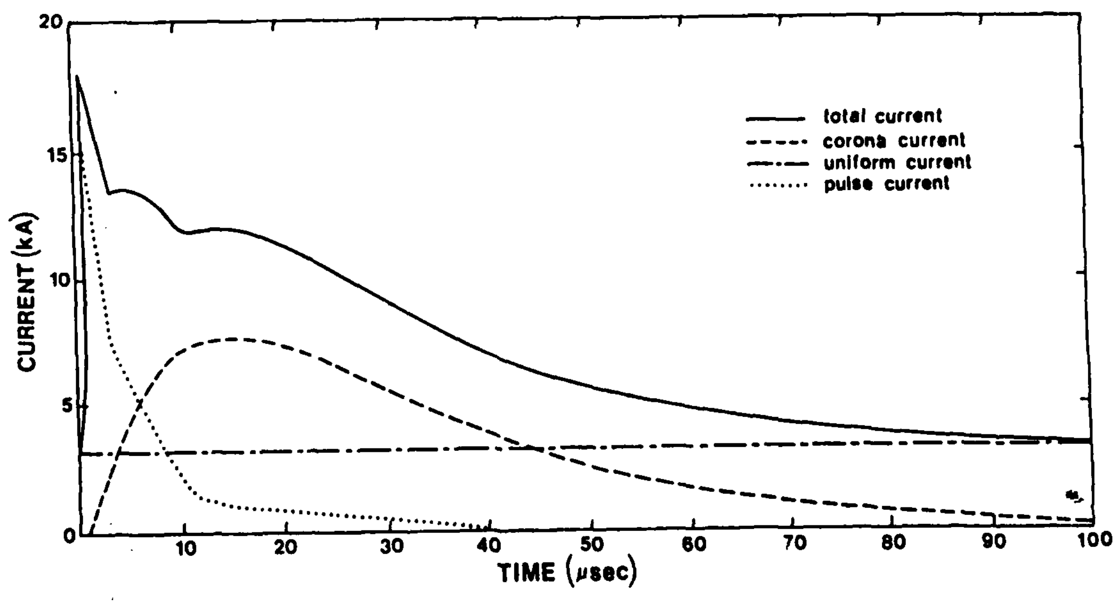

RETURN STROKE CURRENT COMPONENTS AT GROUND FOR A TYPICAL SUBSEQUENT STROKE CALCULATED FROM MEASURED ELECTRIC AND MAGNETIC FIELDS (FROM UMAN)

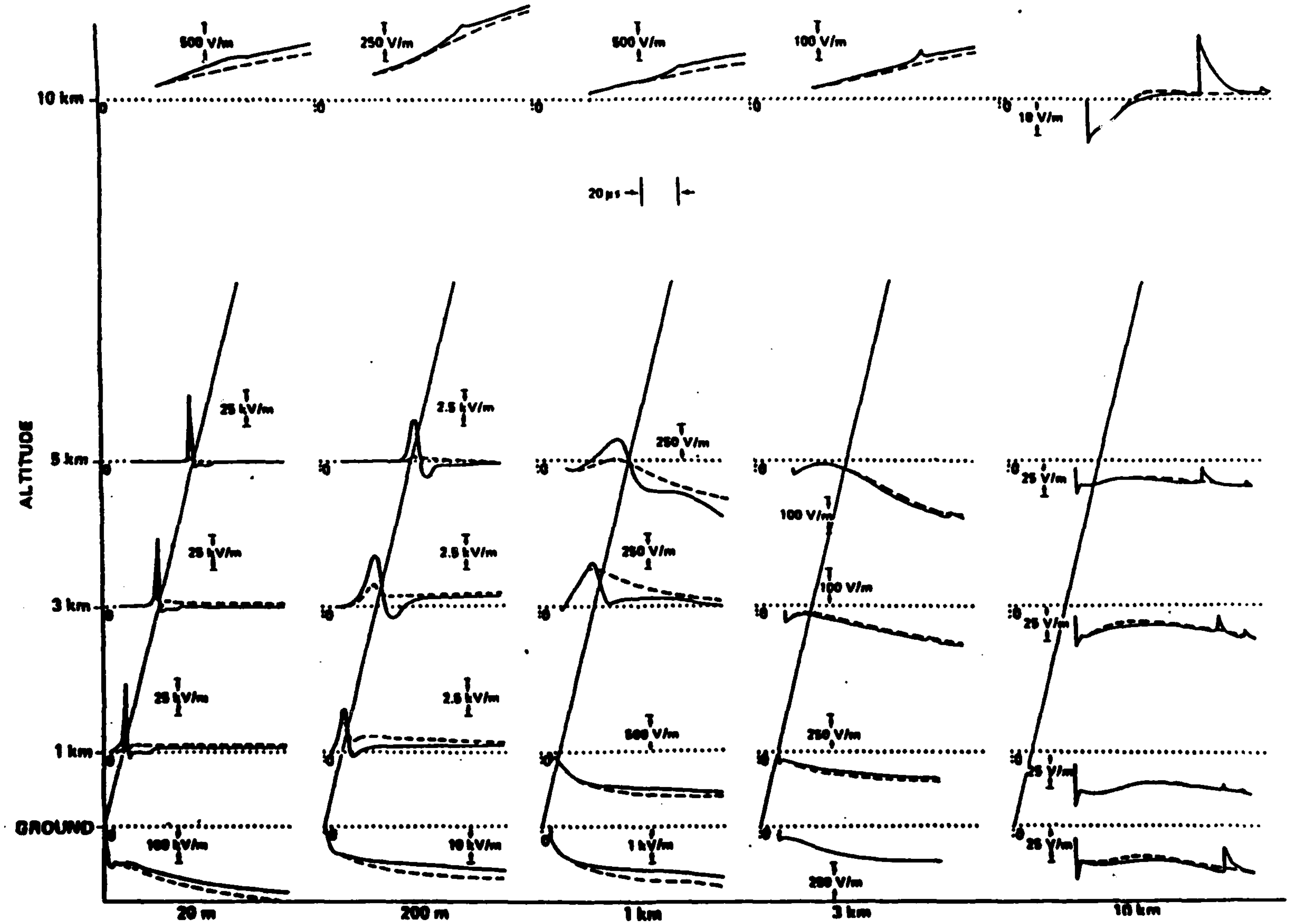

CALCULATED VERTICAL ELECTRIC FIELDS FOR A TYPICAL SUBSEQUENT RETURN STROKE (FROM UMAN)

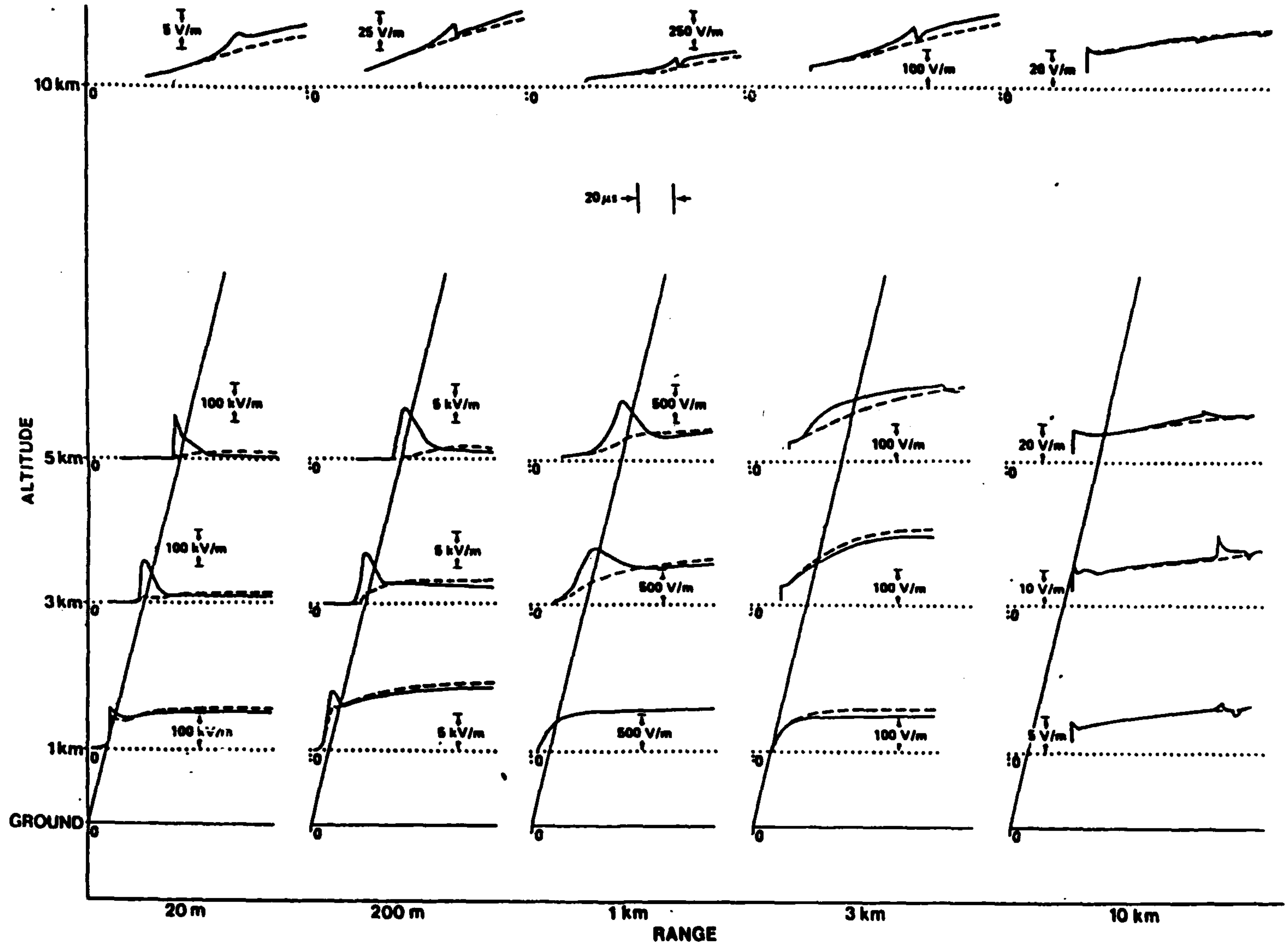

CALCULATED HORIZONTAL ELECTRIC FIELDS FOR A TYPICAL SUBSEQUENT RETURN STROKE (FROM UMAN)

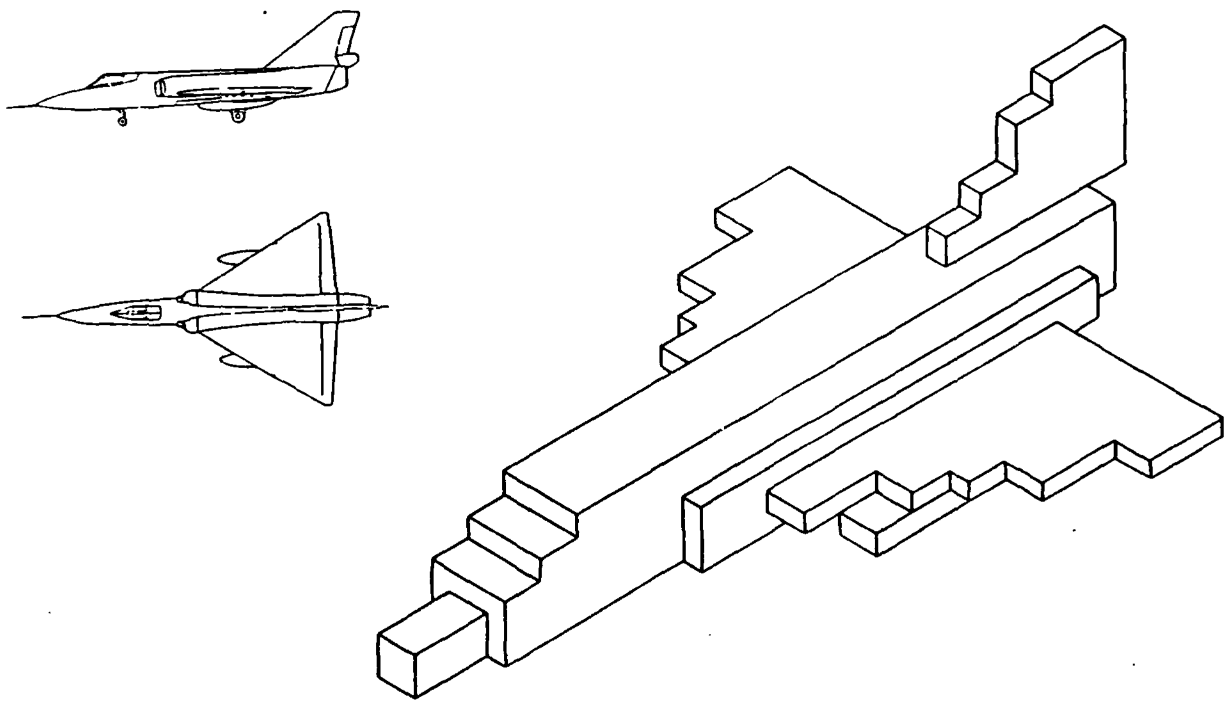

T3DFD MODEL OF F106B

Assumptions: None

Maxwell's Equations

$$-\mu \frac{\partial H_x}{\partial t} = \left(\frac{\partial E_z}{\partial y} - \frac{\partial E_y}{\partial z}\right) \qquad H_x^n(i,j,k) = H_x(x(i),y_0(j),z_0(k),t_H(n))$$

$$-\mu \frac{\partial H_y}{\partial t} = \left(\frac{\partial E_x}{\partial z} - \frac{\partial E_z}{\partial x}\right) \qquad H_y^n(i,j,k) = H_y(x_0(i),y(j),z_0(k),t_H(n))$$

$$-\mu \frac{\partial H_z}{\partial t} = \left(\frac{\partial E_y}{\partial x} - \frac{\partial E_x}{\partial y}\right) \qquad H_z^n(i,j,k) = H_z(x_0(i),y_0(j),z(k),t_H(n))$$

$$\epsilon \frac{\partial E_x}{\partial t} + \sigma E_x = \left(\frac{\partial H_z}{\partial y} - \frac{\partial H_y}{\partial z}\right) - J_x \qquad E_x^n(i,j,k) = E_x(x_0(i),y(j),z(k),t_E(n))$$

$$\epsilon \frac{\partial E_y}{\partial t} + \sigma E_y = \left(\frac{\partial H_x}{\partial z} - \frac{\partial H_z}{\partial x}\right) - J_y \qquad E_y^n(i,j,k) = E_y(x(i),y_0(j),z(k),t_E(n))$$

$$\epsilon \frac{\partial E_z}{\partial t} + \sigma E_z = \left(\frac{\partial H_y}{\partial x} - \frac{\partial H_x}{\partial y}\right) - J_z \qquad E_z^n(i,j,k) = E_z(x(i),y(j),z_0(k),t_E(n))$$

$$x_0(i) = (i-1)\Delta x\ ,\ y_0(j) = (j-1)\Delta y\ ,\ z_0(k) = (k-1)\Delta z\ ,\ t_H(n) = (n-1)\Delta t$$

$$x(i) = (i-1/2)\Delta x\ ,\ y(j) = (j-1/2)\Delta y\ ,\ z(k) = (k-1/2)\Delta z\ ,\ t_E(n) = (n-1/2)\Delta t$$

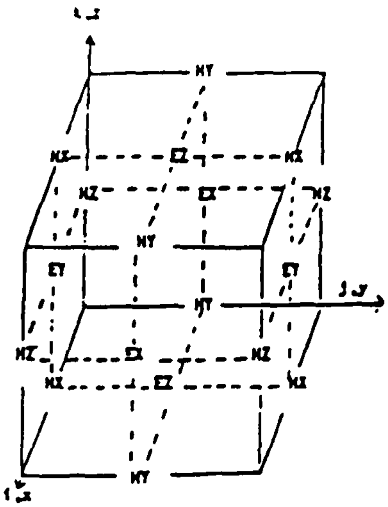

Finite Difference Equations (non-uniform grid allowed)

$$H_x^{n+1}(i,j+1,k+1) = H_x^n(i,j+1,k+1) - \frac{\Delta t}{\mu}\left(\frac{E_z^n(i,j+1,k+1) - E_z^n(i,j,k+1)}{y(j+1) - y(j)}\right) + \frac{\Delta t}{\mu}\left(\frac{E_y^n(i,j+1,k+1) - E_y^n(i,j+1,k)}{z(k+1) - z(k)}\right) \quad \begin{cases} i\in[1,i_{can}] \\ j\in[1,j_{can}-1] \\ k\in[1,k_{can}-1] \end{cases}$$

$$H_y^{n+1}(i+1,j,k+1) = H_y^n(i+1,j,k+1) - \frac{\Delta t}{\mu}\left(\frac{E_x^n(i+1,j,k+1) - E_x^n(i+1,j,k)}{z(k+1) - z(k)}\right) + \frac{\Delta t}{\mu}\left(\frac{E_z^n(i+1,j,k+1) - E_z^n(i,j,k+1)}{x(i+1) - x(i)}\right) \quad \begin{cases} i\in[1,i_{can}-1] \\ j\in[1,j_{can}] \\ k\in[1,k_{can}-1] \end{cases}$$

$$H_z^{n+1}(i+1,j+1,k) = H_z^n(i+1,j+1,k) - \frac{\Delta t}{\mu}\left(\frac{E_y^n(i+1,j+1,k) - E_y^n(i,j+1,k)}{x(i+1) - x(i)}\right) + \frac{\Delta t}{\mu}\left(\frac{E_x^n(i+1,j+1,k) - E_x^n(i+1,j,k)}{y(j+1) - y(j)}\right) \quad \begin{cases} i\in[1,i_{can}-1] \\ j\in[1,j_{can}-1] \\ k\in[1,k_{can}] \end{cases}$$

$$B\cdot E_x^{n+1}(i,j,k) = A\cdot E_x^n(i,j,k) - J_x + \left(\frac{H_z^{n+1}(i,j+1,k) - H_z^{n+1}(i,j,k)}{y_0(j+1) - y_0(j)}\right) - \left(\frac{H_y^{n+1}(i,j,k+1) - H_y^{n+1}(i,j,k)}{z_0(k+1) - z_0(k)}\right) \quad \begin{cases} i\in[1,i_{can}] \\ j\in[1,j_{can}] \\ k\in[1,k_{can}] \end{cases}$$

$$B\cdot E_y^{n+1}(i,j,k) = A\cdot E_y^n(i,j,k) - J_y + \left(\frac{H_x^{n+1}(i,j,k+1) - H_x^{n+1}(i,j,k)}{z_0(k+1) - z_0(k)}\right) - \left(\frac{H_z^{n+1}(i+1,j,k) - H_z^{n+1}(i,j,k)}{x_0(i+1) - x_0(i)}\right) \quad \begin{cases} i\in[1,i_{can}] \\ j\in[1,j_{can}] \\ k\in[1,k_{can}] \end{cases}$$

$$B\cdot E_z^{n+1}(i,j,k) = A\cdot E_z^n(i,j,k) - J_z + \left(\frac{H_y^{n+1}(i+1,j,k) - H_y^{n+1}(i,j,k)}{x_0(i+1) - x_0(i)}\right) - \left(\frac{H_x^{n+1}(i,j+1,k) - H_x^{n+1}(i,j,k)}{y_0(j+1) - y_0(j)}\right) \quad \begin{cases} i\in[1,i_{can}] \\ j\in[1,j_{can}] \\ k\in[1,k_{can}] \end{cases}$$

where

$$A = \left(\frac{\epsilon}{\Delta t} - \frac{\sigma}{2}\right)\ ,\ B = \left(\frac{\epsilon}{\Delta t} + \frac{\sigma}{2}\right)\ ,\ J_x = J_x(t_H(n+1))\ ,\ J_y = J_y(t_H(n+1))\ ,\ J_z = J_z(t_H(n+1))$$

all evaluated at desired E component location

Externally supplied values are tangential electric fields on outer surface of problem space:

$H_x^n(i,j,1)$, $H_y^n(i,j,1)$, $H_x^n(i,j,k_{can}+1)$, $H_y^n(i,j,k_{can}+1)$ all $i\in[1,i_{can}]$, $j\in[1,j_{can}]$

$H_x^n(i,1,k)$, $H_z^n(i,1,k)$, $H_x^n(i,j_{can}+1,k)$, $H_z^n(i,j_{can}+1,k)$ all $i\in[1,i_{can}]$, $k\in[1,k_{can}]$

$H_y^n(1,j,k)$, $H_z^n(1,j,k)$, $H_y^n(i_{can}+1,j,k)$, $H_z^n(i_{can}+1,j,k)$ all $j\in[1,j_{can}]$, $k\in[1,k_{can}]$

3-D Finite Difference Equations in Rectangular Coordinates Set Up with Externally Supplied H Fields

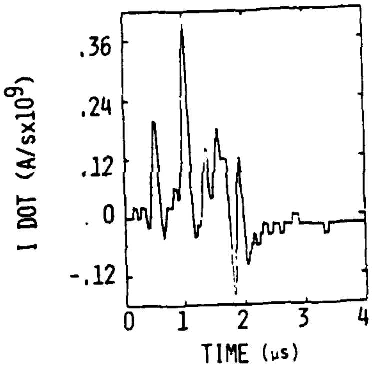

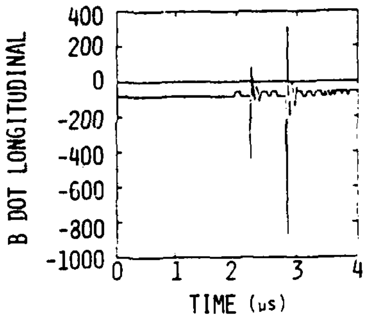

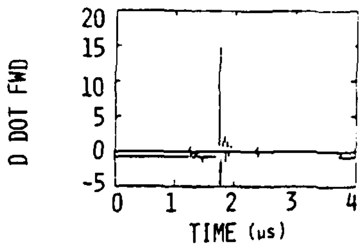

DATA FROM FLIGHT 80-038, RECORD 4

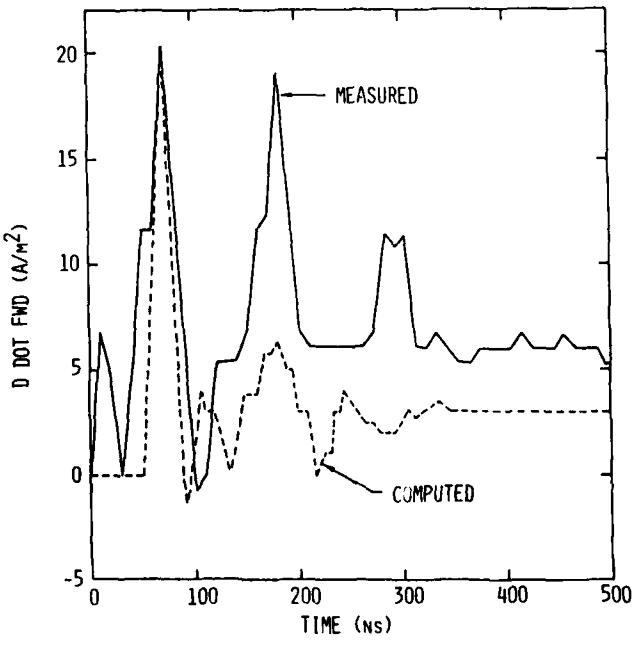

COMPARISON OF MEASURED RESPONSE (FLIGHT 80-18) AND COMPUTED WITH T3DFD AND A 30NS RISE TIME, 590 AMPERE STEP CURRENT SOURCE, NOSE TO TAIL.

CORONA AND STREAMER EFFECTS

by

Dr. R. A. Perala

Electromagnetic Applications, Incorporated

Description of possible corona effects on direct strike data, review of elements and state-of-the-art of corona modeling, and application of corona modeling to lightning/aircraft interaction. Corona to arc transition, importance, and modeling of streamers.

DEFINITIONS

CORONA: A STATE OF THE GASEOUS CONDUCTION PREVIOUS TO ARC FORMATION

STREAMER: A CONDUCTING ARC CHANNEL EMANATING FROM A CORONA REGION

CORONA: BASIC MECHANISM

- REQUIREMENT: FREE ELECTRONS ACCELERATED BY ELECTRIC FIELD

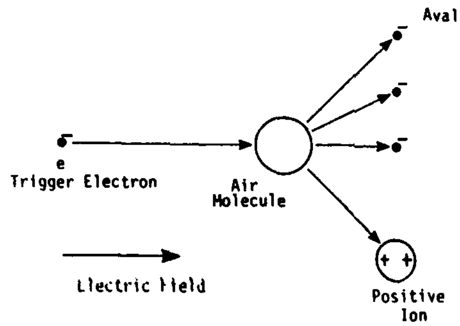

$dn = \alpha n dx$

n = Number of Electrons

x = Distance

α = Townsend Ionization Coefficient

- SOURCE OF FREE (TRIGGER) ELECTRONS: BACKGROUND IONIZATION CAUSED BY COSMIC RAYS; $\sim 2 \times 10^7$ ELECTRON-ION PARIS/(m^3-sec). THIS GIVES AMBIENT AIR CONDUCTIVITY $\sim 10^{-13}$ mho/m.

ELECTRON AND ION LOSS MECHANISMS

- ELECTRON ATTACHMENT TO NEUTRAL AIR MOLECULES TO FORM NEGATIVE IONS
  ATTACHMENT RATE α_E

- RECOMBINATION OF POSITIVE IONS AND ELECTRONS TO FORM NEUTRAL PARTICLES
  RECOMBINATION RATE β

- RECOMBINAZION OF POSITIVE AND NEGATIVE IONS
  RECOMBINATION RATE γ

AIR CHEMISTRY EQUATIONS FOR CORONA

$$\frac{dn_e(t)}{dt} + [\beta n + (t) + \alpha_e - G]\, n_e(t) = Q(t),$$

$$\frac{dn_-(t)}{dt} + [\gamma n + (t)]\, n_-(t) = \alpha_e\, n_e(t),$$

$$\frac{dn_+(t)}{dt} + [\beta n_e(t) + \gamma n_-(t)] = Q(t) + G\, n_e\,(t),$$

AIR CONDUCTIVITY $\quad \sigma = q\,(\mu_e n_e + \mu_i (n_- + n_+)$

- CONDUCTIVITY σ FEEDS BACK INTO MAXWELL'S EQUATIONS

$$\nabla \times \bar{E} = -\mu \frac{\partial \bar{H}}{\partial t}$$

$$\nabla \times \bar{H} = \frac{\epsilon \partial \bar{E}}{\partial t} + \sigma \bar{E}$$

- COEFFICIENTS G, α_e, μ_e IN TURN DEPEND UPON E

- COEFFICIENTS ALSO DEPEND UPON HUMIDITY AND AIR PRESSURE

- If we assume space charge neutrality

$$n_+ = n_e + n_-$$

- However, space charge effects are important for corona, so we need to include:

$$\nabla \cdot \bar{J} + \frac{\partial \rho}{\partial t} = 0$$

$$\rho = (n_+ - n_- - n_e)\, q$$

$$\bar{J} = (n_+ \bar{V}_+ - n_- \bar{V}_- - n_e \bar{V}_e)\, q$$

Also need to include particle dynamics

$$\bar{F}_s = q_s (\bar{E} + \bar{V}_s \times \bar{B}), \text{ s Refers to species}$$

RESULTS FOR A ROD-PLANE GAP.
NUMERICAL RESULTS ASSUME SPACE CHARGE NEUTRALITY.

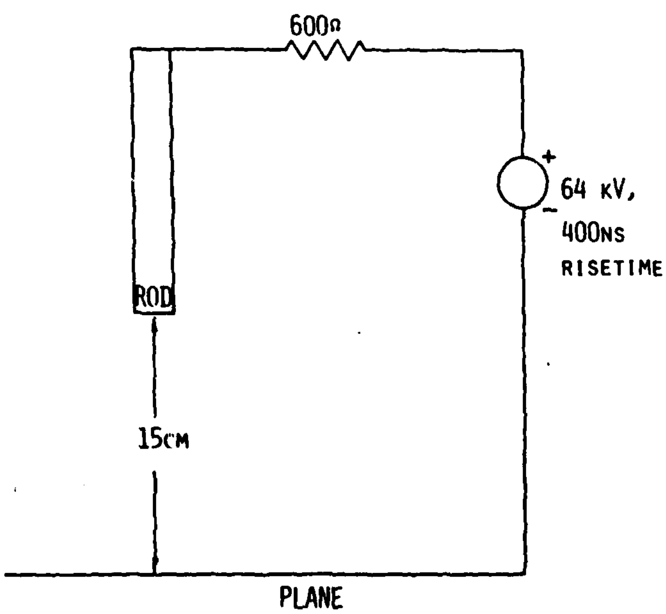

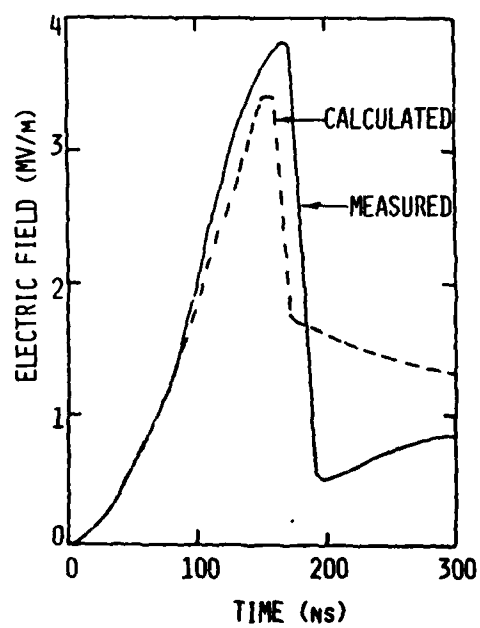

EFFECTS OF NONLINEARITIES

- AIR CONDUCTIVITY MAY SHIELD APERTURES
- AIR BREAKDOWN MAY CAUSE INCREASES IN $\frac{\partial E}{\partial t}$, FOR EXAMPLE, AS INDICATED ON A PREVIOUS SLIDE
- AIRCRAFT COMPLEX RESONANT FREQUENCIES MAY CHANGE BECAUSE CORONA AND STREAMERS EFFECTIVELY EXTEND AIRCRAFT DIMENSIONS

STREAMERS

- BASED ON GROUND MEASUREMENTS, AMPLITUDES LIMITED TO ~100 A
- NO MODEL BASED ON FIRST PRINCIPLES IS KNOWN TO EXIST FOR STREAMER FORMATION AND PROPAGATION
- AT PRESENT, MODELING IS PROBABLY BEST ACCOMPLISHED BY PRESCRIBING NONLINEAR CURRENT SOURCE REPRESENTATIONS

AN ANALYSIS METHOD FOR THE F-106 DIRECT STRIKE DATA

by

Dr. T. F. Trost

Texas Tech University

Summary of characteristics of electric and magnetic fields and currents measured during strikes. Description of laboratory modeling of direct strike fields and currents including test apparatus, airplane model, and data acquisition system. Comparison of model results with in-flight data: Resonances, attachment points, and waveforms. First order interpretation of in-flight data as a lightning input-aircraft response problem.

F-106 DIRECT STRIKE DATA

OBJECTIVES

I. MEASURE STRENGTHS AND WAVEFORMS OF ELECTRIC AND MAGNETIC FIELDS ON AIRCRAFT

II. INTERPRET WAVEFORMS
   A. DETERMINE WHICH CHARACTERISTICS OF WAVEFORMS ARE DUE TO ELECTROMAGNETIC MODES OF AIRCRAFT/CHANNEL
   B. INFER NATURE OF IONIZATION PROCESSES
   C. STATE IMPLICATIONS OF MEASURED WAVEFORMS REGARDING COUPLING TO INTERIOR

APPARATUS FOR
AIRCRAFT-LIGHTNING MODELING

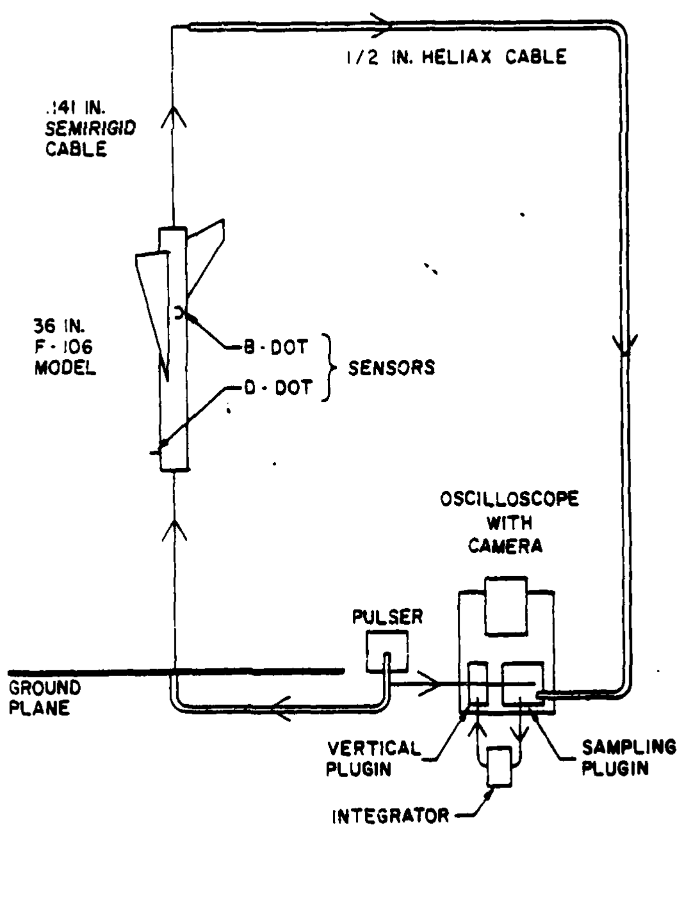

D-DOT AT NOSE

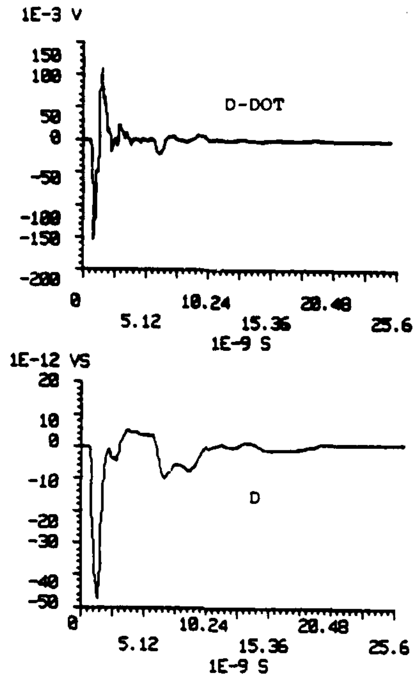

B-DOT AT FUSELAGE

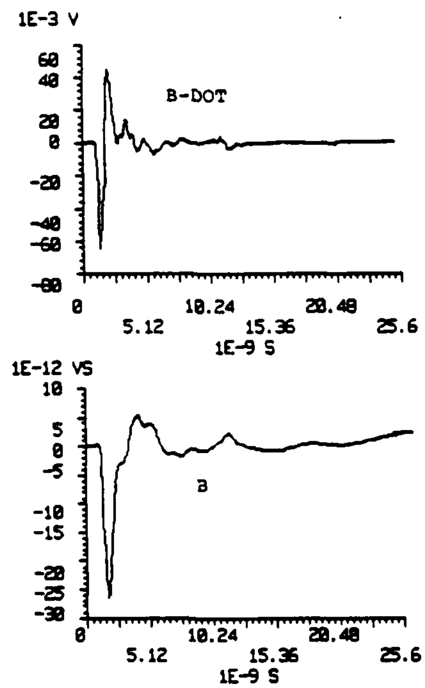

TRANSFER FUNCTIONS
FOR THE F-106 MODEL

FREQUENCY DOMAIN DESCRIPTION

$$\text{TRANSFER FUNCTION} = \frac{\text{FOURIER TRANSFORM OF OUTPUT}}{\text{FOURIER TRANSFORM OF INPUT}}$$

INPUT: B-DOT NEAR LOWER WIRE
OUTPUTS: D-DOT AT NOSE
B-DOT ON FUSELAGE OVER RIGHT WING
B-DOT AT VARIOUS LOCATIONS NEAR SURFACE
D-DOT AT VARIOUS LOCATIONS NEAR SURFACE

EXAMPLES OF TRANSFER FUNCTIONS

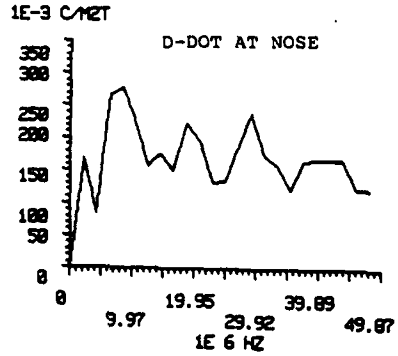

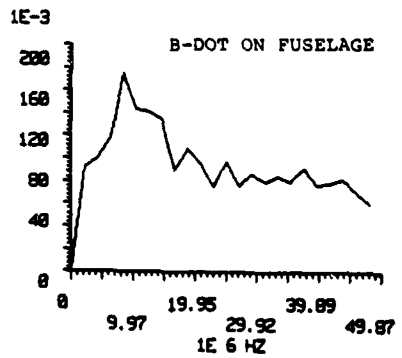

PRONY ANALYSIS OF FIELDS
MEASURED ON THE MODEL

REPRESENT SENSOR OUTPUT WAVEFORMS AS FOLLOWS:

$$V(t) = \sum_{i=1}^{N} A_i e^{\sigma_i t} \cos(\omega_i t + \phi_i)$$

$$= \sum_{i=1}^{2N} R_i e^{s_i t}$$

$s_i = \sigma_i + j\omega_i$ ARE NATURAL FREQUENCIES OR POLES

R_i ARE RESIDUES

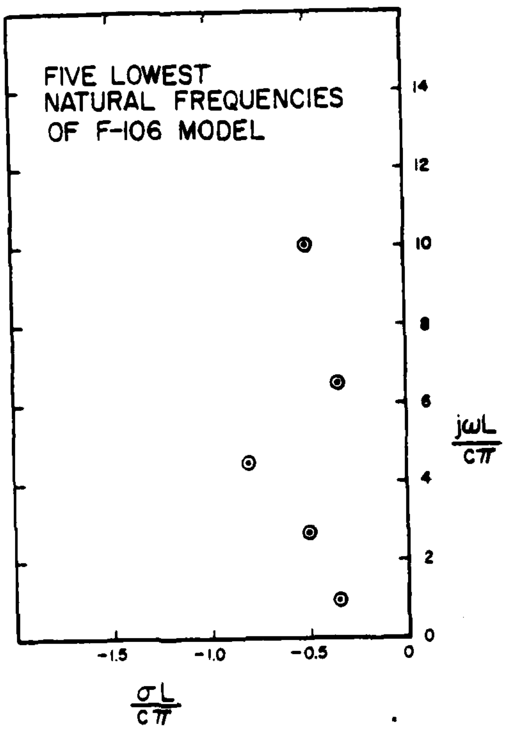

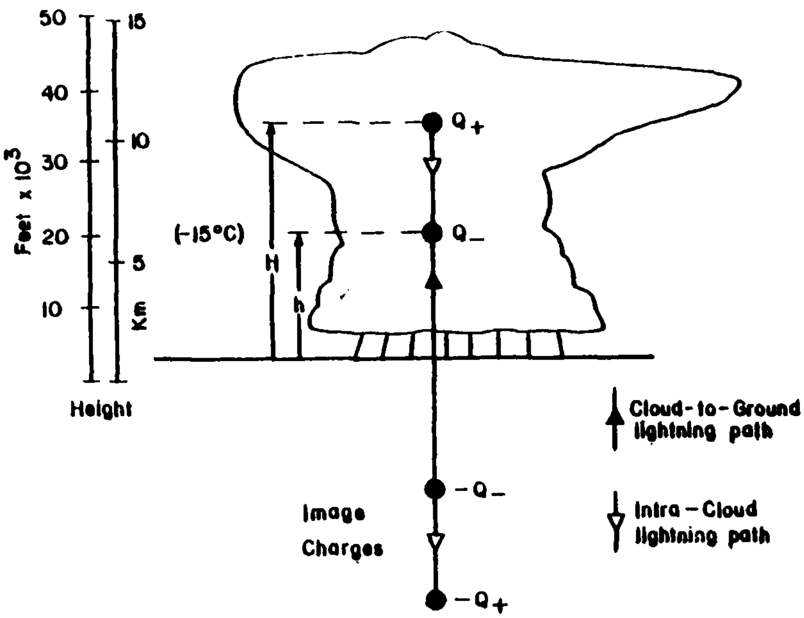

Model of thunderstorm charge distribution.

CHARACTERISTIC TIMES

CORONA CURRENT RISETIME (LABORATORY MEAS.)	10-50 ns
LIGHTNING CURRENT RISETIME (REMOTE ELECTRIC FIELD MEAS.)	30-8000 ns
PERIOD OF LOWEST ELECTROMAGNETIC MODE OF F-106 (LABORATORY SCALE MODEL MEAS.)	110 ns
TIME CONSTANT FOR CHARGING F-106 IN CHANNEL (ESTIMATE)	~250 ns
F-106 DIRECT STRIKE RISETIME OF B	20-40 ns
OF D	20-1000 ns

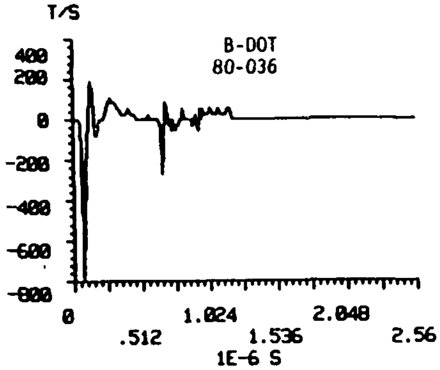
T/S
B-DOT
80-036
400
200
0
-200
-400
-600
-800
0
.512
1.024
1.536
2.048
2.56
1E-6 S

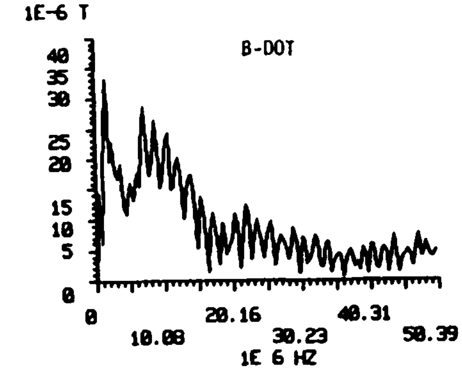
1E-6 T
B-DOT
40
35
30
25
20
15
10
5
0
0
10.08
20.16
30.23
40.31
50.39
1E 6 HZ

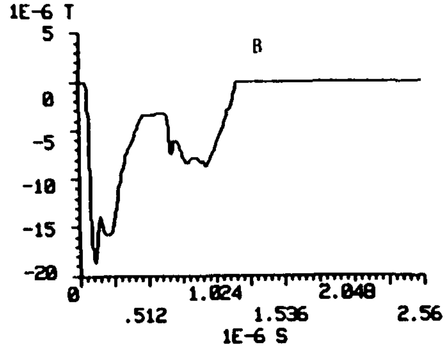
1E-6 T
B
5
0
-5
-10
-15
-20
0
.512
1.024
1.536
2.048
2.56
1E-6 S

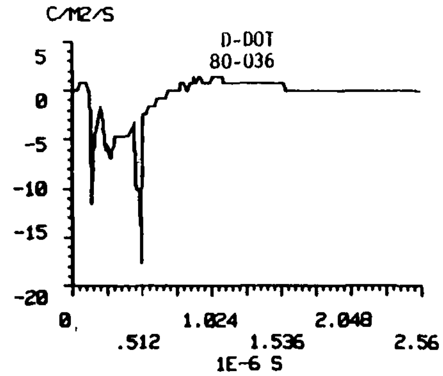
C/M2/S
D-DOT
80-036
5
0
-5
-10
-15
-20
0
.512
1.024
1.536
2.048
2.56
1E-6 S

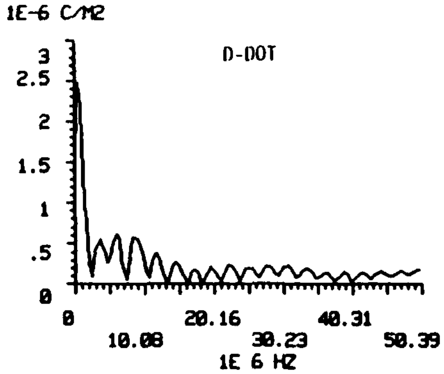
1E-6 C/M2
D-DOT
3
2.5
2
1.5
1
.5
0
0
10.08
20.16
30.23
40.31
50.39
1E 6 HZ

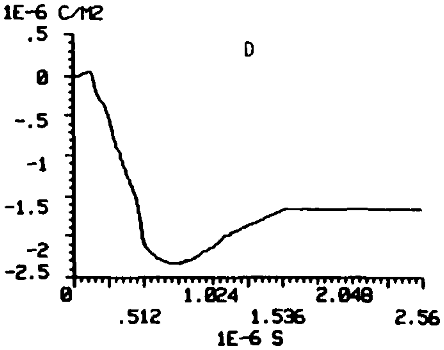
1E-6 C/M2
D
.5
0
-.5
-1
-1.5
-2
-2.5
0
.512
1.024
1.536
2.048
2.56
1E-6 S

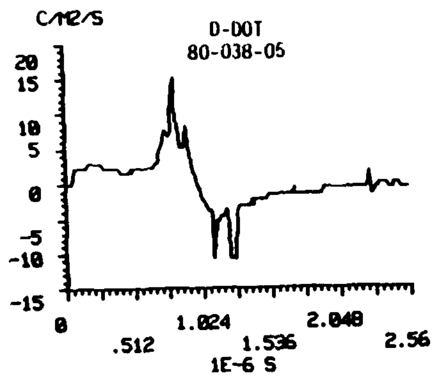
C/M2/S
D-DOT
80-038-05
20
15
10
5
0
-5
-10
-15
0
.512
1.024
1.536
2.048
2.56
1E-6 S

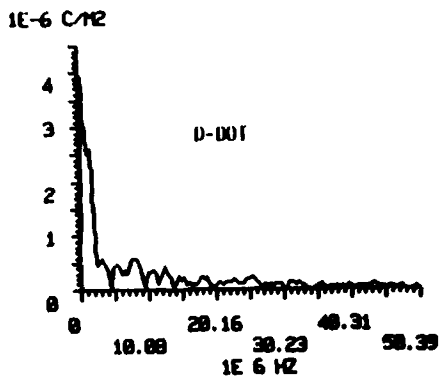
1E-6 C/M2
D-DOT
4
3
2
1
0
0
10.08
20.16
30.23
40.31
50.39
1E 6 HZ

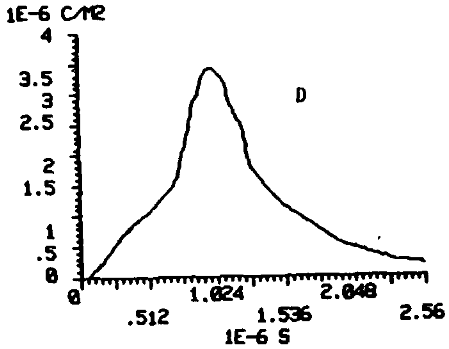
1E-6 C/M2
D
4
3.5
3
2.5
2
1.5
1
.5
0
0
.512
1.024
1.536
2.048
2.56
1E-6 S

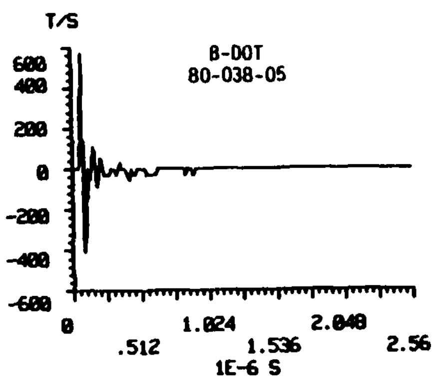
T/S
B-DOT
80-038-05
600
400
200
0
-200
-400
-600
0
.512
1.024
1.536
2.048
2.56
1E-6 S

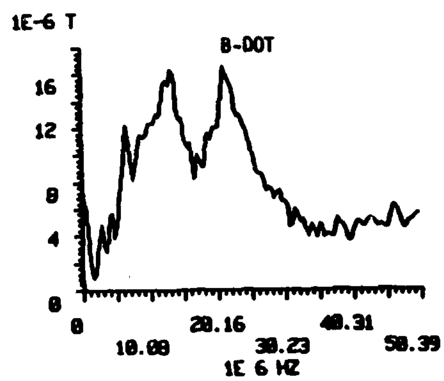
1E-6 T
B-DOT
16
12
8
4
0
0
10.08
20.16
30.23
40.31
50.39
1E 6 HZ

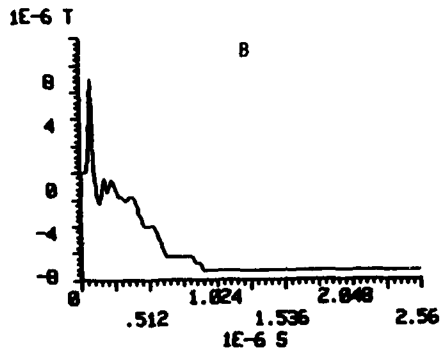
1E-6 T
B
8
4
0
-4
-8
0
.512
1.024
1.536
2.048
2.56
1E-6 S

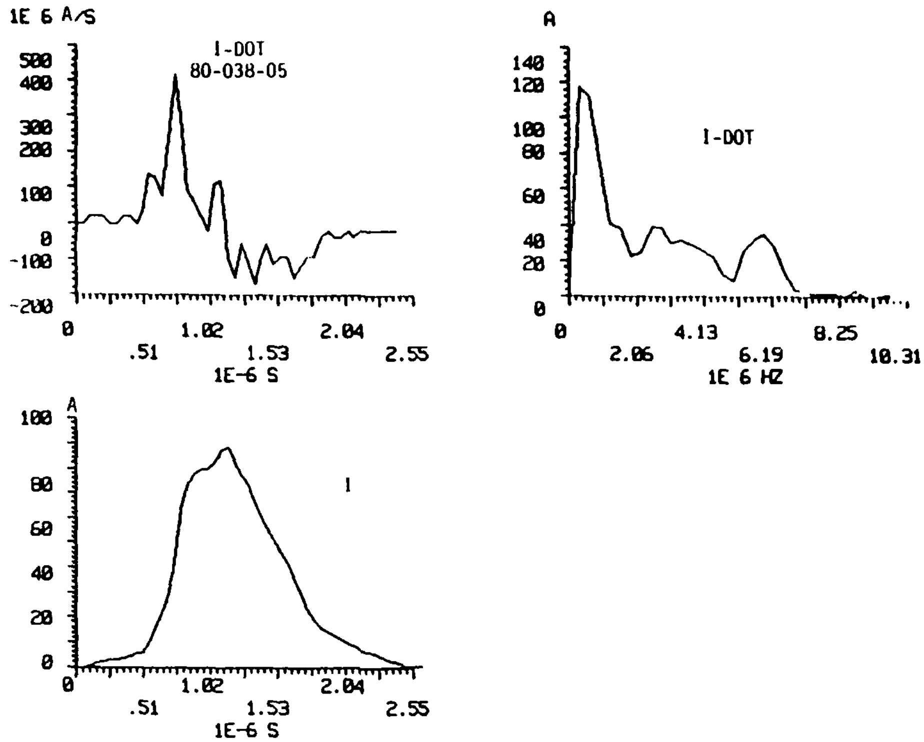

SOME RESULTS FROM COMPARISON
OF MODEL AND IN-FLIGHT DATA

IN-FLIGHT FREQUENCY SPECTRUM PEAKS ARE IN GENERAL AGREEMENT WITH MODES OF MODEL AT 9MHz AND 21 MHz

SHOULD BE ABLE TO *INFER* SOME CHANNEL PROPERTIES FROM IN-FLIGHT SPECTRA

IN-FLIGHT D-DOT WAVEFORMS LONGER DURATION THAN B-DOT WHEREAS DURATIONS SAME ON MODEL

AN OVERVIEW OF THE ELECTRICAL/ELECTROMAGNETIC IMPACT OF ADVANCED COMPOSITE MATERIALS ON AIRCRAFT DESIGN

by

Dr. John C. Corbin, Jr.

Wright-Patterson Air Force Base

The impact of the application of composite structures in aircraft presented from the electromagnetic viewpoint. Fundamental electromagnetic differences between metal and composite aircraft are described and technology developments in shielding effectiveness, joint and fuel system design, and power system/equipment integration are reviewed.

TRENDS IN AIRCRAFT DESIGN

FUEL ECONOMY · NEW ENGINE DESIGNS

· ACTIVE CONTROLS

REDUCED WEIGHT · LIGHTER STRUCTURES

· INCREASED PAYLOAD AND/OR RANGE

DIGITAL ELECTRONICS · HIGH DENSITY PACKAGING

· MICROMINIATURIZATION

· CRITICAL FLIGHT FUNCTIONS

ELECTROMAGNETIC (EM) ENVIRONMENTAL IMPACT

- ELECTRONICS MORE SUSCEPTIBLE TO FAILURE (PERMANENT DAMAGE OR TRANSIENT UPSET)

- CHARACTERISTICS OF THE AIRCRAFT SUBSTANTIALLY CHANGED

TECHNOLOGY TRENDS

TUBES	DISCRETE TRANSISTORS	INTEGRATED CIRCUITS (IC)	LARGE SCALE INTEGRATED CIRCUITS (LSI)	VERY LARGE SCALE INTEGRATED CIRCUITS (VLSI)
 250V 1 WATT/ DEVICE	 TO – 5 12V – 24V 10^{-1} – 10^{-2} WATTS/DEVICE	FLAT PACK  5V – 12V 10^{-2} – 10^{-3} WATTS/TRANS	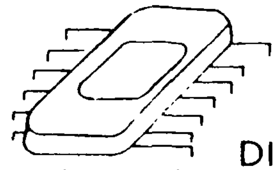 DIP 5V – 7V 10^{-3} – 10^{-4} WATTS/TRANS	CHIP CARRIER 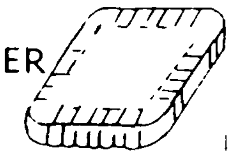 1.5V – 3V 10^{-5} – 10^{-6} WATTS/TRANS
GLASS/ METAL/ CERAMIC	METAL/ CERAMIC	METAL/ CERAMIC/ EPOXY	METAL/ CERAMIC/ EPOXY	CERAMIC/ EPOXY
F – 9, F – 100, F – 106	F – 4, F – 111	F – 14, F – 15	F – 16, F – 18	VSTOL, AFTI
ALUMINUM	ALUMINUM	ALUMINUM/ TITAN	GRAPHITE – EPOXY ALUMINUM	GRAPHITE – EPOXY ?
PRE – 1950'S	1950'S	1960'S	1970'S	1980'S

AD-A114 117 FEDERAL AVIATION ADMINISTRATION TECHNICAL CENTER ATL--ETC F/G 1/3
A COMPENDIUM OF LIGHTNING EFFECTS ON FUTURE AIRCRAFT ELECTRONIC--ETC(U)
FEB 82 N O RASCH
UNCLASSIFIED DOT/FAA/CT-82/30 NL

2 of 3

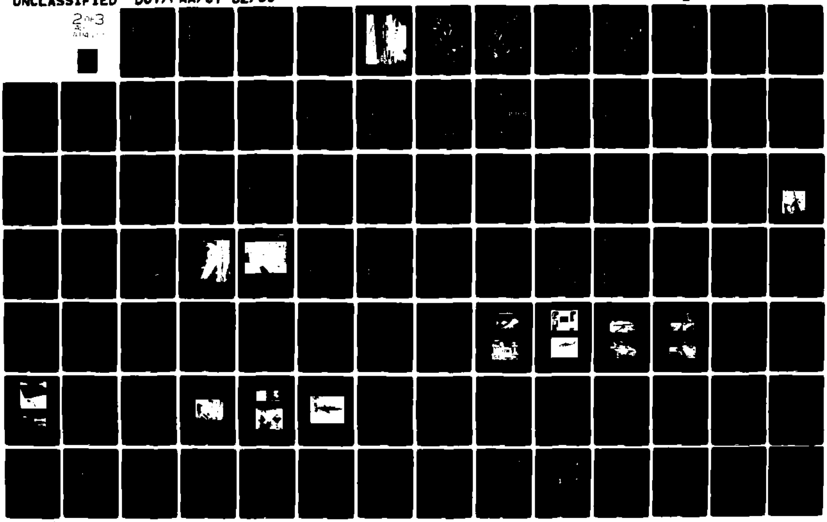

EM FEATURES OF THE ALL-METAL AIRCRAFT

- SHIELDING OF 20 dB OR MORE BETWEEN THE EXTERNAL EM ENVIRONMENT AND INTERNAL AIRCRAFT ELECTRONICS
- READILY AVAILABLE "COMMON GROUND" RETURN PATHS FOR SIGNAL AND POWER
- A LOW RESISTANCE, HIGH CONDUCTIVITY OUTER SKIN FOR CARRYING DIRECT STRIKE LIGHTNING CURRENTS AND DISSIPATING PRECIPITATION STATIC CHARGES
- A RELATIVELY UNBROKEN COUNTERPOISE SYSTEM FOR AIRCRAFT ANTENNAS

ELECTRICAL/ELECTRONIC SYSTEMS

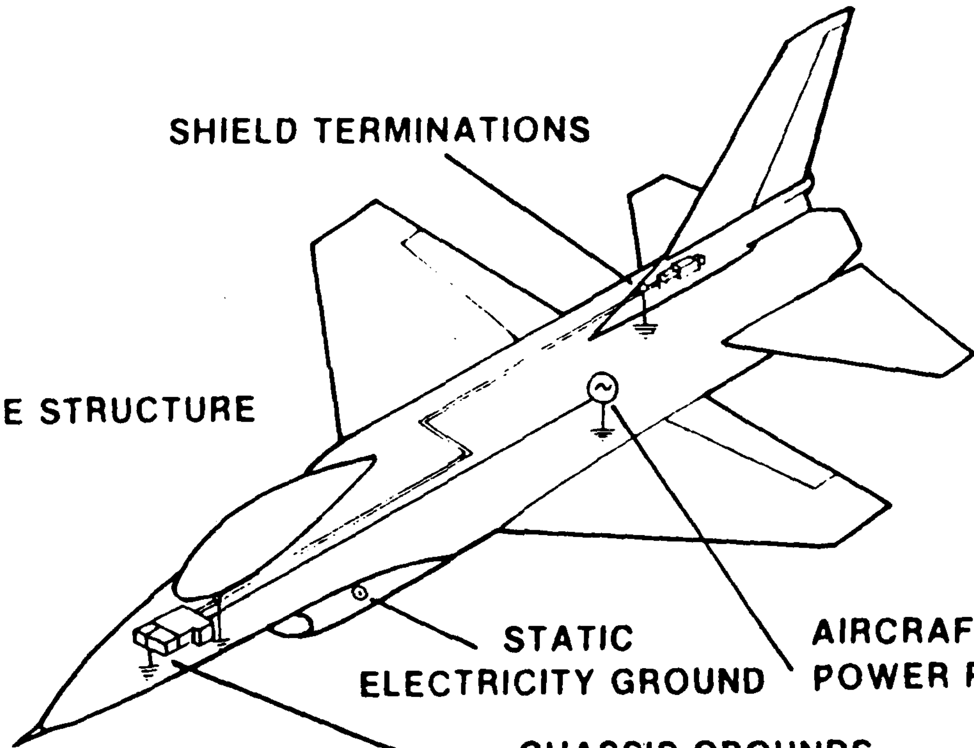

ADVANCED COMPOSITE MATERIALS

- DEFINITION: FIBER-REINFORCED MATERIALS (FIBERS BONDED TO A MATRIX) HAVING PROPERTIES COMPARABLE OR SUPERIOR TO METALS AND FIBERGLASS

- FIBER/MATRIX SYSTEMS IN COMMON USAGE:
  - GRAPHITE/EPOXY
  - BORON/EPOXY
  - KEVLAR/EPOXY
  - HYBRIDS (CARBON, GLASS & KEVLAR)

AIRCRAFT APPLICATIONS

- YF-16 FORWARD FUSELAGE
- F/A 18 HORNET
- AV-8B V/STOL
- 767


U.S. AIR FORCE
01567

F/A-18A MATERIALS DISTRIBUTION

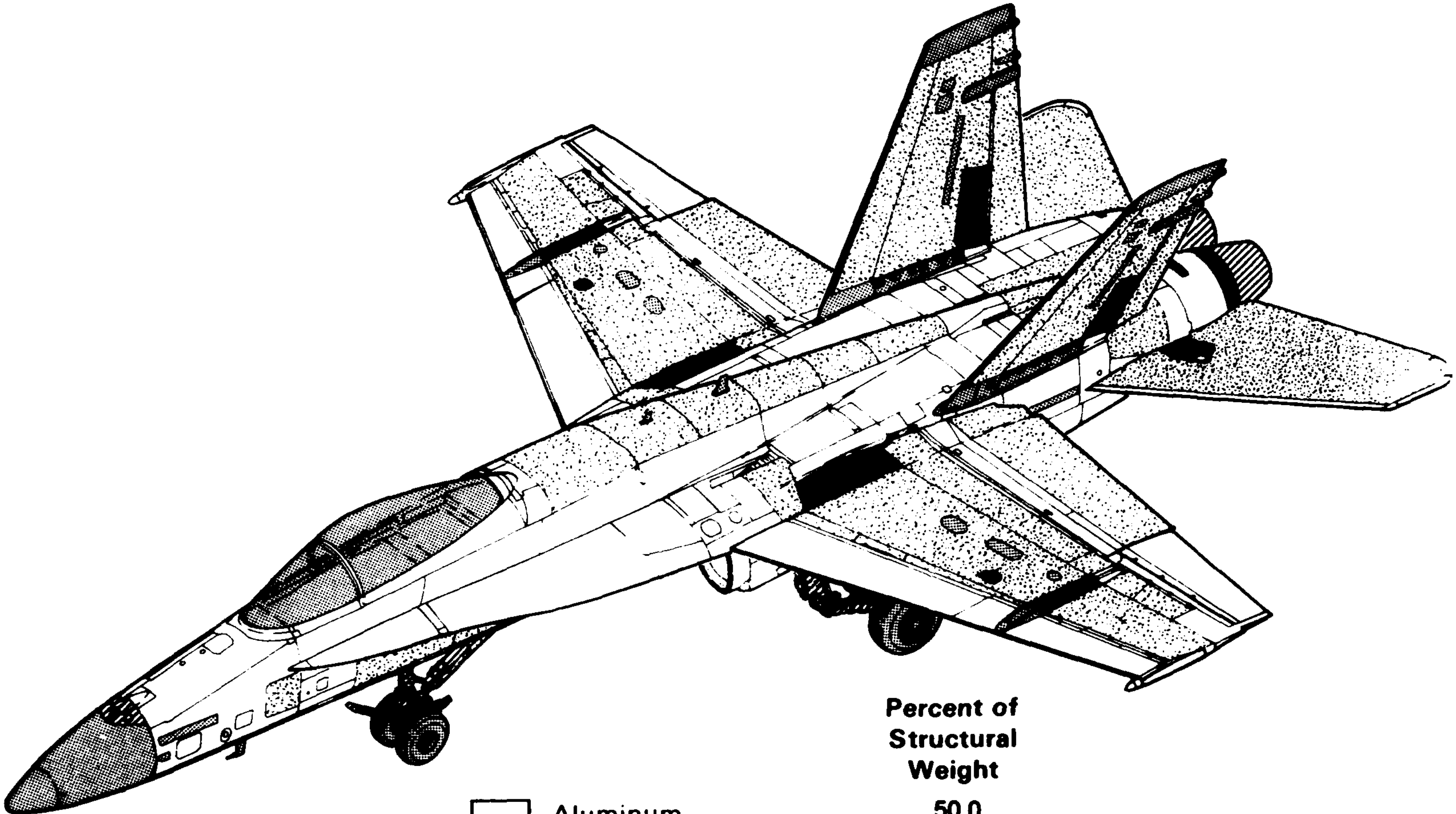

	Percent of Structural Weight
Aluminum	50.0
Steel	15.7
Titanium	13.0
Graphite/Epoxy	9.1
Other	12.2
	100.0

F/A-18A MATERIALS DISTRIBUTION

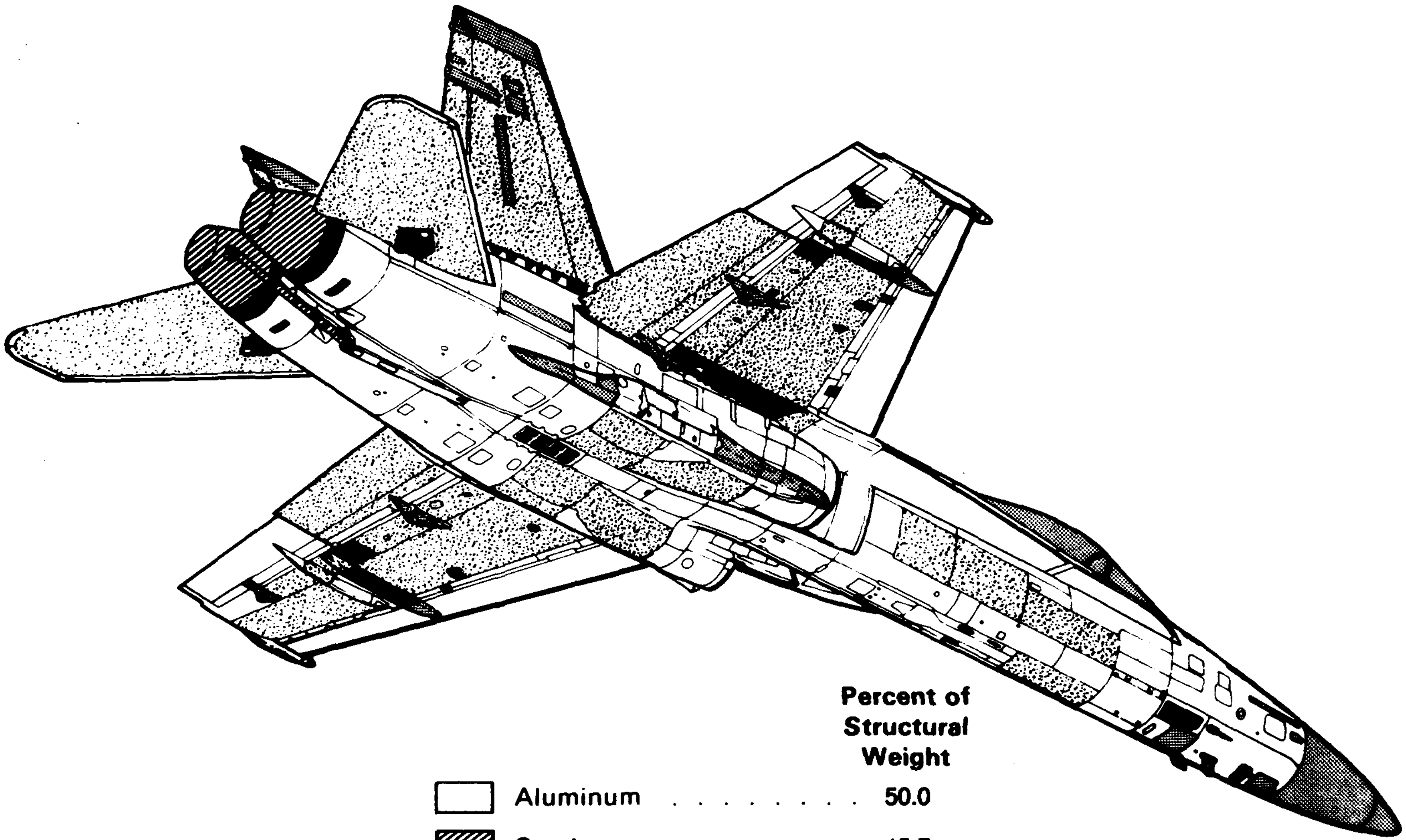

	Percent of Structural Weight
Aluminum	50.0
Steel	15.7
Titanium	13.0
Graphite/Epoxy	9.1
Other	12.2
	100.0

GP13-[illegible]-21
3 FEBRUARY 1981

AV-8B COMPOSITES APPLICATIONS

	STRUCTURAL WEIGHT
GRAPHITE/EPOXY	26.3%
ALUMINUM	47.7%
OTHER	26.0%

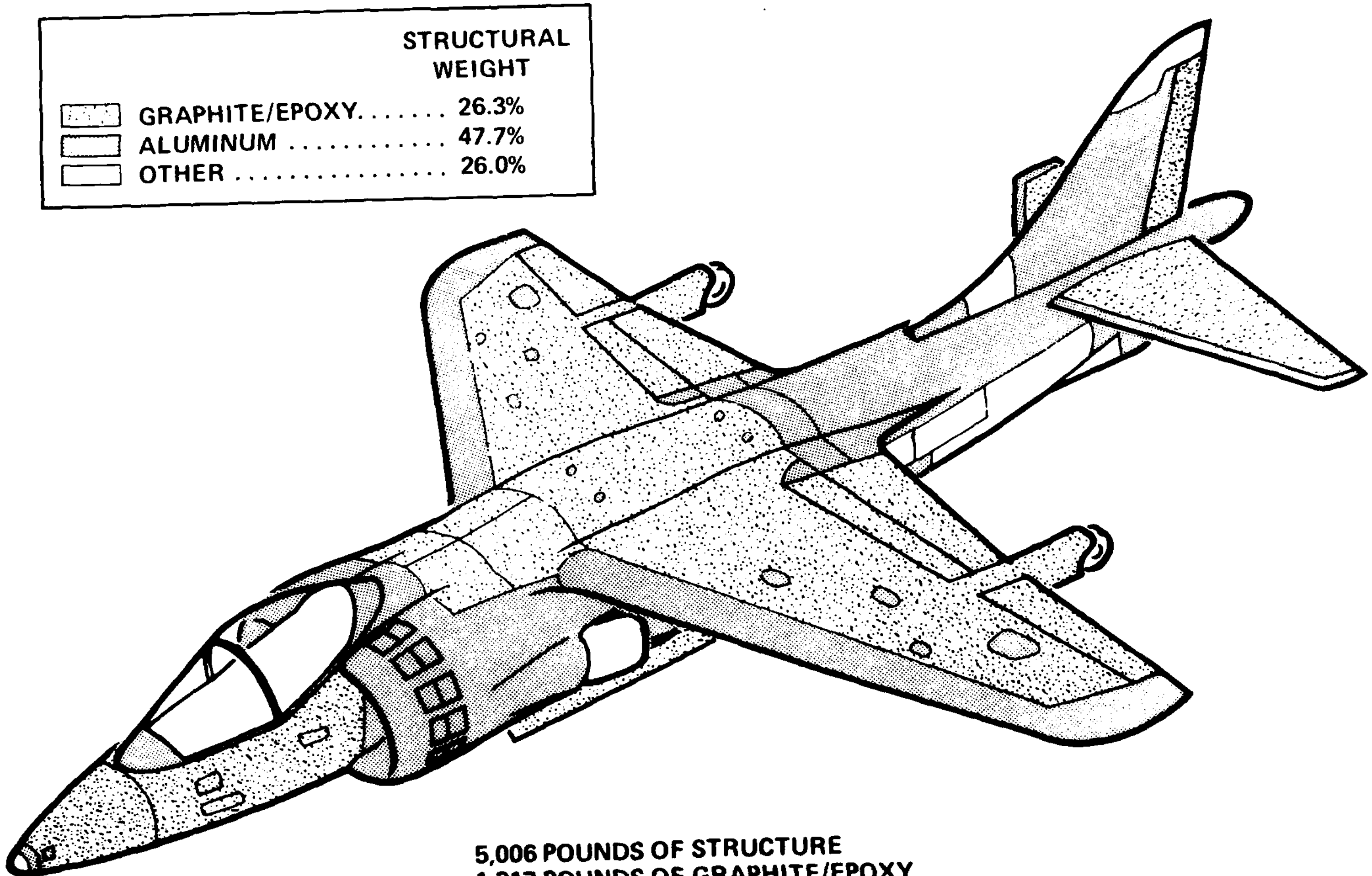

5,006 POUNDS OF STRUCTURE
1,317 POUNDS OF GRAPHITE/EPOXY

767 NON METAL STRUCTURE

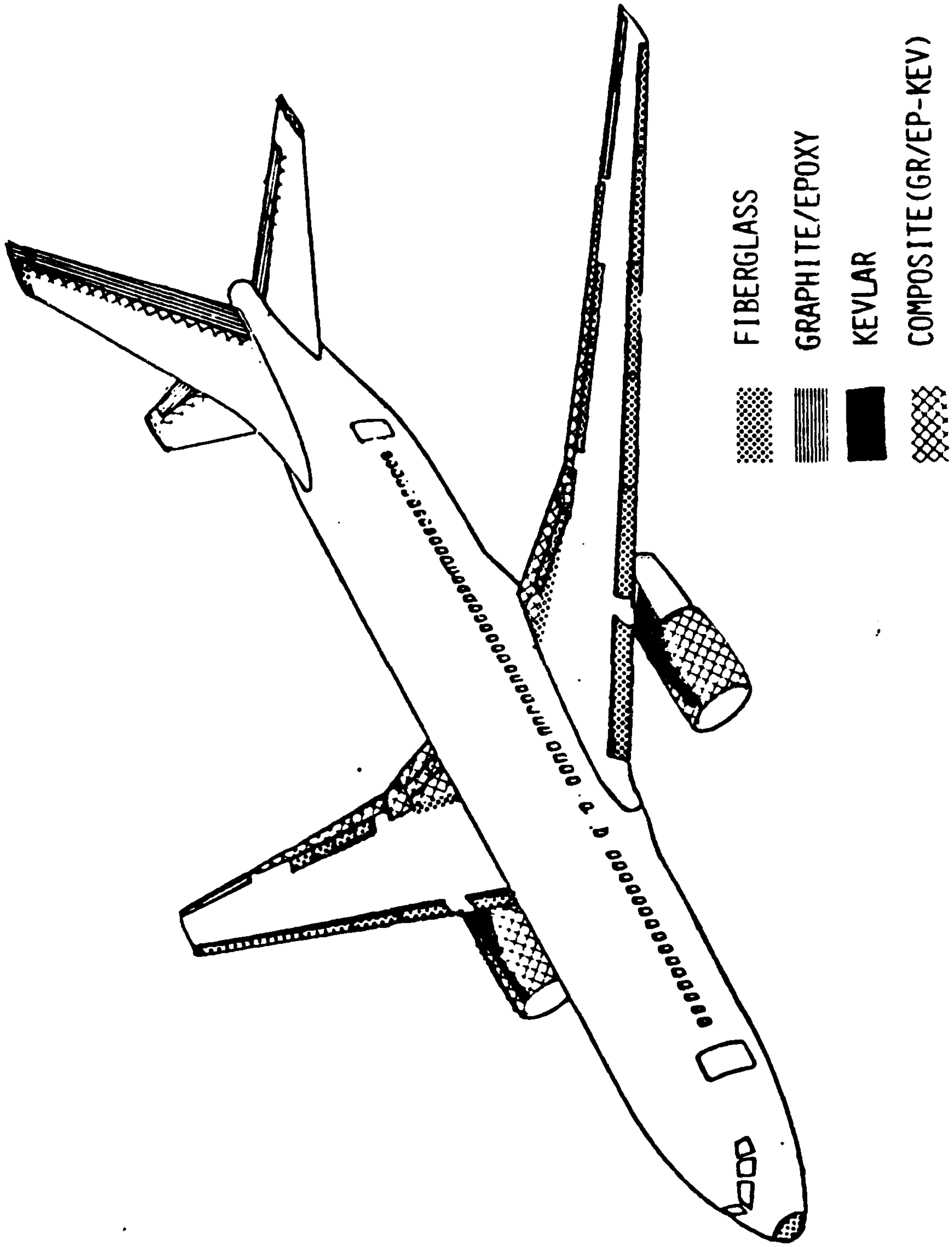

767 NON METAL STRUCTURE

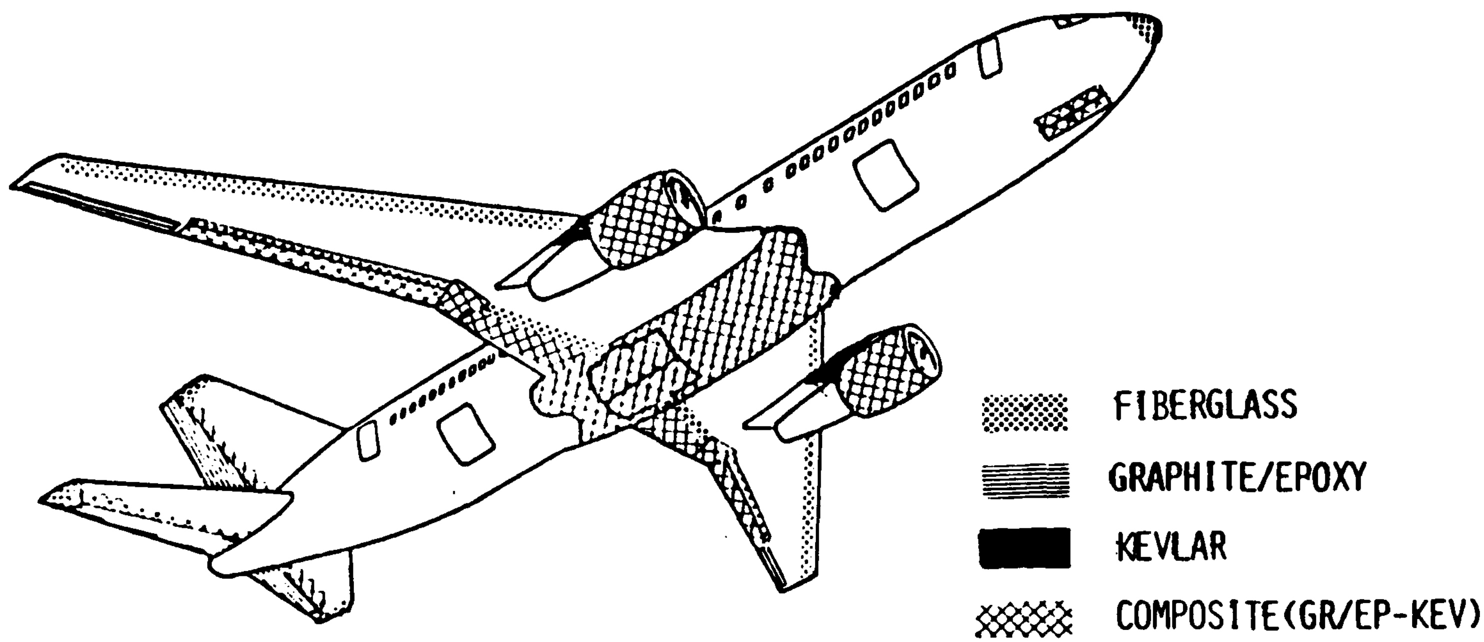

AIR FORCE STUDY (1979)

- **SCOPE:** ASSESS POTENTIAL ELECTRICAL/ ELECTROMAGNETIC IMPACTS OF THE APPLICATION OF ADVANCED COMPOSITE MATERIALS TO AEROSPACE SYSTEMS

- **OBJECTIVES:** IDENTIFY POTENTIAL SUSCEPTIBILITIES OF SYSTEMS

  DETERMINE IF EM ASPECTS ARE BEING FULLY CONSIDERED

  DETERMINE IF EM PROGRAMS ARE IN BALANCE WITH STRUCTURAL PROGRAMS

CONDUCT OF STUDY

- QUESTIONNAIRE SENT TO GOVERNMENT AGENCIES & AEROSPACE CONTRACTORS
- VISITS & IN-DEPTH DISCUSSIONS AT SPECIFIC FACILITIES
- JOINT GOVERNMENT — INDUSTRY MEETING
- BRIEFINGS TO:

SAMSO	NASA
AFWAL	NAVAL ASC
ASD	AFSC (DL/SD)
RADC	USAF (RD)
RAND	DOD (USDR&E)

SCOPE

- MATERIAL CLASS

METALLICS	CONDUCTIVE
GRAPHITE/EPOXIES	
HIGH MODULUS (GY70 - SPECIAL, MISSILE & SPACECRAFT)	REDUCED CONDUCTIVITY
HIGH STRENGTH (T-300, AS - AIRCRAFT)	REDUCED CONDUCTIVITY
FIBER GLASS	DIELECTRIC
KEVLAR	DIELECTRIC

TOPICS

- IMPLEMENTATION ISSUES:
  - DESIGN CAPABILITY
  - DESIGN DATA
- DEVELOPMENT NEEDS
- E/EM CONCERNS
  - LIGHTNING EFFECTS (DIRECT/INDIRECT)
  - STATIC ELECTRIC EFFECTS
  - ANTENNA PERFORMANCE
  - RADAR CROSS-SECTION
  - ELECTROMAGNETIC INTERFERENCE (EMI)
  - ELECTROMAGNETIC COMPATIBILITY (EMC)
  - ELECTROMAGNETIC PULSE (EMP)
  - SYSTEM GENERATED EMP
  - POWER SYSTEM DESIGN
  - SPACE ENVIRONMENT EFFECTS
  - OTHER NUCLEAR EFFECTS

SUMMARIZATION

	INSIGNIFICANT I	MINOR II	INTERMEDIATE III	MAJOR IV	UNKNOWN V	CONDUCTIVITY A	TRANSFER IMPEDANCE B	JOINT IMPEDANCE C	GROUNDING D
LIGHTING DIRECT EFFECT									
STRUCTURAL EFFECTS		X				X			
FUEL SYSTEM EFFECTS			X			X		X	X
LIGHTING INDIRECT EFFECTS			X			X	X	X	X
ANTENNA PERFORMANCE									
HF & LF			X					X	X
VHF -L BAND		X						X	X
ABOVE L BAND			X			X		X	
STATIC ELECTRICITY		X						X	
RADAR CROSS SECTION		X				X			
LOW RCS OBSERVABLE CASE			X					X	
EMI/EMC/EMP			X			X	X	X	X
POWER SUBSYSTEM			X			X		X	X
SYSTEM GENERATED EMP					X	X			
OTHER NUCLEAR EFFECTS					X				
SPACE ENVIRONMENTAL EFFECTS					X				

LEADING CONCERNS

- LIGHTNING
  - SPARK FREE FUEL TANK DESIGN
  - INDIRECT EFFECTS (UPSET/DAMAGE)
- BONDING OF JOINTS AND SEAMS (EMI/EMC, EMP, SGEMP)
  - CORROSION CONTROL
  - ELECTRICAL DURABILITY (A/C AND SPACE)
  - STRUCTURAL/PRODUCIBILITY
- POWER SYSTEM GROUNDING
- HF AND LF ANTENNA TECHNOLOGY
- COMBINED SPACE ENVIRONMENT EFFECTS
- SPECIFIC DATA REQUIREMENTS
- TECHNOLOGY TRANSITION

CONCERNS REFLECT

- MATERIAL PROPERTY DIFFERENCES:
  - REDUCED CONDUCTIVITY
    - REDUCED SURFACE CONDUCTIVITY
    - REDUCED SHIELDING
  - STRUCTURAL JOINT ELECTRICAL CONDUCTIVITY
  - ELECTROCHEMICAL POTENTIAL FOR CORROSION
- LIMITED DATA AND EXPERIENCE:
  - VARYING DEGREES OF CONCERN
  - SOME CONCERNS GENERIC

CONCLUSIONS

- TECHNOLOGY DEVELOPMENT ESSENTIAL IN FIVE MAJOR AREAS:
    - JOINT DESIGN
    - FUEL SYSTEM DESIGN
    - POWER SYSTEM/EQUIPMENT INTEGRATION
    - SHIELDING EFFECTIVENESS
    - RADAR CROSS SECTION

- APPLICATION OF COMPOSITES TO AIRCRAFT IS LOW RISK

- ESTABLISHMENT OF TRI-SERVICE/NASA/FAA WORKING GROUP NEEDED FOR PROGRAM COORDINATION, DEVELOPMENT OF DESIGN GUIDES, HANDBOOKS, STANDARDS AND SPECIFICATIONS, AND DEVELOPMENT OF STANDARD ACCEPTED TEST METHODS FOR CRITICAL AREAS (SUCH AS SHIELDING EFFECTIVENESS)

McAIR ANALYSIS/TEST PROGRAM OF GRAPHITE EPOXY COMPOSITES

- INHERENT SHIELDING
- PANEL SHIELDING
- PANEL/JOINT LEAKAGE
- PANEL JOINT IMPEDANCE
- FUSELAGE SHIELDING
- STATIC WING SHIELDING
- ANTENNA PERFORMANCE
- INTERMODULATION EFFECTS
- LIGHTNING EFFECTS

INHERENT SHIELDING

- COAXIAL LINE FIXTURE (FIGURE 1)
- G/E WASHER SPECIMENS FROM 1, 2, 4, & 8 PLY PANELS
- CW SIGNAL INSERTED/RECEIVED SIGNAL MEASURED
- EFFECTIVE SHIELDING >60 dB FROM 40 KHz - 1 GHz (FIGURE 2)
- SHIELDING PREDOMINANTLY BY REFLECTION

COAXIAL FIXTURE

Coaxial Fixture

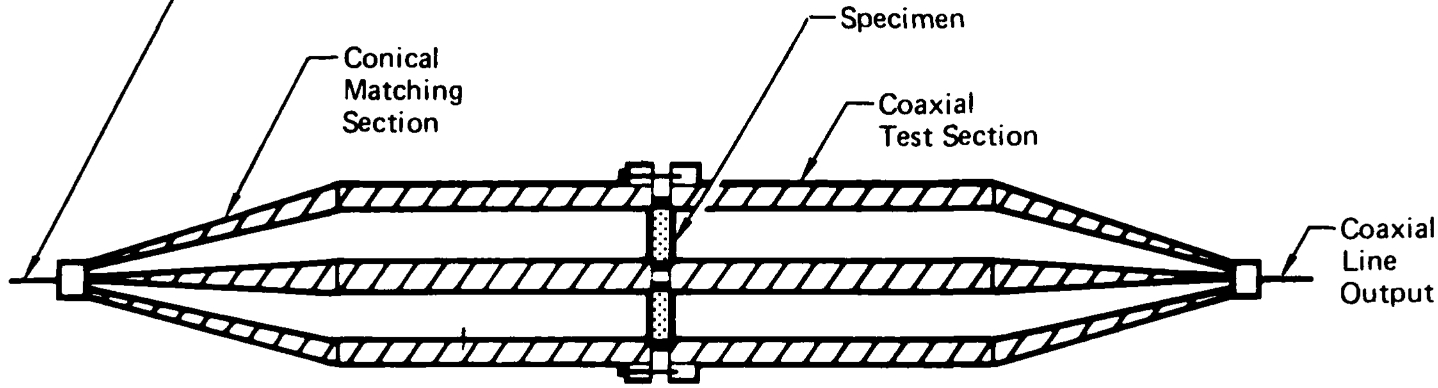

Washer Specimen Mounting Detail

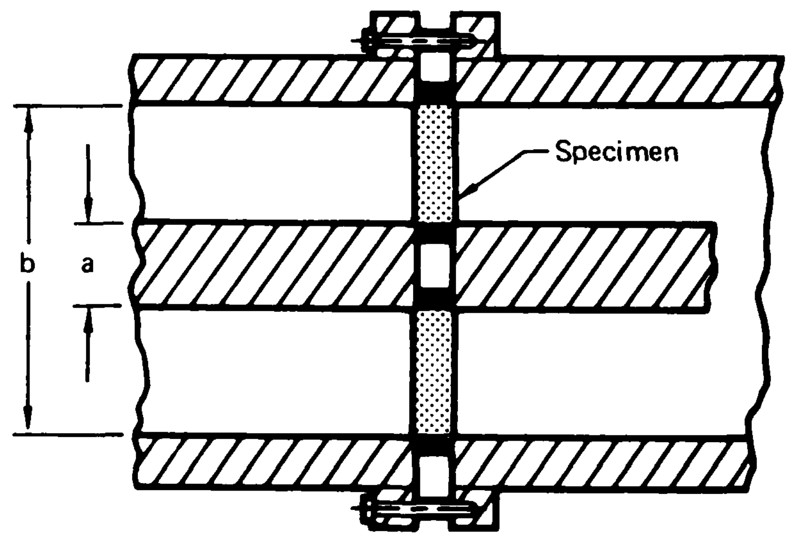

GP03-0153-1

PLANE WAVE SHIELDING MEASURED WITH COAXIAL LINE

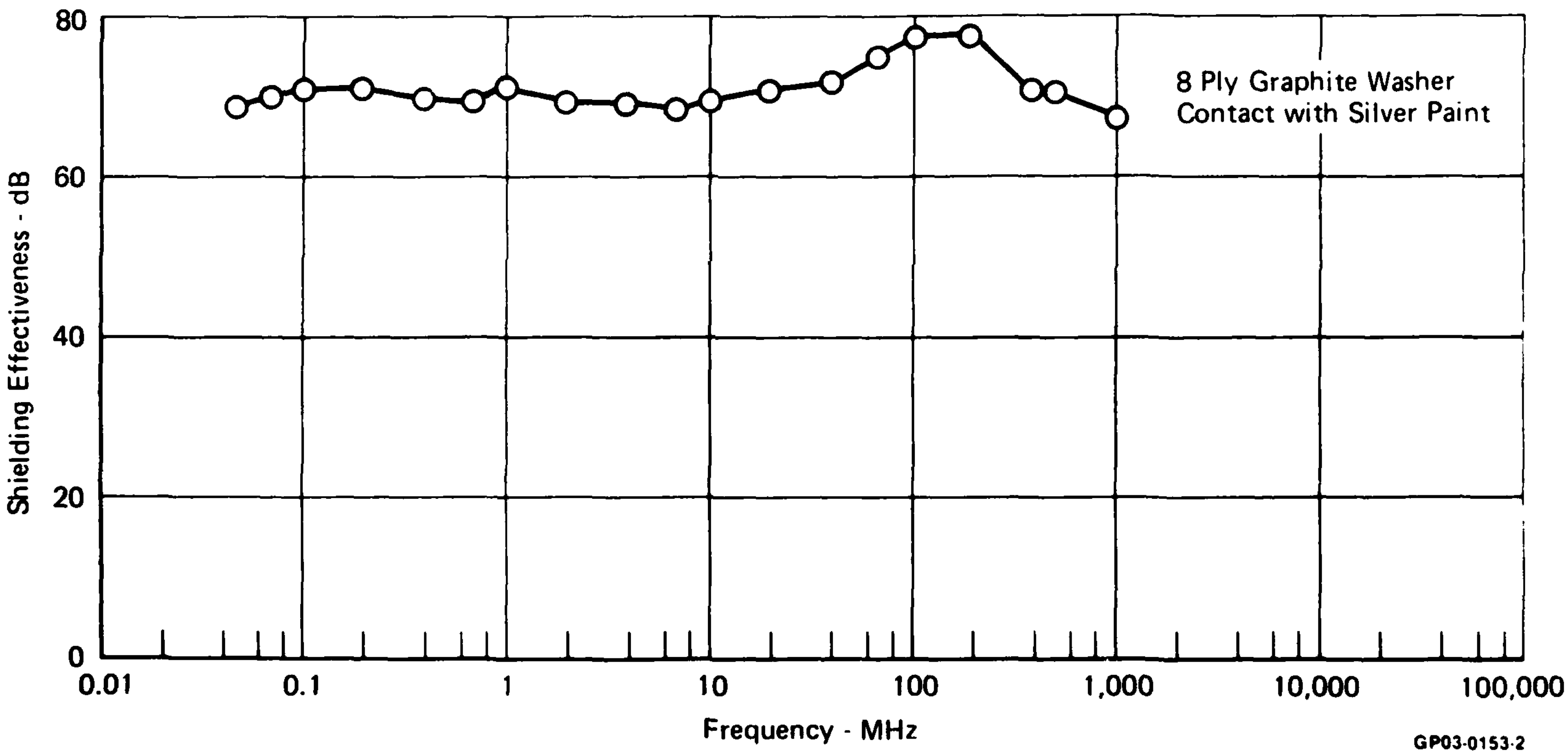

PANEL SHIELDING

- VARIOUS THICKNESSES (1, 2, 4, & 8 PLY)
- VARIOUS CONSTRUCTION TYPES (MONOLYTHIC, HONEYCOMB, SYNTACTIC CORE)
- CUBICAL COPPER BOX FIXTURE (FIGURE 3)
- PLANE WAVE SOURCE (40 KHz - 20 GHz) - ROD ANTENNA SENSOR
- VARIOUS PANEL ATTACHMENTS

    (a) CONTACT MOUNTING (FIGURE 4)
    (b) CONDUCTIVE MOUNTING (EPOXY)
    (c) FASTENER MOUNTING
    (d) CONDUCTING FOIL MOUNTING (FIGURE 5)
    (e) FINGER STOCK MOUNTING

CUBICAL BOX FIXTURE

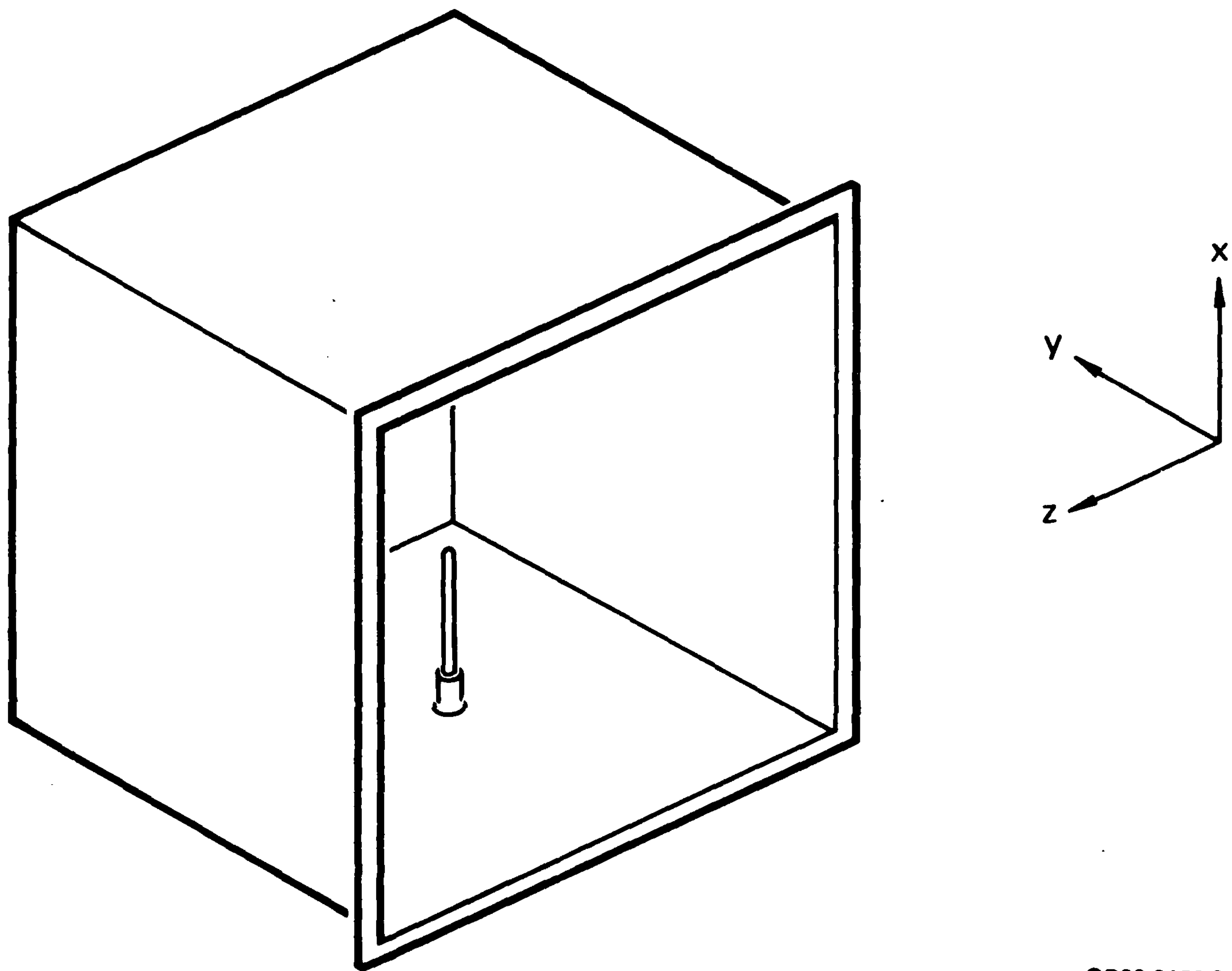

GP03-0153-3

ELECTRIC FIELD SHIELDING FOR GRAPHITE PANELS ON BOX

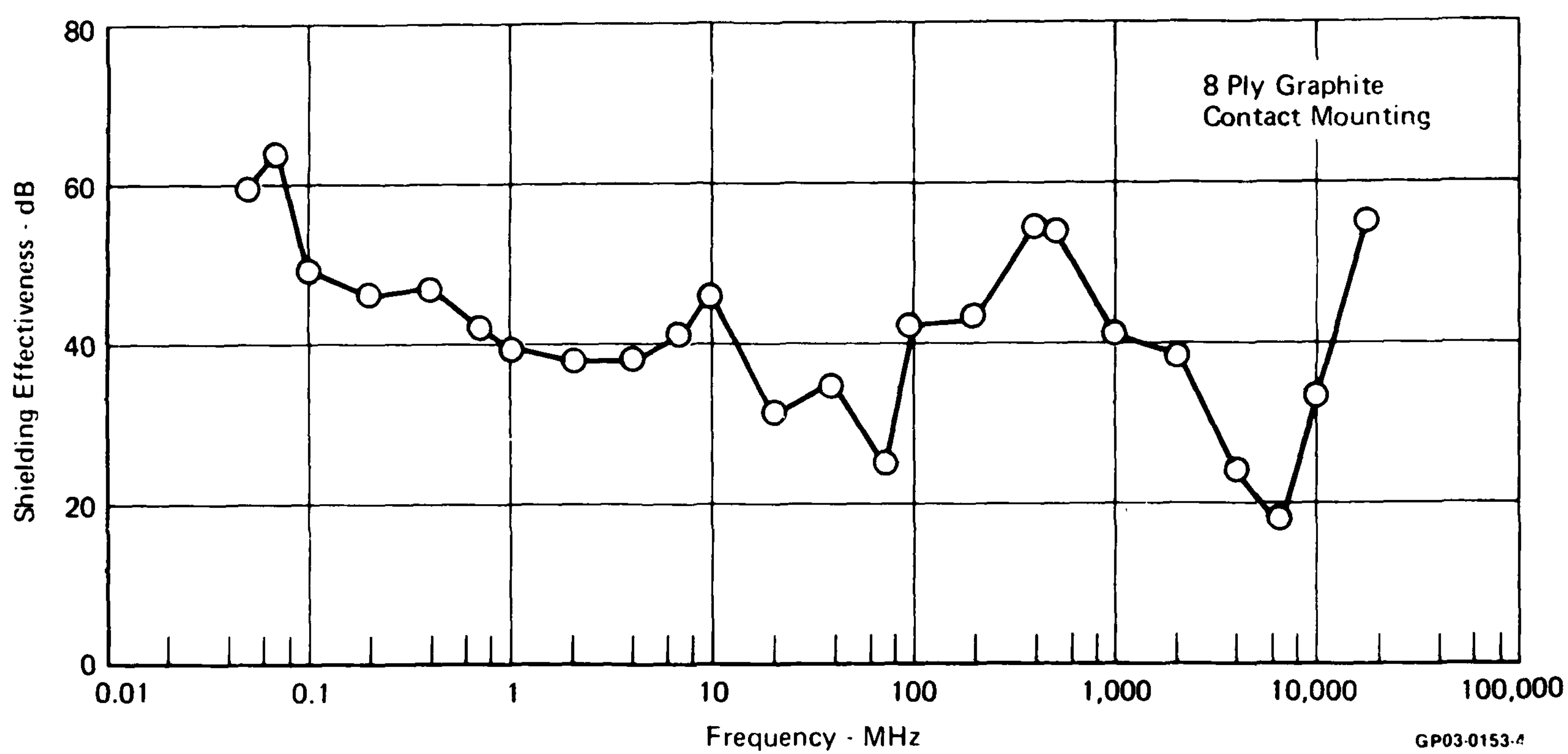

ELECTRIC FIELD SHIELDING FOR GRAPHITE PANELS ON BOX (CAPACITIVELY COUPLED)

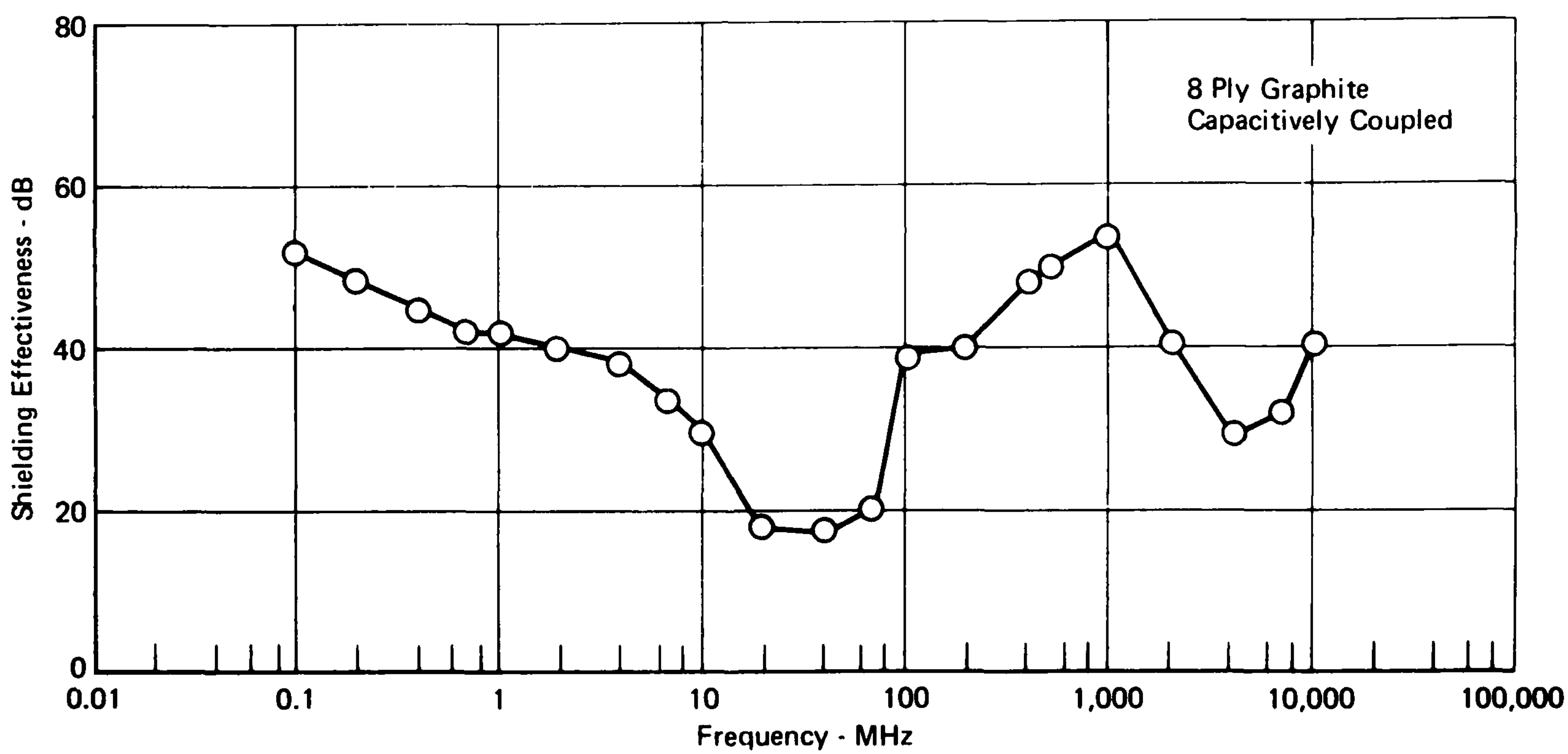

PANEL/JOINT LEAKAGE TESTS

- 13 PANELS TESTED: 4 SOLID, 9 WITH JOINTS (TABLE 1)
- TEST FIXTURE (FIGURE 6)
- RELATIVE PERFORMANCE DATA (TABLE 2)
- CONCLUSIONS
  - TIN PLATING PROVIDED APPRECIABLE PROTECTION IMPROVEMENT THROUGH G/E SINGLE LAP SHEAR JOINTS
  - FINGER STOCKS MOST EFFECTIVE WHEN BONDING IS DESIRED BETWEEN A METALLIC PANEL AND A G/E PANEL
  - TIN PLATING INCREASES SHIELDING EFFECTIVENESS OF NON-JOINTED G/E PANEL

EMI LEAKAGE TEST PANEL LIST

CONFIGURATION IDENT.	CONFIGURATION	JOINT	JOINT SEAL CONFIGURATION
A	G/E Tape Mat'l	None	None
B	G/E Cloth	None	None
C	Aluminum	None	None
D	G/E (Tin Plated)	None	None
G	G/E-Aluminum	Single Lap Shear	Form-In-Place (FIP) Seal
H	G/E-Aluminum	Single Lap Shear	Tin Plated-FIP Seal
J	G/E-Aluminum	Single Lap Shear	FIP Seal
K	G/E-Aluminum	Single Lap Shear	FIP Seal-Finger Stock
L	G/E-G/E	Single Lap Shear	Tin Plated
M	G/E-G/E	Double Lap Shear	Fay Seal
N	Aluminum-Aluminum	Double Lap Shear	Fay Seal
P	G/E-Aluminum	Single Lap Shear	FIP Seal-Finger Stock
R	G/E-G/E	Single Lap	Tin Plated-FIP Seal-Finger Stock

TYPICAL TEST CONFIGURATIONS

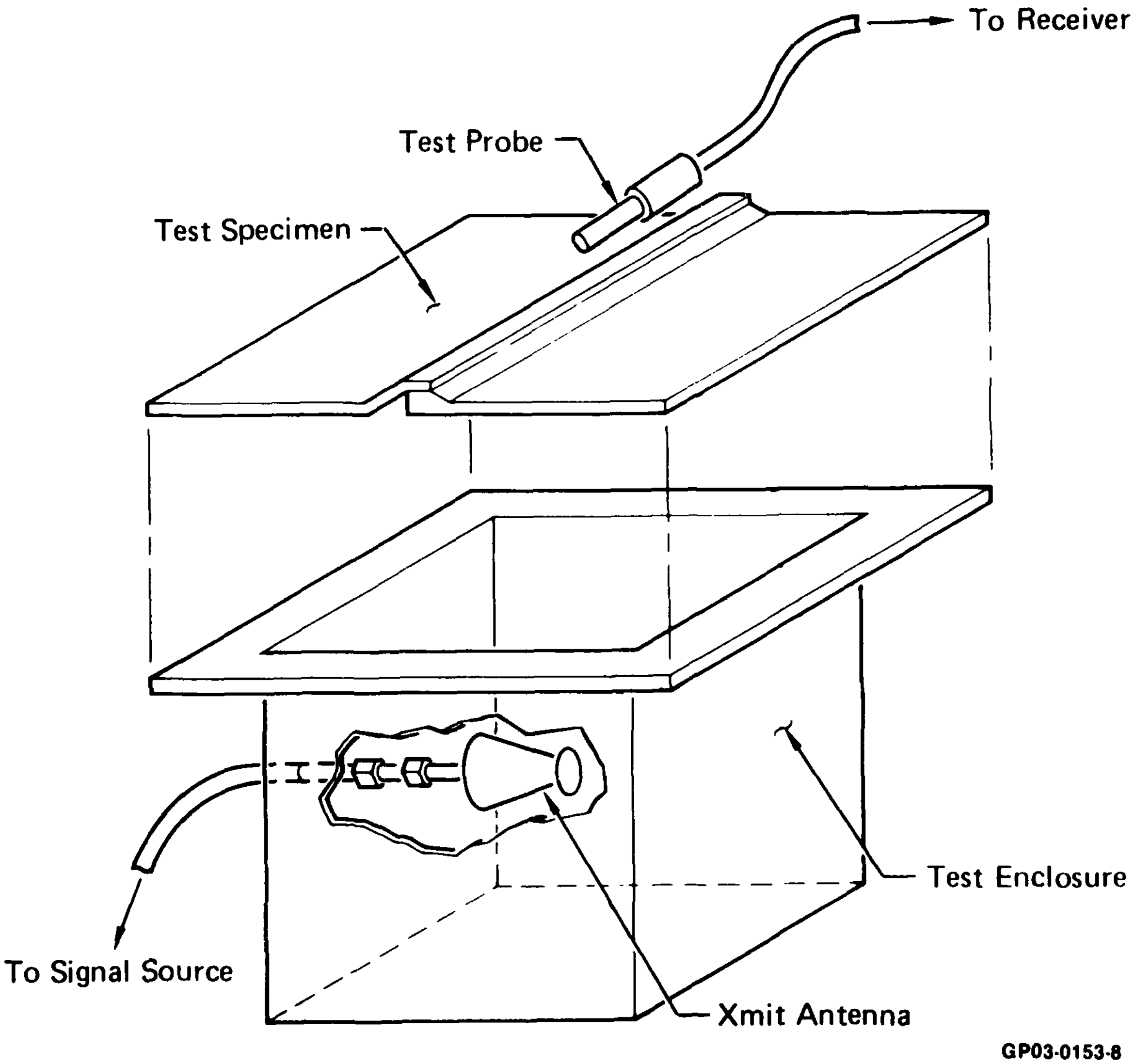

EMI TEST PANEL DATA
RELATIVE PERFORMANCE OF PANELS WITH SEAMS

Test	Panel Description	Seam Preparation (5)	Relative Performance E	Relative Performance H
N	Aluminum-Aluminum	None Double Lap Shear (DLS)	100	97
L	Graphite/Epoxy Cloth - Graphite/ Epoxy Cloth	Tin Plated, Sealed	84	84
P	Aluminum - Graphite/Epoxy Cloth	Bonding Strip, Sealed	69	79
R	Graphite/Epoxy Cloth - Graphite/ Epoxy Cloth	Tin Plated, Bonding Strip Sealed	64	78
G	Aluminum - Graphite/Epoxy Cloth	Sealed	58	99
H	Aluminum - Graphite/Epoxy Cloth	Tin Plated, Sealed	49	96
M	Graphite/Epoxy Cloth - Graphite/ Epoxy Cloth	None (DLS)	50	4
K	Graphite/Epoxy Cloth - Graphite/ Epoxy Cloth	Bonding Strip, Sealed	37	55
J	Graphite/Epoxy Cloth - Graphite/ Epoxy Cloth	Sealed	10	68
C	(4) Aluminum		99	99
D	(4) Tin Plated, Graphite/Epoxy Cloth		95	89
A	(4) Graphite/Epoxy Tape		80	71
B	(4) Graphite/Epoxy Cloth		70	79

NOTES:

1. All panels show relationship to best panel whose value is 100
2. E (electric field)
3. H (magnetic field)
4. One piece panels (no seams)
5. Single lap shear (SLS) unless otherwise indicated
6. The seals are a formed-in-place rubber gasket used to prevent water leaks

PANEL JOINT IMPEDANCE TESTS

- MEASURED JOINT BONDING RESISTANCE/IMPEDANCE AT FREQUENCIES FROM 14 KHz TO 500 KHz (FIGURE 7)
- TESTED SOLID AND JOINTED PANELS (TABLE 3)
- RATIO OF IMPEDANCES OF JOINT TO BULK MATERIAL TABULATED (TABLE 4)
- TIN SPRAYING AT THE JOINT INTERFACE IMPROVED RATIO

ADJACENT GRAPHITE/EPOXY AND ALUMINUM LIGHTNING ATTACHMENT CHARACTERISTICS

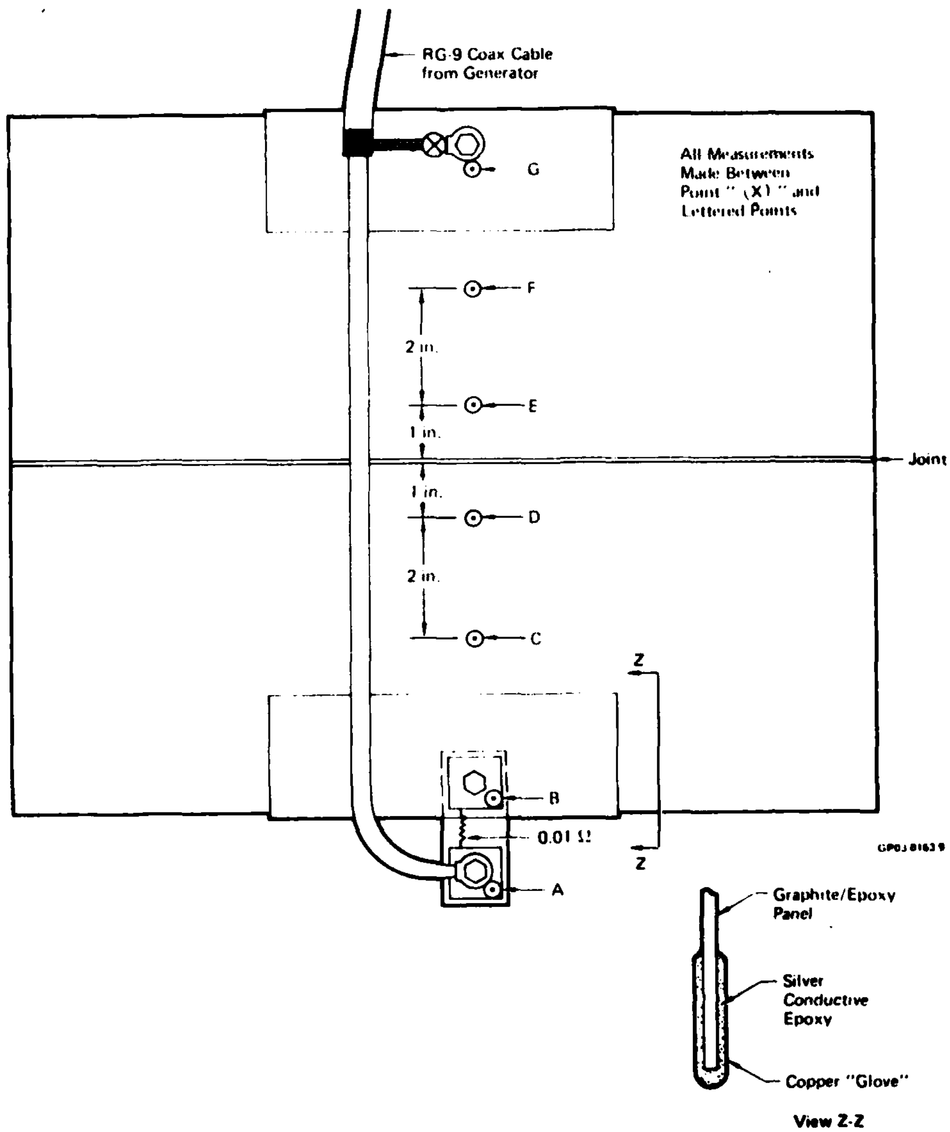

JOINT IMPEDANCE TEST PANEL LIST

CONFIGURATION IDENT.	CONFIGURATION	JOINT	JOINT SEAL CONFIGURATION
B	G/E	None	None
C	Aluminum	None	None
G	G/E-Aluminum	Single Lap Shear	2-Ply Cured Fiberglass
H	G/E-Aluminum	Single Lap Shear	Tin Plate & Form-In Place Seal
J	G/E-Aluminum	Single Lap Shear	Form-In-Place Seal
M	G/E-G/E	Double Lap Shear	Fay Seal
P	Aluminum-G/E	Single Lap Shear	Fip Seal-Finger Stock
R	G/E-G/E	Single Lap Shear	Tin Plate-Fip Seal-Finger Stock

RATIO OF IMPEDANCES

PANEL	TYPE	D.C. RESISTANCE (OHMS)	Ratio of Joint-Impedance to Bulk Material			
			14 KHz	42 KHz	112 KHz	500 KHz
B	G/E Cloth	0.03	1.0	1.0	1.0	1.0
C	Aluminum	0.0	1.0	1.0	1.0	1.0
G	G/E-Alum SLS	0.013	2.3	2.4	2.1	2.8
H	G/E-Alum SLS	0.01	1.0	1.0	1.0	1.0
J	Al-G/E SLS	0.03	7.0	10.4	5.9	1.8
M	G/E DLS	0.41	42.5	42.5	42.5	30.0
P	G/E-Alum SLS	0.013	1.0	1.0	1.0	1.0
R	G/E SLS	0.012	1.0	1.0	1.0	1.0

FUSELAGE SHIELDING

- COMPARED INDUCED VOLTAGES IN TYPICAL AVIONICS BAY FOR METAL AND G/E BOXES (FIGURE 8)
- TESTS CONDUCTED FROM 14 KHz TO 18 GHz
- TESTS CONDUCTED WITH IDENTICAL WIRE BUNDLES, LOAD TERMINATIONS, AND ROUTING LOCATION (FIGURE 9)
- OVER 100 DIFFERENT TEST CONFIGURATIONS (TYPICAL RESULTS SHOWN IN FIGURES 10 AND 11)
- TEST OF SIMULATED FUSELAGE STRUCTURE WITH ACCESS PANEL (FIGURE 12)
- CONCLUSION: LEAKAGE EFFECTS OF JOINTS FOR BOTH ALUMINUM AND G/E ARE DOMINANT FACTOR IN SHIELDING EFFECTIVENESS. LITTLE DIFFERENCE BETWEEN G/E AND ALUMINUM SHIELDING EFFECTIVENESS

FORWARD FUSELAGE EMI TEST ARTICLE

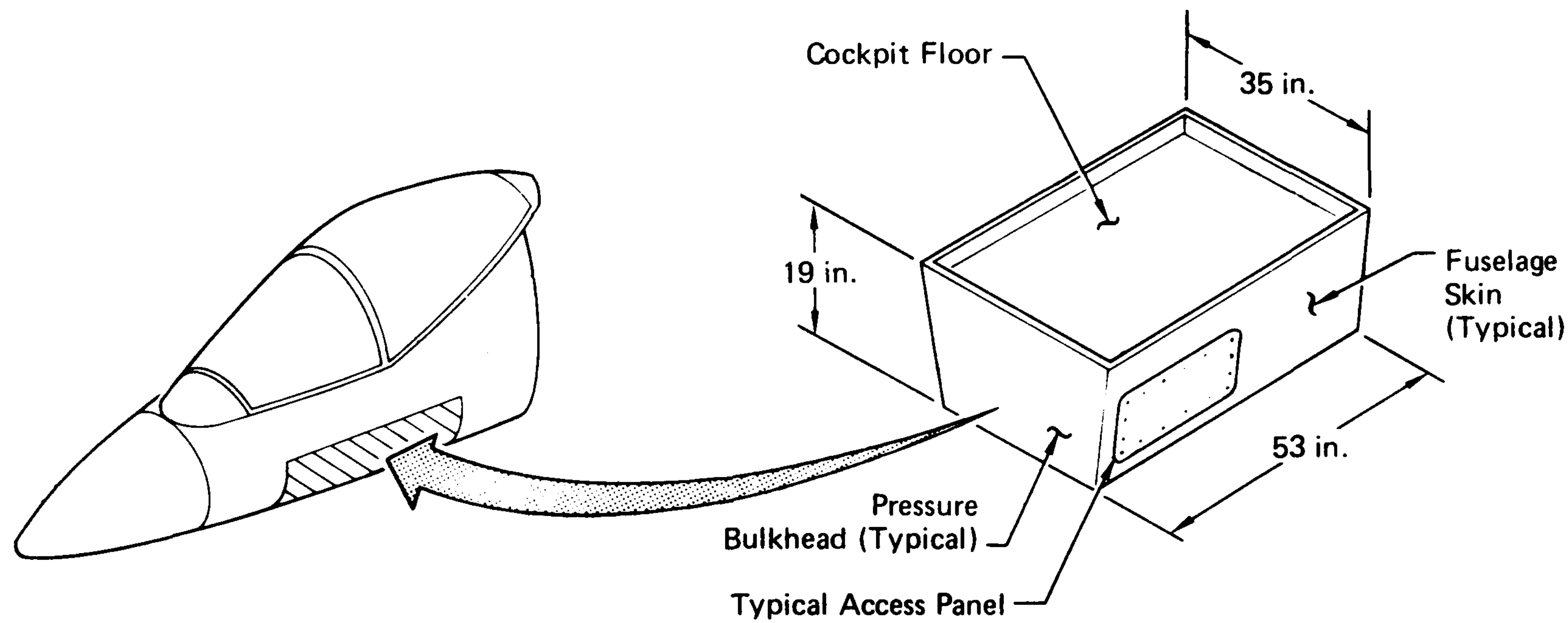

Graphite/Epoxy Test Box and Aluminum Test Box

GP03-0153-10

TRIMETRIC VIEW OF WIRE ROUTING

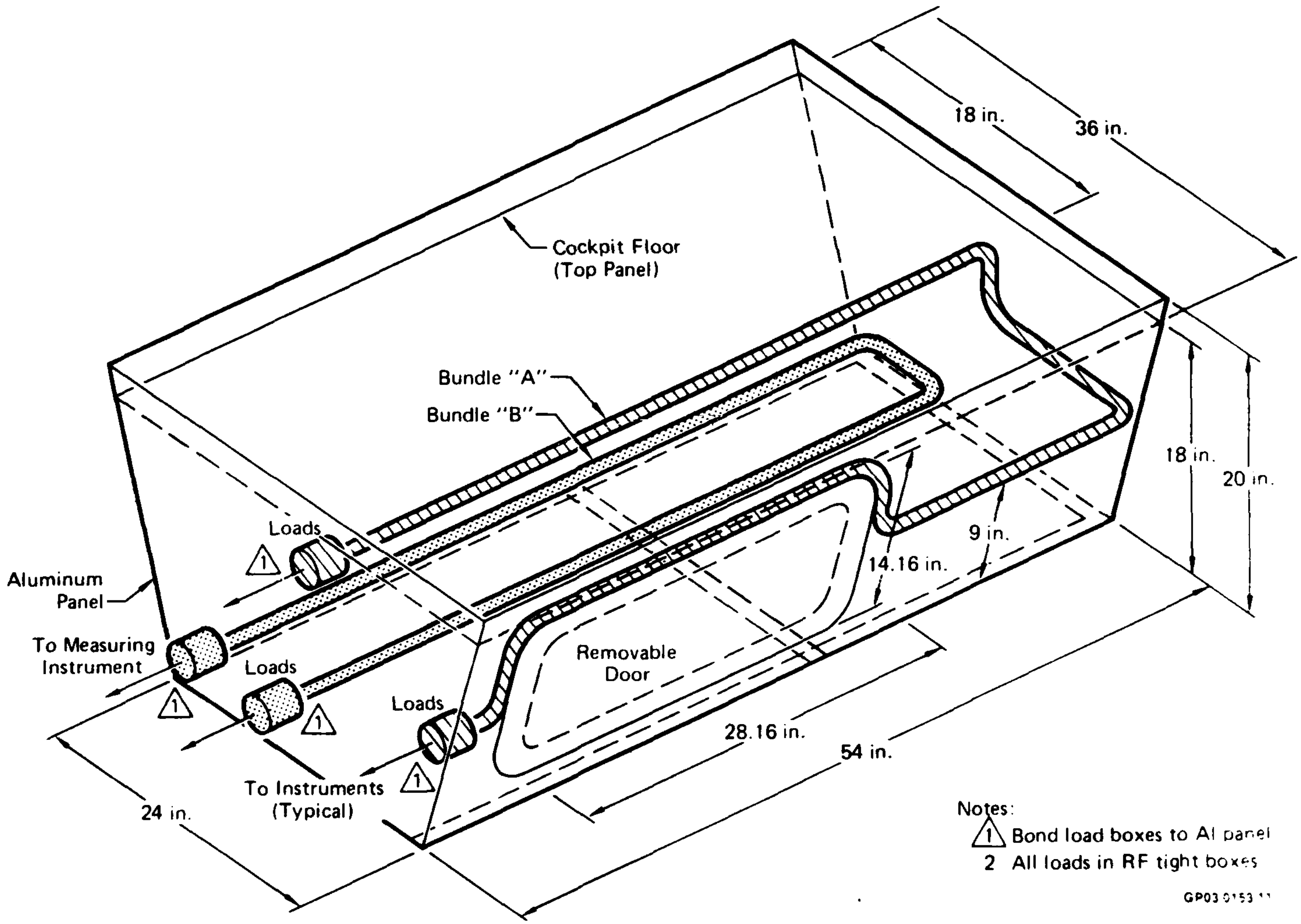

Notes:
1 Bond load boxes to Al panel
2 All loads in RF tight boxes

GP03 0153 11

INDUCED VOLTAGE ON SINGLE WIRE, 1 VOLT/METER FIELD

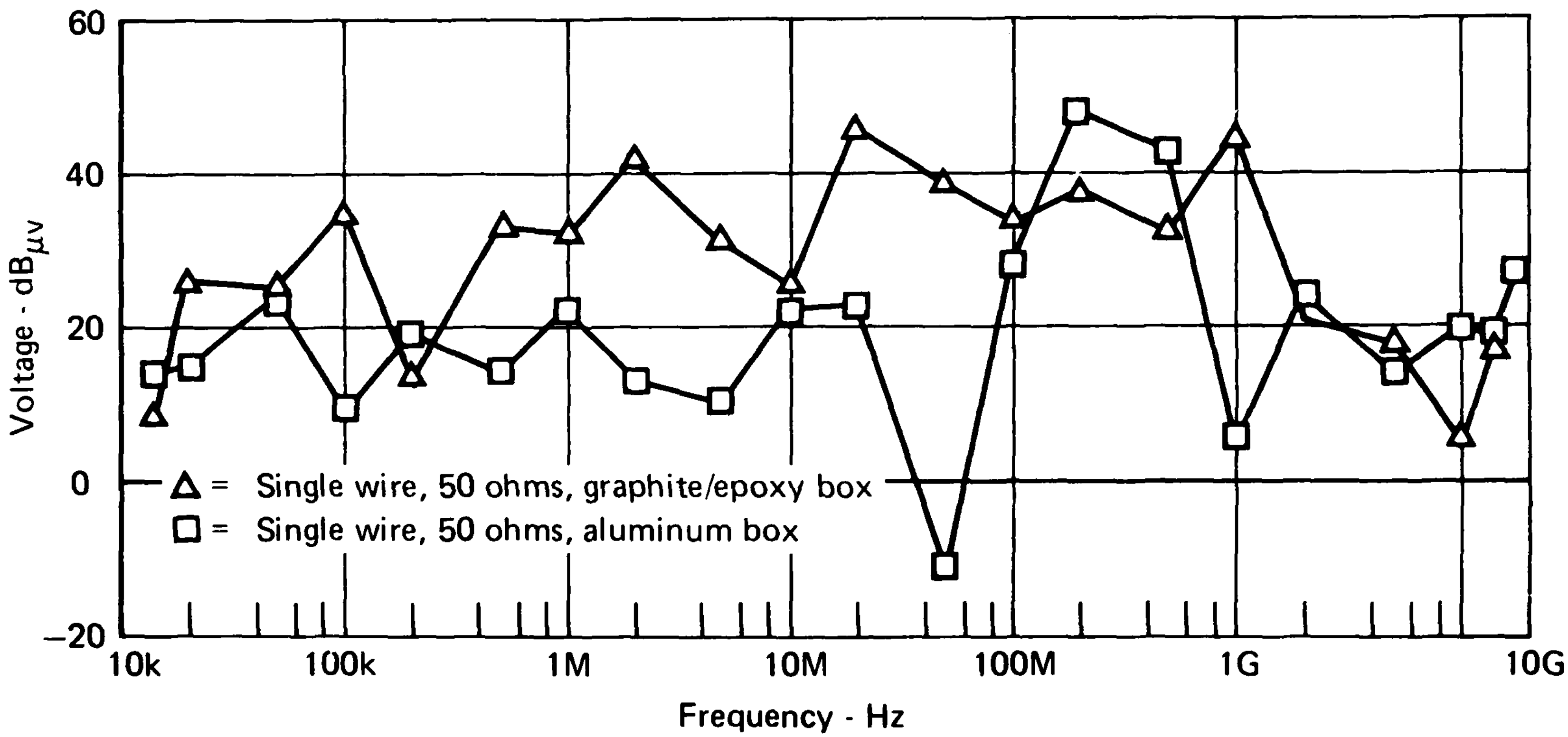

INDUCED VOLTAGE ON TWISTED PAIR, 1 VOLT/METER FIELD

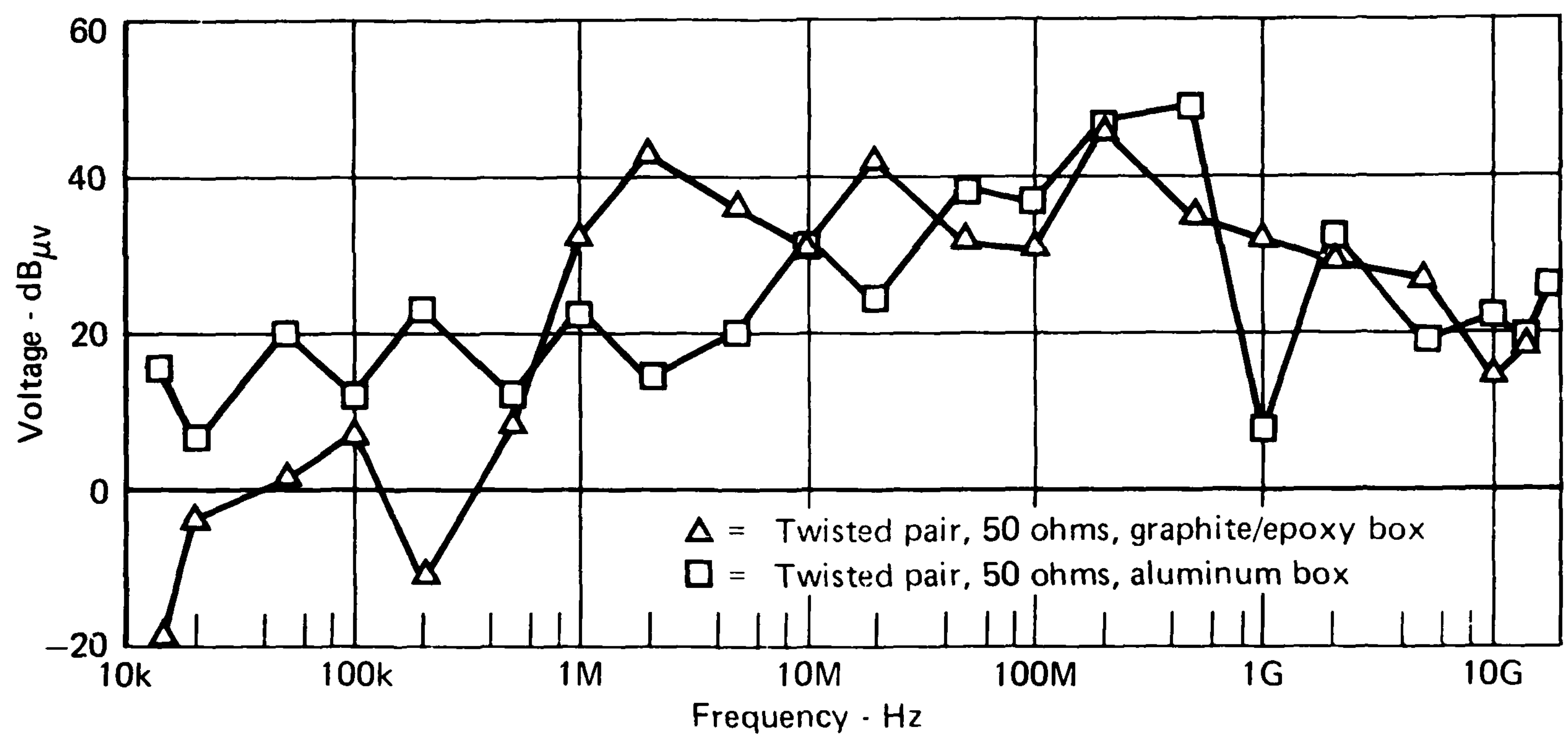

SHIELDING OF ALUMINUM AND COMPOSITE FIXTURES
RELATIVE TO EXPOSED GROUND RETURN WIRE

Test Setup

Simulated Forward Fuselage Structure with Access Panel

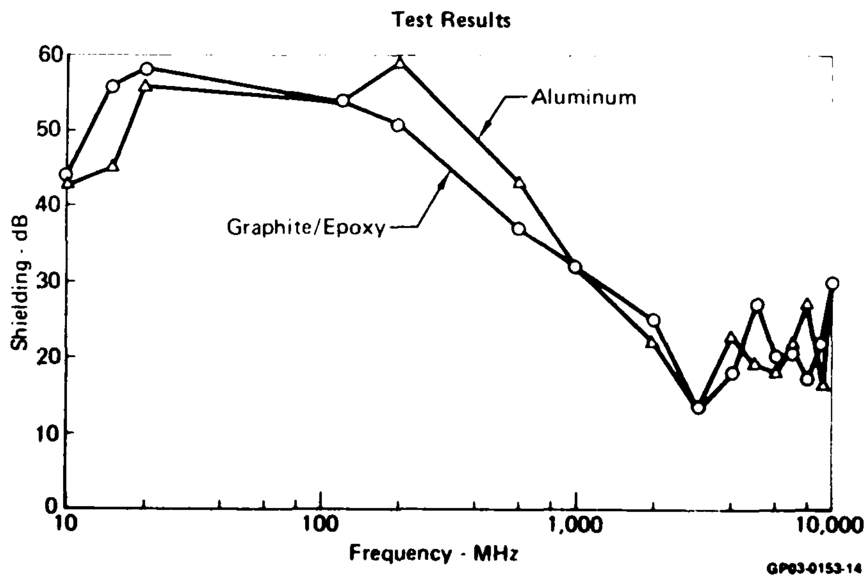

SHIELDING EFFECTIVENESS OF AIRCRAFT STRUCTURES AGAINST MAGNETIC FIELDS

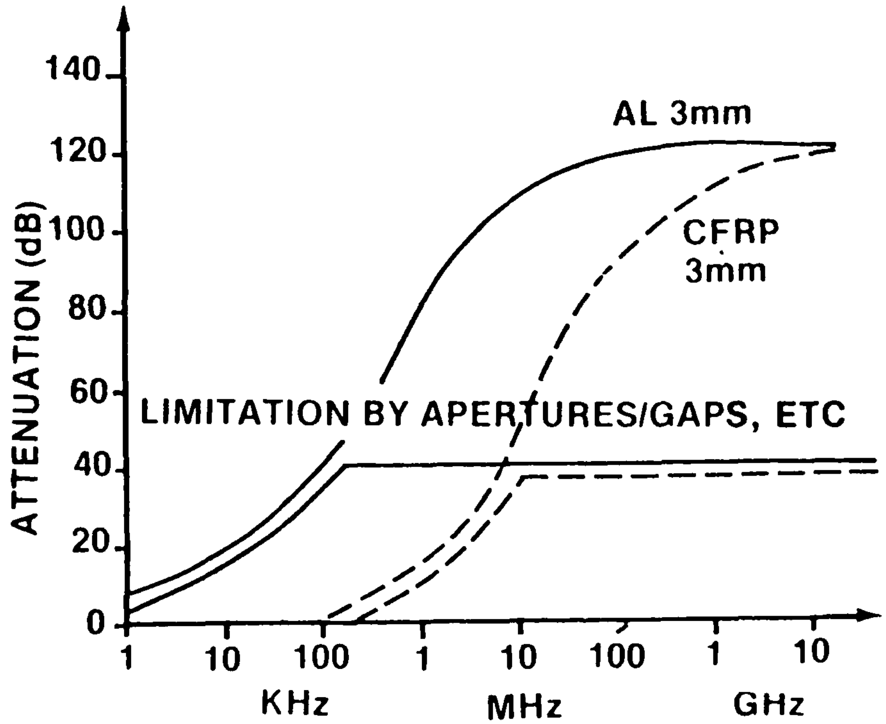

— TYP. METALLIC AIRCRAFT STRUCTURE

- - - TYP. CFRP AIRCRAFT STRUCTURE

STATIC WING SHIELDING TESTS

- USED A FULL SIZE YAV-8B WING ASSEMBLY WITH TERMINATION BOX AT THE WING TIP (FIGURE 13)
- COMPARED INDUCED VOLTAGES FOR WIRES LOCATED UNDER THE METAL LEADING EDGE AND UNDER THE G/E TORQUE BOX SECTION OF THE WING
- TESTS CONDUCTED IN OUTDOOR OPEN AREA AT 14 KHz TO 100 MHz AND ANACHOIC CHAMBER AT 200 MHz TO 18 GHz (FIGURES 15 & 14)
- TESTS SHOWED G/E PROVIDES HIGH DEGREE OF SHIELDING; LITTLE DIFFERENCE IN INDUCED VOLTAGES ON SEPARATE WIRES

EMI TEST ARTICLE

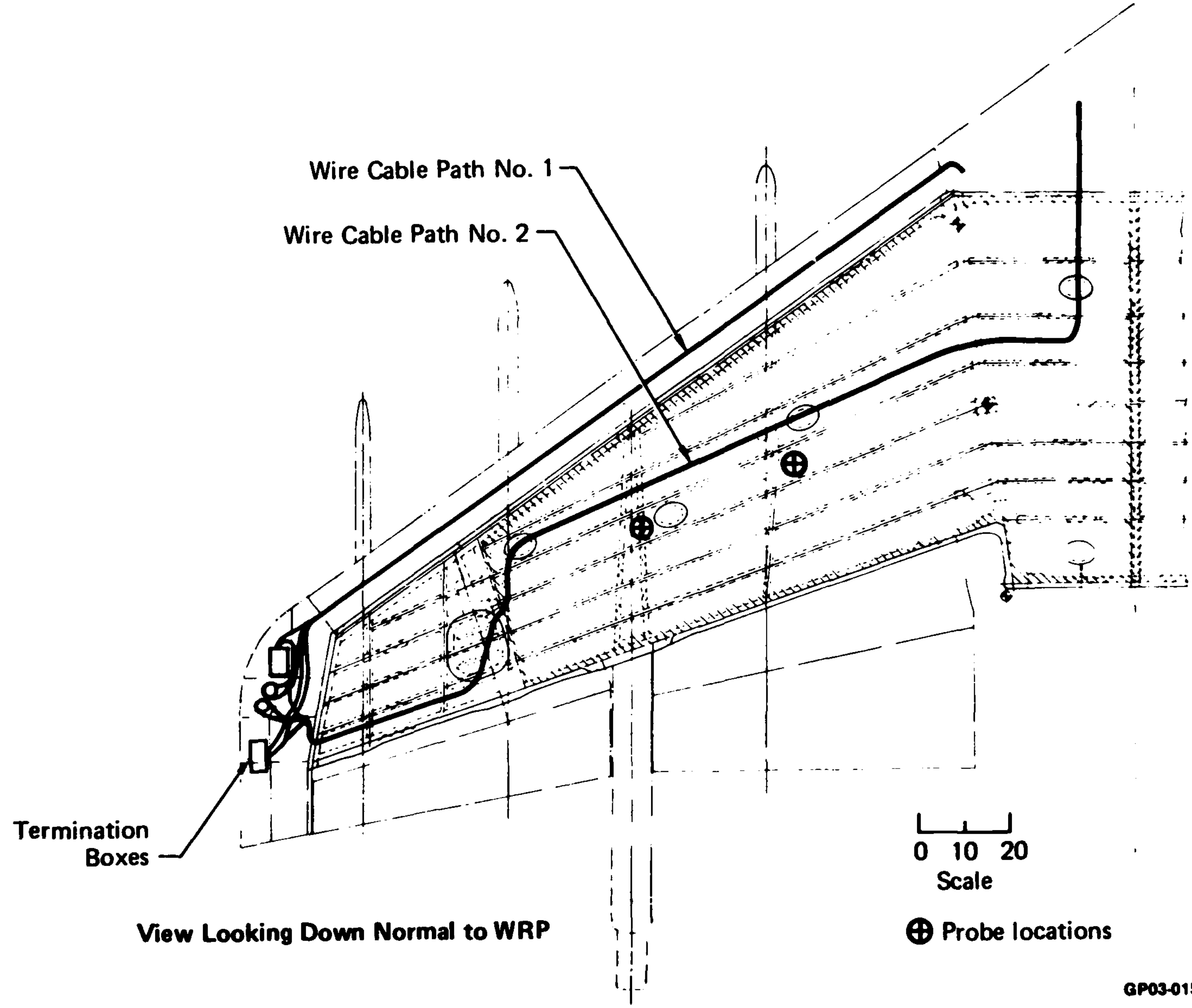

View Looking Down Normal to WRP

GP03-0153-1

EMI OUTDOOR TEST SETUP
(A) ANTENNA, (B) FIELD METER, (C) WING, (D) INSTRUMENTATION BOX

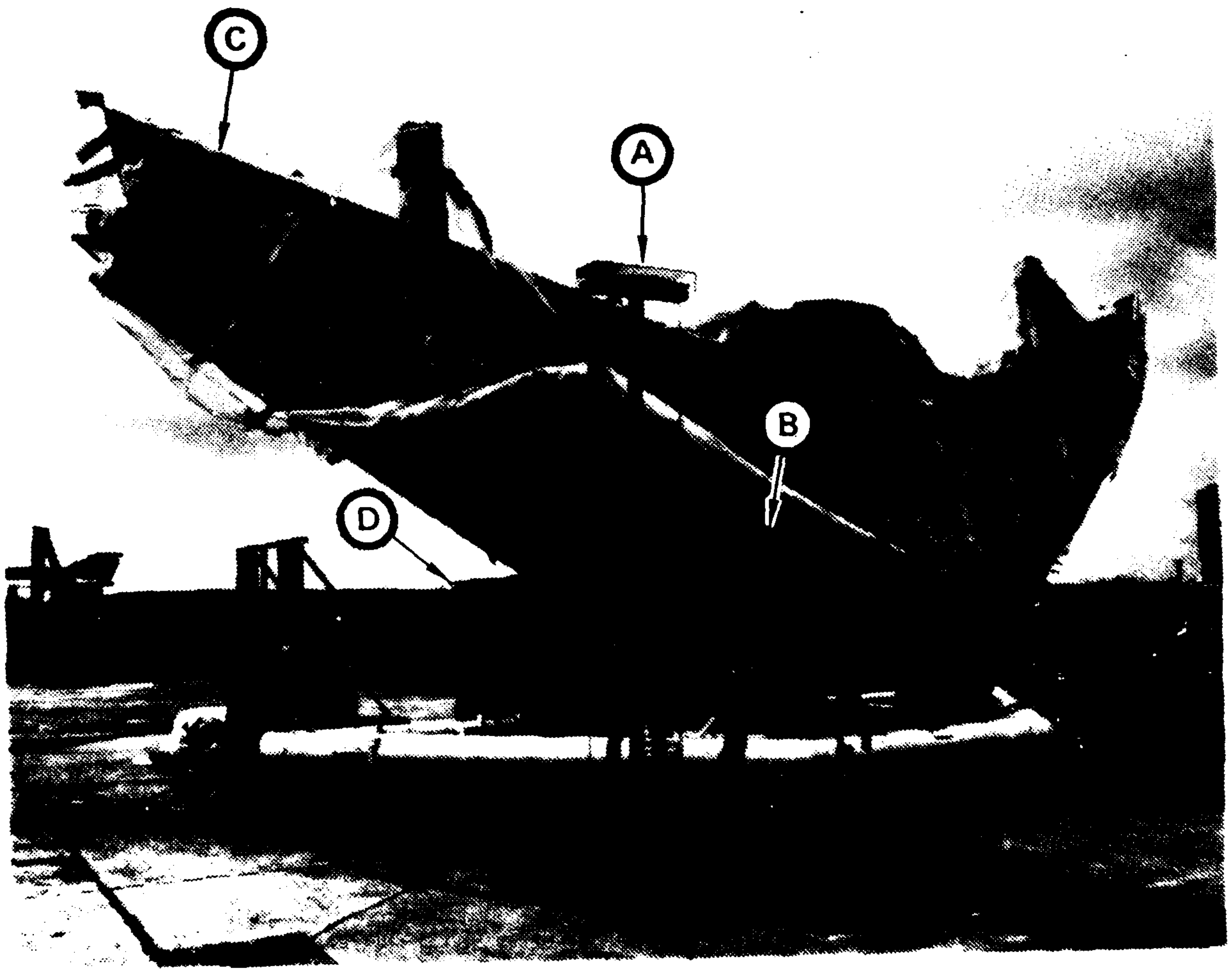

EMI TEST SETUP IN ANECHOIC CHAMBER
(A) ANTENNA, (B) FIELD METER, (C) WING

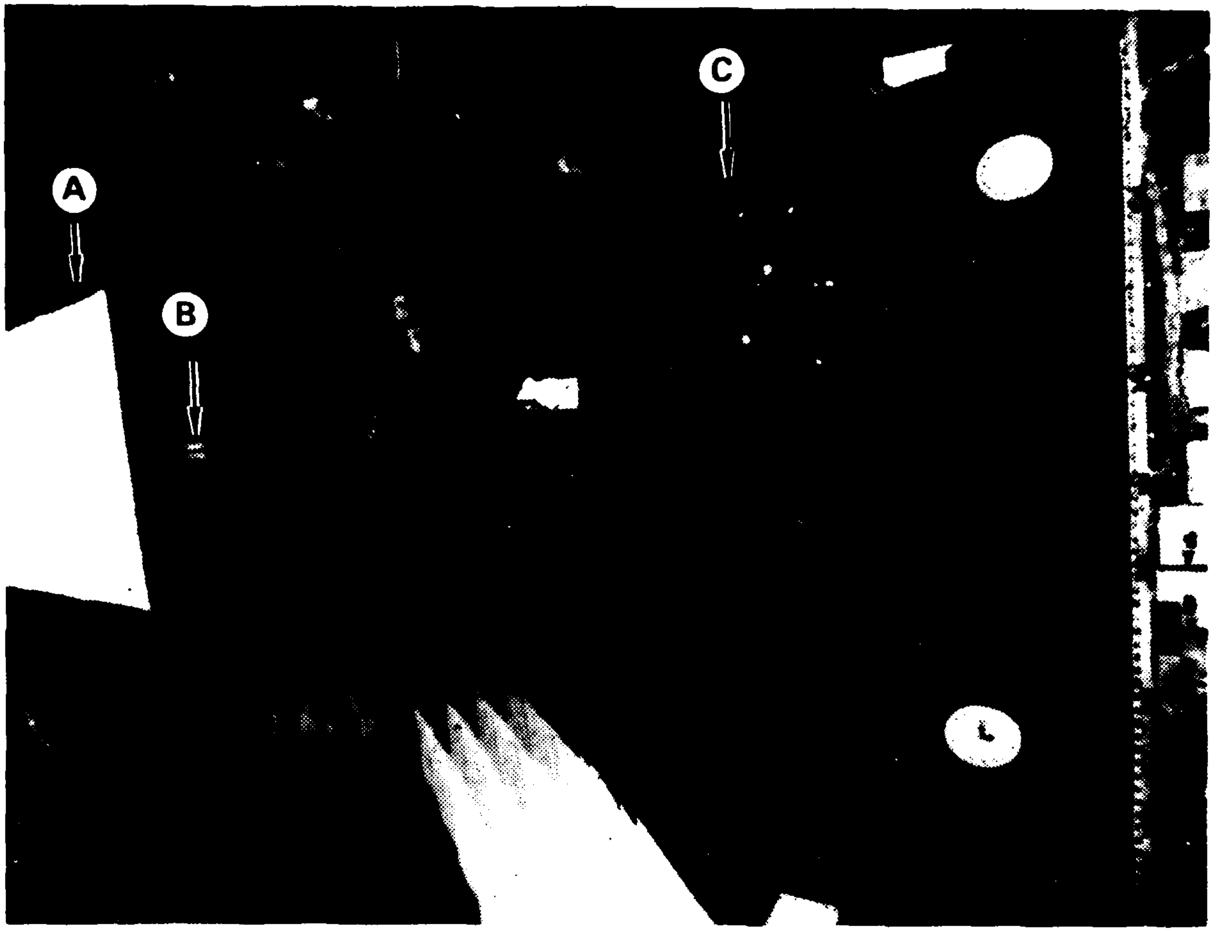

ANTENNA PERFORMANCE TESTS

- PATTERN, GAIN, AND VSWR TESTS CONDUCTED
- USED VARIOUS TEST CONFIGURATIONS TO DETERMINE EFFECTS OF COMPOSITES, GROUND PLANE CONFIGURATION, AND TYPE OF ANTENNA MOUNT
- USED VHF AND TACAN BLADE ANTENNAS AT 400 MHz AND 1 GHz AND A RADAR BEACON STUB ANTENNA AT 10 GHz
- ONLY SMALL PATTERN AND GAIN CHANGES OBSERVED REGARDLESS OF GROUND PLANE OR BASE MOUNTING
- VSWR TESTS SHOWED SLIGHT CHANGES IN GAIN DUE TO SLIGHT CHANGES IN INPUT IMPEDANCE

INTERMODULATION EFFECTS

- CONCERN WITH INTERMODULATION EFFECTS (NONLINEAR JUNCTION) PRODUCED BY GRAPHITE FIBERS IN THE COMPOSITE MATRIX

- NO INTERMODULATION EFFECTS FOUND (NO HARMONICS GENERATED) FROM HIGH CURRENT LEVEL TESTS

LIGHTNING EFFECTS

- NO DAMAGE EXCEPT IN AREA OF ATTACHMENT POINT. THIN METALLIC COATINGS, SCREEN WIRE MESH, OR OTHER CONDUCTIVE LAYERS NEEDED TO SPREAD AND DISSIPATE THE LIGHTNING ENERGY

- ATTACHMENT ZONES FOR PARTIALLY COMPOSITE VEHICLE CAN BE DETERMINED FROM TESTS ON A METAL MODEL

- TESTS SHOWED NO MEASURABLE DIFFERENCE IN ATTACHMENT POINT BEHAVIOR BETWEEN METAL & G/E STRUCTURE (FIGURE 16)

CIRCUIT AND PROBE ATTACHMENT POINTS

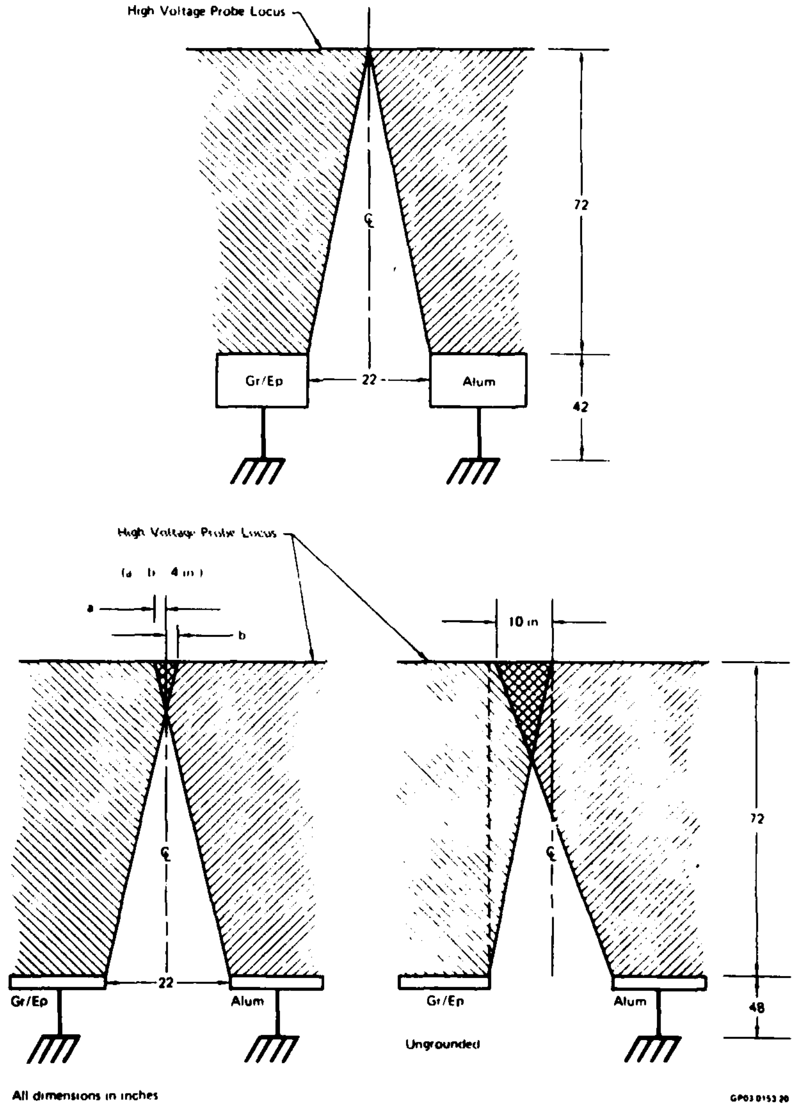

OVERALL FINDINGS

- G/E AIRCRAFT STRUCTURE CAN BE DESIGNED TO PROVIDE ADEQUATE ELECTROMAGNETIC SHIELDING FOR AVIONICS AND ELECTRICAL SUBSYSTEMS

- NO ELECTROMAGNETIC G/E ISSUE HAS BEEN FOUND THAT CANNOT BE HANDLED IN NORMAL AIRCRAFT DESIGN

AV-8B COMPOSITE FORWARD FUSELAGE DEVELOPMENT PROGRAM

MDC REPORT A6398 (MAY 1980) - CONTRACT N00019-76-C-0666

- ASSESSED LIGHTNING PROTECTION DESIGN REQUIREMENTS FOR
  - FORWARD FUSELAGE STRUCTURE
  - AIRFRAME DOORS & PANELS
  - ANTENNAS
  - SENSOR PROBES
  - FORMATION LIGHTS
  - ELECTRICAL POWER
  - AVIONICS

G/E PANELS AND COUPONS WITH BOLTED JOINTS

- THRESHOLD FOR STRENGTH DEGRADATION APPROX 20KA/INCH OF G/E WIDTH FOR PULSED PORTION OF LIGHTNING STROKE AND 150A FOR CONTINUING CURRENT PHASE (FIG 6-61 & 6-62)
- BOLTED JOINTS CAN CARRY RESTRIKE CURRENT AND ARE REMOVABLE WITHOUT HAVING TO DRILL OUT SCREWS
- CONDUCTIVE SURFACE COATING REQUIRED TO PREVENT LIGHTNING PENETRATION OF G/E TEST SPECIMENS (FIG 6-65)

SIMPLIFIED BLOCK DIAGRAM OF LIGHTNING TEST SETUP

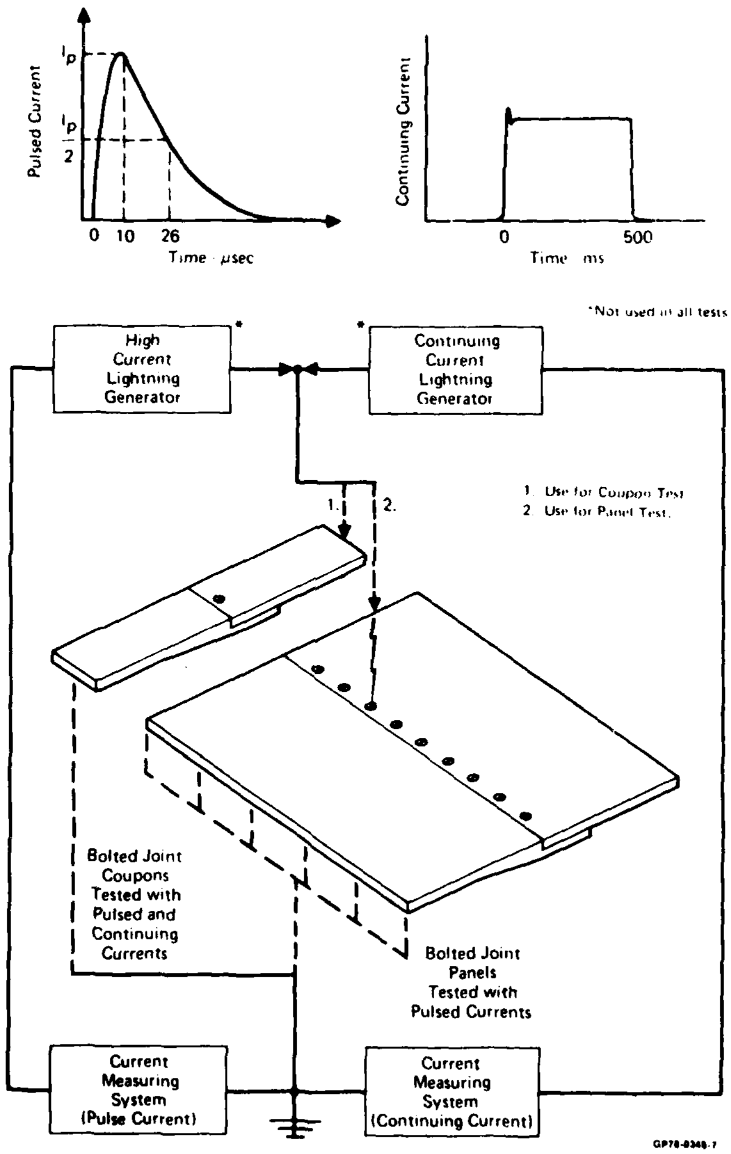

ELECTRICAL POWER

LIGHTNING COUPLING MECHANISMS:

- DIRECT ATTACHMENT TO WIRING (LIGHTS, PROBES, ETC.)
- MAGNETIC INDUCTION (FIG 6-63)
- COMMON MODE INJECTION (FIG 6-64)

PROTECTION REQUIREMENTS:

- DEDICATED WIRES USED AS POWER RETURNS INSTEAD OF STRUCTURE
- INSTALLATION OF LIGHTNING ARRESTORS AT REMOTE POINTS OF POSSIBLE LIGHTNING ENTRY (LIGHTS, PROBES, ETC.)

MAGNETIC COUPLING OF LIGHTNING TO A RECEPTOR

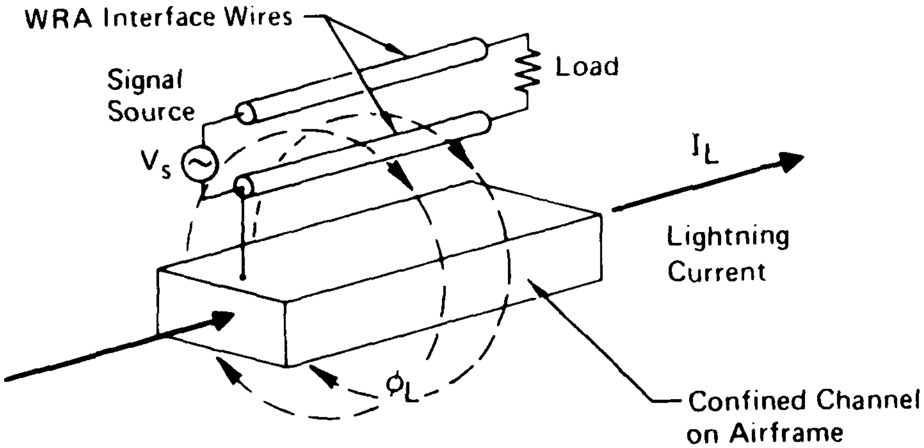

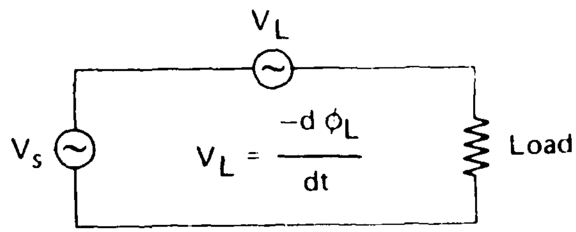

Thevenin Equivalent
Circuit

COMMON MODE LIGHTNING COUPLING TO A RECEPTOR

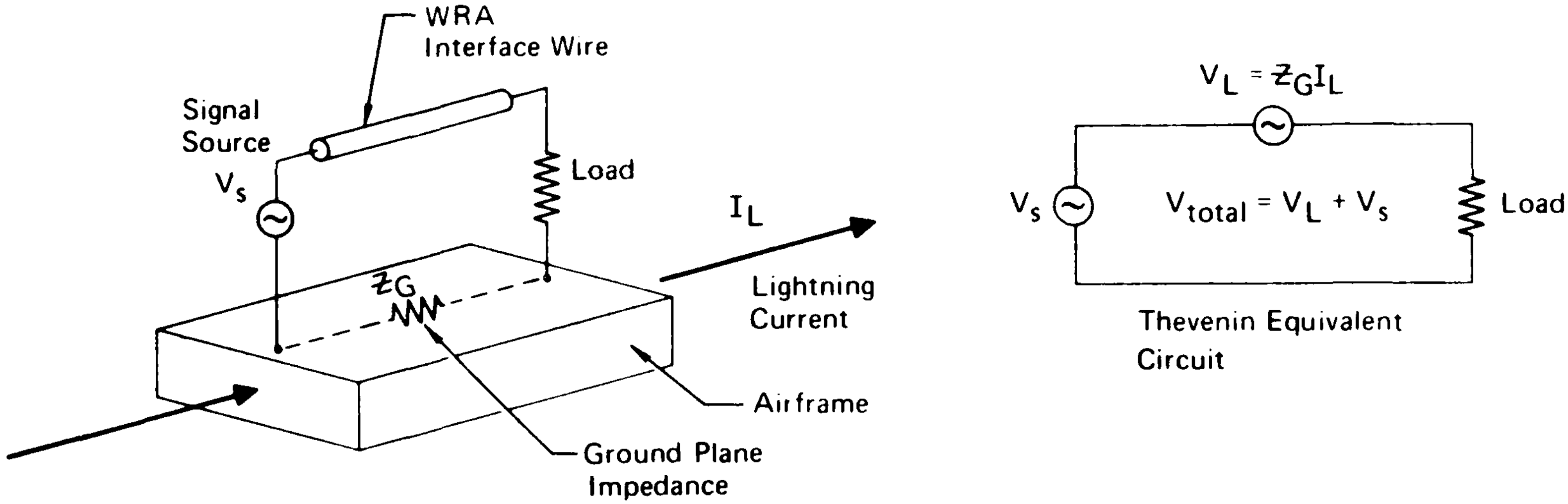

BOEING STUDY PROGRAM

- PROTECTION OF ADVANCED ELECTRICAL POWER SYSTEMS FROM ATMOSPHERIC ELECTROMAGNETIC HAZARDS (AF CONTRACT F33615-79-C-2006)
  - PHASE I
    - TASK 1 - THREAT ASSESSMENT
    - TASK 2 - EVALUATION OF NORMAL DESIGN FOR INHERENT HARDNESS
    - TASK 3 - ADD-ON PROTECTION DEVICE EVALUATION
  - PHASE II
    - TASK 4 - DESIGN GUIDE

TRADE STUDY SUMMARY OF LIGHTNING PROTECTION TECHNIQUES

TYPE CIRCUIT (LOCATION)	SEVERE THREAT LEVEL	TYPE THREAT	INHERENT HARDENING TECHNIQUE	TRANSIENT LEVEL	TYPE OF ADDITIONAL PROTECTION REQUIRED AND TRANSIENT LEVEL			COMMENTS
					1	2	3	
METALLIC WING FIBER-GLASS LEADING EDGE								
1. GENERATORS (ON WINGS)	200 KA	MAGNETIC COUPLING ON FEEDER	FEEDER ROUTED 2 INCHES ABOVE METALLIC SPAR	30 V	-	-	-	PROTECT FOR DIRECT ATTACHMENT ONLY
2. POWER BUS (FUSELAGE)	200 KA	MAGNETIC COUPLING ON FEEDER	FEEDER ROUTED 2 INCHES ABOVE METALLIC SPAR	65 KV	FEEDER SHIELD: 5.4 KV; 295 V	TRANSZORB: 285 V	3 MIL FOIL ON*	SHIELDING COMPARES PIGTAIL & CIRCUMFERENTIAL GROUNDING RESPECTIVELY.
3. WING TIP BEACON LIGHTS	200 KA	MAGNETIC COUPLING ON 20 GAUGE WIRES	ROUTE WIRES NEAR STRUCTURE	2.2 KV AT POWER BUS	WIRE SHIELD: 190 V	TRANSZORB: 285 V	3 MIL FOIL ON* WING: 10.V	TRANSZORBS MUST BE PARALLELED BACK TO BACK IN EACH CASE.
4. WINDSHIELD HEATERS	200 KA	CAPACITIVELY COUPLED ONTO HEATER ELEMENTS	LOCATION OF HEATER ELEMENTS	920 V AT POWER BUS	-	TRANSZORB: 285 V	-	OTHER SIMILAR PROTECTION DEVICES
COMPOSITE WING AND FUSELAGE								
1. GENERATORS (FUSELAGE)	200 KA	DIFFUSION COUPLING ON FEEDERS	MINIMIZED EXPOSED FEEDER	5.8 KV	CIRCUMFERENTIAL* GROUNDED FEEDER SHIELD: 320 V	TRANSZORB: 285 V	-	
2. POWER BUS	200 KA	DIFFUSION COUPLING ON FEEDERS	MINIMIZED EXPOSED FEEDER	2.5 KV	CIRCUMFERENTIAL* GROUNDED FEEDER SHIELD: 130 V	TRANSZORB: 285 V		

* PREFERRED, DUE TO:
1. GREATEST PROTECTION
2. WEIGHT
3. RELIABILITY AND COST

CONCLUSIONS

- ELECTRICAL POWER SYSTEMS IN COMPOSITE STRUCTURE AIRCRAFT CAN BE ADEQUATELY PROTECTED BY A COMBINATION OF STRUCTURAL SHIELDING, WIRE SHIELDING, AND VOLTAGE SUPPRESSION DEVICES

- THE IMPACT OF LIGHTNING ON ADVANCED COMPOSITE MATERIALS AND ADVANCED ELECTRICAL POWER SYSTEMS MUST BE ASSESSED EARLY IN THE DESIGN PHASE FOR NEW AIRCRAFT

- HARDWARE TESTING OF PROTOTYPE SYSTEMS SHOULD BE CONDUCTED TO VERIFY THE ASSESSMENT

REFERENCES

1. COMPOSITE MATERIAL AIRCRAFT ELECTROMAGNETIC PROPERTIES AND DESIGN GUIDELINES, ARC REPORT NO. 50-5779, JANUARY 1981 (CONTRACT N00019-79-C-0634)

2. ELECTROMAGNETIC EFFECTS OF (CARBON) COMPOSITE MATERIALS UPON AVIONICS SYSTEMS, AGARD CONFERENCE PROCEEDINGS NO. 283, LISBON, PORTUGAL, 16-19 JUNE 1980

3. C. D. SKOUBY AND G. L. WEINSTOCK, TECHNIQUES IN THE DESIGN OF GRAPHITE EPOXY STRUCTURES FOR ELECTRICAL PERFORMANCE AND MAINTAINABILITY, FIFTH CONFERENCE ON FIBROUS COMPOSITES IN STRUCTURAL DESIGN, NEW ORLEANS, LOUISIANA, JAN 28, 1981

4. AV-8B COMPOSITE FORWARD FUSELAGE DEVELOPMENT PROGRAM (FINAL REPORT), MDC REPORT NO. A6398, MAY 1980 (CONTRACT N00019-76-C-0666)

5. PROTECTION OF ELECTRICAL SYSTEMS FROM EM HAZARDS, BOEING REPORT NO. D180-26154-2 (FINAL REPORT) AND D180-26154-3 (DESIGN GUIDE), OCTOBER 1981 (CONTRACT F33615-79-C-2006)
AFWAL-TR-81-2117 and 2118

6. F. W. TORTOLANO, HYBRID COMPOSITES, DESIGN NEWS, SEP 21, 1981

STRUCTURAL APPLICATION OF COMPOSITE MATERIALS AND THE DIRECT EFFECTS OF LIGHTNING STRIKES

by

Mr. William E. Howell

Langley Research Center
National Aeronautics and Space Administration

The direct effects of lightning strikes on composite materials and protection approaches will be described. Approaches to EMI shielding which maintain weight advantage and structural integrity over the life of the airframe will be discussed.

SCOPE OF PRESENTATION

- o ADVANCED COMPOSITE MATERIALS
- o APPLICATIONS IN AIRCRAFT STRUCTURES
- o LANGLEY'S RESEARCH ON DIRECT EFFECTS OF LIGHTNING ON COMPOSITE STRUCTURES

MATERIAL PROPERTIES

MATERIAL	PROPERTIES				COST
	STRENGTH, KSI	MODULUS, X 10^3 KSI	DENSITY, LB/IN.^{3}	RESISTIVITY, OHM-CM	$/LB
GRAPHITE-EPOXY	110-225	18	0.055	$0.9\text{-}1.1 \times 10^{-4}$	30
KEVLAR-EPOXY	75-270	11	0.050	*	15
GLASS-EPOXY	75-200	6	0.070	*	10
ALUMINUM	55	10	0.101	2.8×10^{-6}	2

* DIELECTRIC MATERIAL (NON-CONDUCTOR)

NASA
L 81 3777

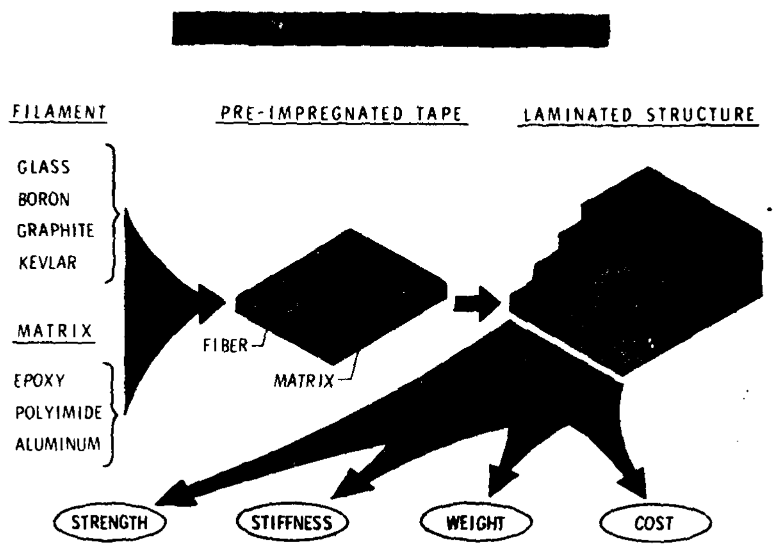

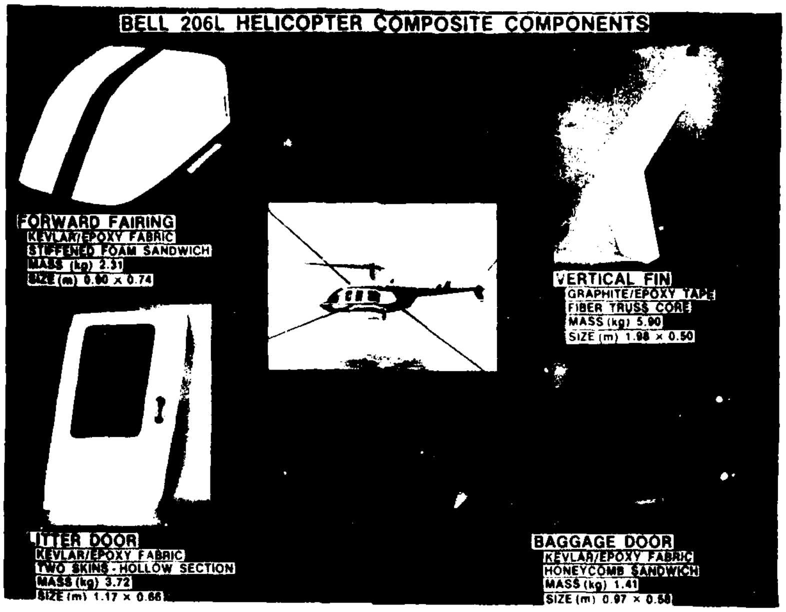
BELL 206L HELICOPTER COMPOSITE COMPONENTS
FORWARD FAIRING
KEVLAR/EPOXY FABRIC
STIFFENED FOAM SANDWICH
MASS (kg) 2.31
SIZE (m) 0.90 x 0.74
VERTICAL FIN
GRAPHITE/EPOXY TAPE
FIBER TRUSS CORE
MASS (kg) 5.90
SIZE (m) 1.98 x 0.50
LITTER DOOR
KEVLAR/EPOXY FABRIC
TWO SKINS - HOLLOW SECTION
MASS (kg) 3.72
SIZE (m) 1.17 x 0.66
BAGGAGE DOOR
KEVLAR/EPOXY FABRIC
HONEYCOMB SANDWICH
MASS (kg) 1.41
SIZE (m) 0.97 x 0.58

GRAPHITE-EPOXY SPOILERS FOR 737 COMMERCIAL FLIGHT SERVICE

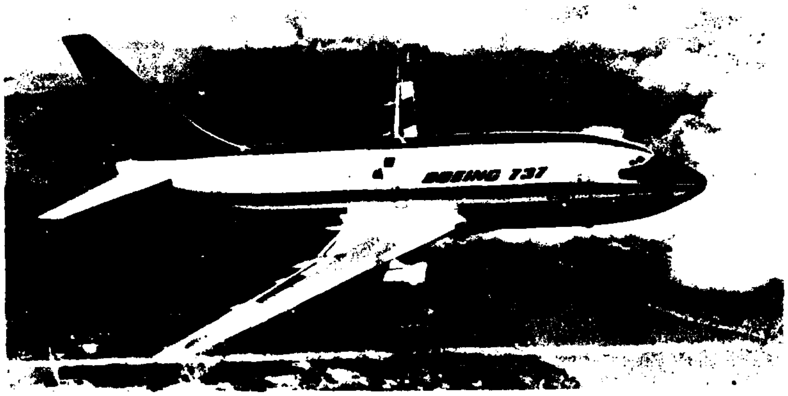

FLIGHT SERVICE EVALUATION OF PRD-49/EPOXY PANELS ON LOCKHEED L-1011 AIRCRAFT

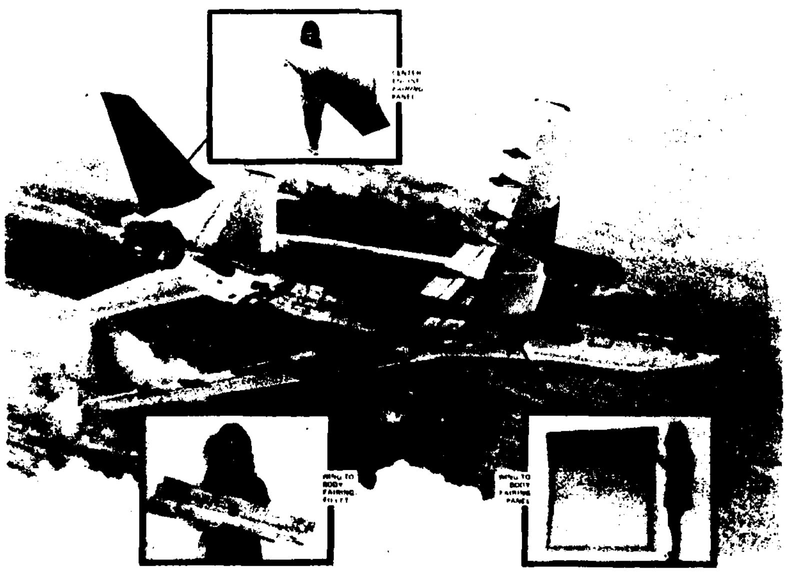

ACEE

COMPOSITE SECONDARY STRUCTURES


BOEING 727 COMPOSITE ELEVATOR


DOUGLAS DC-10 COMPOSITE RUDDER


LOCKHEED L-1011 COMPOSITE AILERON

DC-10 COMPOSITE RUDDER

LIGHTNING DAMAGE

BOEING 767 COMPOSITE STRUCTURE APPLICATIONS

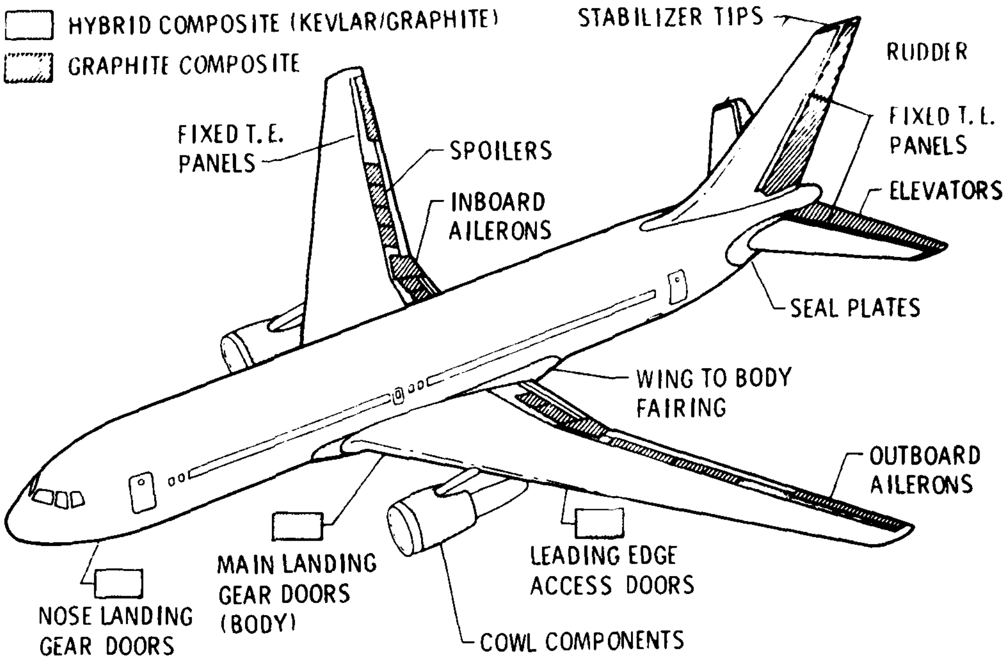

LIGHTNING PROTECTION SYSTEM FOR 727 ELEVATOR

F4A7
6/79

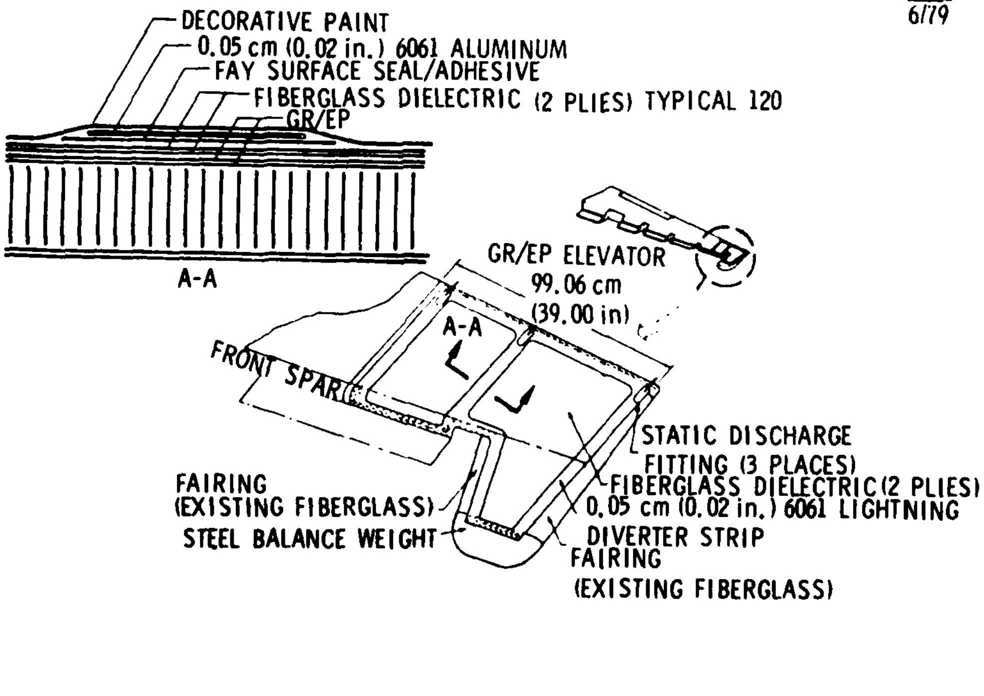

AIRCRAFT STRIKE ZONES

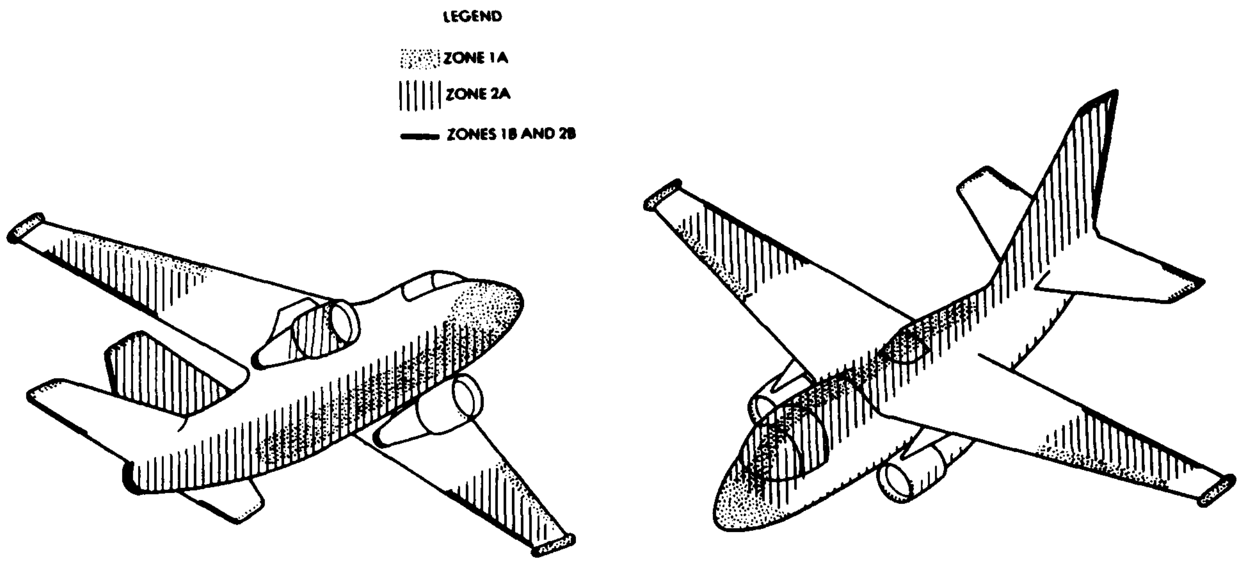

GRAPHITE/EPOXY UPPER AFT RUDDER
DOUGLAS DC-10

F3A
5/76

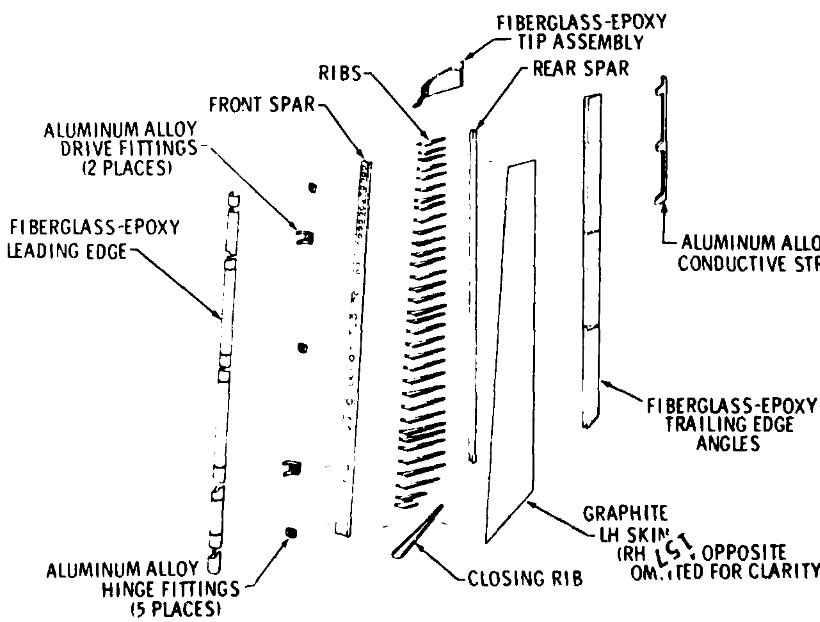

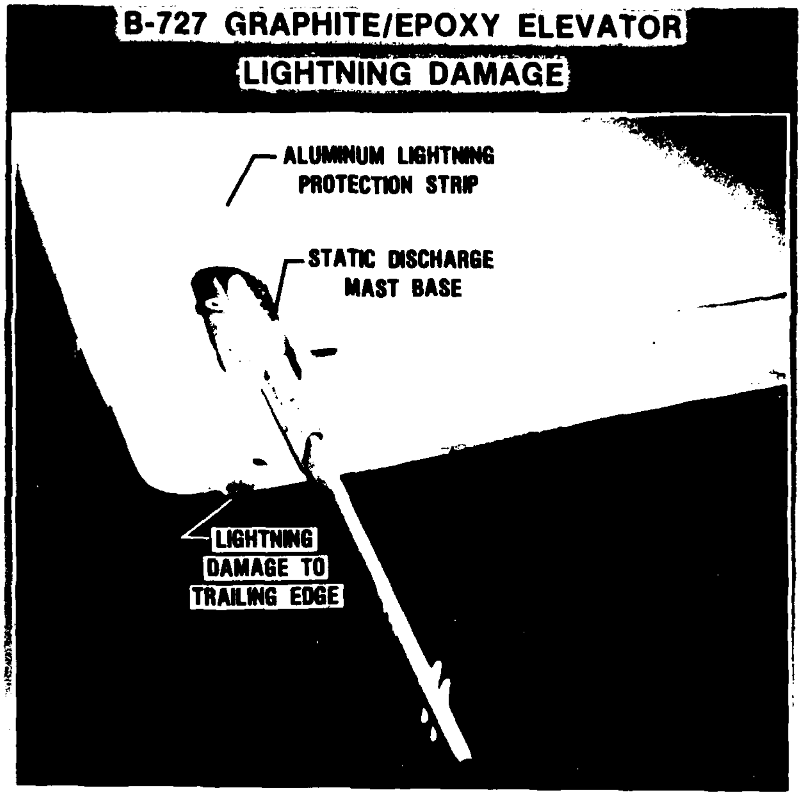

LIGHTNING EFFECTS ON COMPOSITE STRUCTURES

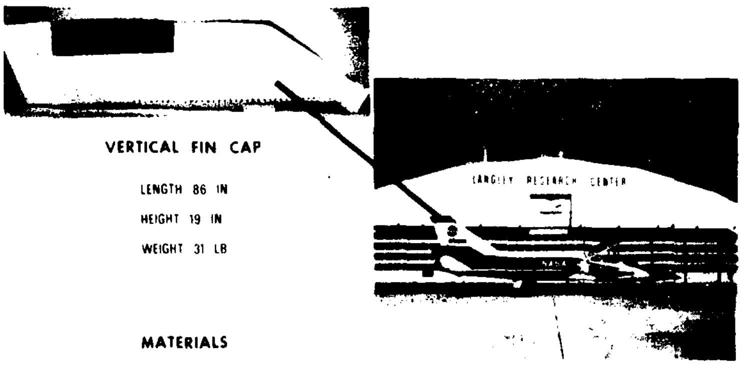

EXAMPLE PROTECTION SYSTEMS

- FLAME SPRAYED ALUMINUM
- ALUMINIZED GLASS (THORSTRAND®)
- ALUMINUM STRIPS/TAPE
- METAL SCREEN OR WIRE MESH

CERTIFICATION CURRENT TEST WAVEFORM COMPONENTS FOR EVALUATION OF DIRECT EFFECTS

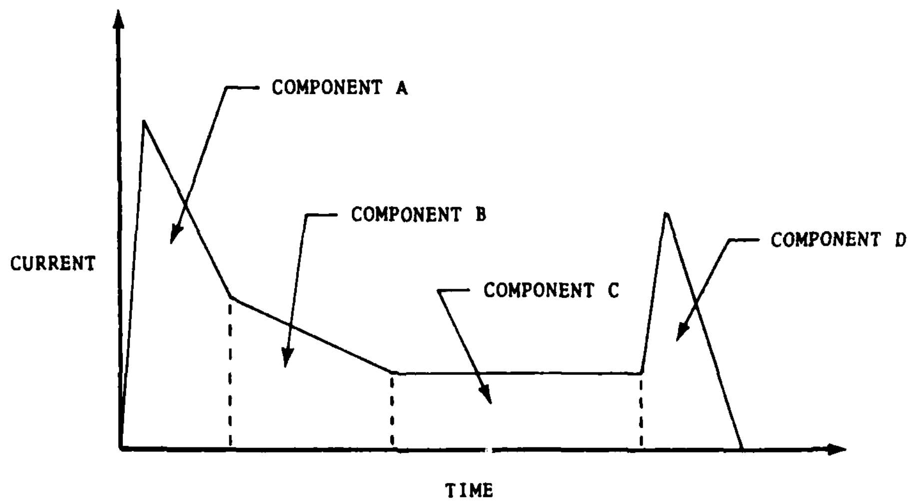

F-106B COMPOSITE FIN TIPS

- o KEVLAR-EPOXY WITH THORSTRAND®
- o GRAPHITE/EPOXY WITHOUT PROTECTION
- o GRAPHITE/EPOXY WITH FLAME SPRAYED ALUMINUM
- o KEVLAR/EPOXY WITH FLAME SPRAYED ALUMINUM

F-106B COMPOSITE FIN TIP ASSEMBLY

EFFECT OF LIGHTNING
ON
KEVLAR/EPOXY WITH THORSTRAND

UNPAINTED | PAINTED

i_p = 105 kA
ACTION INTEGRAL = $0.82 \times 10^6\ A^2 \cdot s$

i_p = 96 kA
ACTION INTEGRAL = $0.47 \times 10^6\ A^2 \cdot s$

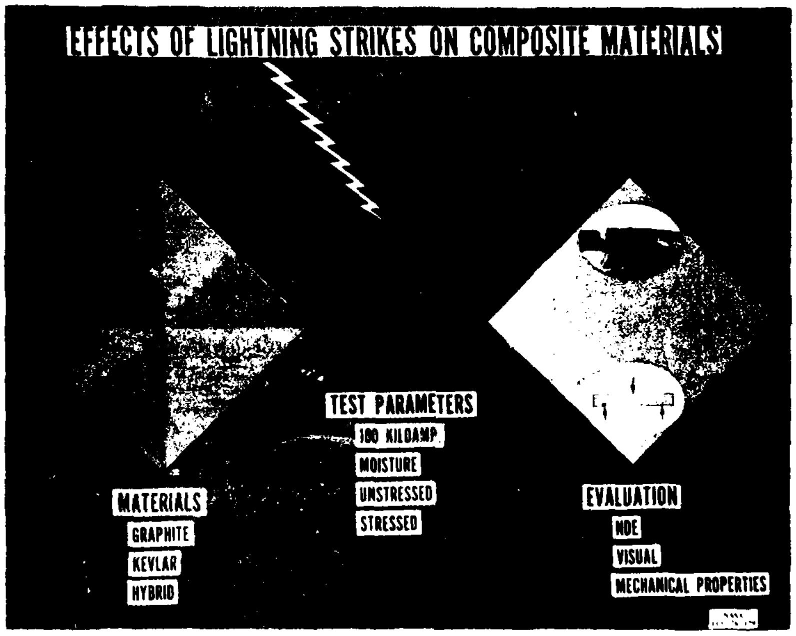


N626BL

CONCLUDING REMARKS

- COMPOSITES EXHIBIT STRUCTURAL ADVANTAGES COMPARED TO METALS
- EXCELLENT IN-SERVICE PERFORMANCE AND MAINTENANCE EXPERIENCE HAVE BEEN ACHIEVED WITH OVER 150 COMPOSITE COMPONENTS DURING 8 YEARS AND OVER 2 MILLION HOURS OF FLIGHT SERVICE WITH NO SIGNIFICANT DAMAGE FROM LIGHTNING STRIKES
- EFFECTS OF LIGHTNING ON COMPOSITE MATERIALS AND LIGHTNING PROTECTION SYSTEMS ARE BEING EVALUATED
- GROUND AND FLIGHT DATA BASE IS BEING DEVELOPED FOR THE ELECTRICAL SAFETY OF AIRCRAFT

LIGHTNING INTERACTION ANALYSIS

by

Dr. Karl S. Kunz

Kunz Associates, Incorporated

Description of lightning interaction analyses and how they are performed including lightning model, aircraft geometry, interior equipment and cable layout, and modeling of interconnecting system. Sample direct strike problem and (generic) expected results. Overview of mathematical basis used in interaction analysis and description of finite difference method.

WHAT IS A LIGHTNING INTERACTION ANALYSIS -

- A MATHEMATICAL TREATMENT OF THE PROPAGATION OF ELECTROMAGNETIC ENERGY FROM A LIGHTNING BOLT TO AN AIRCRAFT AND ON INTO SUSCEPTIBLE INTERIOR EQUIPMENT

- USES EXPERIMENTALLY DETERMINED CHARACTERISTICS AS THE INPUTS OF MATHEMATICAL MODELS

- PREDICTS RESPONSE LEVELS (VOLTAGE AND CURRENT) AT THE INPUTS (PINS) OF SUSCEPTIBLE EQUIPMENT

- ALLOWS UPSET/DAMAGE/FAILURE ASSESSMENTS TO BE MADE FOR THE SUSCEPTIBLE EQUIPMENT

WHY A LIGHTNING INTERACTION ANALYSIS AND NOT JUST EXPERIMENT -

- EXPANDS ON EXPERIMENT
  - SOURCE VARIATIONS, AIRCRAFT MODIFICATIONS AND EQUIPMENT CAN BE ACCOMODATED

- INCREASES UNDERSTANDING
  - MODELING INCREASES UNDERSTANDING AS MODELS ARE REFINED AND MADE MORE ACCURATE

- EFFECTIVE
  - ANALYSIS CAN BE QUICKLY AND INEXPENSIVELY PERFORMED, WHILE ADEQUATE ACCURRACY IS MAINTAINED

HOW IS A LIGHTNING INTERACTION ANALYSIS PERFORMED -

- DEFINE SOURCE (DIRECT STRIKE, RADIATED FIELDS, ETC.), AIRCRAFT (707, 747, ETC.) AND POSSIBLY SUSCEPTIBLE EQUIPMENT (RADAR, NAVIGATIONAL EQUIPMENT, ETC.)

- OBTAIN RELEVANT EXPERIMENTAL DATA, SUCH AS
  - LIGHTNING TIME BEHAVIOR OR SPECTRUM
  - AIRCRAFT GEOMETRY AND CONSTRUCTION
  - INTERIOR EQUIPMENT AND CABLE LAYOUTS
  - ELECTRICAL PARAMETERS (CABLE SIZE, SHIELDING, IMPEDANCE, TERMINATIONS, ETC.)
  - DEVICE UPSET/DAMAGE/FAILURE THRESHOLDS AND MECHANISMS

- MODEL THE INTERCONNECTED SYSTEM OF SOURCE, AIRCRAFT AND EQUIPMENT

- SELECT A MATHEMATICALLY TRACTABLE REALIZATION OF THE MODEL

- CHECK THE MATHEMATICAL MODEL FOR COMPLETENESS AND VALIDITY (COMPARE PREDICTIONS WITH KNOWN EXPERIMENTAL RESULTS)

- PREDICT RESPONSES AT THE SELECTED SUSCEPTIBLE EQUIPMENT

- EXAMINE SENSITIVITY TO PARAMETER VARIATIONS (OPTIONAL "SAFETY" MEASURE)

TYPICAL PROBLEM

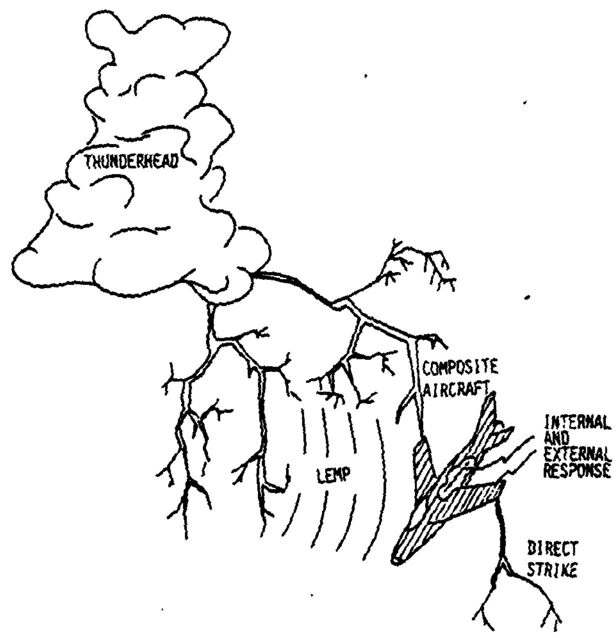

LIGHTNING DETAILS

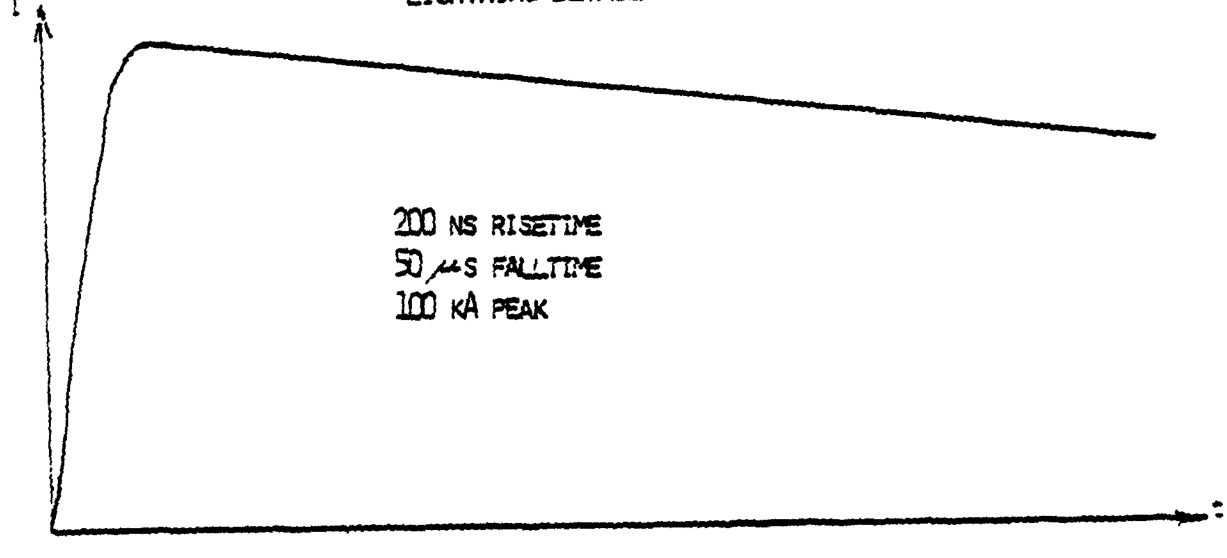

AIRCRAFT DETAILS

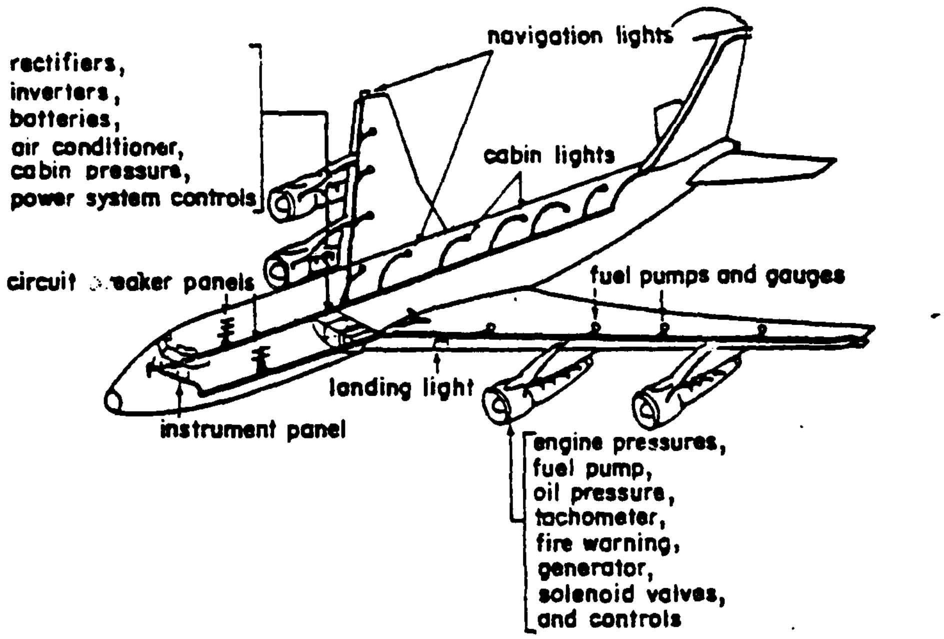

Typical elements and cabling associated with the aircraft power system.

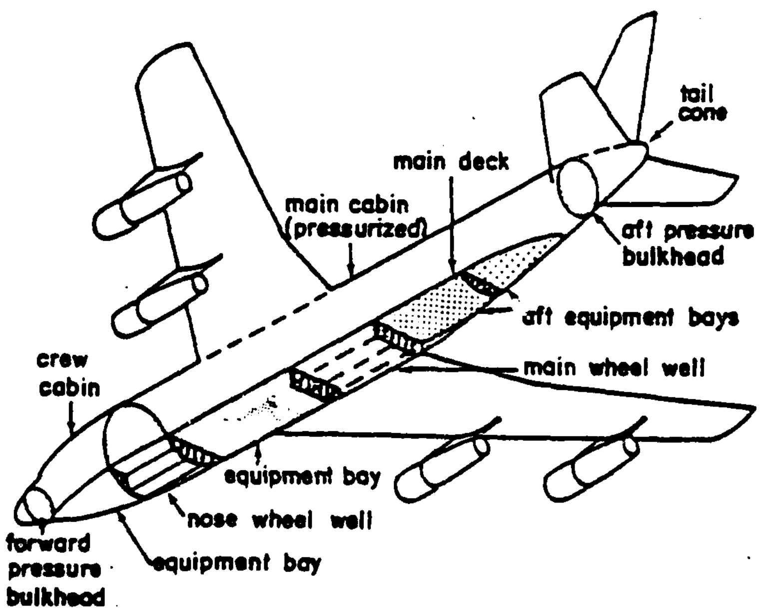

Elementary volumes within the aircraft.

CABLE DETAILS

CABLE TYPES

(TRANSMISSION LINES)

- COAXIAL
- TRIAXIAL
- MULTIAXIAL
- TWINAXIAL
- OPEN LINES
    - STRIPLINE
    - MICROSTRIP
    - TWO-WIRE
    - EDGESTRIP
    - EDGEWIRE
    - WIRE OVER GROUND

MATHEMATICAL REALIZATION -

- GENERAL REQUIREMENTS -

  SOURCE X EXTERIOR RESPONSE X PENETRATION X INTERIOR RESPONSE X SHIELDING EFFECT = RESPONSE AT "PIN"

- EXTERIOR RESPONSE X PENETRATION X INTERIOR RESPONSE MOST DIFFICULT PART

- POSSIBLE APPROACHES (MAY BE COMBINED WITH TRANSMISSION LINE THEORY, BETHE SMALL HOLE THEORY, MULTIPLE RUNS, ETC.)
    - SIMPLE CANONICAL SHAPES
    - MoM THIN WIRE TYPE CODES (EFIE)
    - PATCH CODES (MFIE)
    - FINITE DIFFERENCE TECHNIQUES

CANONICAL SHAPES

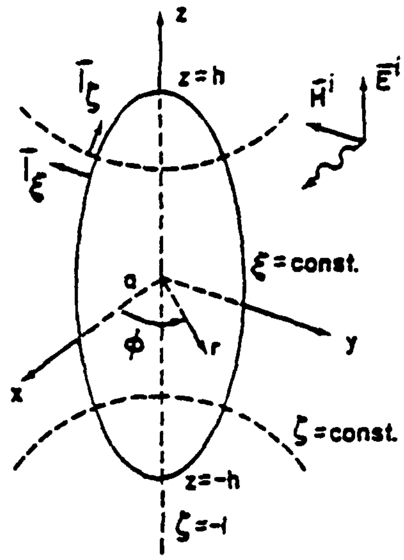

Plane wave broadside incident on a prolate spheroid.

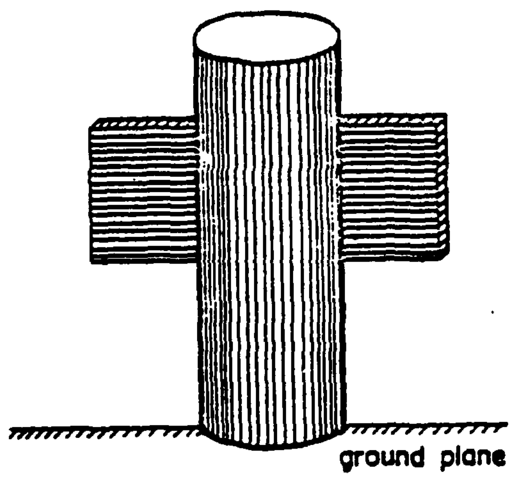

Diagram of flat plate crossed with an electrically thick cylinder.

WIRE MODEL/BOR'S

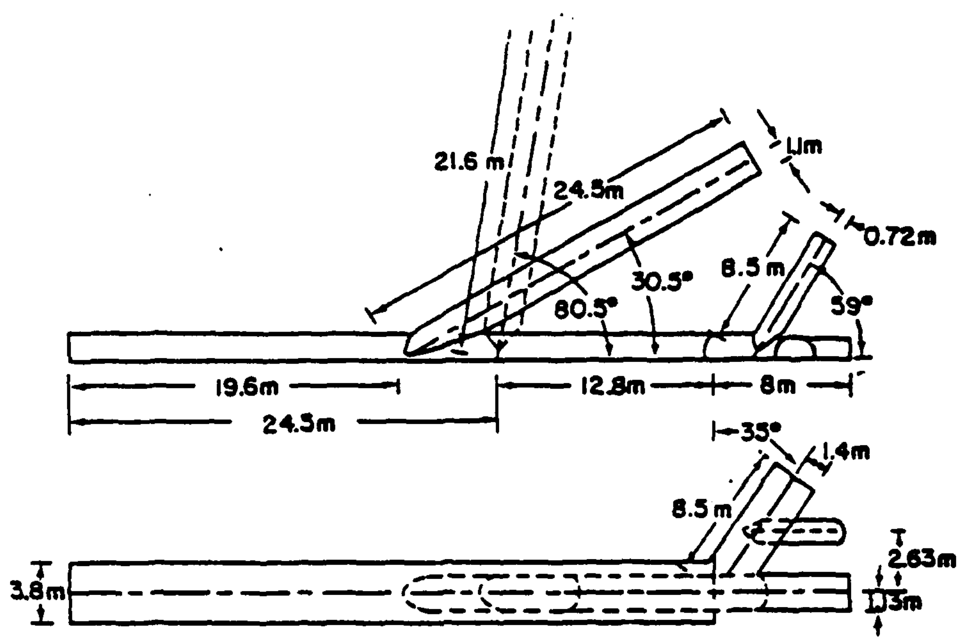

Stick (intersecting cylinders) model of the B-1 aircraft in the wings-forward and wings-swept configurations.

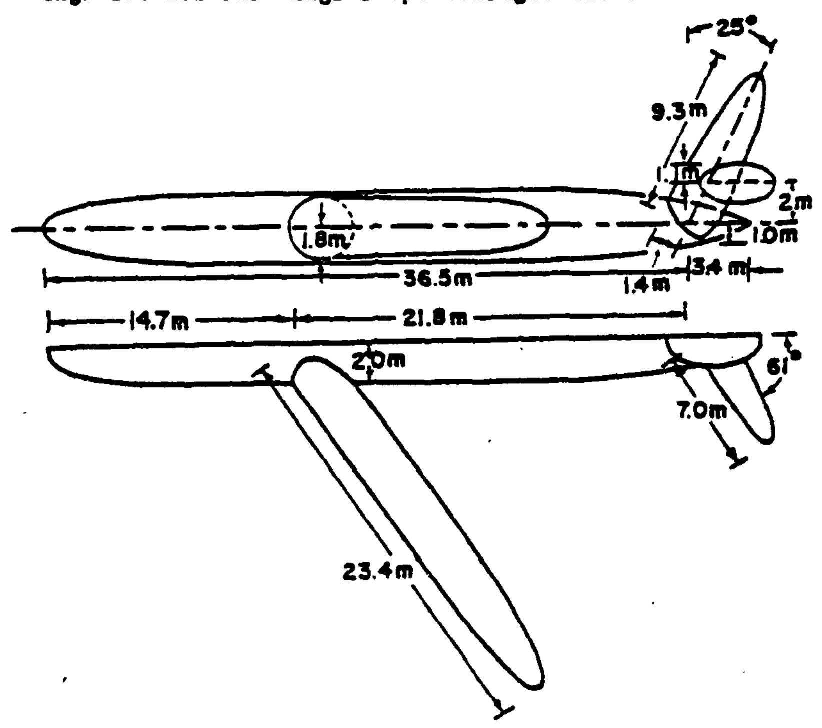

Body-of-revolution model of the EC-135 aircraft. Current zones are indicated with dotted lines.

Some Computational Aspects of Thin-Wire Modeling

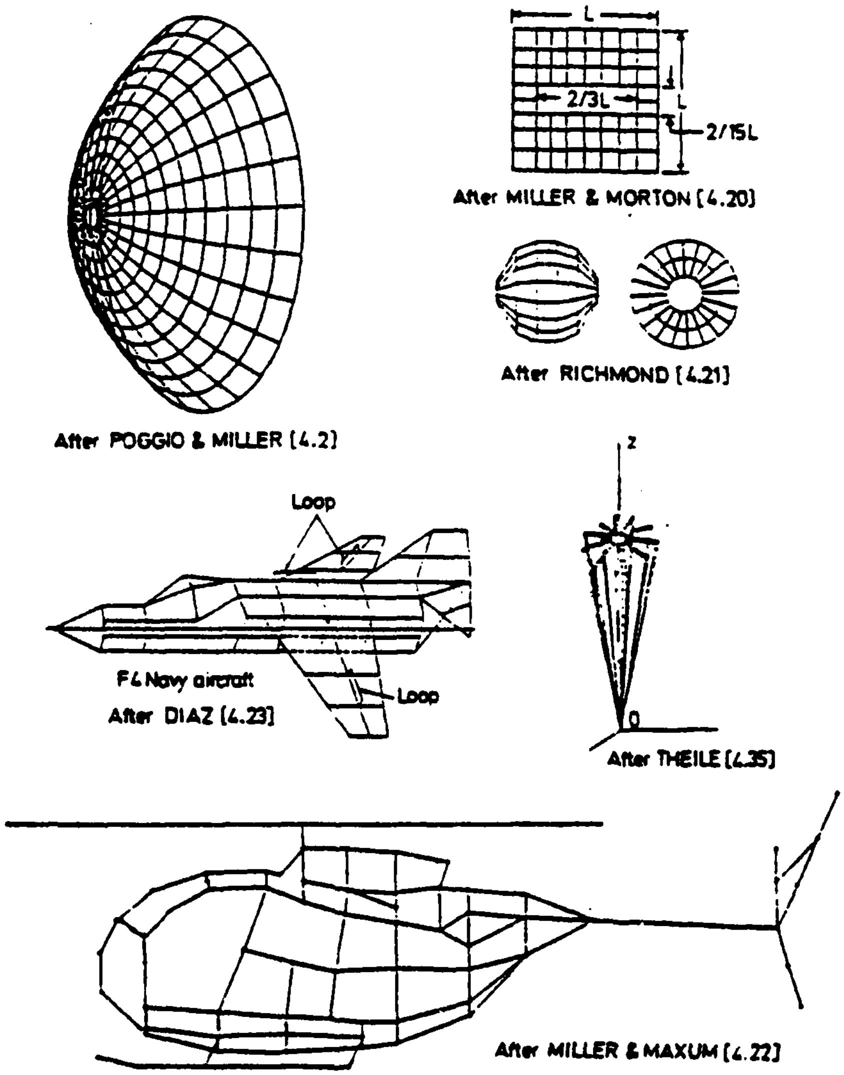

Representative wire grid model structures

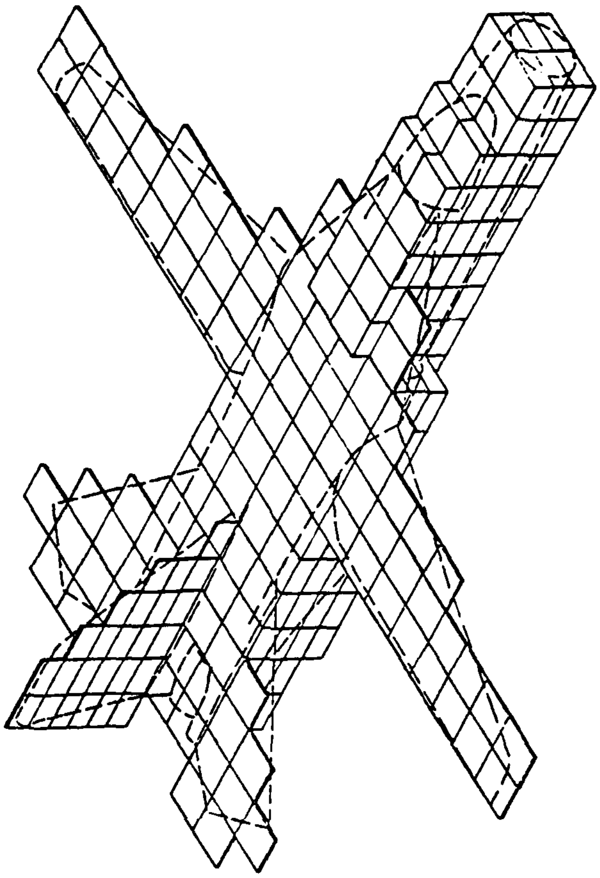

FINITE DIFFERENCE METHOD -

- BASED ON BRUTE FORCE TIME STEPPING OF MAXWELL'S EQUATIONS
- INCORPORATES ANY MATHEMATICALLY EXPRESSIBLE SOURCE, I.E. $I(t) = e^{-\alpha t} - e^{-\beta t}$
- ACCURATE EXTERIOR RESPONSE PREDICTIONS
- WITH EXPANSION TECHNIQUE CAN, ALSO, PERFORM INTERIOR RESPONSE PREDICTIONS AT REASONABLE COST
- CAN HANDLE COMPOSITES, AS WELL AS METAL AIRCRAFT PANELS

DEFINITION OF THE FINITE DIFFERENCE APPROACH

Finite differencing consists of replacing continuous partial derivatives in P.D.E.'s with appropriate finite differences. For example:

$$\partial y \to \Delta(y_n) = y_{n+1} - y_n \; ; \quad \partial^2 y \to \Delta\,[\,\Delta(y_n)] = y_{n+2} - 2y_{n+} + y_n \; ; \text{ etc.}$$

Finite differencing discritizes the P.D.E. and, hence, the problem being solved, i.e.

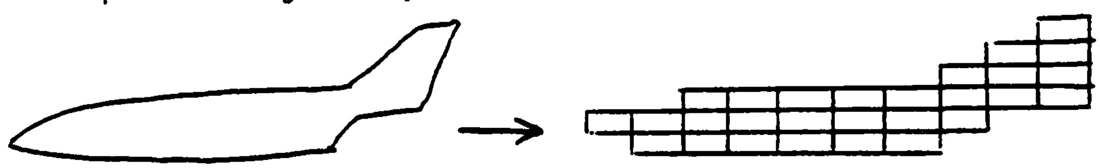

Finite differencing is, therefore, an approximation that in the limit of zero mesh size is exact.

Finite differencing does not require any special model of the problem to facilitate a solution, just the appropriate P.D.E. such as:

$$\frac{1}{\alpha}\frac{\partial T}{\partial \Theta} = \nabla^2 T + Q/k \qquad \text{or} \qquad \left(\frac{\partial e_r}{\partial z} - \frac{\partial e_z}{\partial r}\right) = -\mu_o \frac{\partial h_\phi}{\partial t}$$

(heat equation) (portion of Maxwell Equations for thin scatterer in cylindrical coordinates)

EVOLUTION OF PRECEEDING FINITE DIFFERENCE APPROACH TO EM

- 
- The Maxwell Equations
- Classical Boundary Value Solutions
- Introduction of Computers/Computer Oriented Numerical Analysis
- Integral Equation Approaches (EFIE and MFIE)
- Finite Difference as presently applied to EM coupling

  1) feasibility of application to realistic problems -
     K.S. Lee - "Num. Sol. of Int. Bound. Val. Prob. Involving Maxwell's Equas. in Iso. Media", IEEE Transactions A and P, May,1966.
  2) application in 2D to realistic problem with radiation boundary condition -
     D.E. Merewether - "Trans. Currents Induced on a Metallic Body of Rev. by an EM Pulse", IEEE Transactions on EMC, May, 1971.
  3) formulation of 3D code with radiation boundary condition -
     R. Holland - "THREDE: A Free-Field EMP Coupling and Scattering Code", Mission Research Corp., AMRC-R-95, Sept., 1976.

4) application to complex scattering object with comparison to experiment -
   K.S. Kunz and K.M. Lee - "A Three-Dim. Finite-Diff. Solu. to the Ext. Response of an Aircraft to a Complex Transient EM Environment: Part 1 -The Method and Its Implementation and Part 2 - Comparison of Predictions and Measurements", IEEE Transactions on EMC, May, 1978.
5) expand subvolume in a second run for increased spatial and frequency resolution -
   K.S. Kunz and L.T. Simpson - "A Technique for Increasing the Resolution of Finite-Difference Solutions of the Maxwell Equations", IEEE Transaction on EMC November, 1981
6) generalize the 3D code to treat lossy dielectrics -
   R. Holland, L.T. Simpson and K.S. Kunz - "Finite-Difference Analysis of EMP Coupling to Lossy Dielectric Structures", IEEE Transactions on EMC, August, 1980.

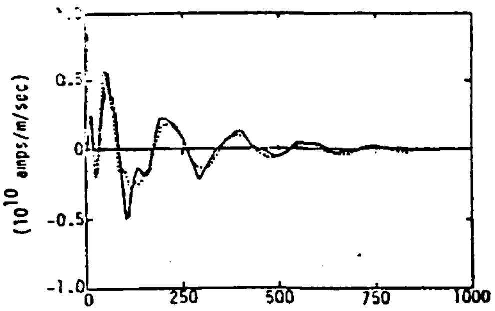

Fig. 17. T.P. R1, $\dot{J}_A(t)$, $E \parallel$ Fuselage.

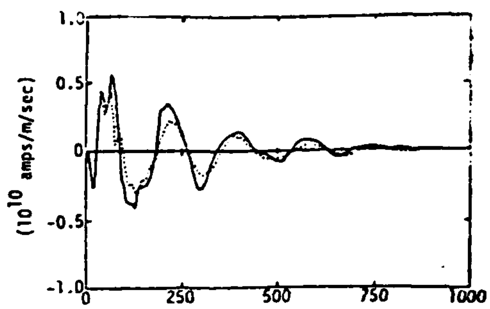

Fig. 21. T.P. 382, $\dot{J}_A(t)$, $E \parallel$ Fuselage.

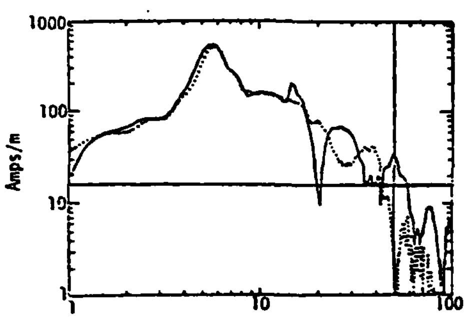

Fig. 18. T.P. R1, $\dot{J}_A(t)$, $E \parallel$ Fuselage.

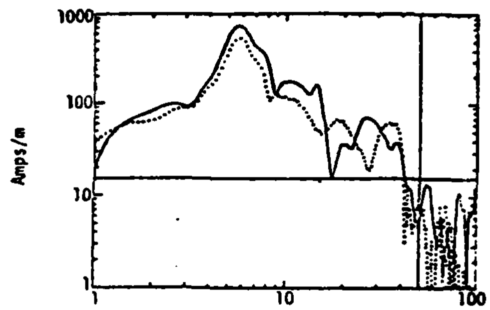

Fig. 22. T.P. 382, $\dot{J}_A(\omega)$, $E \parallel$ Fuselage.

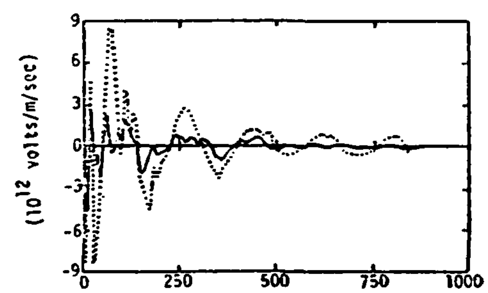

Fig. 19. T.P. R1, $\dot{Q}(t)$, $E \parallel$ Fuselage.

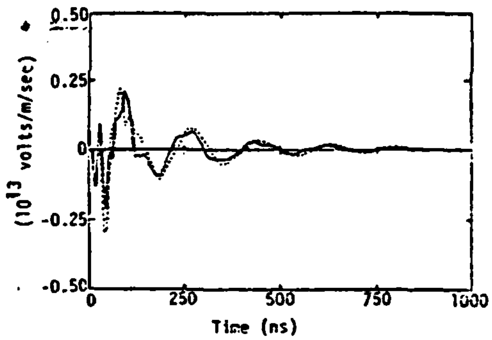

Fig. 23. T.P. 382, $\dot{Q}(t)$, $E \parallel$ Fuselage.

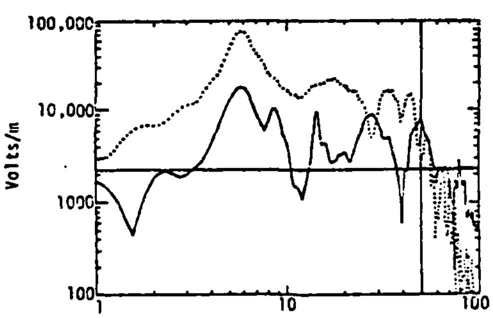

Fig. 20. T.P. R1, $\dot{Q}(\omega)$, $E \parallel$ Fuselage.

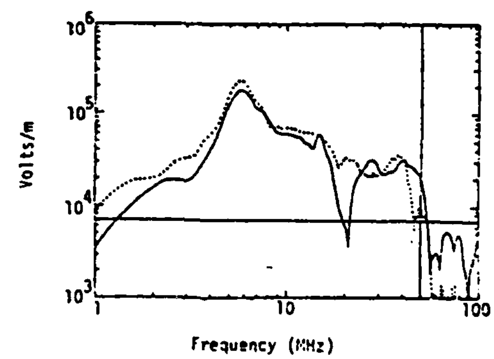

Fig. 24. T.P. 382, $\dot{Q}(\omega)$, $E \parallel$ Fuselage.

SAMPLE PERFECTLY CONDUCTING A/C RESULTS

INCREASED RESOLUTION USING EXPANSION TECHNIQUE

- A/C UNEXPANDED -

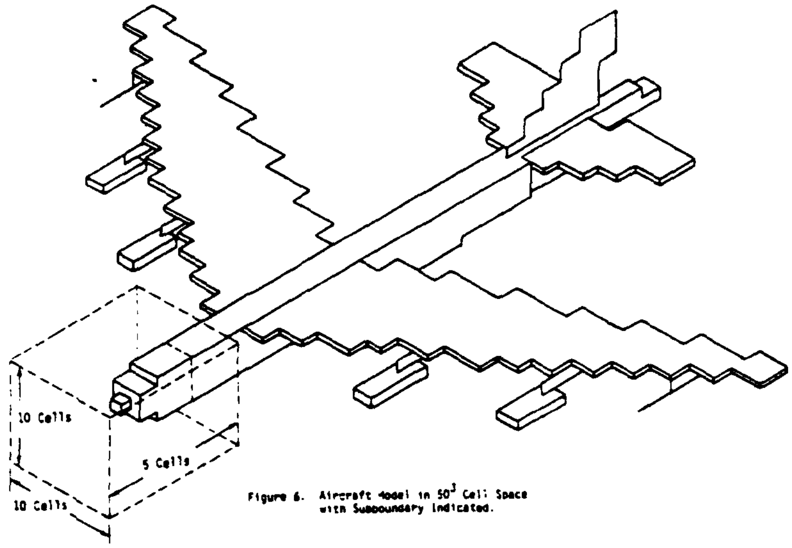

Figure 6. Aircraft Model in 50^3 Cell Space with Subboundary Indicated.

- A/C EXPANDED -

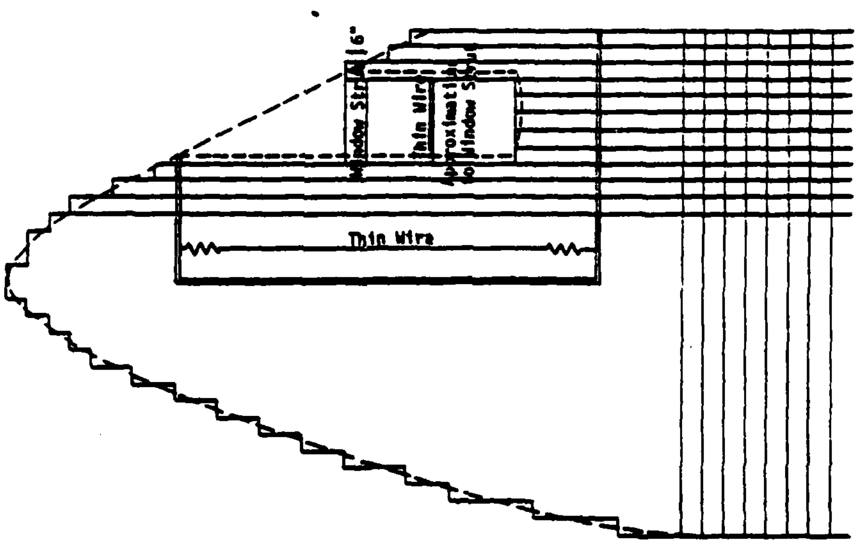

Figure 7. Expanded Run Showing Cockpit Area Detail.

LOSSY DIELECTRIC CAPABILITIES

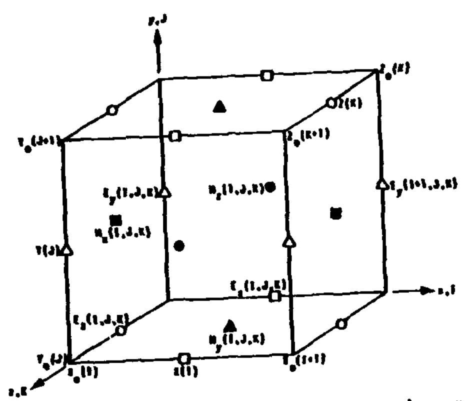

Fig. 1. Convention for imposing the (I, J, K) indexes on the (x, y, z) problem space, and location of the six field evaluation points in a typical cell.

The lossy-dielectric version of THREDE is based upon

$$\mu \frac{\partial H^s}{\partial t} + \sigma^* H^s = -\nabla \times E^s - \sigma^* H^i - (\mu - \mu_0) \frac{\partial H^i}{\partial t}$$

$$\epsilon \frac{\partial E^s}{\partial t} + \sigma E^s = \nabla \times H^s - \sigma E^i - (\epsilon - \epsilon_0) \frac{\partial E^i}{\partial t} .$$

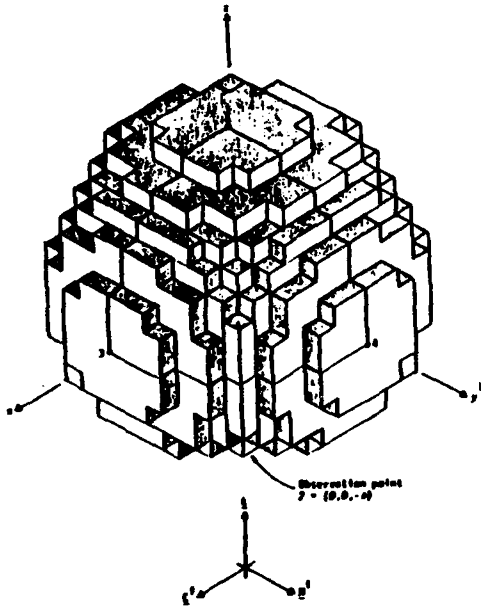

Fig. 2. THREDE model of a dielectric sphere with incident field and observation points indicated. The numbered observation points marked in this figure refer to the observation points cited in Figs. 3-20

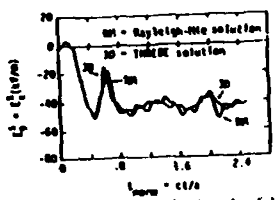

Fig. 3. $E_\theta{}^t = +E_z{}^t$ at observation point 1 (pole of dark hemisphere) for $\epsilon = 9\epsilon_0$

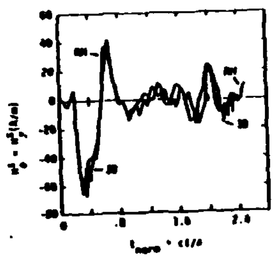

Fig. 4. $H_\phi{}^t = +H_y{}^t$ at observation 1 for $\epsilon = 9\epsilon_0$

Fig. 5. $E_\theta{}^t = -E_z{}^t$ at observation point 2 (pole of illuminated hemisphere) for $\epsilon = 9\epsilon_0$

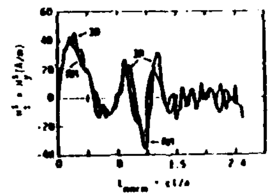

Fig. 6. $H_\phi{}^t = +H_y{}^t$ at observation point 2 for $\epsilon = 9\epsilon_0$

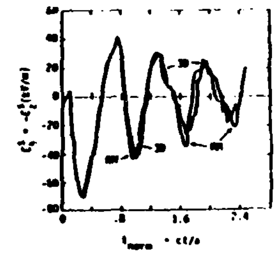

Fig. 7. $E_\theta{}^t = -E_z{}^t$ at observation point 3 for $\epsilon = 9\epsilon_0$

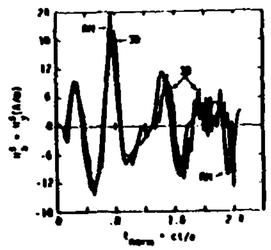

Fig. 8. $H_\phi{}^t = +H_y{}^t$ at observation point 3 for $\epsilon = 9\epsilon_0$

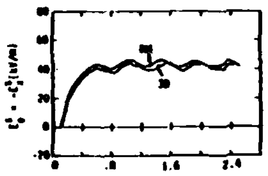

Fig. 9. $E_\phi{}^s = -E_z{}^s$ at observation point 4 for $\epsilon = 9\epsilon_0$.

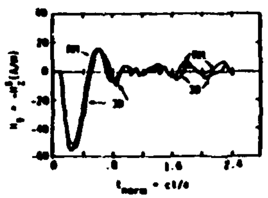

Fig. 10. $H_\phi{}^s = -H_z{}^s$ at observation point 4 for $\epsilon = 9\epsilon_0$.

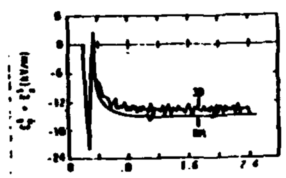

Fig. 11. $E_\theta{}^s = +E_z{}^s$ (unfiltered) at observation point 1 (pole of dark hemisphere) for $\epsilon = 2\epsilon_0$.

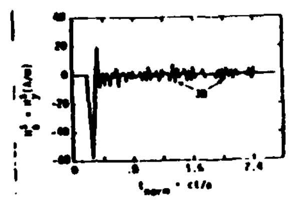

Fig. 12. $H_\phi{}^s = +H_y{}^s$ (unfiltered) at observation point 1 for $\epsilon = 2\epsilon_0$.

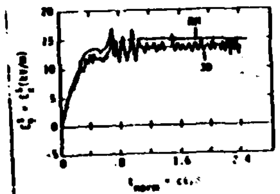

Fig. 13. $E_\theta{}^s = -E_z{}^s$ (unfiltered) at observation point 2 (pole illuminated) hemisphere) for $\epsilon = 2\epsilon_0$.

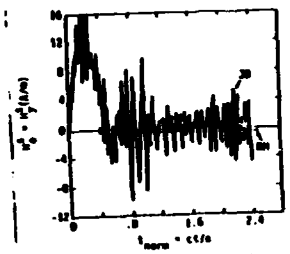

Fig. 14. $H_\phi{}^s = +H_y{}^s$ (unfiltered) at observation point 2 for $\epsilon = 2\epsilon_0$.

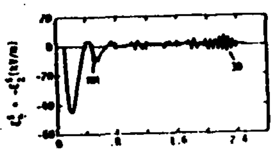

Fig. 15. $E_\theta{}^s = -E_z{}^s$ (unfiltered) at observation point 3 for $\epsilon = 2\epsilon_0$.

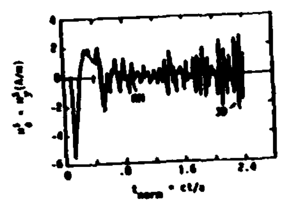

Fig. 16. $H_\phi{}^s = +H_y{}^s$ (unfiltered) at observation point 3 for $\epsilon = 2\epsilon_0$.

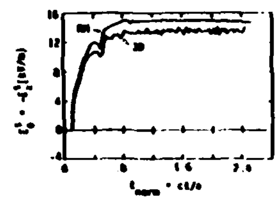

Fig. 17. $E_\theta{}^s = -E_z{}^s$ (unfiltered) at observation point 4 for $\epsilon = 2\epsilon_0$.

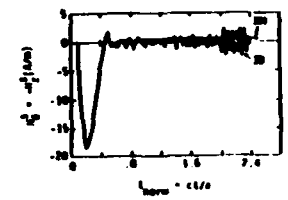

Fig. 18. $H_\phi{}^s = -H_z{}^s$ (unfiltered) at observation point 4 for $\epsilon = 2\epsilon_0$.

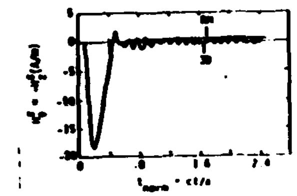

Fig. 19. $H_\phi{}^s = +H_y{}^s$ ($\omega_{co} = 2.5\ c/a$) at observation point 2 for $\epsilon = 2\epsilon_0$; compare with the unfiltered result shown in Fig. 14.

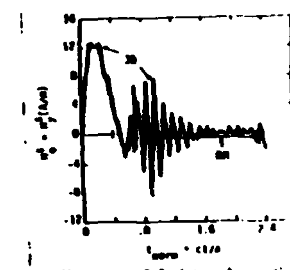

Fig. 20. $H_\phi{}^s = -H_z{}^s$ ($\omega_{co} = 2.5\ c/a$) at observation point 4 for $\epsilon = 2\epsilon_0$; compare with the unfiltered result shown in Fig. 18.

INTERIOR COUPLING APPROACH

Contiguous Skin Model of the Aircraft for Diffusion Calculations

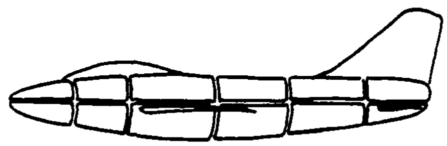

Perfectly Conducting Aircraft with Seams

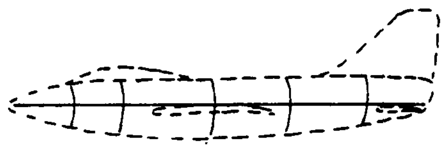

Complement of the Seam Model

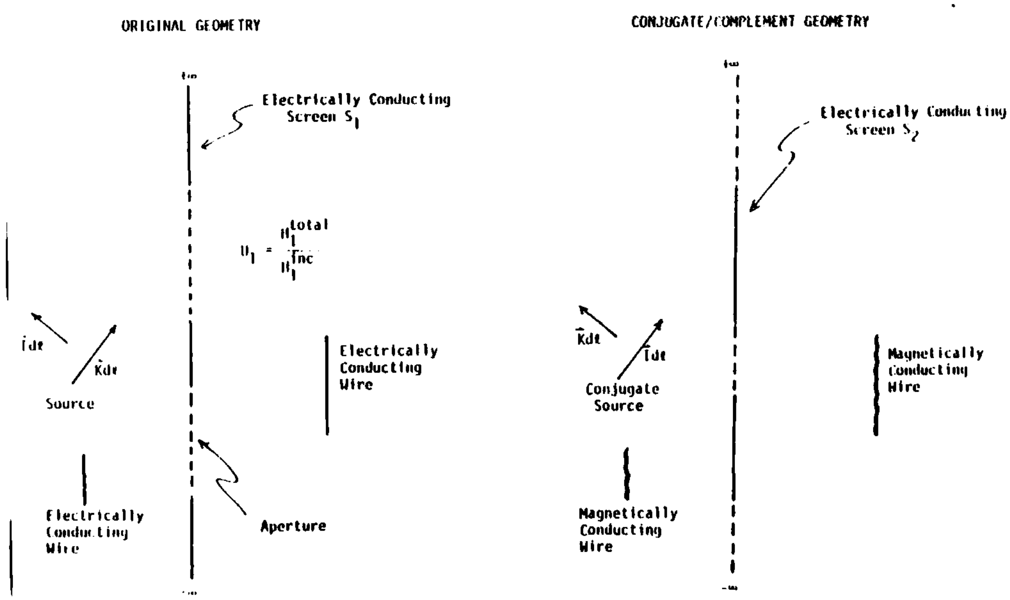

Original and Conjugate/Complement Geometry - Planar Screen Example

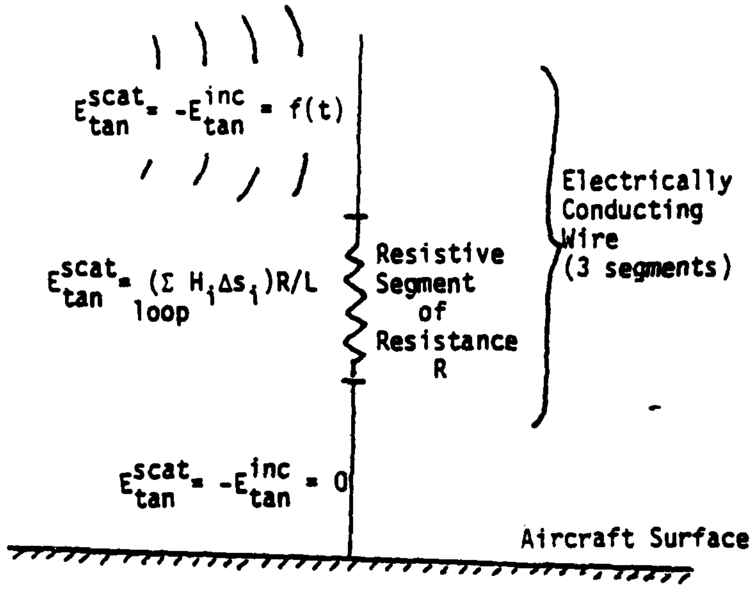

Lightning Channel Source

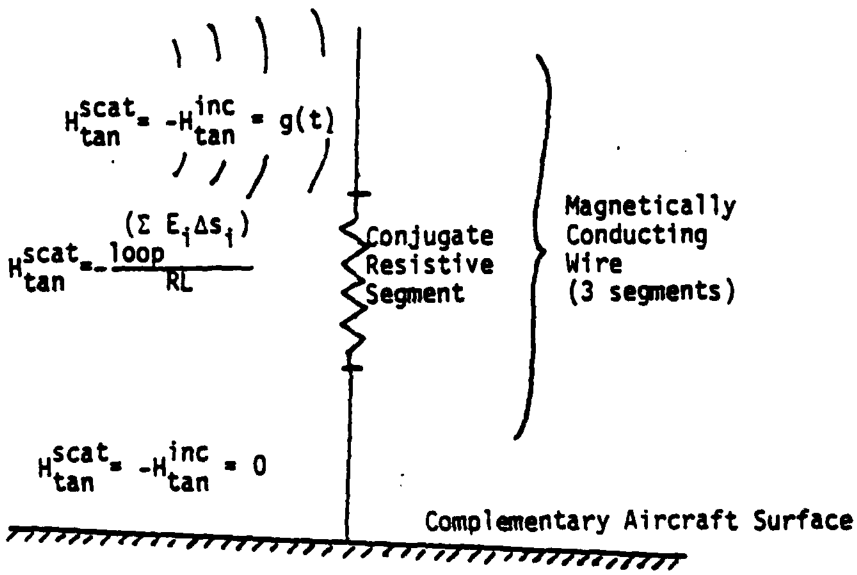

Conjugate Lightning Channel Source

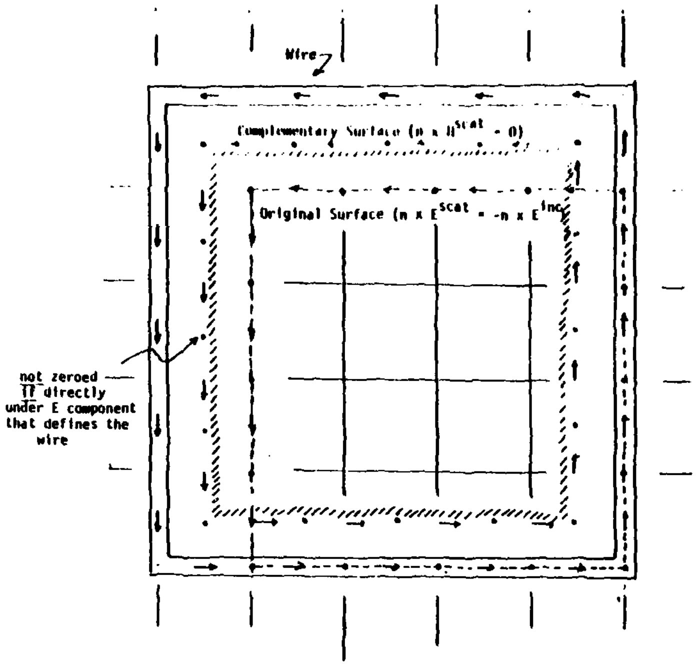

Finite Difference Formulation of the Complementary Aircraft Surface Showing the Half Cell Displacement and the Wire Model of the Seam Girdling the Surface

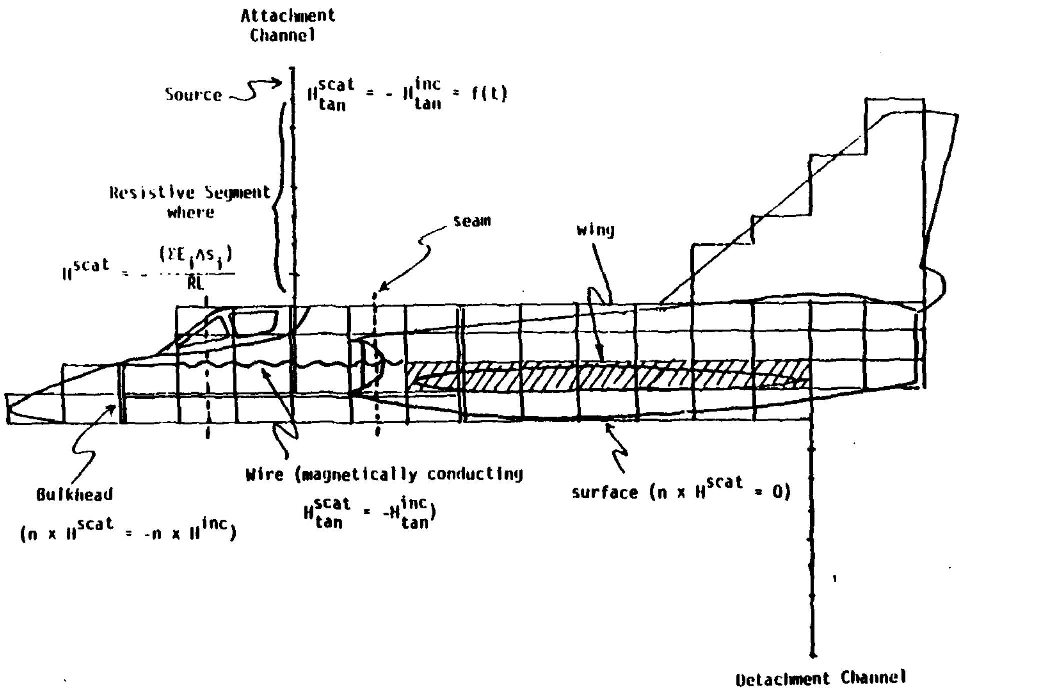

Couple Conjugate/Complement Geometry as Formulated for Finite Difference Applications

PIN PREDICTIONS - SINGLE MULTILAYERED CABLE

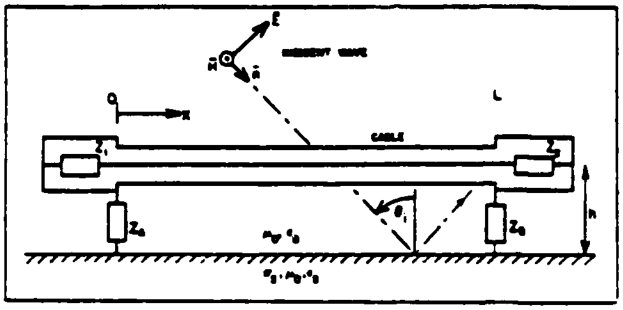

Model of aerial cables.

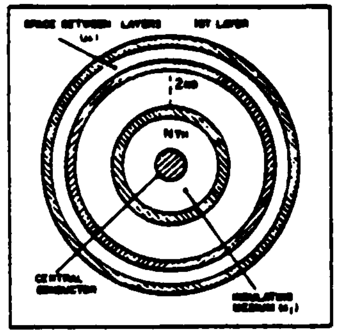

Model of shielded cables.

- USE F.D. TO FIND CURRENTS ALONG CABLE SHEATH, I_b

- USE SURFACE TRANSFER IMPEDANCE, Z_T, AS DEFINED BY SCHELKUNOFF, TO FIND THE INTERIOR CURRENTS:

$$I_a(x) = \int_0^L G_{I1}(x,x') \cdot Z_T \cdot I_b(x')dx' \quad *$$

WHERE G_{I1} IS THE APPROPRIATE GREEN'S FUNCTION THAT INCORPORATES THE CORRECT BOUNDARY CONDITIONS FOR THE GEOMETRY AT HAND

- EVALUATE I_a $(x = L)$ TO FIND THE CURRENT AT THE PIN

- EVALUATE THE VOLTAGE ACROSS THE DEVICE CONNECTED TO THE PIN, V_d, USING THE PIN CURRENT AND THE DEVICE'S IMPEDENCE Z_d, I.E. $V_d = I_a(x = L)Z_d$.

*ONLY DIFFUSION THROUGH SHIELD CONSIDERED

AD-A114 117 FEDERAL AVIATION ADMINISTRATION TECHNICAL CENTER ATL--ETC F/G 1/3
A COMPENDIUM OF LIGHTNING EFFECTS ON FUTURE AIRCRAFT ELECTRONIC--ETC(U)
FEB 82 N O RASCH
UNCLASSIFIED DOT/FAA/CT-82/30 NL

3 of 3

END
DATE
FILMED
6-82
DTIC

EXPECTED RESULTS -

- EXTERIOR RESPONSE - SIMILAR TO PERFECTLY CONDUCTING A/C RESPONSES
- INTERIOR CABLE RESPONSE, WIRE EXTERIOR - WEAKLY DAMPED SINUSOID, SEE BELOW
- PIN RESPONSE - SIMILAR TO WIRE EXTERIOR

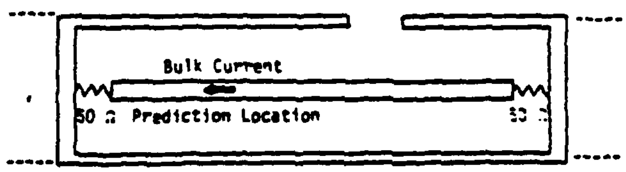

Interior Geometry of Expanded Region

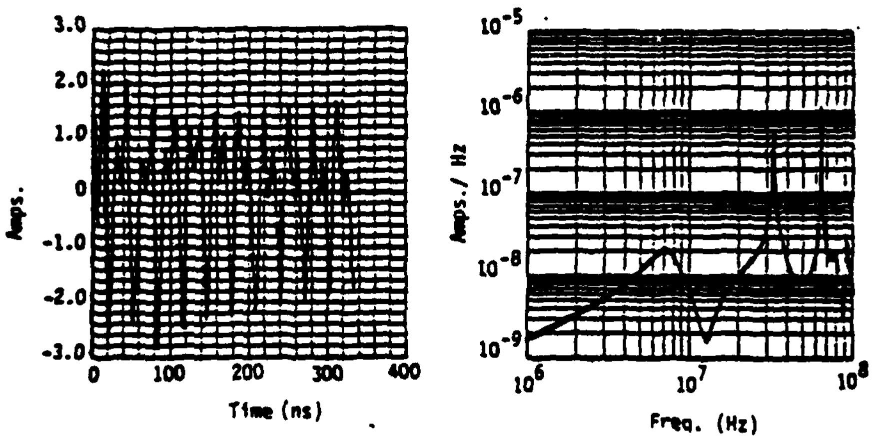

Sample of Predicted Results

SUMMARY

FEATURES

° Any fuselage exterior geometry can be modeled, including:

  - composites
  - conducting panels
  - mix of composite and metal

° Various coupling pathways can be modeled, including:

  - diffusion through composite panels
  - seams around panels
  - small apertures around doors/hatches/wheel wells, etc.
  - large apertures such as windows

° *Detailed interior geometries* can be treated, including:

  - individual wires with various terminations
  - surrounding "fill"
  - adjacent wires to within a cell size (~0.05m or ~2" at best)

° Fast risetime (~30-50ns) pulses can be easily incorporated

° Non-linear effects can be modeled

  - attachment points can be selected based on experience, while detachment points can be selected based on fields exceeding preset thresholds
  - interior arcing can be modeled similarly

AREAS OF APPLICATION

- Exterior I and V response predictions as a function of:
  - position
  - A C construction (metal or composite or mix)
  - excitation source
  - attachment/detachment location
- Interior Responses
  - interior field levels
  - wire currents
  - transfer functions
- Hazard Assessment
  - induced current damage
  - field induced upset
  - fuel ignition from arcing
- Protection Measures Evaluation
  - field/charge and current penetration reduction (from covered seams, mesh across windows, etc.)
  - arc suppression (from cable rerouting, interior geometry changes, etc.)
  - protective device effects (depends on "threat" spectrum, device location, device operations, etc.)

INTERMITTENT/TRANSIENT FAULTS IN DIGITAL COMPUTERS

by

Dr. Gerald M. Masson

Johns Hopkins University

Need and objectives of digital system upset assessment methodology: The definition of upset. Description of approach being developed for assessing upset potential of digital systems. Upset model types and importance of burst error models; dominant importance of program transition models. Definition and use of system state probability transition matrix in upset analyses. Example of upset tolerant microcontroller.

FAULT ANALYSIS

* FAULTS
  - PERMANENT
  - INTERMITTENT
  - TRANSIENT
  - I/T
* MODELS
  - STUCK-AT
* TESTS
  - DETECTION
  - LOCATION

FAULT TOLERANCE

* DUPLEX SYSTEMS
  - ROLLBACK
* TMR SYSTEMS
  - ROLLAHEAD
* DIAGNOSABLE SYSTEMS
  - INTELLIGENT UNITS

MICROPROCESSOR CONTROLLERS

* HARDWARE
  - CENTRAL PROCESSING UNIT (CPU)
  - READ-ONLY MEMORY (ROM)
  - READ/WRITE MEMORY (RAM)
  - INPUT/OUTPUT DEVICES (I/O)
  - SUPPORT LOGIC
* SOFTWARE
  - LOOKUP TABLES
  - CHARACTERIZATION
    I. INPUT SENSORS SCANNED
    II. DATA PROCESSING
    III. CONTROL SIGNALS TO ACTUATORS

FAULTS IN MICROPROCESSORS

* CPU TESTING
* RECOVERY STRATEGIES
  - DUPLICATION
  - TMR
  - WATCHDOG TIMER

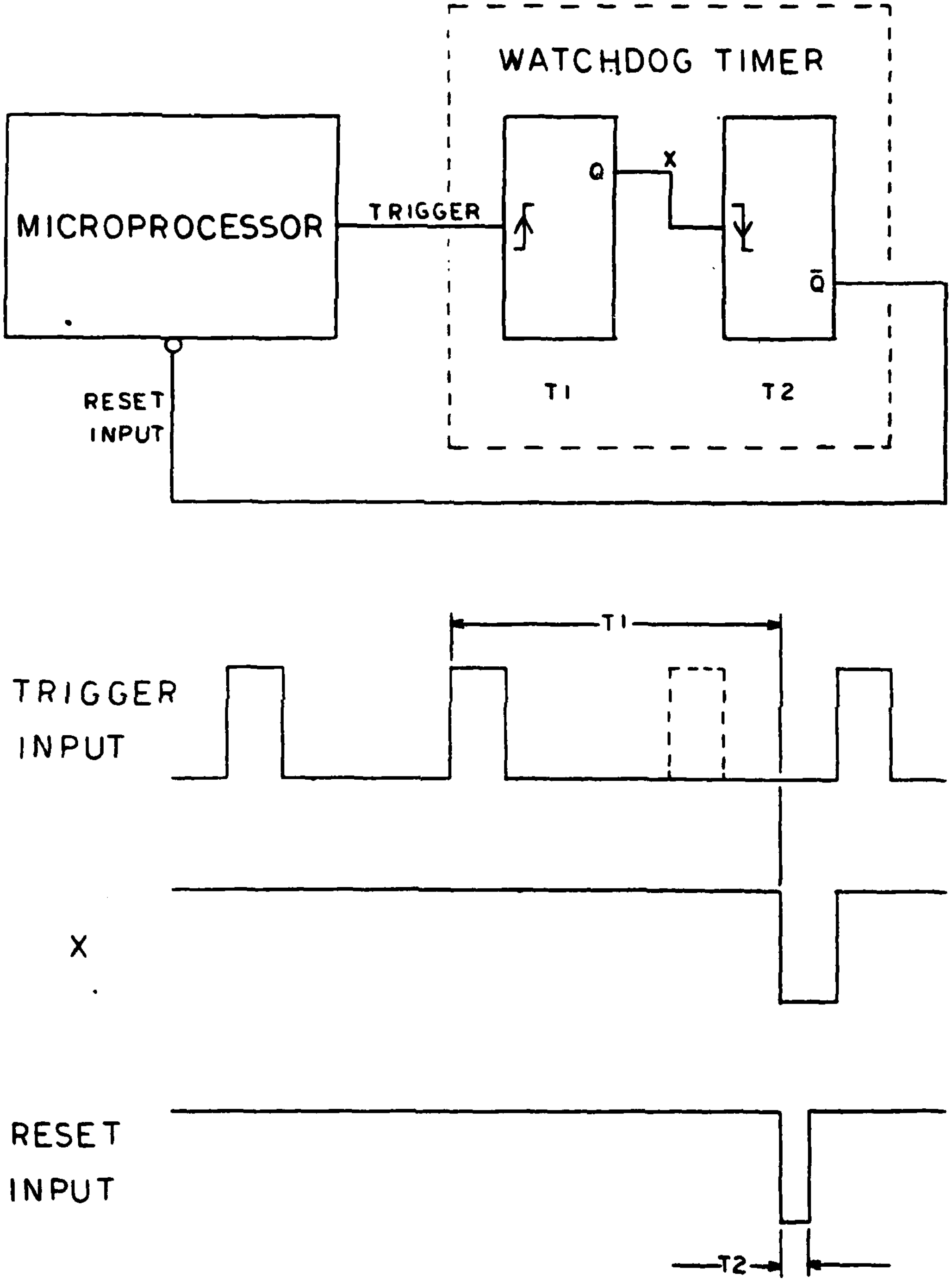

FIGURE 1. WATCHDOG TIMER

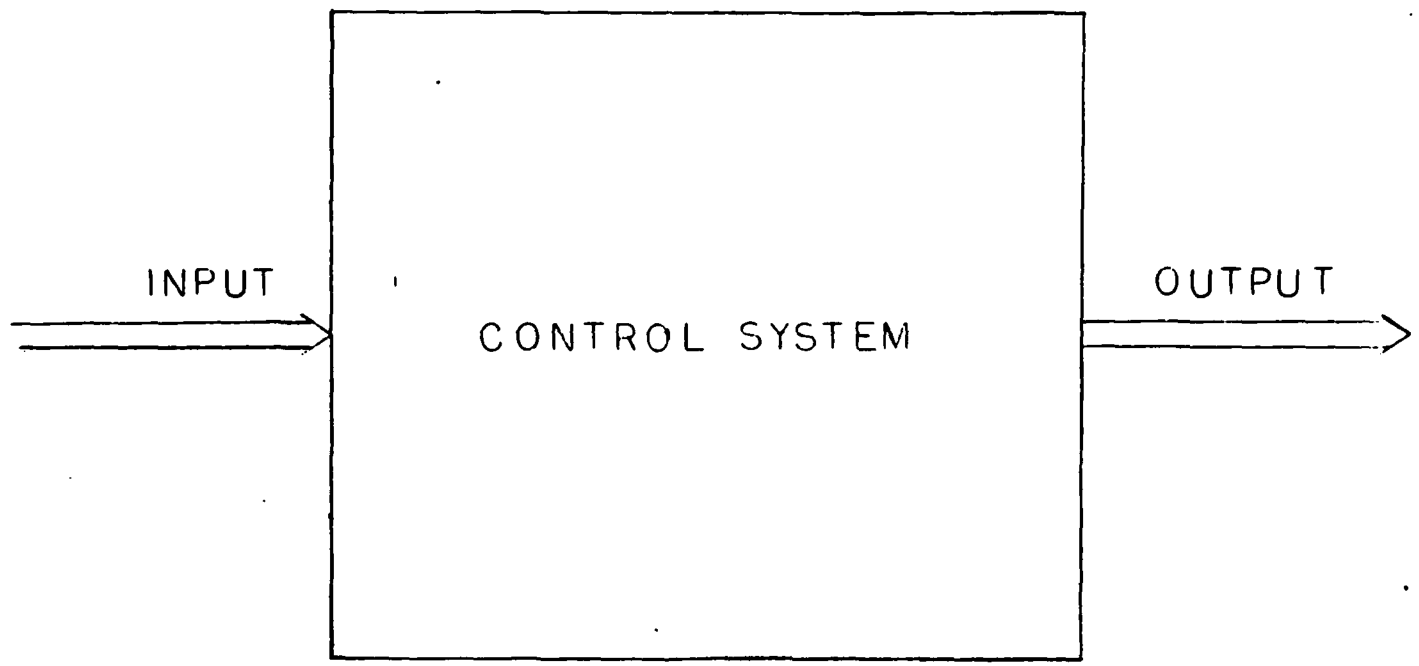

FIGURE 2. CONTROL SYSTEM CONSIDERED ALONE

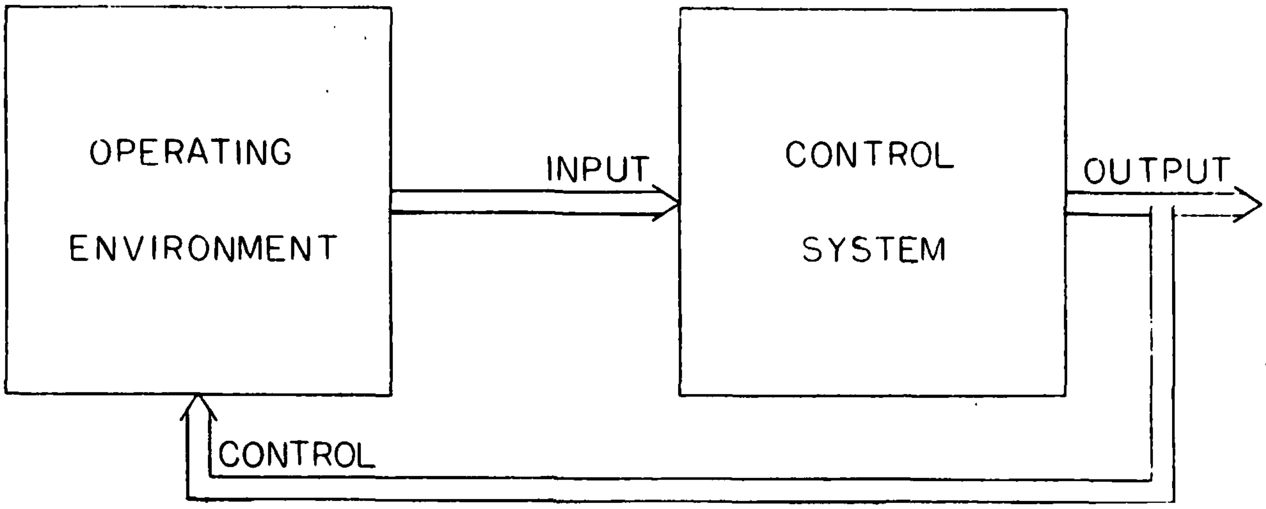

FIGURE 3. CONTROL SYSTEM SITUATED IN ITS ENVIRONMENT

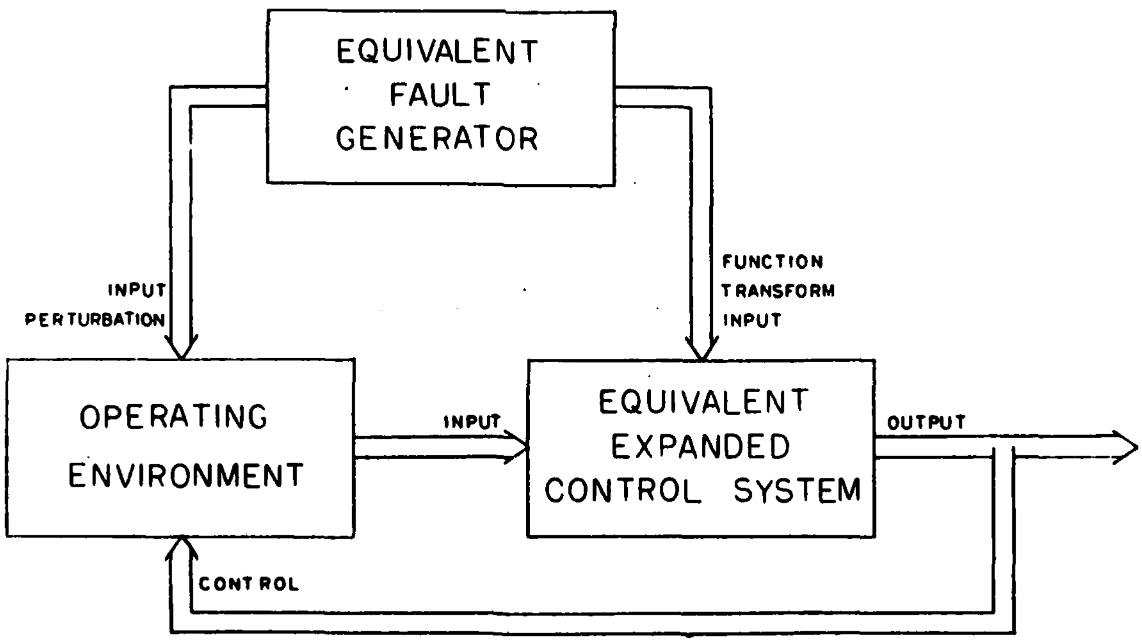

FIGURE 4. CONTROL SYSTEM SITUATED IN EQUIVALENT HOSTILE ENVIRONMENT

FAULT/SYSTEM INTERACTION

* CONTROL SYSTEM INTERACTS WITH ENVIRONMENT

* INTERMITTENT/TRANSIENT FAULTS
  - SYSTEM "TRANSIENT" RESPONSE
  - SYSTEM "STEADY STATE" RESPONSE

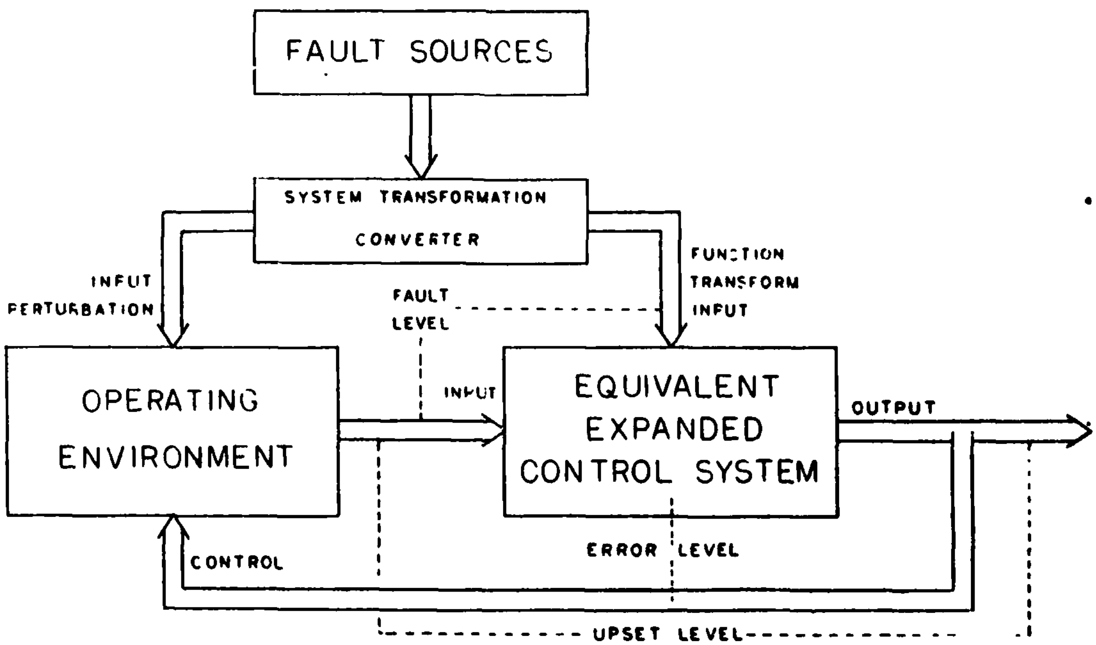

FIGURE 5. CONTROL SYSTEM SITUATED IN HOSTILE ENVIRONMENT

FAULTS, ERRORS, AND UPSETS

- FAILURES
  - CIRCUIT LEVEL
  - ANALOG NATURE
- FAULTS
  - LOGICAL LEVEL
  - DIGITAL NATURE
  - LOGICAL DIFFERENCE AT FAULT SITE
- ERRORS
  - LOGICAL LEVEL
  - DIGITAL NATURE
  - DUE TO PROPAGATION OF FAULTS
  - LOSS OF SYNCHRONIZATION PROBLEM
    NEW DEFINITION
- UPSETS
  - SYSTEM LEVEL
  - FUNCTIONAL NATURE
  - TRANSFER FUNCTION

CONTAINMENT SETS

- A FINITE SET OF MUTUALLY EXCLUSIVE FUNCTIONAL STATES
- COVERS ALL POSSIBLE SYSTEM TRANSFER FUNCTIONS
- INCLUDES
  - VALID STATES
  - ERRONEOUS STATES

CONTAINMENT SET TRANSITIONS

TRANSITION MATRIX:

$T=[p_{ij}]$, WHERE p_{ij} IS THE PROBABILITY OF A TRANSITION FROM STATE j TO STATE i , GIVEN THAT AN ERROR HAS OCCURRED

$$L(K+1) = T\,L(K) \quad , \quad L(K) = \begin{bmatrix} p_0 \\ p_1 \\ \vdots \\ p_n \end{bmatrix}$$

$p_i(K)$ IS THE PROBABILITY OF BEING IN CONTAINMENT STATE $L_i \in \{L\}$ AFTER K UPSETS

AFTER K UPSETS,

$$L(K) = T^K\,L(0)$$

FAULT ANALYSIS AND SYSTEM VALIDATION

* SINGLE UPSET ENVIRONMENT
  - P_{11} OF $T\left[P_{ij}\right]$ OF MAJOR CONCERN
* MULTIPLE UPSET ENVIRONMENT
  - P_{11} OF T^K FOR LARGE K OF MAJOR CONCERN

* EXAMPLE

$$T^* = \begin{bmatrix} 3/4 & 15/16 \\ 1/4 & 1/16 \end{bmatrix} , \qquad T^{**} = \begin{bmatrix} 7/8 & 1/8 \\ 1/8 & 7/8 \end{bmatrix}$$

$$\lim_{K\to\infty} (T^*)^K = \begin{bmatrix} 15/19 & 15/19 \\ 4/19 & 4/19 \end{bmatrix} , \quad \lim_{K\to\infty} (T^{**})^K = \begin{bmatrix} 1/2 & 1/2 \\ 1/2 & 1/2 \end{bmatrix}$$

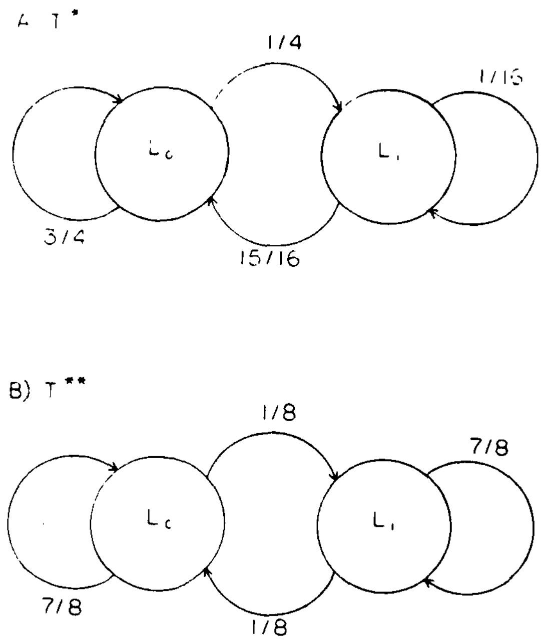

FIGURE 6. TWO 2-LOOP IMPLEMENTATIONS

FAULT TOLERANCE

- CONTAINMENT SET AND TRANSITION MATRIX ANALYSIS PROVIDES FEEDBACK TO IMPROVE DESIGNS
- REMOVAL OF ERRONEOUS ELEMENTS FROM THE CONTAINMENT SET AUTOMATICALLY PROVIDES FAULT TOLERANCE

CONTAINMENT SET FOR MICROPROCESSORS

* PROGRAM TYPES
  - EXITING
  - LOOPING
* TAKE THE CONTAINMENT SET TO CONSIST OF ALL POSSIBLE LOOP PROGRAMS
  - INCLUDES VALID LOOPS
  - INCLUDES ERRONEOUS LOOPS

GIVEN THE EXECUTION OF LOOP PROGRAM $L_i \in \{L\}$, UPSETS CAN BE CHARACTERIZED AS:

(1) DATA CHANGE --
DATA VALUES ARE MODIFIED, BUT EXECUTION REMAINS IN L_i

(2) PROGRAM BUMP --
EXECUTION TEMPORARILY DIVERGES FROM L_i BUT EVENTUALLY RETURNS TO L_i

(3) PROGRAM TRANSITION --
EXECUTION JUMPS FROM L_i TO L_j, $L_i \neq L_j$

PROGRAM TRANSITION = STEADY STATE OPERATIONAL DEVIATION
TRANSITION INTO INVALID EMBEDDED LOOP = SYSTEM CRASH

	ADDRESS	CONTENTS
NORMAL EXECUTION	N	OP-CODE
ERRONEOUS EXECUTION	N+1	DATA

NORMAL EXECUTION	N	OP-CODE
ERRONEOUS EXECUTION	N+1	DATA 0
ERRONEOUS EXECUTION	N+2	DATA 1

ERRONEOUS EXECUTION	N	DATA TABLE
ERRONEOUS EXECUTION	N+1	DATA TABLE
.	.	.
.	.	.
.	.	.

FIGURE 7. ERRONEOUS LOOP INSTRUCTION EXECUTION

Result	Addr	Data	L0 Code	L1 Code	L2 Code	Other
L0	0000	00				NOP
.	.	.				.
.	.	.				.
.	.	.				.
L0	00C9	00				NOP
L0	00CA	3E	MVI A,0C3H			
L1	00CB	C3		JMP 0D3H		
L0	00CC	D3	OUT 0			
L0	00CD	00				NOP
L0	00CE	22	LXI H,0CFC3H			
L2	00CF	C3			JMP 0CFH	
L0	00D0	CF				RST 1
L0	00D1	00	NOP			
L0	00D2	32	STA 0CBC3H			
L1	00D3	C3		JMP 0CBH		
L0	00D4	CB				RSTV
L0	00D5	00	NOP			
L0	00D6	C3	JMP 0CAH			
L0	00D7	CA				JZ 0
L0	00D8	00				NOP
L0	00D9	00				NOP
.	.	.				.
.	.	.				.
.	.	.				.
L0	00FE	00				NOP
L0	00FF	C7				RST 0

Figure 8. An Erroneous Loop Example for the 8085

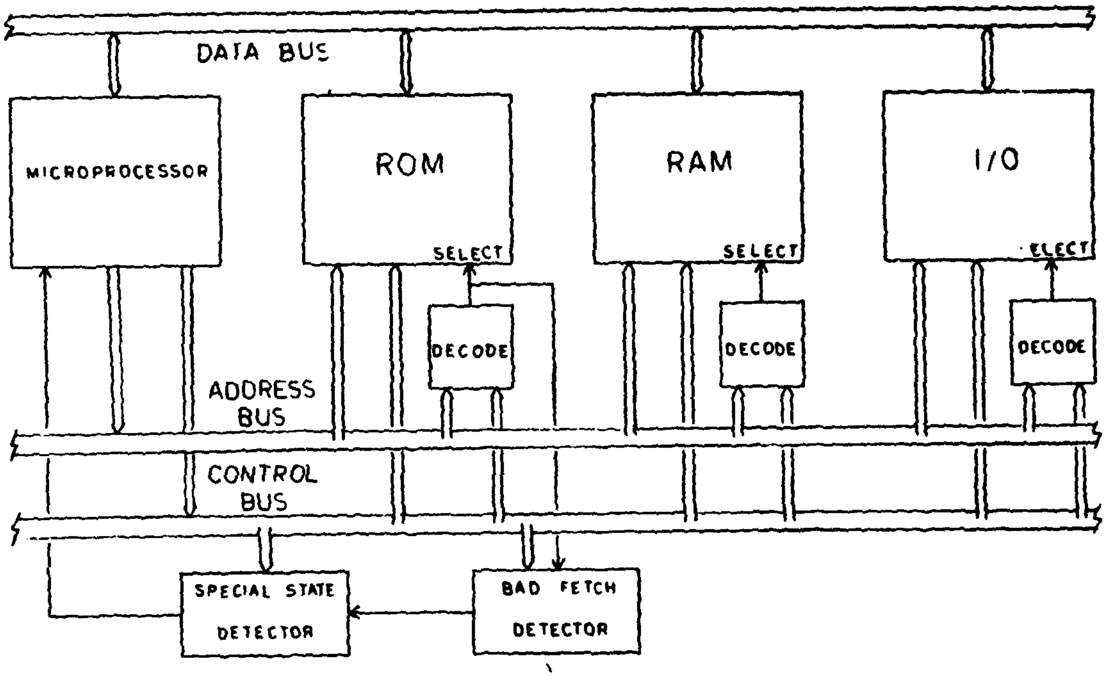

FIGURE 9. CONTROLLER WITH CONTAINMENT HARDWARE

PROGRAM PATH DIVERTERS

* HARDWARE
  - CLOCK STOP
  - HALT
  - READY
  - HOLD
  - INTERRUPTS

* SOFTWARE
  - JUMP CATEGORY INSTRUCTIONS
  - CALL CATEGORY INSTRUCTIONS
  - RETURN CATEGORY INSTRUCTIONS

  (+ EFFECTS OF "UNDEFINED" INSTRUCTIONS)

** A PROGRAM STRUCTURAL ANALYSIS IS MADE BASED ON PATH DIVERTERS **

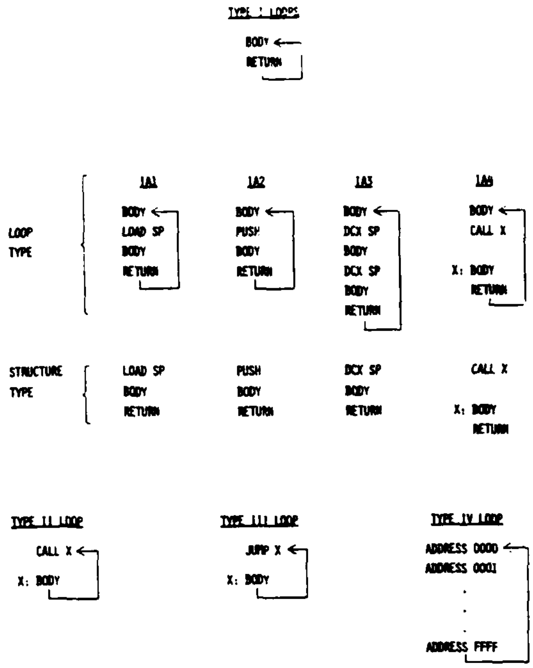

FIGURE 10. LOOP STRUCTURES

FAULT TOLERANT CONTROLLER DESIGN RULES

* HARDWARE
    - CONTINUOUS CLOCK
    - UNCONDITIONAL INSTRUCTION EXECUTION
      (OP-CODE FETCH DETECTION)
    - BAD FETCH DETECTOR
      (ROM RESTRICT MECHANISM)
    - OPTIONAL SAFE ROM
    - REQUIRES 2-3 INTEGRATED CIRCUITS

TABLE I

CRASH-PROOF SOFTWARE DESIGN RULES SUMMARY

1. PROGRAM EXECUTION FROM RAM IS PROHIBITED.

2. EXIT FROM TEMPORARY LOOPS MUST BE GUARANTEED.

3. STABLE LOOPS MUST INCLUDE A CALL TO A CHECK SUBROUTINE, WHICH GUARANTEES ALL ASSUMPTIONS THE PROGRAM REQUIRES FOR CONTINUED EXECUTION. (THESE INCLUDE ASSUMPTIONS ON I/O, INTERRUPTS, AND VARIABLES.)

4. RETURN FROM ALL POSSIBLE INTERRUPTS MUST BE GUARANTEED.

5. SUBROUTINES CANNOT CALL THEMSELVES.

6. SUBROUTINES CANNOT MODIFY THE STACK POINTER OR THE RETURN ADDRESS.

7. WITHIN SUBROUTINES, MEMORY STORE INSTRUCTIONS WHICH PERMIT A VARIABLE STORE ADDRESS MUST GUARANTEE THAT THE REGISTER USED AS THE ADDRESS POINTER CANNOT POINT TO THE STACK SPACE.

8. INSTEAD OF USING RET OR RCN INSTRUCTIONS, A JMP OR JCN TO A SPECIAL RETURN ROUTINE WHICH GUARANTEES THAT THE STACK POINTER POINTS WITHIN THE STACK SPACE BEFORE RETURNING MUST BE USED. (THE RETURN ROUTINE CONTAINS THE ONLY RET INSTRUCTION IN THE ENTIRE PROGRAM.)

9. A STACK WALL MUST BE ADDED. (LEAVE UNUSED ROM SPACE AS 00 OR FF.)

10. THE PCHL INSTRUCTION CANNOT BE USED.

11. EITHER A SAFE ROM MUST BE USED, OR ALL ERRONEOUS LOOPS AND ERRONEOUS CALLS TO ADDRESSES WHICH, WHEN CONSIDERED TO BE SUBROUTINES, DO NOT SATISFY EITHER RULE 5, 6, 7, OR 8 MUST BE REMOVED.

FAULT TOLERANT CONTROLLER TEST SYSTEM

* NOISY POWER SUPPLY TEST SOURCE
* DUAL LED CONTROLLERS
* UNMODIFIED SOFTWARE
  - LED 1.1
  - LED 4.6
* CRASH-PROOF SOFTWARE
  - LED 2.2
  - LED 3.3
  - LED 3.4
  - LED 5.2
  - OVERHEAD

    LED 2.2/LED 1.1 = 8.5 %

    LED 5.2/LED 4.6 = 14 %

    LED 3.3/LED 2.2 = 35 %

    LED 3.3/LED 1.1 = 47 %

SOFTWARE TOOLS

* DESIGN AIDS FOR FAULT TOLERANCE IMPLEMENTATION
* INTERACTIVE USE PROVIDES EFFECTIVE AND EFFICIENT DESIGN
* SAFE
  - PRODUCES SAFE ROM CONTENTS FROM SOURCE CODE
  - OUTPUT USED AS INPUT TO LOOP
* LOOP
  - LOCATES BANNED PROGRAM STRUCTURES
  - LOCATES ERRONEOUS LOOPS
  - PROVIDES CHECK ON INTENTIONAL LOOPS

LOOP ANALYSIS OF LED 1.1, PAGE 1

```
% LOOP LED1.1.OBJ LED1.1.SAFE
LOOP SEARCH? Y
ONLY VALID (V,v) OR ERRONEOUS (E,e) ? E
LOOP: ERRONEOUS
00FB F5          PSH PSW
00FC 00          NOP
00FD C3 F3 00    JMP  00F3
00F3 05          DCR B
00F4 C8          RZ

LOOP SEARCH? N
LIST CALLS? Y
ONLY VALID (V,v) OR ERRONEOUS (E,e) ? E
LOOP: ERRONEOUS
036D FC 07 F8   CM   F807      [I/O]

LOOP: ERRONEOUS
0395 FC 0F FE   CM   FE0F      [I/O]

LOOP SEARCH? N
LIST CALLS? N
LIST MEMORY STORES? Y
ONLY VALID (V,v) OR ERRONEOUS (E,e) ? V
LOOP: VALID
006A 77          MOV M,A

LOOP: VALID
00AC 34          INR M

LOOP: VALID
00B3 36 00       MVI M, 00

*** MAIN AND SWTCH SET AS ERRONEOUS ***

% LOOP LED1.1.OBJ LED1.1.SAFE
LOOP SEARCH? Y
ONLY VALID (V,v) OR ERRONEOUS (E,e) ? V
LOOP: VALID
009D CD EB 01    CALL  01EB
00A0 0D          DCR C
00A1 C2 9D 00    JNZ   009D

LOOP: VALID
00F3 05          DCR B
00F4 C8          RZ
00F5 23          INX H
00F6 7E          MOV A,M
00F7 23          INX H
00F8 FE F0       CPI   F0
00FA C2 F5 00    JNZ   00F5
00FD C3 F3 00    JMP   00F3

LOOP: VALID
00F5 23          INX H
00F6 7E          MOV A,M
00F7 23          INX H
00F8 FE F0       CPI   F0
00FA C2 F5 00    JNZ   00F5

LOOP: VALID
00F3 05          DCR B
00F4 C8          RZ
00F5 23          INX H
00F6 7E          MOV A,M
```

TABLE II

LED Program Comparisons

Program	Bytes (Hex)	Bytes (Dec)	Features
LED 1.1	03BB	955	* Functional
LED 2.2	040C	1036	* Functional * Crash-proof
LED 3.3	0577	1399	* Functional * Crash-proof with SAFE ROM * State encode
LED 3.4	0578	1400	* Functional * Crash-proof * State encode
LED 4.6	039A	922	* Functional
LED 5.2	0419	1049	* Functional * Crash-proof

CONCLUSIONS

- DIRECT APPLICATION TO MICROPROCESSOR CONTROLLERS
  - TRADE-OFFS
  - MEASUREMENTS
  - COMPARISON WITH WATCHDOG TIMER
  - LANGUAGE CONSIDERATIONS
    - ASSEMBLY LANGUAGE
    - COMPILED LANGUAGES
    - INTERPRETIVE LANGUAGES
  - CPU SELECTION REQUIREMENTS AND ARCHITECTURAL RECOMMENDATIONS
    - ROM RESTRICT MECHANISM
    - TEST MODES
    - UNDEFINED OP-CODES
- APPLICATION TO LARGE COMPUTER SYSTEMS
  - MONITORS
  - DIAGNOSABLE SYSTEMS
  - THEORY EXPANSION

A MICROPROCESSOR-BASED UPSET TEST METHOD

by

Ms. Celeste M. Belcastro

Langley Research Center
National Aeronautics and Space Administration

Description of a microprocessor-based upset testing method employing transient waveforms randomly injected into a digital unit. Upset test data presented along with preliminary observations.

OUTLINE

- BACKGROUND
- RESEARCH OBJECTIVES OF UPSET TESTING
- UPSET TEST DESIGN CRITERIA
- UPSET TEST HARDWARE IMPLEMENTATION
- PRELIMINARY OBSERVATIONS
- FUTURE PLANS

PROBLEM CAUSED BY LIGHTNING

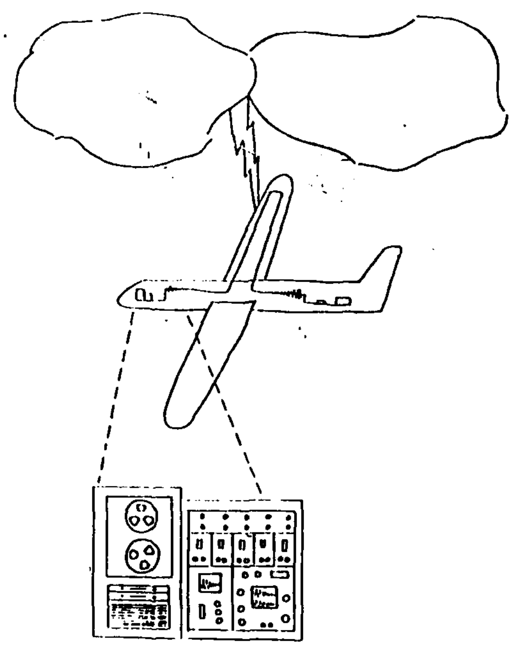

INDUCED EFFECTS TESTING LEVELS

- SYSTEM AND SUBSYSTEM ASSESSMENT -

  CABLE EXCITATION

  - CHANGING MAGNETIC FIELD IN A COUPLING TRANSFORMER
  - TRANSVERSE ELECTROMAGNETIC WAVES GENERATED ON PARALLEL-PLATE TRANSMISSION LINES

- INDIVIDUAL UNIT ASSESSMENT -

  INTERFACE CIRCUIT INJECTION

  - DIRECT APPLICATION OF TRANSIENT WAVEFORMS TO PIN CONNECTIONS

RESEARCH OBJECTIVES

- SHORT RANGE
  - DEVELOP A METHODOLOGY TO TEST A DIGITAL SYSTEM FOR UPSETS
- LONG RANGE
  - CHARACTERIZE UPSET PHENOMENA
  - DEVELOP DIGITAL FAULT SIGNATURES THAT MODEL UPSETS
    - DIAGNOSTIC EMULATION
    - UPSET VULNERABILITY ASSESSMENT

UPSET TEST CRITERIA

- CHOOSE A CANDIDATE PROCESSOR/CONTROLLER
- INJECT TRANSIENT SIGNALS RANDOMLY
  - ENHANCE SIMULATION
  - AVOID SYNCHRONIZATION
- IDENTIFY PROCESSOR'S INTERNAL STATE WHEN INJECTION OCCURS
  - DETERMINE IF UPSET OCCURS INDEPENDENTLY OF PROCESSING STATE
- VARY THE TRANSIENT SIGNAL INJECTION POINT
  - DETERMINE IF UPSET SUSCEPTIBILITY IS UNIFORM THROUGHOUT THE PROCESSING SYSTEM
- OBTAIN BIT PATTERNS
  - DEVELOP FAULT SIGNATURES

CANDIDATE PROCESSOR/CONTROLLER

INTEL µP UNIT -

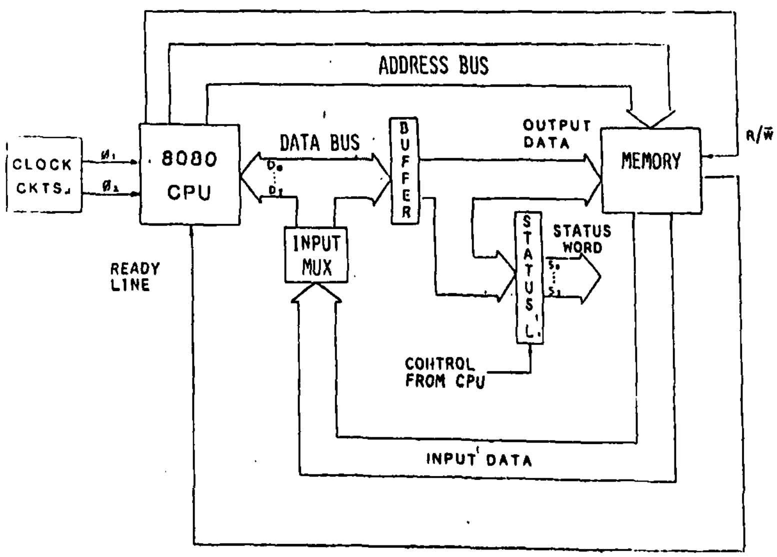

PROGRAMMING HIERARCHY

PROGRAMMER

↓

8080 INSTRUCTION SET
(244 INSTRUCTIONS)

↓

PROGRAM

↓

OPERATION CODE (OP-CODE)

↓

8080 μP

↓

INSTRUCTION CYCLES

↓

MACHINE CYCLES (IDENTIFIED BY STATUS BITS)

↓

STATES

↓

CLOCK CYCLES ($\emptyset_2$)

MICROPROCESSOR MACHINE CYCLES

TYPE OF MACHINE CYCLE	STATUS BITS S7	S6	S5	S4	S3	S2	S1	S0	NO. OF CLOCK CYCLES
INSTRUCTION FETCH	1	0	1	0	0	0	1	0	4 OR 5
MEMORY READ	1	0	0	0	0	0	1	0	3
MEMORY WRITE	0	0	0	0	0	0	0	0	3 OR 4
STACK READ	1	0	0	0	0	1	1	0	3
STACK WRITE	0	0	0	0	0	1	0	0	3
INPUT	0	1	0	0	0	0	1	0	3
OUTPUT	0	0	0	1	0	0	0	0	3
INTERRUPT	0	0	1	0	0	0	1	1	5
HALT	1	0	0	0	1	0	1	0	3x
INTERRUPT WHILE HALT	0	0	1	0	1	0	1	1	5

UPSET TEST CONFIGURATION

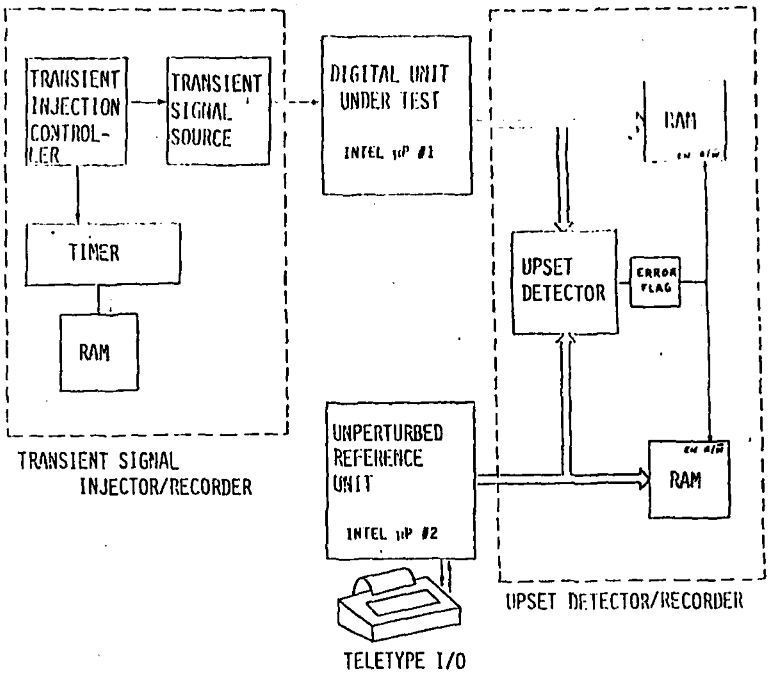

LIGHTNING INDUCED EFFECTS WAVEFORMS

- DAMPED SINUSOID

- DECAYING EXPONENTIAL

DAMPED SINUSOIDAL WAVEFORM

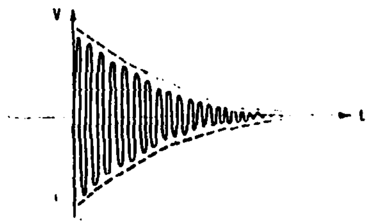

WAVEFORM	FREQUENCY	t_r (ns)	t_d
1	1 MHz (±20%)	50 max	Amplitude decreases
2	10 MHz (±20%)	5 max	25-50% in 4 cycles

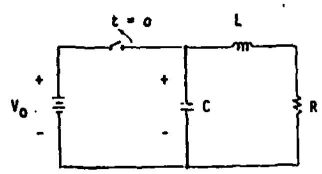

$$\frac{R}{2L} = \frac{-\ell n 0.5}{t_d}$$

$$C = \frac{1}{L\left[4\pi^2 f^2 + \left(\frac{R}{2L}\right)^2\right]}$$

1 MHz

R = 68 Ω
L = 196 μH
C = 129 ρF

10 MHz

R = 47 Ω
L = 13.5 μH
C = 18.7 ρF

DECAYING EXPONENTIAL WAVEFORM

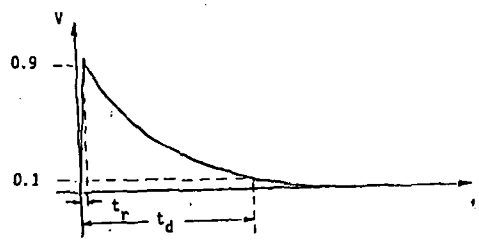

WAVEFORM	t_r (ns)	t_d (μs)
3	500 max	170 (±20%)
4	100 max	2 (±20%)

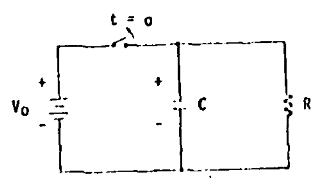

$$RC = \frac{t_d}{\ell n 0.1}$$

t_d = 170 μs

R = 1.0 KΩ
C = 0.0068 μF

t_d = 2 μs

R = 1.0 KΩ
C = 470 ρF

PRELIMINARY OBSERVATIONS

- UPSET HAS BEEN INDUCED AND OBSERVED IN THE LABORATORY
  - UPSET DOES NOT OCCUR AFTER EACH TRANSIENT SIGNAL INJECTION
    - IMPLIES CORRELATION BETWEEN UPSET AND PROCESSING STATE

- NORMAL FUNCTION IS RESTORED BY RESETTING AND/OR REPROGRAMMING THE SYSTEM

- STATUS BIT SEQUENCES HAVE BEEN RECORDED THAT DO NOT CORRESPOND TO AN 8080 MACHINE CYCLE
  - IMPLIES UNDEFINED PROCESSING STATES BEING ENTERED

FUTURE PLANS

- COMPLETE THE FOLLOWING UPSET TEST MATRIX

$$\begin{bmatrix} \text{PIN LEVEL-} \\ \mu\text{P CHIP} \\ \\ \text{CONNECTOR} \\ \text{LEVEL-} \\ \text{CPU CARD} \end{bmatrix} \times \begin{bmatrix} \text{WAVEFORM 1} \\ \text{WAVEFORM 2} \\ \text{WAVEFORM 3} \\ \text{WAVEFORM 4} \end{bmatrix} \times \begin{bmatrix} \text{DATA BUS LINES} \\ \text{ADDRESS BUS LINES} \\ \text{CONTROL LINES} \\ \text{- - - - - - - - -} \\ \text{I/O LINES} \end{bmatrix}$$

- PERFORM A STATISTICAL ANALYSIS OF THE TIME DATA TO RELATE UPSET TO
  - INTERNAL STATE OF THE CANDIDATE PROCESSOR
  - TRANSIENT SIGNAL INJECTION POINT

- UTILIZE A SOFTWARE SIMULATION APPROACH TO DEVELOP FAULT SIGNATURES FROM THE STATUS BYTE DATA

DIAGNOSTIC EMULATION ANALYSIS--NEED AND TECHNIQUE

by

Mr. Gerard E. Migneault

Langley Research Center
National Aeronautics and Space Administration

A brief description of the problem of determining failure modes will clarify the usefulness of emulation. The discussion will cover the relationship of complexity, definitional flaws, specific software dependent behavior and lumped parameter analytical models. Deterministic and stochastic application possibilities of emulation will be identified, as will implementation details — at the level of a conceptual scheme and in terms of supporting components. A sample application will be described. Future possible directions will be identified.

CHARACTERISTICS OF FAULT TOLERANCE

- REDUNDANCY
- ERROR DETECTION
- CONTINUED OPERATION
  -- RECOVERY

●●● INCREASED COMPLEXITY

- SAFETY REQUIREMENT IMPLIES PROBABILITY OF SYSTEM FAILURE IN 10-HOUR FLIGHT LESS THAN ABOUT 10^{-9}

- FAULT INTOLERANT SYSTEM
  WORST COMPONENT/DEVICE
  MTTF $\sim 10^{10}$ HOURS
  NOT FEASIBLE TODAY

- SYSTEM MUST TOLERATE FAULTS AND BE MAINTAINED

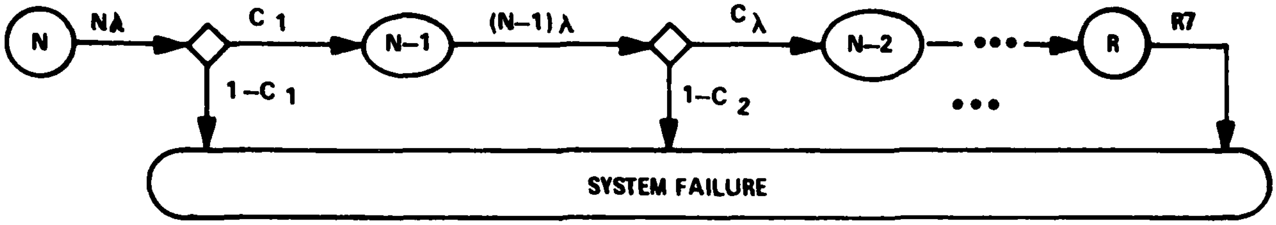

$$\frac{\text{SYSTEM MTTF}}{\text{DEVICE MTTF}} = \sum_{j=R}^{N} \frac{a_{N-j}}{j}$$

$$a_0 = 1 ,\ a_K = \prod_{k=1}^{j} c_k$$

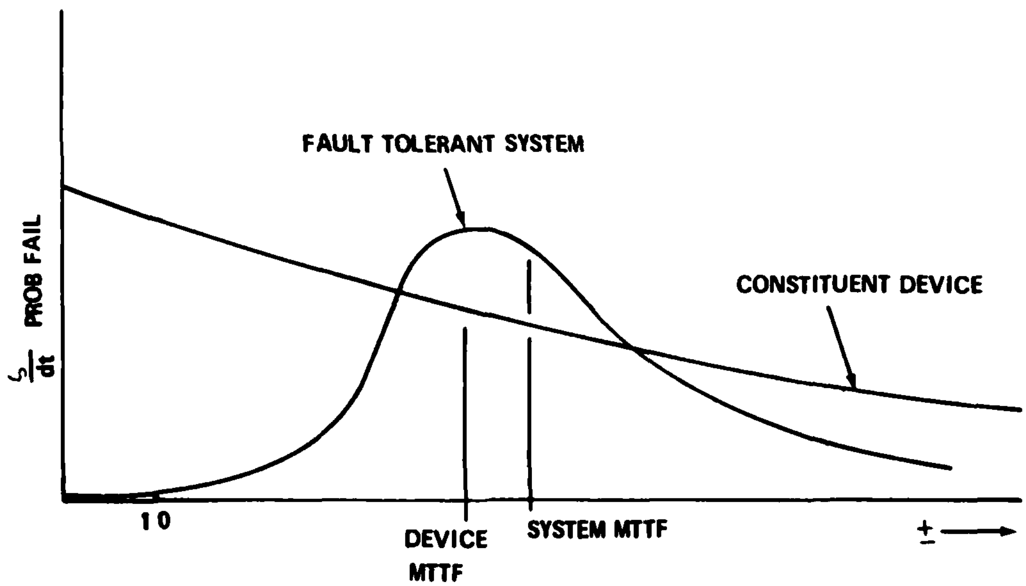

MAINTAINED FAULT TOLERANT SYSTEM

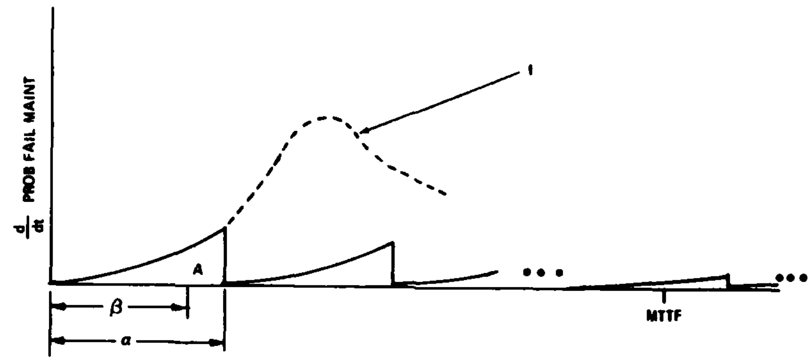

- $MTTF_{MAINT} = \frac{\alpha}{A} + \beta - \alpha$

  $\sim$ 10 10 HOURS

$$A = \int_o^{\alpha} f(t)$$

$$\beta = \int_o^{\alpha} t\, f(t)$$

- $MTTR_{EPAIR} \longrightarrow \frac{\text{DEVICE MTTF}}{\text{No. OF DEVICES}}$
- ECONOMICS ⟶ MULTIFUNCTION DEVICES
- MORE COMPLEXITY

TOLERANCE OF DEFINITIONAL FLAWS SOFTWARE PRIME CULPRIT

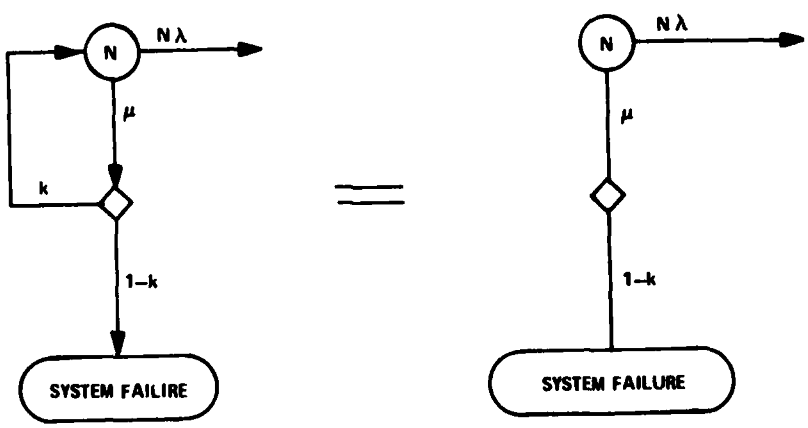

TOLERANCE OF DEFINITIONAL FLAWS

SOFTWARE PRIME CULPRIT

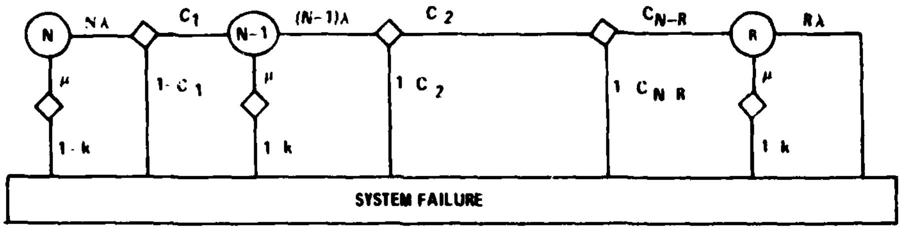

H/W+S/W FAULT TOLERANT MODEL

- **ANALYTICAL SOLUTION TECHNIQUE**

$$\text{PROB FAIL} = 1-e^{-[N\lambda+\mu(1-k)]t}\sum_{\ell=0}^{N-R} a_{\ell}\binom{n}{\ell}\left(e^{\lambda t}-1\right)$$

- **BUT**

$0.999999 < C_1 \leq 1$

$0.9999 < C_2 \leq 1$

$0 \leq \mu(1-k)\quad 0.000\,000\,000\,1$

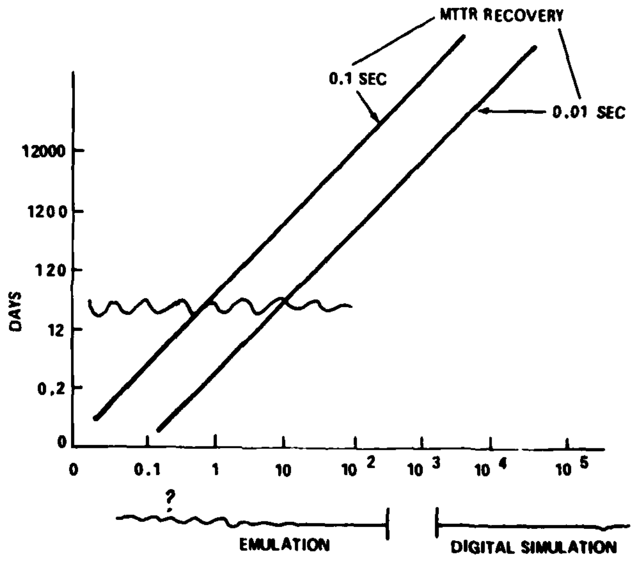

TEST DURATION FOR 10^7
FAULT INSERTIONS FOR
~2000 GATE EQUIVALENTS CPU
WITH ARBITRARY MEMORY
AND SOFTWARE

OBJECTIVE

DEVELOPMENT AND SPECIFICATION OF AN EMULATION TECHNIQUE FOR GENERATING STATISTICALLY SIGNIFICANT QUANTITIES OF FAILURE MODES EFFECTS DATA OF HIGHLY RELIABLE COMPUTER SYSTEMS

JUSTIFICATION

- IN HIGHLY RELIABLE, FAULT TOLERANT SYSTEMS SYSTEM FAILURE MODES DUE TO DESIGN FLAWS BECOME SIGNIFICANT - PERHAPS DOMINANT
- CREDIBILITY OF ANALYTICAL RELIABILITY MODELS IS DEPENDENT UPON AMOUNT OF DATA FROM WHICH INPUT PARAMETERS ARE DERIVED
- HIGH RELIABILITY (10^{-9}) OF SYSTEMS BEING ANALYZED PRECLUDES USE/LIFETIME TESTING OF ACTUAL SYSTEMS BECAUSE OF INORDINATELY LONG MTTF's
- NO OTHER MEANS IDENTIFIED TO ACQUIRE SUFFICIENT DATA FOR THE ABOVE.

TECHNICAL APPROACH

- DEVELOPMENT OF FAST EMULATION ALGORITHMS CAPABLE OF SUPPORTING FAULT INSERTION
  - GATE LOGIC LEVEL
  - HYBRID LEVELS
    GATE/CHIP/REGISTER/INSTRUCTION COMBINATIONS
- IMPLEMENTATION OF ALGORITHMS IN A HORIZONTALLY MICROPROGRAMMABLE COMPUTER AS AN ALGORITHM TEST BED WITH OPERATIONS SYSTEMS
- DEVELOPMENT AND SPECIFICATION OF NEEDED SUPPORT CAPABILITIES
  - META COMPILERS/ASSEMBLERS
  - DATA RECORDING CAPABILITIES
  - RUN TIME CONTROL FUNCTIONS
  - FAULT TABLE GENERATORS
  - H/W DESCRIPTION TRANSLATOR
  - ENVIRONMENT SIMULATOR/INTERFACING
  - DATA POST PROCESSORS
  - OPERATOR GRAPHICS

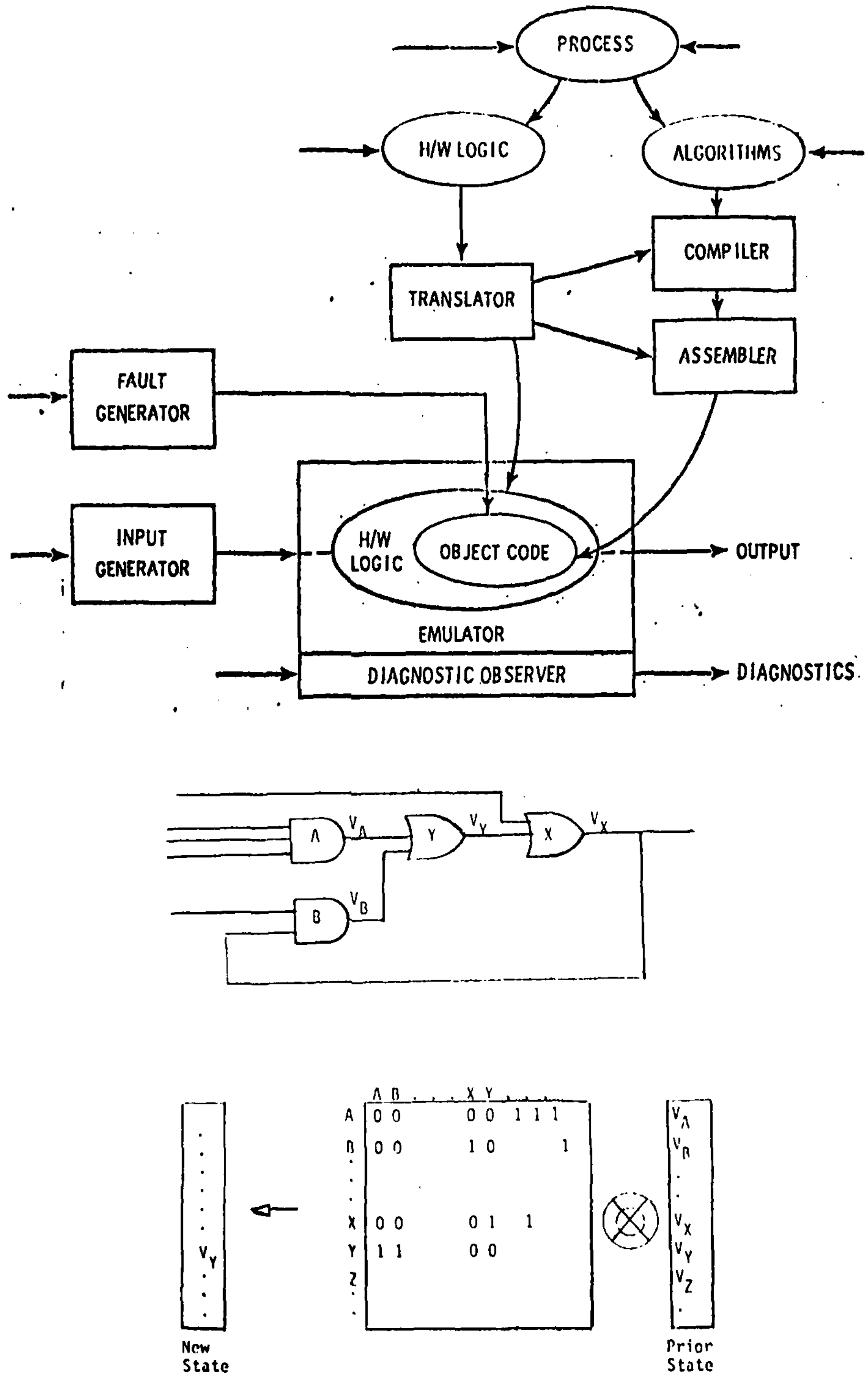

CONCEPTUAL EMULATION SCHEME

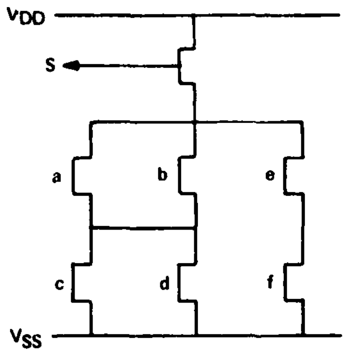

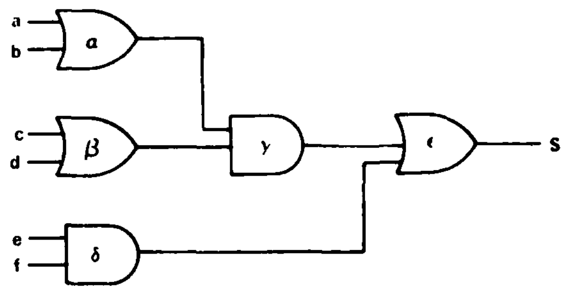

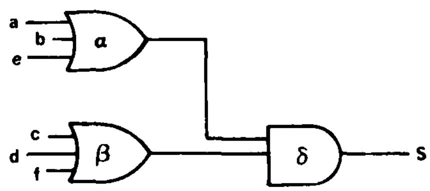

	a	b	c	d	e	f	α	β	γ	δ	ε
α	1	1	0	0	0	0	0	0	0	0	0
β	0	0	1	1	0	0	0	0	0	0	0
γ	0	0	0	0	0	0	1	1	0	0	0
δ	0	0	0	0	1	1	0	0	0	0	0
ε	0	0	0	0	0	0	0	0	1	1	0
S	0	0	0	0	0	0	0	0	0	0	1

SAMPLE LATENT FAULT ANALYSIS

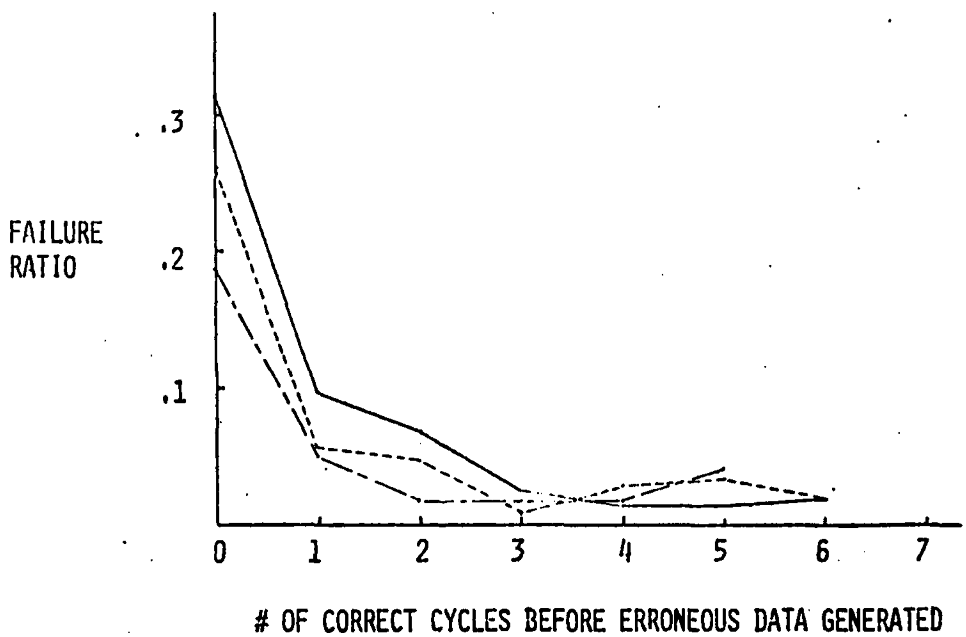

DIAGNOSTIC EMULATION APPLICATIONS

DETERMINISTIC:

- HARDWARE LOGIC DESIGN ANALYSIS.
- SOFTWARE DESIGN ANALYSIS.
- SYSTEM (H/W & S/W) EFFICIENCY/MISMATCH ANALYSIS.
- H/W/S/W/SYSTEM FAILURE MODES & EFFECTS ANALYSIS
- SYSTEM PERFORMANCE ANALYSIS IN A SIMULATED MISSION

DIAGNOSTIC EMULATION APPLICATIONS

STATISTICAL:

- LATENT FAULT ANALYSIS AND MODELING.
- COVERAGE DETERMINATION AND MODELING.
- TRANSIENT FAULT ANALYSIS.

DIGITAL SYSTEM HARDWARE DESCRIPTION TECHNIQUE USED IN EMULATION

by

Mr. Robert M. Thomas, Jr.

Langley Research Center
National Aeronautics and Space Administration

A technique to translate a digital circuit description into the form required to emulate the circuit at the gate and flip-flop level is described. This technique, implemented as computer programs, takes as input a description of the integrated circuit and translates the description into tables for the emulation. Integrated circuit description language is described.

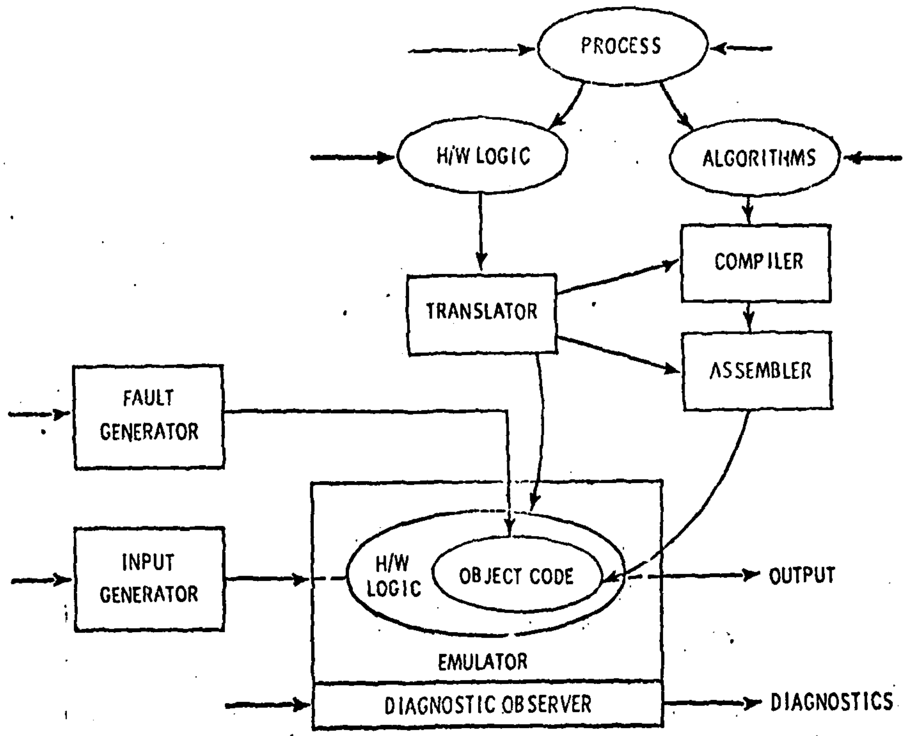

OUTLINE

- HARDWARE DESCRIPTION LANGUAGE
- TRANSLATION
- FAULT GENERATION AND INSERTION

HARDWARE DESCRIPTION LANGUAGE

SYSTEMATIC RULES FOR EXPRESSING HARDWARE LOGIC
IN A FORM USABLE BY THE TRANSLATOR.

SOURCE OF INFORMATION

SCHEMATICS

- INTEGRATED CIRCUIT TYPES
- INTERCONNECTIONS
- NAMES OF EACH IC

INTEGRATED CIRCUIT DATA SHEETS

- GATE/FLIP-FLOP MODELS

HARDWARE DESCRIPTION LANGUAGE

LANGUAGE ELEMENTS

GATE TYPES:	AND, OR, NOT, NAND, NOR, EXCLUSIVE OR, EXCLUSIVE NOR
FLIP-FLOP TYPES:	D, J-K, R-S, T
INTEGRATED CIRCUIT IDENTIFIERS:	ALPHA-NUMERIC
INTEGRATED CIRCUIT CONNECTIONS:	PIN TO PIN

CHIP DESCRIPTION

```
$ CHIP DEFINITION $
TYPE !
POWER !
DESCRIPTION !
UNUSED PINS !
FUNCTIONS !
   G-S =
   G-A =
   G-R =
   G-C =
   G-A' =
   G-B' =
   G-C' =
   G-D 0 =
   G-D 1 =
   G-D 2 =
   G-D 3 =
   G-D 4 =
   G-D 5 =
   G-D 6 =
   G-D 7 =
   G-W (P-6) =
   G-Y (P-5) =
   END CHIP $
```

LATCHED PARALLEL TO SERIAL CONVERTER SCHEMATIC

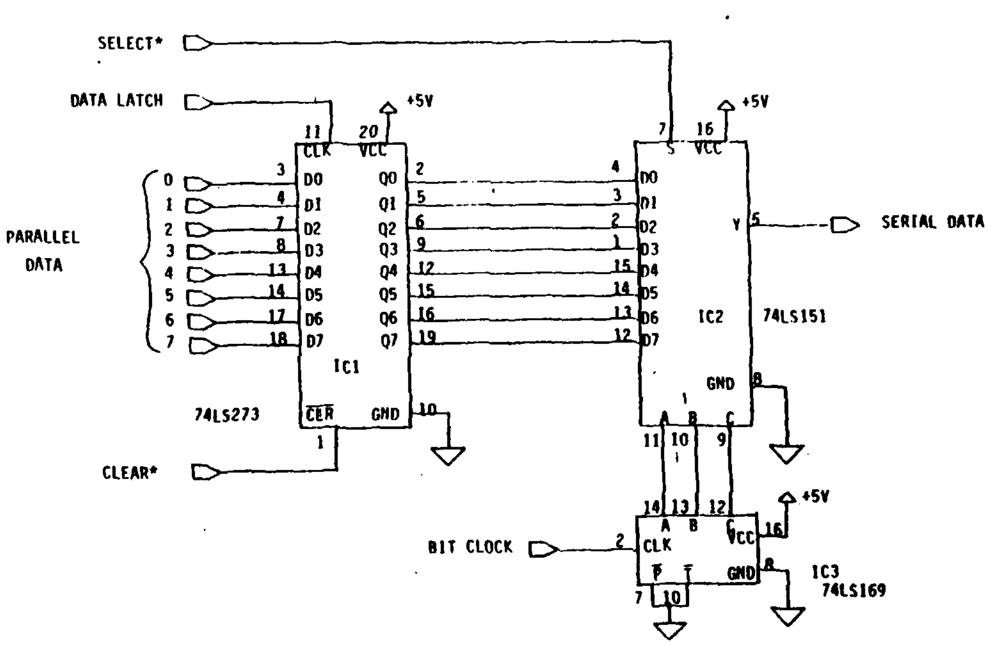

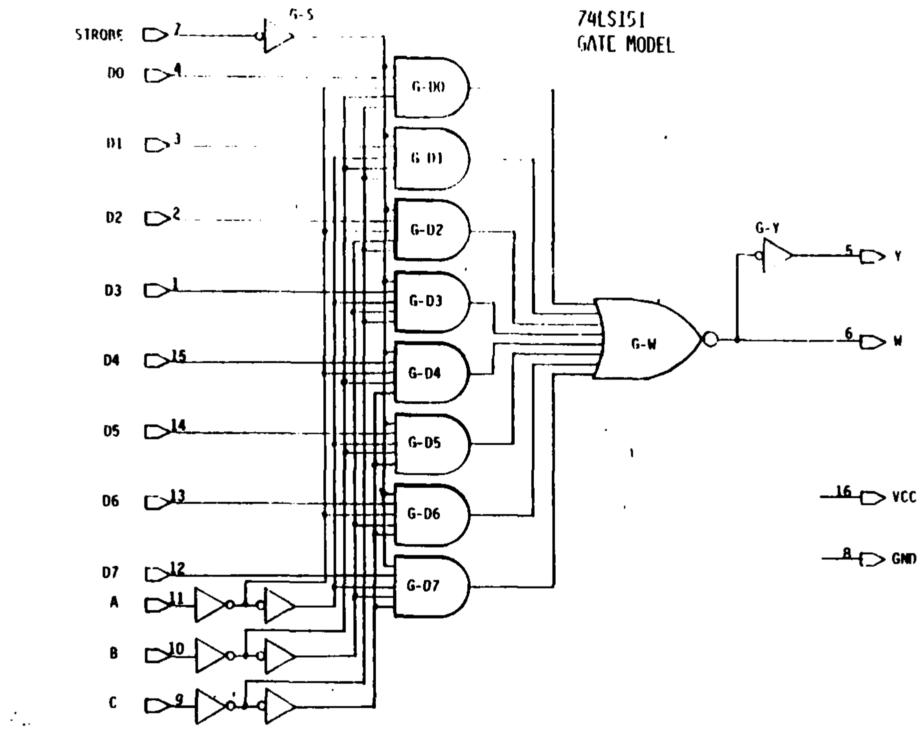

CHIP DESCRIPTION FOR 74LS151

```
$ CHIP DEFINITION $
TYPE : SN54LS151
POWER : VCC = P-16, GND = P-8
DESCRIPTION : ONE OF EIGHT DATA SELECTORS MULTIPLEXERS.
UNUSED PINS : NONE
FUNCTIONS :
  G-S = NOT(P-7)
  G-A = AND(P-11)
  G-B = AND(P-10)
  G-C = AND(P-9)
  G-A' = NOT(G-A)
  G-B' = NOT(G-B)
  G-C' = NOT(G-C)
  G-D0 = AND(G-S, P-4, G-A', G-B', G-C')
  G-D1 = AND(G-S, P-3, G-A, G-B', G-C')
  G-D2 = AND(G-S, P-2, G-A', G-B, G-C')
  G-D3 = AND(G-S, P-1, G-A, G-B, G-C')
  G-D4 = AND(G-S, P-15, G-A', G-B', G-C)
  G-D5 = AND(G-S, P-14, G-A, G-B', G-C)
  G-D6 = AND(G-S, P-13, G-A', G-B, G-C)
  G-D7 = AND(G-S, P-12, G-A, G-B, G-C)
  G-W(P-6) = NOR(G-D0,G-D1,G-D2,G-D3,G-D4,G-D5,G-D6,G-D7)
  G-Y(P-5) = NOT(G-W)
$ END CHIP $
```

INTEGRATED CIRCUIT NAME TABLE

NAME	IC TYPE
IC 1	74LS273
IC 2	74LS151
IC 3	74LS169

INTEGRATED CIRCUIT CONNECTION TABLE

OUTPUT	DESTINATION	SIGNAL NAME (OPTIONAL)
IC 1-2	IC 2-4	
IC 1-5	IC 2-3	
IC 1-6	IC 2-2	
IC 1-9	IC 2-15	
IC 1-12	IC 2-14	
IC 1-15	IC 2-13	
IC 1-16	IC 2-12	
IC 1-19		
IC 2-5	OUTPUT CONNECTOR	SERIAL DATA
IC 3-14	IC 2-11	
IC 3-13	IC 2-10	
IC 3-12	IC 2-9	

TRANSLATION PROCESS

TRANSLATION PROCESS

CONVERT A PSEUDO ENGLISH CIRCUIT DESCRIPTION TO A PACKED BINARY ENCODED FORM REQUIRED BY THE EMULATION ALGORITHM

REJECT DESCRIPTION THAT DOES NOT FOLLOW PRECISELY THE HARDWARE DESCRIPTION LANGUAGE RULES

EMULATION MATRIX

SOURCE

DESTINATION	G-S	G-A	G-B	G-C	G-A'	G-B'	G-C'	G-DO . . .
G-S								
G-A								
G-B								
G-C								
G-A'		x						
G-B'			x					
G-C'								
G-DO	x				x	x	x	
.								
.								
.								

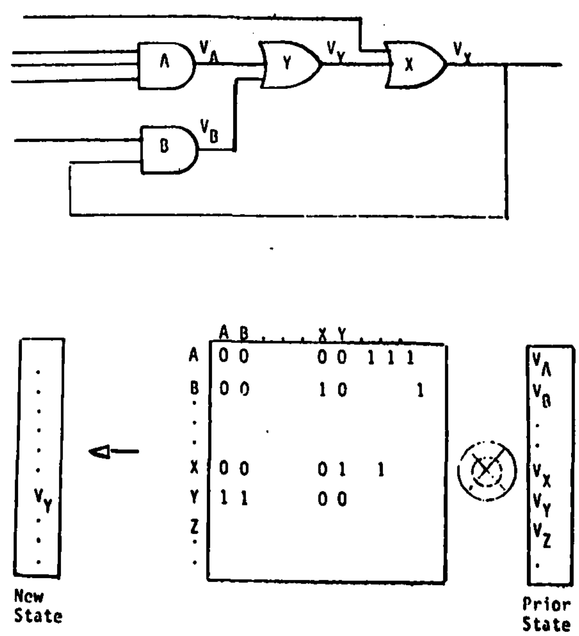

CONCEPTUAL EMULATION SCHEME

FAULT GENERATION AND INSERTION

FAULT SELECTION

- MANUAL - SELECTED BY EXPERIMENTER
- AUTOMATIC - RANDOMLY SELECTED

FAULT INSERTION

- MODIFY EMULATION MATRIX TO REFLECT FAULT

FAULT OCCURRENCE

- INFORMATION TO EMULATION ALGORITHM AS TO WHEN FAULT OCCURS

SUMMARY

DEVELOPING THE TOOLS TO SUPPORT GATE/FLIP-FLOP LEVEL EMULATION OF DIGITAL COMPUTERS

- HARDWARE DESCRIPTION LANGUAGE
- TRANSLATOR PROGRAM
- FAULT GENERATOR PROGRAMS

THE NEED FOR TRANSIENT DATA IN A CARE III RELIABILITY ANALYSIS

by

Mr. Salvatore J. Bavuso

Langley Research Center
National Aeronautics and Space Administration

The recently developed CARE III (Computer-Aided Reliability Estimation) computer program incorporates a transient/intermittent fault model that is mathematically accurate in contrast to many existing reliability evaluator programs which employ approximations for the transient/intermittent model. The CARE III transient/intermittent model will be discussed and compared to existing approximating models. Computational complexity arising from the use of the CARE III transient/intermittent model will also be addressed.

ADVANCED RELIABILITY ASSESSMENT TECHNIQUES

OBJECTIVE: DEVELOP A CAPABILITY TO ASSESS THE RELIABILITY OF ANY FAULT-TOLERANT COMPUTER-BASED SYSTEM, INCLUDING EXECUTIVE SOFTWARE

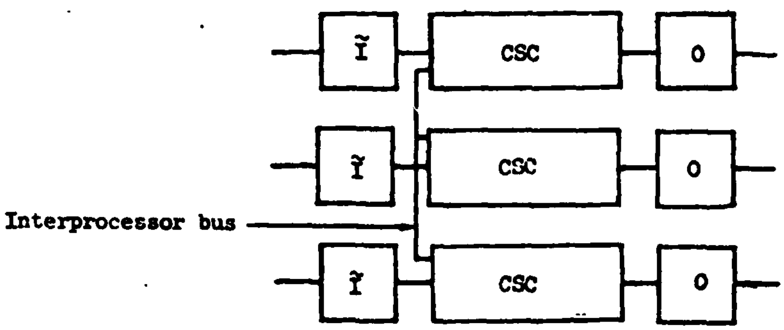

Triplex computer architecture.

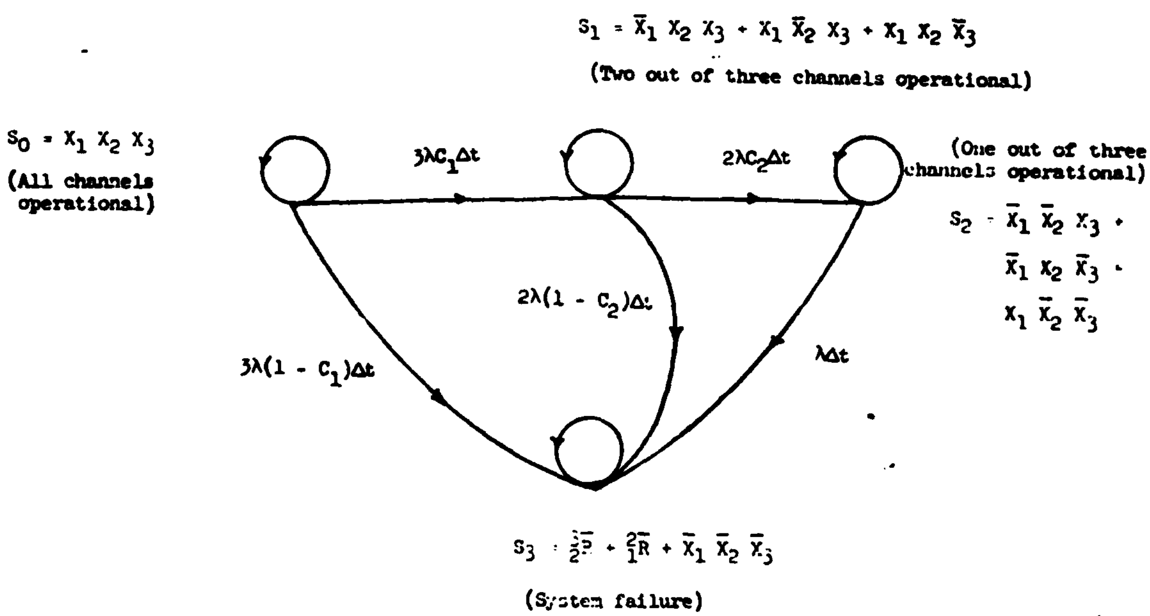

Markov state space model of triplex channel RCS.

$$P_0(t + \Delta t) = P_0(t) - 3\lambda C_1 \Delta t P_0(t) - 3\lambda\left(1 - C_1\right)\Delta t P_0(t)$$

$$\lim_{\Delta t \to 0} \frac{P_0(t + \Delta t) - P_0(t)}{\Delta t} = \frac{dP_0(t)}{dt} = -3\lambda P_0(t)$$

$$\frac{dP_0(t)}{dt} = -3\lambda P_0(t)$$

$$\frac{dP_1(t)}{dt} = 3\lambda C_1 P_0(t) - 2\lambda P_1(t)$$

$$\frac{dP_2(t)}{dt} = 2\lambda C_2 P_1(t) - \lambda P_2(t)$$

$$\frac{dP_3(t)}{dt} = 3\lambda(1 - C_1)P_0(t) + 2\lambda(1 - C_2)P_1(t) + \lambda P_2(t)$$

where P_0 is the probability of the system being in state S_0, that is

$$P_0 = P\left(S_0\right) \qquad P_1 = P\left(S_1\right)\ P_2 = P\left(S_2\right)\ P_3 = P\left(S_3\right)$$

and the initial conditions are

$$P_0(0) = 1 \qquad P_1(0) = P_2(0) = P_3(C) = 0$$

$$P_0(t) = e^{-3\lambda t}$$

$$P_1(t) = 3C_1\left(e^{-2\lambda t} - e^{-3\lambda t}\right)$$

$$P_2(t) = 3C_1C_2\left(e^{-\lambda t} - 2e^{-2\lambda t} + e^{-3\lambda t}\right)$$

$$P_3(t) = 1 - \left[P_0(t) + P_1(t) + P_2(t)\right]$$

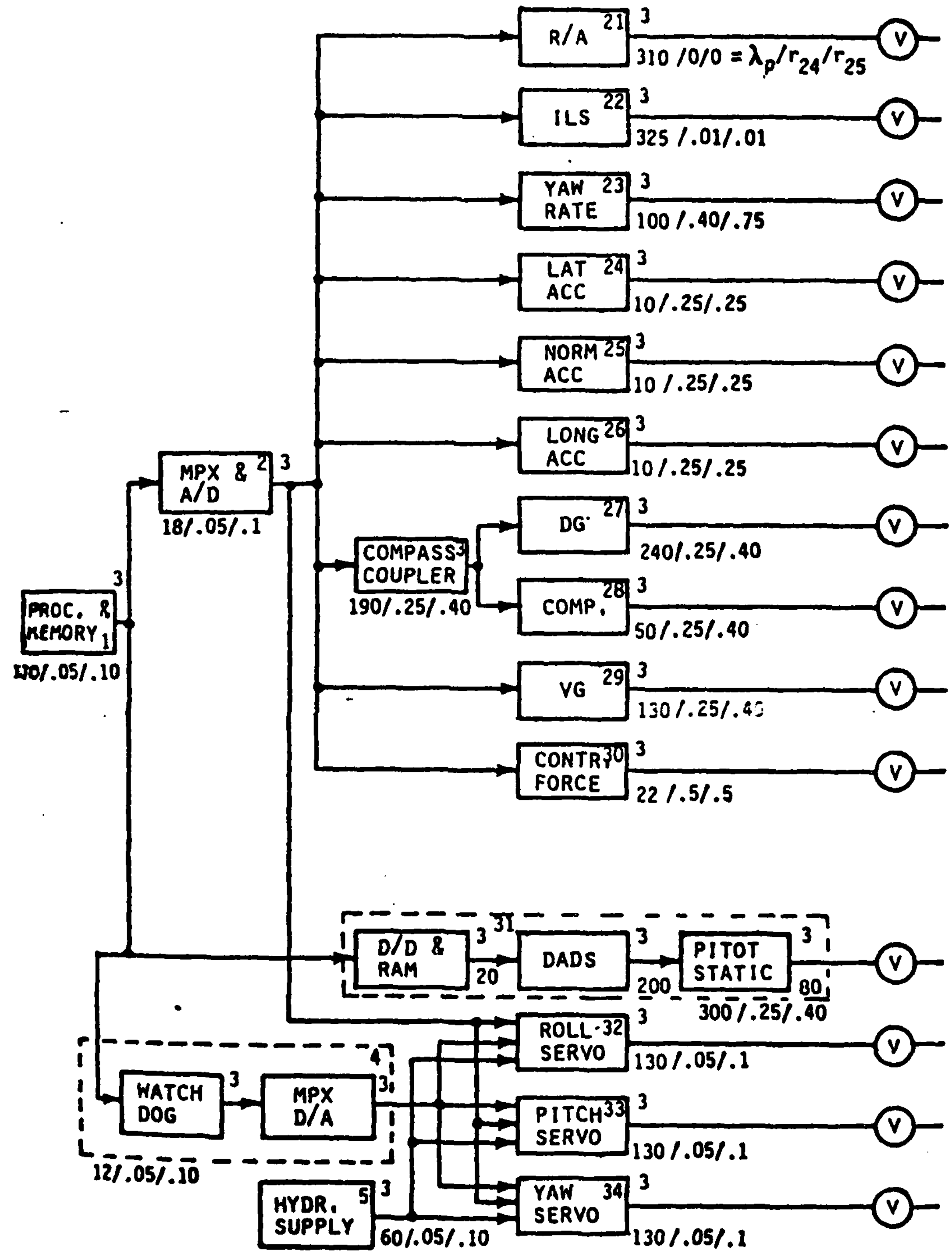

FOR CWS, DELETE R/A AND ILS

Near-Term ARCS Dependency Tree

DELINEATION OF HARDWARE AND SOFTWARE ANOMALIES

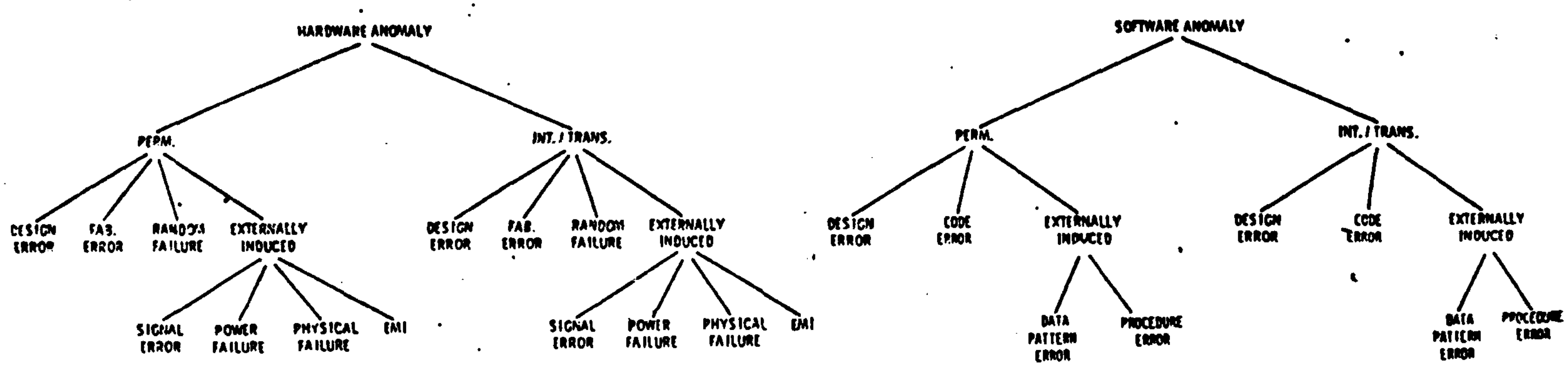

Delineation of hardware and software anomalies.

NUMBER OF STATES NEEDED FOR A MARKOV MODEL

LET: n = NUMBER OF "COUPLED" STAGES

k_i = NUMBER OF POSSIBLE FAULT TYPES IN iTH STAGE

ℓ_i = NUMBER OF POSSIBLE FAULT STATES/TYPE IN iTH STAGE

m_i = NUMBER OF MODULE FAILURES THAT CAN BE TOLERATED IN THE iTH STAGE

THEN NUMBER OF STSTEM STATES N IS

$$N = \prod_{i=1}^{n} \left[\sum_{j=0}^{m_i} \binom{k_i \ell_i + j - 1}{j} \right]$$

E.g., If $n = 4$ and $k_i = 2$, $\ell_i = 3$, $m_i = 2$ for all i, $N = 614{,}656$

$$\text{CARE III} \quad N = 2 \prod_{i=1}^{n} (m_i + 1) = 162$$

CARE III APPROACH

- DEFINE SYSTEM STATE ONLY IN TERMS OF NUMBER OF EXISTING FAULTS
- INDEPENDENTLY EVALUATE TRANSITION PARAMETERS AS A FUNCTION OF DISTRIBUTION OF POSSIBLE FAULT TYPES AND STATES
- DETERMINE RELIABILITY USING KOLMOGOROV'S FORWARD DIFFERENTIAL EQUATIONS
- NUMBER OF STATES DRASTICALLY REDUCED; TRANSITION RATES NECESSARILY TIME-DEPENDENT 81 vs 614,656

COMPUTER AIDED RELIABILITY ESTIMATION

(CARE III)

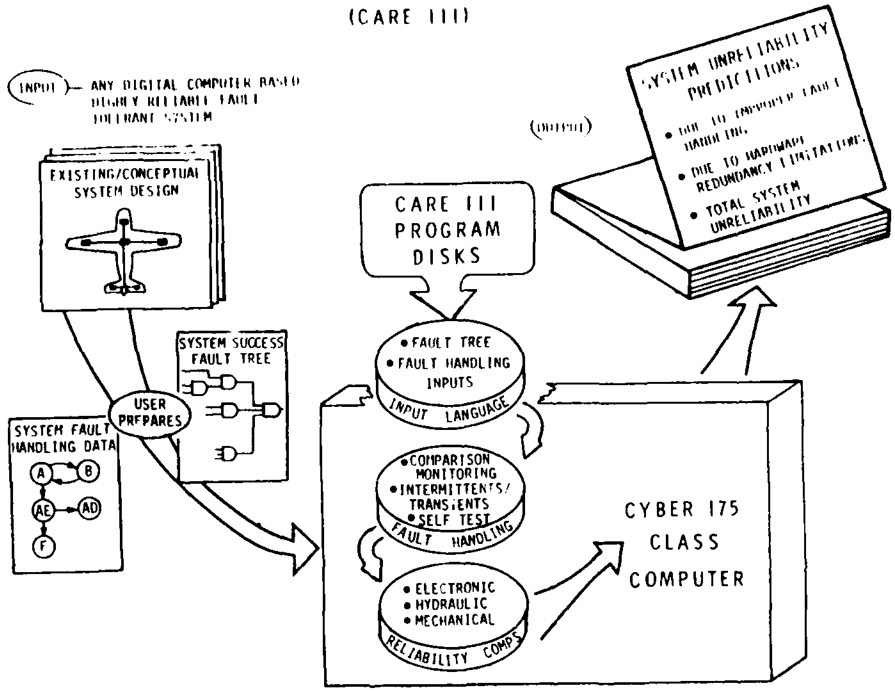


```
100- $FLTTYP  NFTYPS=1,DEL=3.6E2,CVPRNT=T,DBLDF=5.0E-2,CVPLOT=T$
110- $STAGES  NSTGES=2,N=10,5,M=2,2,IRLPCD=4,RLPLOT=T$
120- $FLTCAT  NFCATS=2*1,JTYP(1,1)=1,JTYP(1,2)=1,
130-          RLM(1,1)=1.0E-4,RLM(1,2)=1.0E-5$
140- $RNTIME  FT=10.,SYSFLG=T,CPLFLG=T$
150- SIFT1 FAULT-TREE 7-1-81
160- 1 2 3 3
170- 3 0 1 2
180- SIFT1 CRITICAL-FAULT PAIRS
190- 1 15 16 18
200- 1 1 10
210- 2 11 15
220-16 2 1 2 3 4 5 6 7 8 9 10
230-17 2 11 12 13 14 15
240-18 0 16 17
```

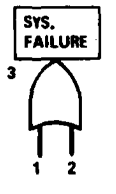

SYSTEM TREE

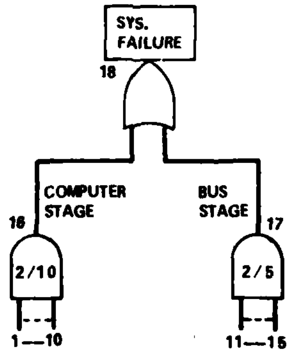

2 : : 5 BUS FORM A CRITICAL PAIR CAUSES A SYSTEM FAILURE

CRITICAL PAIR FAULT TREE

SYSTEM FAILS IF STAGE 1 OR 2 FAILS OR A CRITICAL FAULT PAIR OCCURS.

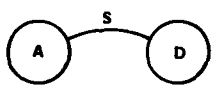

FAULT MODEL

PERMANENT, TRANSIENT/INTERMITTENT FAULT ANALOG

	PERMANENT FAULT	TRANSIENT/INTERMITTENT FAULT
LOGICAL FAULT MODEL AFTER FAULT ARRIVAL	S-A-1/S-A-0 DETERMINISTIC: $\tau_F \leq \tau < \infty$	S-A-1/S-A-0 STOCHASTIC τ FOR DURATION OF S-A-1 AND S-A-0 EXPONENTIAL: $f(t) = \alpha e^{-\alpha t}$
FAULT ARRIVAL MODEL	WEIBULL: $f(t) = w\lambda t^{w-1}e^{-\lambda t^w}$ EXPONENTIAL: $f(t) = \lambda e^{-\lambda t}$	

TRANSIENT AND PERMANENT FAULTS
CONVENTIONAL MARKOV MODEL
2-UNIT SYSTEM

λ_p = PERMANENT FAILURE RATE (ARRIVAL RATE)

λ_T = TRANSIENT RATE (ARRIVAL RATE)

1 = PROPORTION OF TRANSIENTS THAT ARE MISTAKEN FOR PERMANENT FAILURES

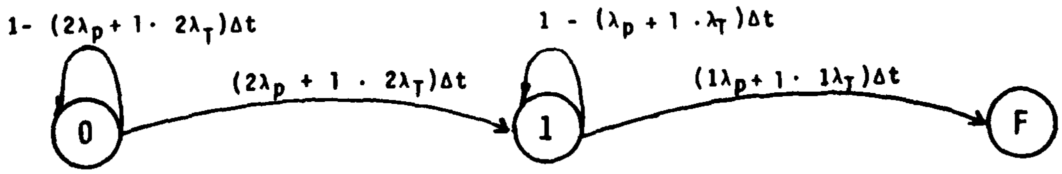

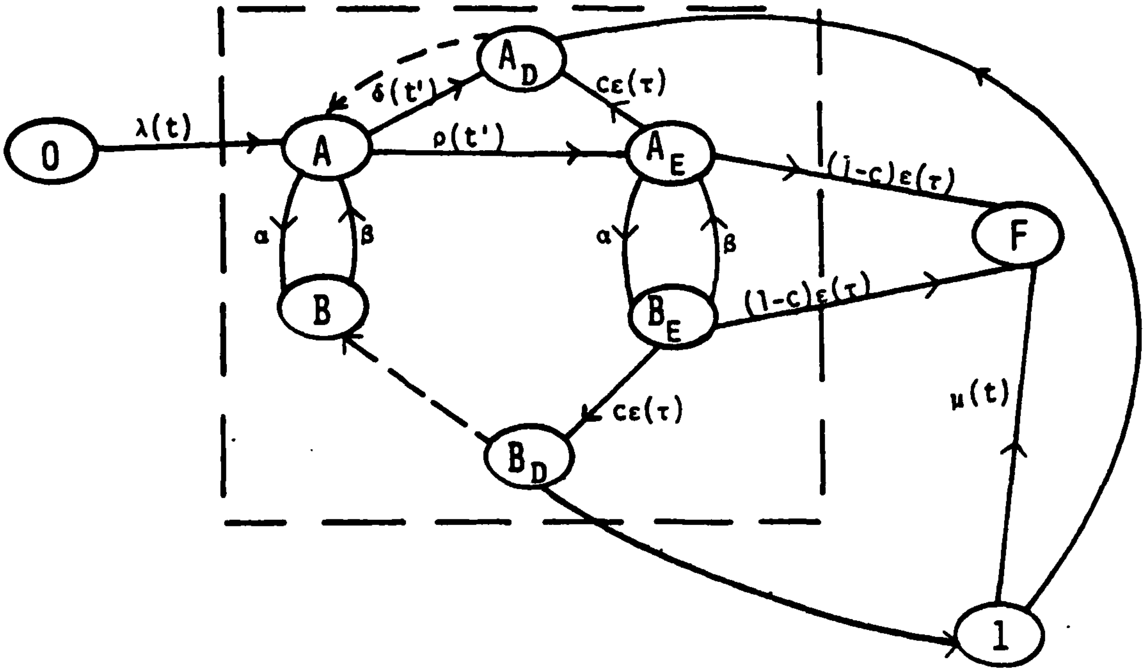

Overall reliability model of two-unit system.

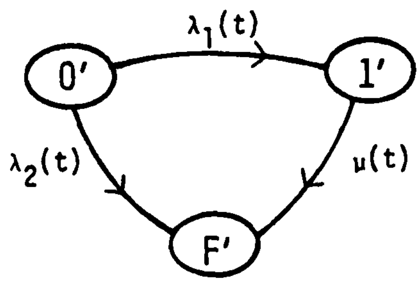

Aggregated reliability model for a two-unit system.

- System states defined by number of failed modules of each type
- Transition rates determined by averaging overall failure types and states

SINGLE-FAULT MODEL EQUATIONS

	VARIABLE
$\phi(t) = \alpha e^{-\beta t}\int_0^t e^{-(\alpha-\beta)\tau} r(\tau)d(\tau)d\tau$	FEEAR(IT)
$P_a(t) = e^{-\alpha t} r(t)d(t) + \beta\int_0^t \phi(t-\tau)P_a(\tau)d\tau$	PA(IT)
$P_b(t) = \phi(t) + \beta\int_0^t \phi(t-\tau)P_b(\tau)d\tau$	PB1(IT)
$P_e(t) = \int_0^t e^{-\alpha\tau}\rho(\tau)d(\tau)e(t-\tau)d\tau + \beta\int_0^t \phi(t-\tau)P_e(\tau)d\tau$	PERR(IT)
$p_e(t) = e^{-\alpha t}\rho(t)d(t) + \beta\int_0^t \phi(t-\tau)p_e(\tau)d\tau$	PEAR(IT)
$p_{\bar{e}}(t) = e^{-\alpha t}\delta(t)r(t) + \beta\int_0^t \phi(t-\tau)p_{\bar{e}}(\tau)d\tau$	PNEAR(IT)
$p_f(t) = (1-C)\int_0^t p_e(\tau)\varepsilon(t-\tau)d\tau$	PFLD(IT)
$\Psi_A(t) = C\int_0^t p_e(\tau)\varepsilon(t-\tau)\left(\frac{\beta + \alpha e^{-(\alpha+\beta)(t-\tau)}}{\alpha+\beta}\right)d\tau + p_{\bar{e}}(t)$	PSIA(IT)
$\Psi_B(t) = \frac{\alpha C}{\alpha+\beta}\int_0^t p_e(\tau)(1 - e^{-(\alpha+\beta)(t-\tau)})\varepsilon(t-\tau)d\tau$	PSIB(IT)

Double Fault Model

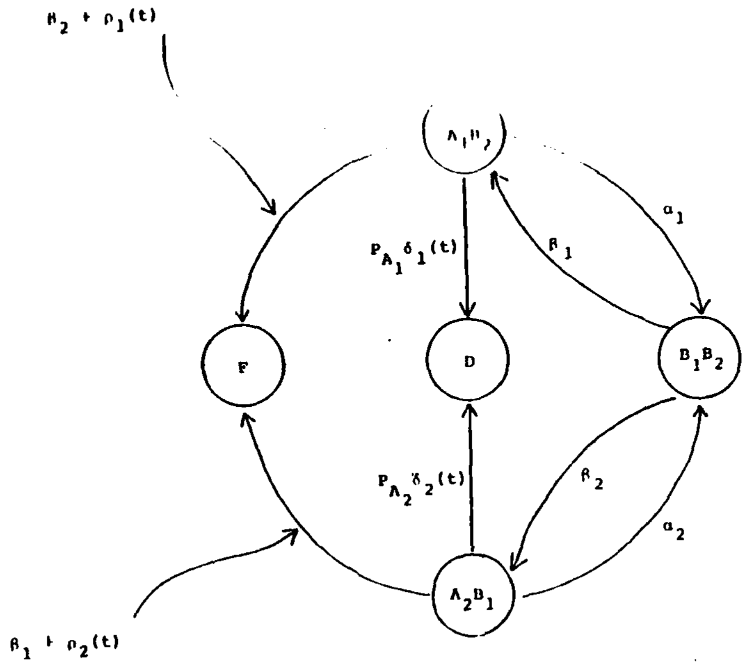

ADVANCED RELIABILITY ASSESSMENT DEVELOPMENT